

University of Southampton Research Repository ePrints Soton

Copyright © and Moral Rights for this thesis are retained by the author and/or other copyright owners. A copy can be downloaded for personal non-commercial research or study, without prior permission or charge. This thesis cannot be reproduced or quoted extensively from without first obtaining permission in writing from the copyright holder/s. The content must not be changed in any way or sold commercially in any format or medium without the formal permission of the copyright holders.

When referring to this work, full bibliographic details including the author, title, awarding institution and date of the thesis must be given e.g.

AUTHOR (year of submission) "Full thesis title", University of Southampton, name of the University School or Department, PhD Thesis, pagination

UNIVERSITY OF SOUTHAMPTON

FACULTY OF MEDICINE

THE PATHOGENESIS OF PLEURAL EMPYEMA CAUSED BY STREPTOCOCCUS PNEUMONIAE

by

Claire Jane Heath

Thesis submitted for the degree of Doctor of Philosophy

October 2011

Dedication

I dedicate this work to my Grandad, Mr John Jennings, whose unfaltering love and encouragement made me believe anything is possible.

Love you always Granch. X

Acknowledgements

Foremost, I cannot begin to express my gratitude to my supervisor, Dr. Myron Christodoulides, who has consistently gone above and beyond the call of duty to provide support, both professionally and personally. Thank you for always having an open door, a lending ear and a shoulder to cry on, sometimes literally.

Thanks also to Professor John Heckels for his overall guidance and support throughout this project.

Thanks are also due to Dr. Jason Hinds for his invaluable guidance and advice on bacterial microarray analysis, and also to Dr. Kate Gould for her technical support in microarray analyses.

I am also indebted to Colin Nicholson for his patience and unnerving accuracy in the technicalities of human transcriptome microarray analysis. Thanks also to Professor Paddy Tighe for his assistance in the analysis of human arrays.

I would also like to thank Dr. Helen Parker for being so approachable and for giving up her time to teach me the art of on-chip RNA analysis and for encouraging me to keep trying when things were not going quite to plan.

Thank you also to Dr. Ben Nicholas for his technical advice on FACS methodology and also to Achika Keys for her practical assistance in FACS analysis.

Mostly, I am sincerely grateful to all of my friends in Southampton for making the last four years so incredibly enjoyable. Thank you Megan, Becca, Jenny and Jo. In particular, thank you my dear friend and colleague Annie, for always being cheerful enough for the both of us, for being my biggest fan and for all of the late night discussions, some of which were even on the topic of microbiology. I also undoubtedly owe my sanity to my wonderful housemate Carolina, who kept me fed and watered during the process of writing this thesis.

Finally, without the love and support, both emotional and financial, of my fantastic family I would not be where I stand today. Thank you all for your love and belief in me.

ABSTRACT

The clinical incidence of paediatric empyema has been increasing in the UK and indeed worldwide over the last decade. Empyema is defined as the fibropurulent stage of pleural disease, characterised by the presence of pus in the pleural cavity.

Understanding of the aetiology of this disease was hindered by the fact that routine culture of patient samples is often negative due to the administration of antibiotics. The advent of molecular techniques however, has identified *Streptococcus pneumoniae* as the main causative organism of this disease.

In the current study, an *in vitro* model of empyema has been established and the pathogen-host interactions between human pleural mesothelial cells and *Streptococcus pneumoniae* were investigated. Different pneumococcal strains, including mutants deficient in various putative virulence genes and also clinical empyema isolates were examined.

We observed that compared to laboratory strains, clinical isolates adhered poorly to host cells, yet were still able to elicit cell death. The innate immune response was characterised by very low expression of pro-inflammatory cytokines, although these cells did respond to other bacterial stimuli, suggesting that the pneumococcus may employ a suppressive mechanism.

In addition, the transcriptome of both the bacteria and the host was examined during infection. Analysis of bacterial gene expression revealed that, in our model, the well characterised pneumococcal virulence genes were not differentially regulated, suggesting that these genes, which have been shown to be important in bacterial colonisation and invasion, are constitutively expressed in empyema-causing strains. Rather, genes involved in metabolic and bacteriostasis showed the greatest levels of differential activation and we suggest that genes which enable the bacteria to overcome host offences are equally important to the virulence.

In pleural cells, genes involved in mitochondrial dysfunction were differentially regulated during pneumococcal infection, perhaps indicating that in addition to the direct toxicity exerted by the bacteria, the induction of metabolic distress, and perhaps inactivation of some host innate defences, also contributes to the pathogenesis of disease.

CONTENTS

DEDICA	ATION	i
ACKNO	WLEDGEMENTS	ii
ABSTRA	ACT	V
INDEX		vii
LIST OF	FIGURES	xvii
LIST OF	TABLES	xxi
DECLA	RATION OF AUTHORSHIP	XXV
СНАРТ	ER 1 INTRODUCTION	1
1.1 7	THE BIOLOGY OF PNEUMOCOCCAL DISEASE	1
1.1.1	Disease Burden	i
1.1.2	Risk Factors	4
1.1.3	Invasive pneumococcal diseases	
1.1.4	Seasonality of Pneumococcal Disease	8
1.1.5	Anatomy and function of the lungs and pleura	8
1.2 F	PARAPNEUMONIC EFFUSIONS AND EMPYEMA	12
1.2.1	What is Empyema?	12
1.2.2	Classification of parapneumonic effusions	12
1.2.3	Clinical incidence	13
1.2.4	Aetiology	14
1.2.5	Pathophysiology	14
1.2.6	Signs and Symptoms	15
1.2.7	Diagnosis	15
1.2.8	Management	18
1.3 S	STREPTOCOCCUS PNEUMONIAE	20
1.3.1	Cultivation	20
1.3.2	The History of the Pneumococcus	21

1.3.3	Pneumococcal Serotyping	21
1.3.4	History of Pneumococcal vaccines	23
1.3.5	Nasopharyngeal Carriage of Pneumococci	25
1.3.6	Pneumococcal disease-causing serotypes	25
1.3.7	Pneumococcal Virulence Factors	30
1.4 1	MMUNITY TO THE PNEUMOCOCCUS	34
1.4.1	Complement	35
1.4.2	Toll-like Receptors	36
1.4.3	Nucleotide binding and Oligomerisation Proteins	37
1.4.4	Recognition of the Polysaccharide Capsule	38
1.5 I	HYPOTHESES AND OBJECTIVES	40
CHAPT	ER 2 MATERIALS AND METHODS	41
2.1	GENERAL REAGENTS	41
2.2	CHARACTERISATION OF HUMAN PLEURAL MESOTHELIAL CELL LINE	41
2.2.1	Culture and passage	41
2.2.2	Cryopreservation	42
2.2.3	Resuscitation of cryopreserved cells	43
2.2.4	Immunocytochemistry of cellular markers in cultured human pleural mesothelial cells	43
2.2.5	Characterisation of Toll-Like Receptor expression in MET-5A cells	44
2.3	CHARACTERISATION OF STREPTOCOCCUS PNEUMONIAE	45
2.3.1	In vitro culture of pneumococcal strains	46
2.3.2	Cryopreservation of bacteria	48
2.3.3	Quantification of bacterial suspensions	48
2.3.4	Preparation of infection suspensions	48
2.3.5	Characterisation of capsule expression	49
2.3.6	Characterisation of haemolytic activity	49
2.4 I	NVESTIGATION OF BACTERIAL ASSOCIATION WITH HUMAN PLEURAL	
MESOTI	HELIAL CELLS	50
2.4.1	Ouantification of total bacterial association	50

2.4.2	Quantification of bacterial invasion of pleural mesothelial cells	51
2.4.3	Visualisation of pneumococcal adherence to Met-5A cells by Scanning Electron Microso	copy52
2.5 A	ANTIGENIC STIMULATION OF PLEURAL MESOTHELIAL CELLS.	53
2.5.1	Pre-Stimulation of pleural mesothelial cells with TNF-α	53
2.5.2	Production of bacteria-derived antigens	53
2.5.3	Stimulation of pleural cells with antigens	55
2.5.4	Assessment of cytokine degradation by pneumococci	56
	QUANTIFICATION OF CYTOKINE PRODUCTION BY PLEURAL MESOTHELIAL FOLLOWING BACTERIAL ASSOCIATION AND ANTIGEN STIMULATION.	56
2.7 A	ANALYSIS OF PNEUMOCOCCAL GENE EXPRESSION PROFILE DURING INFECT	ION
OF HUM	IAN PLEURAL MESOTHELIAL CELLS.	58
2.7.1	Recovery of pneumococci from pleural mesothelial cell monolayers	58
2.7.2	Extraction of RNA from adherent pneumococci and Met-5A cells	59
2.7.3	Assessment of RNA quantity and integrity	59
2.7.4	Bacterial RNA Labelling	62
2.8 V	VALIDATION OF BACTERIAL GENE EXPRESSION	64
2.8.2	Synthesis of cDNA by reverse transcription	67
2.8.3	Quantitative Polymerase Chain Reaction	67
2.9 A	ANALYSIS OF GENE EXPRESSION PROFILE OF MET-5A CELLS DURING INFECT	ΓΙΟΝ
WITH ST	TREPTOCOCCUS PNEUMONIAE	68
2.9.1	Manufacture and Quality Control of Human Microarray Slides	69
2.9.2	Synthesis of First Strand cDNA	70
2.9.3	Synthesis of Second Strand cDNA	71
2.9.4	Purification of cDNA	71
2.9.5	In-vitro transcription to synthesise amino-allyl RNA (aRNA).	72
2.9.6	Purification of aRNA	72
2.9.7	Dye-coupling and clean up of aRNA	73
2.9.8	Purification of dye-labelled aRNA	73
2.9.9	Pre-hybridisation processing of microarray slides.	74

2.9.	10 Fragmentation of microarray probes	74	
2.9.	11 Microarray slide hybridisation	75	
	PTER 3 RESULTS – PNEUMOCOCCAL INTERACTIONS WITH HUMAN RAL MESOTHELIAL CELLS	77	
3.1 CELL	CHARACTERISATION OF THE HUMAN PLEURAL MESOTHELIAL LINE MET-5A		77
3.2	CHARACTERISATION OF CAPSULE EXPRESSION IN S. PNEUMONIAE ISOLATES	78	
3.3 MESO	ASSOCIATION OF <i>STREPTOCOCCUS PNEUMONIAE</i> WITH HUMAN PLEURAL OTHELIAL MET-5A CELLS	80	
3.4 MICRO	VISUALISATION OF BACTERIAL ASSOCIATION BY SCANNING ELECTRON OSCOPY	84	
3.5 PNEU	INVASION OF HUMAN PLEURAL MESOTHELIAL CELLS BY STREPTOCOCCUS MONIAE.	87	
3.6	QUANTITATION OF CYTOTOXICITY OF S. PNEUMONIAE TO MET-5A CELLS	91	
3.7	CYTOKINE RESPONSES OF MET-5A CELLS TO BACTERIAL INFECTION	92	
3.8	PRE-STIMULATION OF MET-5A CELLS WITH TNF-A	96	
3.9 MESO	INVESTIGATION OF TOLL-LIKE RECEPTOR EXPRESSION IN PLEURAL OTHELIAL CELLS	98	
3.10	ANTIGENIC STIMULATION OF MET-5A CELLS	100	
3.11	CYTOKINE DEGRADATION BY S. PNEUMONIAE	101	
3.12	SUMMARY	103	
	PTER 4 RESULTS – GENE EXPRESSION IN STREPTOCOCCUS PNEUMONIAE OWING HUMAN CELL INTERACTION	105	
4.1	ANALYSIS OF DIFFERENTIAL GENE EXPRESSION IN STREPTOCOCCUS		
PNEU	MONIAE DURING INFECTION OF MET-5A CELLS.	105	
4.1.	1 Optimisation of bacterial RNA extraction method	105	
4.2	MICROARRAY ANALYSIS OF DIFFERENTIAL GENE EXPRESSION IN	111	
	PTOCOCCUS PNEUMONIAE FOLLOWING ASSOCIATION WITH MET-5A CELLS.	111	
4.3		121	
_	PTER 5 RESULTS - GENE EXPRESSION IN HUMAN PLEURAL MESOTHELIAI S FOLLOWING CHALLENGE WITH PNEUMOCOCCI	123	

5.1 ANALYSIS OF GENE EXPRESSION IN HUMAN PLEURAL MESOTE	HELIAL CELLS
FOLLOWING CHALLENGE WITH STREPTOCOCCUS PNEUMONIAE.	123
5.1.1 Differential gene expression in Met-5A cells infected with pneumococci-	-derived antigens. 130
5.1.2 Pathway analysis of differential human gene expression	137
5.2 Summary.	143
CHAPTER 6 DISCUSSION AND CONCLUSIONS	145
6.1 INTERACTIONS OF <i>STREPTOCOCCUS PNEUMONIAE</i> WITH PLEUF CELLS 145	RAL MESOTHELIAL
6.2 MICROARRAY ANALYSIS OF DIFFERENTIAL GENE EXPRESSION	N IN
$STREPTOCOCCUS\ PNEUMONIAE\ FOLLOWING\ ADHERENCE\ TO\ HUMAN$	PLEURAL
MESOTHELIAL CELLS.	156
6.3 GENE EXPRESSION IN HUMAN PLEURAL MESOTHELIAL CELLS	FOLLOWING
INFECTION WITH STREPTOCOCCUS PNEUMONIAE.	165
6.4 FUTURE WORK.	169
CHAPTER 7 REFERENCES	173

LIST OF FIGURES

Figure 1-1. Geographical burden of mortality caused by pneumococcal disease
Figure 1-2: Geographical distribution of incidence of pneumococcal disease
Figure 1-3 : A map of pneumococcal disease burden worldwide.
Figure 1-4: The anatomy of the lungs and pleura.
Figure 1-5: The microscopic anatomy of the pleura
Figure 1-6: An X-ray image showing empyema in a paediatric patient.
Figure 1-7: Pneumococcal serotypes isolated from children with uncomplicated versus complicated pneumonia
Figure 2-1 : Spectrophotometric analysis of bacterial and human RNA.
Figure 2-2: Agilent RNA Nano Chips used to assess the integrity and homogeneity of bacterial RNA 6
Figure 3-1 : Immunocytochemical characterisation of Met-5A cells
Figure 3-2: Negative capsule staining of Streptococcus pneumoniae.
Figure 3-3: Total association of pneumococci with human pleural mesothelial cells
Figure 3-4: Scanning Electron Micrographs of pneumococcal interactions with pleural mesothelial cells
Figure 3-5: Invasion of Met-5A cells by S. pneumoniae.
Figure 3-6: Lactate Dehydrogenase release from Met-5A cells following infection with S. pneumoniae
Figure 3-7: The pro-inflammatory response of Met-5A cells to pneumococcal infection
Figure 3-8: The anti-inflammatory response of Met-5A cells to pneumococcal infection
Figure 3-9: TNF- α – induced pro-inflammatory cytokine production in Met-5A cells
Figure 3-11 Stimulation of Met-5A cells with bacterially derived antigens
Figure 3-12: Investigation of the potential of pneumococci to degrade TNF-α in vitro

Figure 4-1: Analysis of bacterial RNA quality following disruption of Met-5A cells and pneumocoo	cci
using various methods of differential lysis.	07
Figure 4-2: Quantification of bacterial RNA following infection of 30x 75cm ² cell culture flask w	ith
pneumococci at an MOI of 250 bacteria/cell	08
Figure 4-3: Analysis and quantification of bacterial RNA following trypsin detachment	10
Figure 4-4: LOWESS normalisation was applied to bacterial microarrays to compensate	for
heterogeneity between slides and inherent experimental variability	12
Figure 4-5: Differentially expressed bacterial genes were identified by the application of a series	of
filtering algorithms to the data	13
Figure 4-6: Mean expression fold changes in pneumococcal genes which exhibited ≥ 2-fold different	tial
expression	15
Figure 5-1: Overlaid microarray scan images illustrating differential gene expression in human pleu	ral
mesothelial cells following infection with Streptococcus pneumoniae	24
Figure 5-2: Illustration of commonly expressed genes in Met-5A cells following challenge with live	or
heat-attenuated pneumococci, or pneumococcal lysates	35
Figure 5-3: Pathway analysis of differential gene expression in Met-5A cells following challenge with	S.
pneumoniae derived antigens1	41

LIST OF TABLES

Table 1-1 Summary of global IPD incidence and disease burden.
Table 1-2: Pneumonia-causing organisms. Error! Bookmark not defined.
Table 1-3: Serotypes included in pneumococcal vaccines
Table 1-4: Pneumococcal serotypes that cause invasive disease in children aged 5 years and under, listed
in decreasing order of prevalence for each geographical region
Table 1-5: Pneumococcal serotypes that cause invasive disease in children over 5 years of age and adults, listed in decreasing order of prevalence for each geographical region
Table 1-6: Empyema-causing pneumococcal serotypes, ranked in decreasing order of prevalence 29
Table 2-1: Antibodies used for the staining of cellular markers
Table 2-2: Streptococcus pneumoniae strains used in this study
Table 2-3: Primer pairs for RT-qPCR validation of differentially expressed pneumococcal genes 66
Table 3-1: The proportion of total bacteria adherent to Met-5A cell monolayers.
Table 3-2: Invasion of pneumococci as a proportion of total associated bacteria
Table 3-3: Inhibition of TNF-α-induced production of pro-inflammatory cytokines by Met-5A cells following pneumococcal infection
Table 4-1: Up-regulated pneumococcal genes following adherence to human pleural mesothelial cells
Table 4-2: Downregulated pneumococcal genes following adhesion to human pleural mesothelial cells
Table 5-1: Differential gene up-regulation in Met-5A cells following infection with D39 strain Streptococcus pneumoniae.
Table 5-2: Differential gene down-regulation in Met-5A cells following infection with D39 strair Streptococcus pneumoniae.
Table 5-3: Differential gene up-regulation in Met-5A cells following challenge with the lysate of D39
strain Streptococcus pneumoniae

Table 5-4: Differential gene down-regulation in Met-5A cells following challenge with the lysate of D39
strain Streptococcus pneumoniae
Table 5-5: Differential gene up-regulation in Met-5A cells following infection with S1-H strain
Streptococcus pneumoniae. 129
Table 5-6: Differential gene down-regulation in Met-5A cells following infection with S1-H strain
Streptococcus pneumoniae
Table 5-7: Differential gene up-regulation in Met-5A cells following challenge with the lysate of S1-F
strain Streptococcus pneumoniae
Table 5-8: Differential gene down-regulation in Met-5A cells following challenge with the lysate of S1-
H strain Streptococcus pneumoniae
Table 5.0: Differential came up regulation by Mot 5.4 calls following shallongs with heat attenuates
Table 5-9: Differential gene up-regulation by Met-5A cells following challenge with heat-attenuated
D39 strain Streptococcus pneumoniae
Table 5-10: Differential gene down-regulation by Met-5A cells following challenge with heat-attenuated
D39 strain Streptococcus pneumoniae
Table 6-1: List of known virulence determinants of Streptococcus pneumoniae. 158

DECLARATION OF AUTHORSHIP

I, C	laire Jane Heath
dec	lare that the thesis entitled
The	pathogenesis of pleural empyema caused by Streptococcus pneumoniae
	the work presented in the thesis are both my own, and have been generated by me as the result of my original research. I confirm that:
•	this work was done wholly or mainly while in candidature for a research degree at this University; where any part of this thesis has previously been submitted for a degree or any other qualification at this University or any other institution, this has been clearly stated; where I have consulted the published work of others, this is always clearly attributed; where I have quoted from the work of others, the source is always given. With the exception of such quotations, this thesis is entirely my own work; I have acknowledged all main sources of help; where the thesis is based on work done by myself jointly with others, I have made clear exactly what was done by others and what I have contributed myself; none of this work has been published before submission.
Sign	ned:
Dat	e:

CHAPTER 1 INTRODUCTION

1.1 The Biology of Pneumococcal disease

1.1.1 Disease Burden

Pneumococcal disease kills over 1.6 million people globally each year, and between 700,000 and 1 million of these are children under five years of age, making *Streptococcus pneumoniae* the single largest killer of young children, accounting for 11% of deaths in children (O'Brien *et al.* 2009)

Of all deaths attributable to pneumococcal disease, more than 98% occur in developing countries, and in fact, just 10 countries in Asia and sub-Saharan Africa account for around 60% of all pneumococcal deaths world wide, as outlined in the most comprehensive meta-analysis of recent years (O'Brien *et al.* 2009) (Figure 1-1).

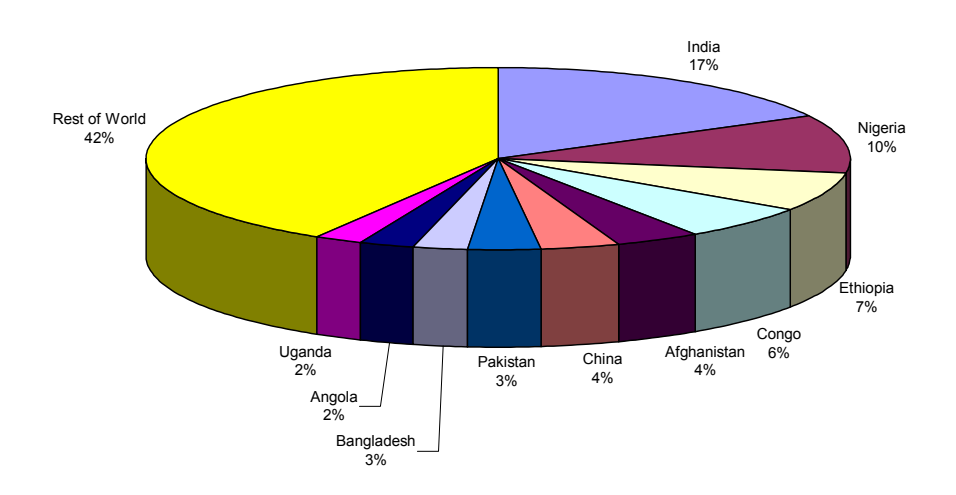


Figure 1-1. Geographical burden of mortality caused by pneumococcal disease

Data adapted from epidemiological data presented by (O'Brien et al. 2009)

Moreover, this enormous global disease burden is likely to be a gross underestimate, due to the limited availability and performance of diagnostic tests and limited access to care and treatment facilities.

A comprehensive meta-analysis performed by O' Brien and colleagues estimated that there were 14.5 million cases of pneumococcal disease annually worldwide. Disease incidence however, varied greatly geographically, ranging from 188-6387 cases per 100,000 children <5 years old and again, just 10 countries accounted for over 60% of the total number of cases of pneumococcal disease worldwide (Figure 1-2), of which seven were included in those countries with the highest number of pneumococcal deaths.

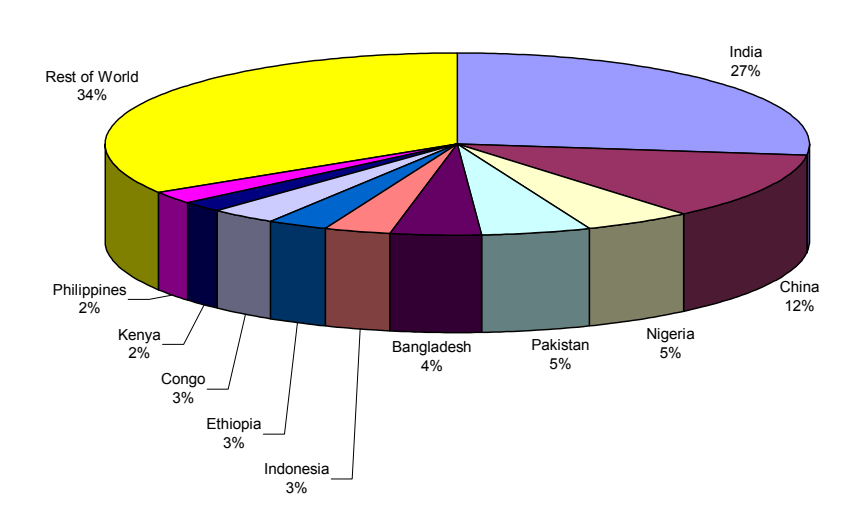


Figure 1-2: Geographical distribution of incidence of pneumococcal disease

Africa has the highest overall incidence rate of pneumococcal disease and also the highest rate of pneumococcal mortality (Figure 3), although Asia has the greatest number of cases in absolute numbers, due to the larger population. The burden of pneumococcal disease is lowest in Europe, each in terms of number of cases, relative incidence rate and also rate of mortality. Death rate is defined as the number of people per 100,000 of the population to die from a given cause, whereas case fatality rate (CFR) is the proportion of deaths within a population of people with a particular condition. These epidemiological data are summarised in Table 1-1.

	Global	Africa	Americas	Eastern Mediterranean	Europe	S.E. Asia	Western Pacific
Total							
No. of cases	14,500,000	4,060,000	713,000	1,510,000	260,000	5,480,000	2,430,000
Incidence rate	2331	3627	920	2358	504	2991	1842
Mortality rate	133	399	43	156	29	102	33
No. of deaths	826,000	447,000	33,100	100,100	15,100	187,000	43,700
• HIV +ve	91,300	88,300	500	800	100	1400	200
• HIV– ve	735,000	359,000	32,600	99,300	15,000	186,000	43,600
Pneumonia							
No. of cases	13,800,000	3,810,000	648,000	1,450,000	23,800	5,330,000	2,340,000
Incidence rate	2228	3397	836	2264	462	2911	1775
No. of deaths	741,000	406,000	24,300	92,100	13,000	169,000	36,500
Death Rate	119	362	31	144	25	92	28
CFR	5%	11%	4%	6%	5%	3%	2%
Meningitis							
No. of cases	103,000	43,100	9500	9700	3300	24,200	13,100
Incidence rate	17	38	12	15	6	13	10
No. of deaths	60,500	31,700	4500	5500	1300	13,700	3700
Death Rate	10	28	6	9	3	7	3
CFR	59%	73%	48%	57%	38%	57%	29%
Other IPD							
No. of cases	538,000	215,000	55,400	50,500	18,600	122,000	76,100
Incidence rate	87	192	71	79	36	67	58
No. of deaths	25,200	9500	4300	2500	800	4700	3500
Death Rate	4	8	6	4	2	3	3
CFR	45%	58%	37%	44%	29%	44%	22%

Table 1-1 Summary of global IPD incidence and disease burden.

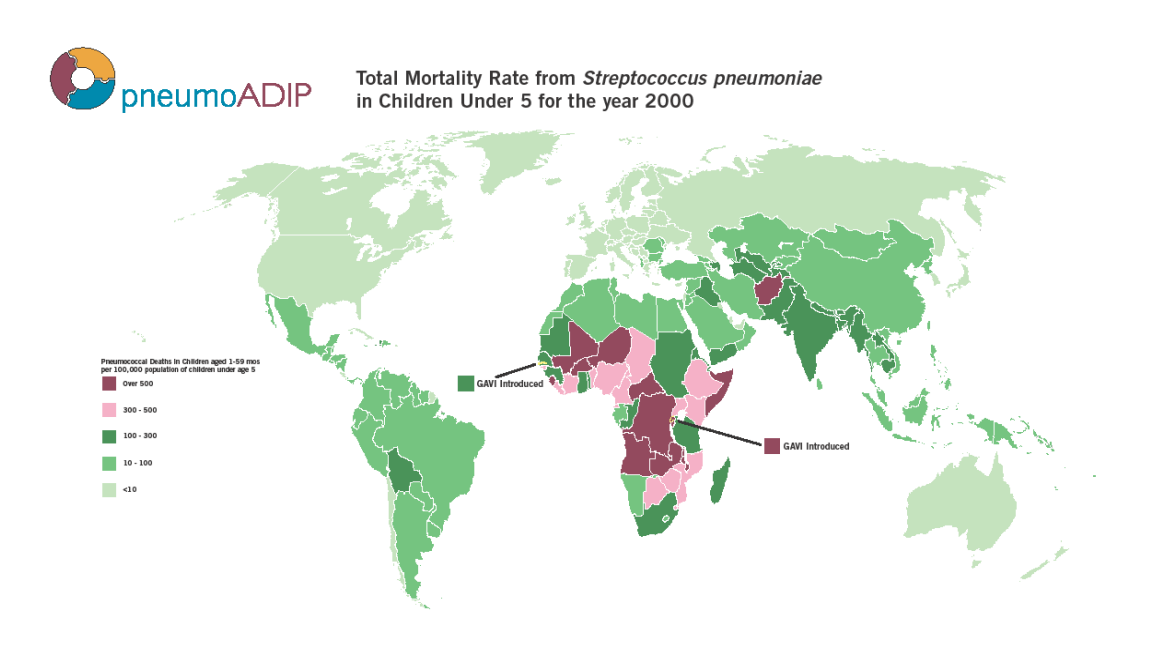


Figure 1-3: A map of pneumococcal disease burden worldwide

http://www.preventpneumo.org/datatools/upload/pcv_wo_intro_status_10.pdf

In the developed world, pneumococcal disease burden occurs disproportionately in children under the age of 2 years and the elderly. In addition, some ethnic populations, including Native American Indians, Alaskan indigenous populations and Australian Aboriginals, are at much higher risk (Black 2008; Langley *et al.* 2008). In the UK, 5000-6000 cases of invasive pneumococcal disease are reported to the Health Protection Agency (HPA) annually (Kaye 2008).

1.1.2 Risk Factors

Several risk factors contribute to the heavy burden of pneumococcal disease in the developing world. The coincident prevalence of other diseases such as such as HIV and sickle cell anaemia increase the risk of infection, with HIV-infected children 20-40 times more likely to acquire pneumococcal disease((APPG) 2008). In 2000, an estimated 826,000 deaths occurred in children aged under-5 years old as a result of pneumococcal disease, of whom 91,300 were HIV-positive (Table 1-1) The prevalence of overcrowding and malnutrition in developing countries further increases the risk of disease.

In developed countries, risk factors for pneumococcal disease include extremes of age, underlying co-morbidities such as chronic cardiovascular disease and asthma. In addition, a correlation has been reported between increased disease risk and several lifestyle factors including cigarette smoking, excessive alcohol consumption and high BMI (Feldman and Anderson 2009)

1.1.3 Invasive pneumococcal diseases

Invasive pneumococcal disease (IPD) is clinically defined as the isolation of bacteria from a normally sterile site (McDonald 2011). Some of the specific manifestations of IPD are described below.

1.1.3.1 Pneumonia

Pneumonia is the leading cause of death in children worldwide, killing an estimated 1.8 million children every year, accounting for 20% of all deaths in children under 5 years of age (WHO 2007). There are approximately 155 million cases of childhood pneumonia every year, (WHO 2009) and although it affects people everywhere, it is most prevalent in South Asia and sub-Saharan Africa.

Streptococcus pneumoniae is the most common cause of pneumonia worldwide, causing approximately 36% of all pneumonias in children((APPG) 2008). However, pneumonia can be caused by a number of infectious agents, including viruses, fungi and bacteria, as summarised in Table 1-2.

Bacteria	Streptococcus pneumoniae		
	Haemophilus influenzae		
	Staphylococcus aureus		
	Less commonly		
	Mycoplasma pneumoniae		
	Chlamydia pneumoniae		
	• Legionella pneumophila		
Viruses	Respiratory Syncytial Virus (RSV)		
	Varicella Zoster Virus		
	Influenza types A and B Viruses		
Fungi	Pneumocystis jiroveci		

Table 1-2: Pneumonia-

causing organisms.

1.1.3.2 Bacteraemia/Septicaemia

S. pneumoniae can infect the bloodstream after entering the body (bacteraemia) and cause blood poisoning (septicaemia). If this occurs, bacteria can be transported to numerous organs, most notably to the membranes surrounding the brain, the meninges, where it can cause life threatening meningitis.

1.1.3.3 Meningitis

Meningitis, inflammation of the membranes surrounding the brain and spinal cord, in particular, the arachnoid and the pia mater, is the most life threatening form of invasive pneumococcal disease. Most cases occur in babies and children under 18 months of age.

The epidemiology of bacterial meningitis has changed dramatically in the last 20 years. Before a remarkably successful vaccination campaign, *Haemophilus influenzae* was a major cause of meningitis. Currently however, pneumococci are the most important cause of bacterial meningitis in children and adults in the US and Europe and mortality is greatest in this form (Hoffman and Weber 2009). However, the most

common meningitis-causing pathogen in developed countries is *Neisseria meningitidis* (meningococci).

The global incidence of pneumococcal meningitis is around 17 per 100,000 children with an estimated 103,000 cases in 2000 (O'Brien *et al.* 2009). In the UK, in 2007, there were approximately 200 reported cases of pneumococcal meningitis (HPA, 2008).

Symptoms include headache, fever, lethargy, photosensitivity, stiff neck and vomiting. Rapid diagnosis and treatment is essential, as even in developed countries where appropriate treatment and supportive care is available, the mortality rate from pneumococcal meningitis is around 20% (APPG, 2008). In the developing world, this proportion is around 50%, even amongst hospitalised patients.

Additionally, 25-50% of survivors may develop neurological sequelae, including hearing loss, blindness, speech difficulties and other significant motor and cognitive impairments, due to damage to various areas of the brain and nerves.

1.1.3.4 Otitis Media

Otitis media (infection of the middle ear) is the most common manifestation of pneumococcal disease. It affects infants and young children, with a peak in incidence in the 6-18 month age group. In the USA, two-thirds of children have had an episode of otitis media by 12 months of age, and more than 80% by the time they are 3 years old. *Streptococcus pneumoniae* accounts for 30-50% of cases of acute otitis media, while *Haemophilus influenzae* causes around 15-30% of infections, and *Moraxella catarrhalis* represents 5-15% of cases (Durbin 2004)

Most children who develop pneumococcal otitis media recover completely, although some develop chronic otitis media (fluid in the middle ear) which can impair hearing and potentially lead to deafness.

1.1.4 Seasonality of Pneumococcal Disease

The observation that the incidence of pneumococcal infections increase every winter has been documented by several investigators (Talbot et al. 2005). Although this phenomenon remains to be fully explained, seasonality has been attributed to various factors including cold weather, photoperiod, crowding together of susceptible hosts, decreases in humidity, increases in associated viral infections and air pollution. In the USA, one study describes a distinctly seasonal pattern of pneumococcal disease, increasing from approximately 10 cases per 100,000 of the population during the summer to around 35 cases per 100,000 of the population during the winter (Dowell et al. 2003). More specifically, in adult cases, a peak in the rate of pneumococcal infections to between 50-75 cases per 100,000 was observed during the last week of December and the first week of January in each of the study years. These investigators also showed that there was a significant correlation between incidence of pneumococcal disease and temperature (p<0.0001) and also minutes of darkness (p<0.0001). The correlation between pneumococcal disease and precipitation, however, was poor. Paradoxically, Alaska one of the coldest states, did not have an elevated disease rate and also did not display the consistent seasonal variation that was observed in all of the other US surveillance sites.

1.1.5 Anatomy and function of the lungs and pleura

The lungs are a pair of cone shaped organs located in the thoracic cavity either side of the heart. Each lung is divided into lobes by fissures, with three lobes in the right lung and two in the left. The right lung is thicker and wider than the left lung and because the diaphragm muscle is higher on the right side, and because of the location of the liver below it, the right lung is slightly shorter than the left. In humans, the trachea divides into the two main bronchi that enter at the root of each lung. The bronchi continue to divide within the lung and, after multiple divisions, give rise to terminal bronchioles which lead to alveolar sacs. Alveolar sacs are comprised of clusters of alveoli. The individual alveoli are surrounded by capillaries and it is here that gas exchange actually occurs. Deoxygenated blood is pumped through the pulmonary artery to the lungs, where oxygen diffuses into the bloodstream and is exchanged for carbon dioxide in the haemoglobin of erythrocytes. The newly oxygenated blood

returns to the heart via the pulmonary vein to be pumped back into systemic circulation (Figure 1-4) (Jantz and Antony 2008)

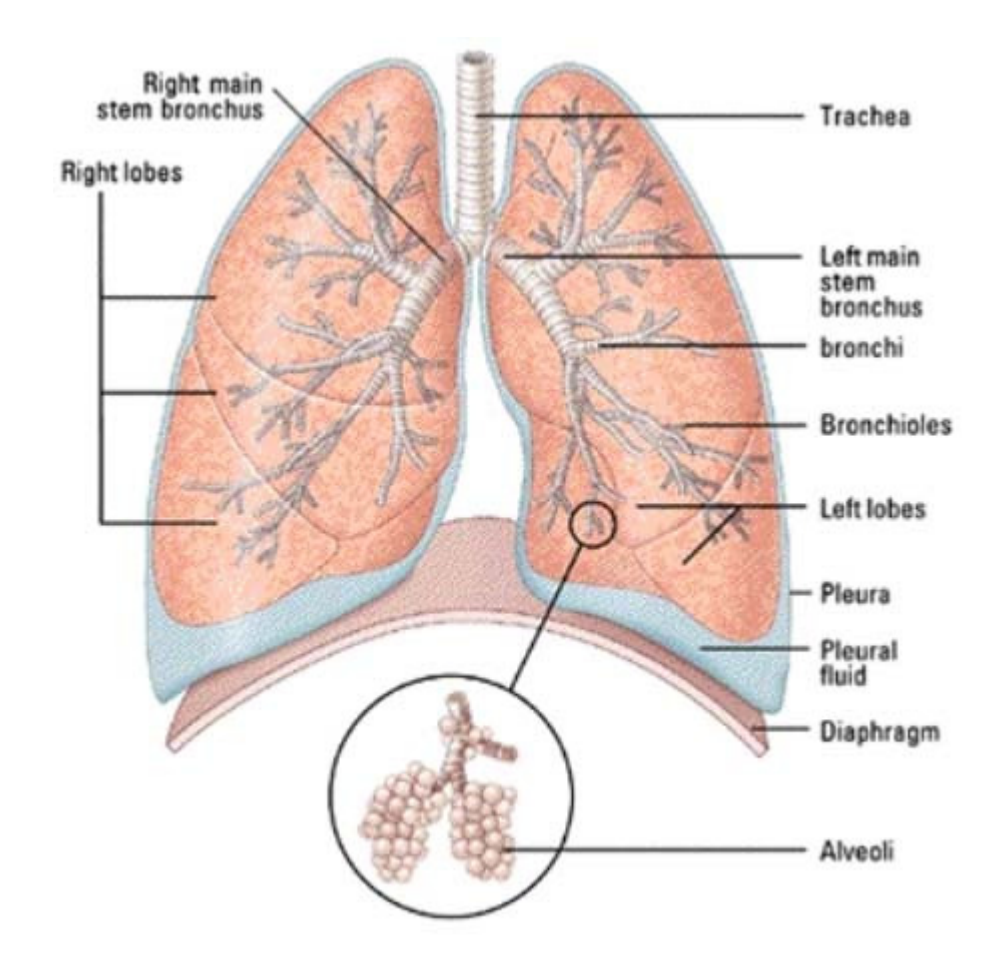


Figure 1-4: The anatomy of the lungs and pleura.

http://howardhughes.trinity.duke.edu/uploads/assets/image/lungs.jpg.

1.1.5.1 The pleurae

In human anatomy, the lungs are surrounded by two mesodermally derived serous membranes called the pleurae, which are each approximately $30\text{-}40\mu m$ thick. These serve to reduce friction generated by the expansion and deflation of the lungs during the respiratory cycle, which creates movement between the lung surface and the chest wall.

The parietal pleura lines the chest wall, diaphragm, thoracic apex and mediastinum, while the visceral pleura is tightly attached to the lung, and the membranes meet at the hilum (lung root) where the major airways and pulmonary vessels penetrate. The space between the two membranes is termed the pleural cavity, which is moistened by a film of serous fluid and maintained at around 10-20µm across. In humans the right and left pleural cavities are entirely separated from each other and from the mediastinum and the pericardial cavities.

The pleurae are each composed of a monolayer of mesothelial cells that loosely overlie a basement membrane. The connective tissue of the pleural basement membrane is a complex network of capillaries, originating from the bronchial arterial vessels, and lymphatic connections which drain into the mediastinal, intercostal and sternal lymph nodes (Jantz and Antony 2008) (Figure 1-5). It is the accumulation of fluid here during infection (pleural effusion), that can eventually lead to empyema.

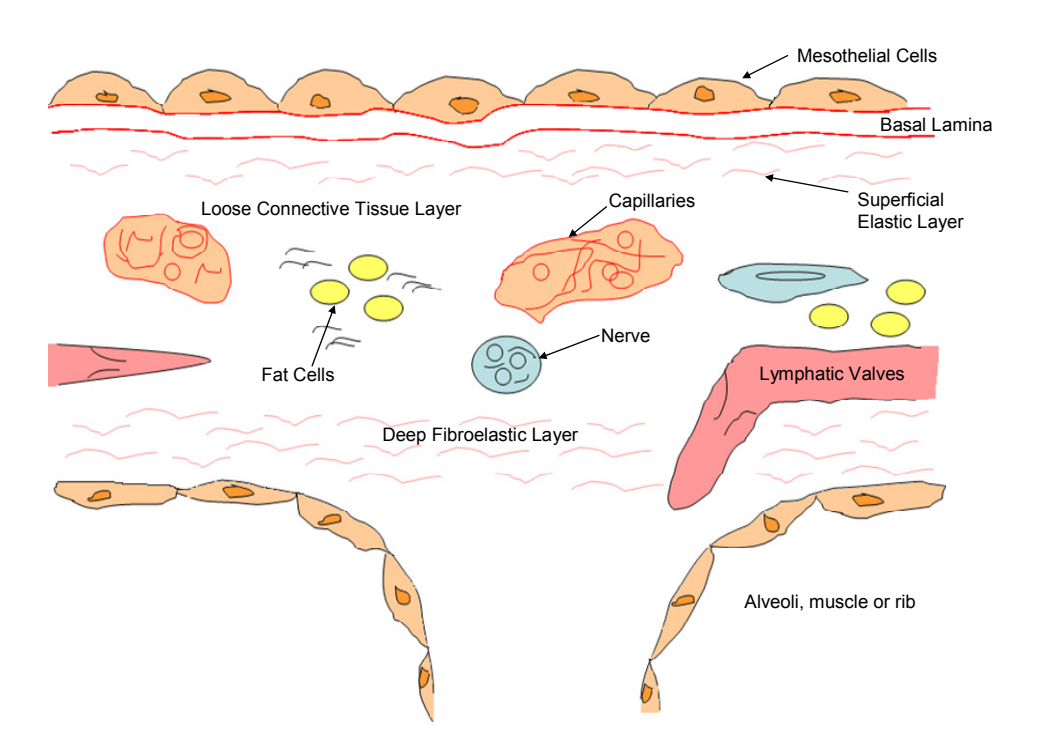


Figure 1-5: The microscopic anatomy of the pleura

1.1.5.1.1 Pleural Mesothelial Cells

Mesothelial cells form the monolayer mesothelium which covers the connective tissue at the basal lamina of the pleura. These cells adhere to one another at their apical side, which when *in situ* is oriented into the pleural space, via tight junctions, with intermediate and desmosome junctions also occasionally present. However, at the basal surface, cells are more loosely associated and are not attached to each other, allowing them to stretch and slide over each other during respiratory movements.

These cells have been shown to exhibit heterogeneous morphologies regionally, and may appear flattened or cuboidal (Michailova *et al.* 1999) with individual cell size ranging from 16.4±6.8 to 41.9 ±9.5μm in diameter and from < 1 to 4μm thick. However, no differences have been found between cells composing the visceral and parietal pleura (Wang 1974). Mesothelial cell nuclei are ovoid with prominent nucleoli. The abundance and thickness of the cytoplasm may vary, but consistently contains mitochondria and rough and smooth endoplasmic reticulum. Metabolic activity is also evidenced by the presence of Golgi apparatus, polyribosomes, intermediate fibrils and glycogen granules (Chretien J 1985).

Microvilli are present diffusely yet irregularly on the surface of mesothelial cells. Each microvillus is approximately 0.1µm in diameter and between 3-6µm in length. The microvilli are thought to play a key role in the formation and absorption of the lubricating film of pleural fluid, since pinocytic vesicles are often seen in association with microvilli (Andrews and Porter 1973).

1.1.5.1.2 Normal physiology of pleural fluid

Pleural fluid is secreted by the parietal pleura, originating from the systemic circulation. Its reabsorption occurs mainly through lymphatic drainage, again exclusively on the parietal pleural side. Fluid passes between the small capillaries of the parietal pleura and the pleural cavity, according to the net hydrostatic-oncotic

pressure. Movement of fluid between the pleural cavity and the lung interstitium is restricted by the presence of intercellular tight junctions as previously described.

In humans, the volume of pleural fluid is 0.26 ± 0.1 ml/kg of bodyweight and contains approximately 1.7×10^3 cells/ml. This number is comprised of approximately 75% macrophages, 23% lymphocytes, less than 3% polymorphonuclear cells and approximately 2% free mesothelial cells (Noppen *et al.* 2000).

1.2 Parapneumonic Effusions and Empyema

1.2.1 What is Empyema?

Strictly defined, empyema is the presence of pus in the pleural cavity in association with underlying pneumonia. It is an advanced stage of the continuum of parapneumonic effusion that occurs following pleural infection.

1.2.2 Classification of parapneumonic effusions

Parapneumonic effusion and empyema are stages of a spectrum of pleural disease, and are best defined by the staging of the pleural fluid associated with infection (Balfour-Lynn *et al.* 2005)

- Exudative: characterised by the accumulation of fluid in the pleural cavity, with a low white cell count, without the presence of loculations (simple parapneumonic effusion).
- Fibropurulent: fibrin is deposited in the pleural space, which gives rise to loculations. White cell count is increased and pleural fluid thickens (complicated parapneumonic effusion), eventually becoming pus (empyema).
- Organisational: the pleural cavity is infiltrated by fibroblasts, and the intrapleural membranes thicken and lose elasticity. Organised pleural loculations may be present, which can cause lung entrapment and impair function.

In an attempt to help guide management, Hamm and Light added another stage that precedes the exudative stage, which they termed the "pleuritis sicca" stage (Hamm and Light 1997), characterised by inflammation of the pleura which manifests as chest pain and pleural rub, although this does not necessarily progress to the exudative stage. These investigators also assigned reference pH and lactate dehydrogenase levels to each stage of pleural effusion to aid diagnosis and therapy.

1.2.3 Clinical incidence

Parapneumonic effusions are common, and often expected, complications of bacterial pneumonia, occurring in over 40% of cases (Balfour-Lynn *et al.* 2005). In adults, empyema develops in approximately 5% of patients with bacterial pneumonia, while the incidence in children hospitalised with pneumonia has been reported to be around 0.6%. One study in the USA reported the 'attack rate' of empyema to be 10.3% (Byington *et al.* 2002), which is much higher than had been previously reported in either adults or children.

The incidence of empyema in children is increasing and although the mortality rate is very low, it is associated with significant morbidity. This increasing incidence of paediatric empyema was first reported in the West Midlands, UK, in 1997 (Rees et al. 1997), and the trend has since been confirmed throughout the UK, Europe and North America (Playfor et al. 1997; Byington et al. 2002; Gupta and Crowley 2006; Langley et al. 2008; Spencer and Cliff 2008), occurring in 3.3 per 100,000 children (Hardie et al. 1996). In fact, over the duration of the Byington et al. study from 1993 to 1999, the incidence of paediatric empyema as a complication of pneumonia increased 5-fold, from 1 per 100,000 to 5 per 100,000 of the population aged less than 19 years. Similarly, Gupta and Crowley reported an increase from 14 per million to 26 per million in paediatric admissions for pyothorax between 1995 and 2003, with the increase most prominent in 1-4 year olds (Gupta and Crowley 2006). A Canadian study by Finley et al., found an alarmingly disproportionate increase of 463% in empyema in children aged 1-4 years, compared to an overall increase of 12.4% in the general population (Finley et al. 2008). Although it has not been definitively proven, some studies suggest that empyema is more prevalent in males than females (Gupta and Crowley 2006).

1.2.4 Aetiology

The epidemiology of empyema has changed significantly since the discovery and use of antibiotic agents with different spectra of activity for treating pneumonia. In the 1940s, *Streptococcus pneumoniae* and group A streptococci were the most common causative agents of pleural empyema, until the widespread introduction of penicillin and sulphonamides resulted in a decline in these supporative complications of pneumonia. In the 1950s, *Staphylococcus aureus* was the prevalent organism linked with empyema. However, the advent of penicillinase-resistant penicillins in the 1960s brought about a decrease in pneumonia caused by *S. aureus* and, by the 1980s, *Haemophilus influenzae* type b had emerged as a prevalent causative organism.

However, differences in inclusion/exclusion criteria, pleural sampling and bacterial culture techniques, have rendered much of the historical data unhelpful. Furthermore, understanding the aetiology of empyema has been hindered by the fact that, in most cases, routine bacterial culture is negative, presumably due to the administration of antibiotics before sample collection. However, the advent of molecular techniques, such as polymerase chain reaction (PCR), has identified *Streptococcus pneumoniae* as currently the most common causative organism of empyema in the USA (Byington *et al.* 2002) and also in the UK (Eastham *et al.* 2004). Eastham *et al.* implicated *S. pneumoniae* as the causative pathogen in 31 out of 36 cases of pneumonia (Eastham *et al.* 2004)

1.2.5 Pathophysiology

In healthy adults, the pleural space contains 0.3ml/kg body weight of pleural fluid. The circulation of this fluid is finely balanced by its secretion and absorption by lymphatic vessels in the parietal pleura, at a rate of approximately 0.02-0.1ml/kg/hr. However, these lymphatics are able to cope with several hundred millilitres of additional fluid per 24hrs, and so it is only when an imbalance in pleural fluid formation and drainage occurs that a pleural effusion may result (Miserocchi 1997).

Under normal physiological conditions this fluid has a very low protein concentration (0.1g/l), and contains only a small number of cells (up to 100cells/µl), which are predominantly lymphocytes. However, during infection, increased vascular

permeability facilitates the influx of pathogens and their toxins into the pleura. Here, pathogens interact with the mesothelial cells that line the pleural space, and stimulate them to release various cytokines, including interleukin-1 (IL-1), IL-6, IL-8, tumour necrosis factor-α (TNF-α) and platelet activating factor (Quadri and Thomson 2002) resulting in the migration of various immune cells such as lymphocytes, neutrophils and eosinophils to the pleura. In addition, these inflammatory mediators further increase the permeability of local capillaries, exacerbating fluid accumulation. Activation of the coagulation cascade results in a decrease in fibrinolysis, and thus the deposition of fibrin in the pleura, which causes the thick "rind" formation and loculations seen in empyema (Jaffé and Balfour-Lynn 2005).

1.2.6 Signs and Symptoms

Children with a parapneumonic effusion/empyema usually present with clinical manifestations of bacterial pneumonia: cough, dyspnoea (shortness of breath), tachypnoea (rapid shallow breathing), fever, lethargy and pleuritic chest pain.

1.2.7 Diagnosis

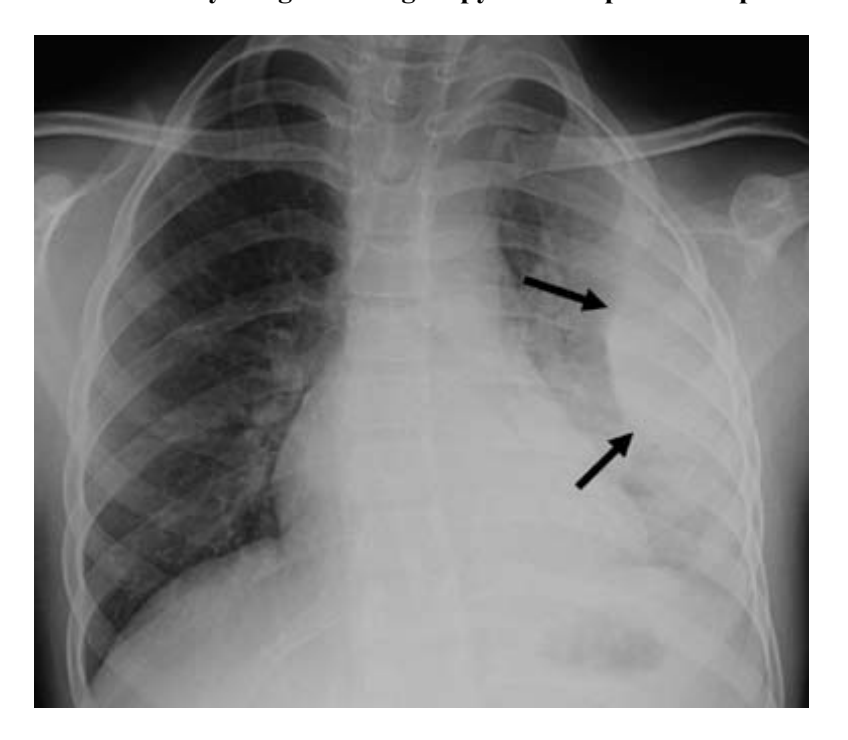
1.2.7.1 Physical Examination

Parapneumonic pleural effusion/empyema is suggested by a unilateral decrease in chest wall expansion, dullness to percussion and reduced or absent breath sounds (Balfour-Lynn *et al.* 2005; Jaffé and Balfour-Lynn 2005; Ampofo *et al.* 2008).

1.2.7.2 Chest Radiography

Patients with suspected pleural effusion initially undergo a chest X-ray to confirm the presence of pleural fluid and to exclude other conditions, such as underlying malignancy. However, radiographs alone cannot differentiate between empyemas and parapneumonic effusions.

Figure 1-6: An X-ray image showing empyema in a paediatric patient.



The image shows a radiograph of a complicated parapheumonic effusion in a child, with arrows indicating a loculation resulting from pus formation and fibrin deposition. Image reproduced with authors permission (Calder and Owens 2009).

1.2.7.3 Ultrasound

Chest ultrasonography is used to detect the presence of fluid in the pleural cavity. It is also useful in detecting fibrous strands and fluid loculations, and in determining the size of the effusion.

1.2.7.4 Computerised Tomography

The role of CT scanning in diagnosing empyema, particularly in paediatrics is controversial, due to the relatively high levels of radiation. The presence of pleural thickening and fluid in the pleural cavity can be detected by ultrasound, thus the British Thoracic Society (BTS) guidelines recommend that CT scans are not performed routinely, but in cases where there are atypical empyema presentations *e.g.* underlying tumour or lung abscess (Balfour-Lynn *et al.* 2005)

1.2.7.5 Blood Tests

- **Blood Cultures** Blood cultures are often negative in empyema patients, due to prior treatment with broad range antibiotics. However, samples are sent for culture in order that the causative organism maybe identified and any antibiotic resistance is detected. Antimicrobial therapy can then be tailored to the case accordingly.
- Full Blood Counts Initial blood cell counts in empyema patients often reveal anaemia, leucocytosis and thrombocytosis in response to the initial infection
- Acute Phase Reactants. C-reactive protein and erythrocyte sedimentation rate (ESR) are usually markedly elevated at presentation. Although these parameters are unable to distinguish viral from bacterial disease, serial measurements may be helpful in monitoring patient progress.

1.2.7.6 Pleural Fluid Analysis

In all cases of empyema, it is imperative that pleural fluid is sent for microbiological analysis, so that a causative organism maybe identified. However, the yield of bacterial culture of pleural fluid is low ($\sim 60\%$). It is thought that this reflects effective antimicrobial therapy prior to sample collection, although other postulations include the presence of biofilms in the pleura, the suggestion that the continued presence of bacteria is not necessary for the ongoing inflammatory response following the initial invasion, and lack of sensitivity of conventional culture techniques (Brims *et al.* 2010). Alternative non-culture techniques such as specific and broad range PCR and latex agglutination testing may improve rates of identification.

In adults, biochemical analysis of the pleural fluid, in particular lactate dehydrogenase (LDH), glucose and pH measurements, plays an important part in the management of pleural effusions. However, the BTS guidelines suggest that biochemical analysis does not alter the management of paediatric empyema and so should not be routinely performed in children.

1.2.8 Management

1.2.8.1 General

The overall objective of empyema treatment is to control infection and reestablish normal pleural circulation, thus restoring normal lung function. In order to minimise morbidity, basic supportive measures can be taken to maintain good oxygen saturation (>92%) and hydration. Administration of antipyretics and analgesia will also relieve symptoms.

1.2.8.2 Antibiotics

Most parapneumonic effusions will respond dramatically to antimicrobial chemotherapy and supportive care, and may not require any further intervention (Quadri and Thomson 2002; Sonnappa and Jaffe 2007).

Antibiotic choice for the treatment of empyema is largely guided by local policy, reflects whether the effusion is secondary to community-acquired or nosocomial pneumonia, and is dependent on the child's immune status. Generally, broad-spectrum agents are used in the first instance to ensure adequate removal of S. pneumoniae. Although penicillin-resistance is increasing in general, most serious disease-causing strains of S. pnemoniae in the UK are still susceptible to penicillin (Davies et al. 2003). The British Thoracic Society (BTS) guidelines suggest intravenous treatment with amoxicillin, co-amoxiclay or cefaclor in children under 5 years of age (Davies et al. 2003). Patients with penicillin allergy may be treated with clindamycin, and children older than 5 years may be prescribed an oral macrolide such as erythromycin to also provide cover against Mycoplasma pneumoniae and Fusobacterium due to the increased prevalence of these organisms in older children. An antistaphylococcal agent such as flucloxacillin may also be included if Staphylococcus aureus is suspected as a causative agent, and is mandatory if pneumatoceles (thin-walled, gas-filled spaces within the lung) are observed. Where pulmonary aspiration is a risk or there is a history of thoracic surgery, metronidazole maybe included in the treatment regimens to cover anaerobes. Where possible, antimicrobial treatment should be guided by microbiology results, and consultation of local microbiologists may be of value in areas where antibiotic resistance is an issue.

1.2.8.3 Thoracentesis

In adults, thoracentesis is routinely performed in order that biochemical analysis of the pleural fluid may guide management, However, this procedure often requires sedation or anaesthesia and so is not recommended for children (Jaffé and Balfour-Lynn 2005).

1.2.8.4 Chest Tube Drainage

Chest tube drainage has long been used in the treatment of pleural effusions. Small soft pig-tail catheters are inserted under local anaesthetic and light sedation, and the pleural fluid/pus is drained.

1.2.8.5 Fibrinolytics

The formation of fibrin associated with empyema results in the formation of loculations of pus and fluid making chest tube drainage difficult. The intrapleural instillation of fibrinolytic agents, such as urokinase, streptokinase and tissue plasminogen activator, lyses fibrous strands and clears lymphatic pores, thus facilitating drainage.

1.2.8.6 Surgery

Patients for whom medical management of empyema has failed, will require surgical intervention (Balfour-Lynn *et al.* 2005). The surgical options are:

- Open decortication surgical removal of the thickened fibrous pleura and pyogenic material and direct irrigation of the pleural cavity. This is a long and complex procedure that leaves a large scar along the rib line.
- Mini-thoracotomy an open debridement procedure performed through a smaller incision
- Video Assisted Thoracoscopic Surgery (VATS) this procedure is a thorascopic decortication performed through three ports made in the chest. One port is used for insertion of the camera, and the others for surgical instruments. Interest in the use of VATS as a primary treatment for paediatric empyema has increased over the last decade, with proponents citing that compared to

conventional surgery, VATS limits damage to the skin, nerves and muscle, and minimises the risk of post-operative infection and cosmetic scarring

Despite the increasing incidence of paediatric empyema, there is little consensus on the best management approach, due to the lack of evidence from properly controlled clinical trials. Treatment largely depends on local policy and practice, the availability and preferences of thoracic surgeons and, particularly in the case of VATS, the availability of equipment and personnel properly trained in its use.

1.3 Streptococcus pneumoniae

Streptococcus pneumoniae (the pneumococcus) is a Gram-positive anaerobe of the genus Streptococcus. It is identifiable by its production of α -haemolysis on blood agar, bile solubility and its inhibition by ethyl hydrocupereine (optochin). The organism is usually observed as pairs of cocci (diplococci), although they may occur as single cocci or in short chains. Individual cells are $0.5-1.25\mu m$ in diameter and are non motile.

1.3.1 Cultivation

Pneumococci are fastidious organisms, growing best at 5% carbon dioxide. Around a fifth of fresh clinical isolates require fully anaerobic conditions and in all cases a source of catalase is required for growth, to neutralise the large quantities of hydrogen peroxide produced by the bacteria. In complex media containing blood, at 37°C, the pneumococcus has a doubling time of 20-30 minutes.

On blood agar, colonies characteristically produce a zone of α (green) haemolysis. This differentiates pneumococci from group A streptococcus which are β -haemolytic, but not from other commensal α -haemolytic viridans streptococci. Therefore, diagnostic tests routinely employ tests such as inulin fermentation, bile solubility and optochin sensitivity to differentiate the pneumococcus from *Streptococcus viridans*.

Pneumococci undergo spontaneous phase variation, switching between transparent and opaque phenotype. While the transparent variant is adapted to nasopharyngeal colonisation, the opaque colony type is more adept to survival in the blood.

1.3.2 The History of the Pneumococcus

In 1881, Streptococcus pneumoniae was simultaneously and independently isolated by U.S Army physician George Sternberg (Sternberg 1881) and French chemist Louis Pasteur (Pasteur 1881). Both researchers injected human saliva into rabbits; Pasteur using the saliva from a child that had died of rabies, and Sternberg using his own saliva, and subsequently recovered diplococci from the blood of these rabbits, thus demonstrating the pathogenic potential of these organisms in animals. The organism was named Microbe septicemique du salive by Pasteur and Micrococcus pasteuri by Sternberg and in 1886 Fraenkel referred to this organism as the Pneumococcus due to its propensity to cause pulmonary disease (Fraenkel 1886). In 1920, the organism was redesignated Diplococcus pneumoniae due to the pairs of cocci seen in association with pneumonia (Winslow 1920). It was not until 1974 that Streptococcus pneumoniae was given its present name (Deibel 1974) primarily due to its characteristic growth as chains of cocci in liquid media.

1.3.3 Pneumococcal Serotyping

Streptococcus pneumoniae is classified into 93 immunologically distinct sero<u>types</u> (Calix and Nahm 2010), each producing a polysaccharide capsule which is unique in its biochemical composition. Those strains that exhibit antibody cross-reactivity, due to antigenic similarities such as shared saccharides, are then categorised within the same sero<u>group</u>, of which there are 46.

The quellung (swelling) reaction, devised by Neufeld (Neufeld 1902), forms the basis of serotyping and relies on the "swelling" of the capsule upon binding of homologous antibody. In fact, this reaction is the result of an *in situ* immunoprecipitation leading to a change in the refractory index of the capsules and thus their opacity. The reliability and reproducibility of the Quellung reaction has meant that it is still the gold standard test used for pneumococcal serotyping today. However, the labour-intensiveness, high cost of specific antisera, subjectivity in

interpretation and technical expertise required, have driven the development of various more high-throughput typing technologies.

In 1970, Kirkman *et al.* described a method of bacterial agglutination to determine capsular phenotype. In this, serogroup-specific antibodies bound to pneumococci resulting in bacterial "clumping", visible by macroscopic inspection thus negating the requirement for a microscope (Kirkman *et al.* 1970). This technique was developed further by Kronvall and colleagues in 1973 (Kronvall 1973; Christensen 1975), whereby serogroup specific pneumococcal antibodies were conjugated by their Fc domains to the surface of formalin fixed *Staphylococcus aureus* via association with protein A on the staphylococcal surface. The binding of homologous pneumococci via the available antigen recognition (Fab) domains resulted in macroscopic coagglutination of the bacteria, which was readily visually discernable. In 1986, this coagglutination method was extended to allow determination of serotypes within serogroups (Smart 1986) and in 1993 the Statens Serum Institut in Denmark described a simplified "chessboard" method of serotype deduction using a series of antisera pools (Sorensen 1993).

The availability of conjugate vaccines has renewed scientific interest in pneumococcal capsular typing, since optimal vaccine formulation is based serotype prevalence data (Hausdorff *et al.* 2000) and constant population surveillance is necessary to assess vaccine efficacy (Whitney *et al.* 2003; Kaplan *et al.* 2004) and the degree of serotype replacement by non-vaccine types (Lipsitch 2000; Weinberger *et al.* 2011). The ever-increasing demand for rapid and reliable results has encouraged the development of more high-throughput molecular and multiplex typing techniques. In 2000, Park and colleagues reported the development of a latex-bead based flow-cytometric assay which could simultaneously distinguish between 15 of the most common serotypes isolated in clinical disease. This method used latex beads of various sizes and red fluorescent properties, which were coated with the polysaccharide of 1 of 15 serotypes. Beads were then incubated with the lysate of the pneumococcal isolate to be typed and a rabbit anti-capsule antibody pool, capable of binding all 15 of the serotypes. These antibodies bind preferentially to polysaccharide in the lysate, therefore, when the beads were washed to remove the lysate and the incubated with

fluorescence-conjugated anti-rabbit IgG, fluorescence would be inhibited on those beads where there had been a match between the serotype of the lysate and the serotype of the bead-bound polysaccharide (Park *et al.* 2000). This technology was subsequently extended by Yu *et al.* to accurately identify 36 serotypes, including closely related serotypes within a serogroup, with the authors implying that the method was thus universally applicable to all pneumococcal capsular types (Yu *et al.* 2008). However, flow-cytometry is an expensive technology and therefore several investigators have sought to employ more molecular techniques of serotype determination.

Genotypic characterisation of the pneumococcal capsule has been enabled by the description of the capsular loci sequences of the first 90 serotypes by Bentley *et al.* followed by the discovery and capsular sequencing of the 3 most recent pneumococcal serotypes (Bentley *et al.* 2006; Park *et al.* 2007; Jin *et al.* 2009; Calix and Nahm 2010). Methods of multiplex and sequential PCR have been designed that probe for serotype specific genes within the capsular synthesis locus (Brito *et al.* 2003; Pai *et al.* 2006) High sequence homology amongst some closely related serotypes however, resulted in cross-reactivity, for example between serotypes within serogroups 6 and 18 (Pai *et al.* 2006). This necessitated differentiation by conventional immunological techniques in these isolates, although the process was greatly streamlined.

1.3.4 History of Pneumococcal vaccines

In 1911, Wright *et al.* developed a crude, whole-cell heat-killed pneumococcal vaccine to immunise South African gold miners, who had an extremely high incidence of serious pneumococcal infections (Wright 1914). During the 1940's, controlled clinical trials were conducted on the safety and efficacy of bivalent, trivalent and quadrivalent vaccines (MacLeod 1945), which led to the commercial production of two hexavalent vaccines. However, the advent of penicillin reduced the urgency of research into pneumococcal disease prevention. Despite the substantial impact of antimicrobial drugs on the mortality of pneumococcal infection, Austrian and Gold Brooklyn, between 1952 and 1962 with a particularly high mortality rate in the elderly (Austrian 1964) This initiated research into and the development of polyvalent

polysaccharide vaccines (PPVs), and a 14-valent vaccine (PPV14) received licensure in the United States in 1977. This was replaced by a 23 valent vaccine (PPV23) which was licensed in the United States in 1983 and in the UK in 1992. The pneumococcal serotypes represented in these vaccines are shown in Table 1-3.

Vaccine	Serotypes Included
PPV14	1, 2, 3, 4, 6A, 7F, 8, 9N, 12F, 14, 18C, 19F, 23F, 25.
PPV23 (Pneumovax 23)	1, 2, 3, 4, 5, 6B, 7F, 8, 9N, 9V, 10A, 11A, 12F, 14, 15B, 17F, 18C, 19A, 19F, 20, 22F, 23F,
PCV-7 (Prevenar)	4, 6B, 9V, 14, 18C, 19F
PCV-13	1, 3, 4, 5, 6A, 6B, 7F, 9V, 14, 18C, 19A, 19F, 23F

Table 1-2: Serotypes included in pneumococcal vaccines

As discussed previously, rates of invasive pneumococcal disease are highest during the first 2 years of life. However, pneumococcal capsular polysaccharides are T-cell independent antigens that induce limited antibody responses in children under 2 years. Conjugation of polysaccharide antigens to carrier proteins renders the immune response T-cell dependent, leading to higher antibody titres in infants. In addition, memory B cells are produced and primed for "booster" responses in which high concentrations of specific antibodies are rapidly produced upon subsequent doses of vaccine (Butler *et al.* 1999).

The 7-valent pneumococcal conjugate vaccine (PCV7) contains the polysaccharide of serotypes 4, 6B, 9V, 14, 18C, 19F and 23F, reflecting the 7 most prevalent serotypes in the USA and Canada (Hausdorff et al. 2000). Polysaccharide antigens are conjugated to a non-toxic diphtheria variant carrier protein. This vaccine was licensed for use in the US in 2000 and in the UK in 2001, for use in children under 5 years of age in certain at-risk groups.

1.3.5 Nasopharyngeal Carriage of Pneumococci

S. pneumoniae is commonly carried asymptomatically as a commensal organism in the nasopharynx of healthy children. It is believed that carriage rates range from <10% during the first few weeks of life, to 100% within the first few years of life, and nearly all children have at least one episode of pneumococcal carriage during their early childhood (Sleeman et al. 2001). Certain pneumococcal serotypes are much more likely to be associated with nasopharyngeal carriage than with invasive disease, and these include most of the serotypes represented in the PCV-7 vaccine, with the exception of serotype 4. Members of serogroups 10, 11, 13, 15, 33 and 35 are also routinely isolated from carriage (Hausdorff et al. 2005)

1.3.6 Pneumococcal disease-causing serotypes

In the UK, prior to the introduction of PCV-7 into the routine childhood immunisation schedule, the most commonly isolated pneumococcal serotypes from the nasopharynx of children were the vaccine serotypes 6B, 9V, 19F, and 23F, the vaccine-related serotypes 6A and 19A, and the non-vaccine serotypes 3, 15 and 21 (Brueggemann and Spratt 2003). Notwithstanding the diversity of pneumococcal serotypes, only a small number are associated with the majority of invasive and non-invasive disease in children under 5 years of age (Clarke *et al.* 2004), although predominating serotypes may vary with time, age, geography and disease manifestation. A meta-analysis of more than 70 studies demonstrated that in each geographical region, less than 10 serogroups account for the majority of invasive disease (Hausdorff *et al.* 2000), and these are summarised in Tables 1-4 and 1-5 below.

Region	IPD-causing serotypes	
United States and Canada	14, 6B/A, 19F/A, 18C/B/F, 23F/B/A	
Europe	14, 6B/A, 19F/A, 18C/B/A/F, 23F/A/B, 9V, 4, 1	
Asia	1, 19F/A, 6B/A, 5, 14	
Africa	6B/A, 14, 1, 19F/A, 23F	
Latin America	14, 6B/A, 5, 1, 19F/A	
Oceania	14, 6B/A, 19F/A, 23F/B, 18C/A	

Table 1-3: Pneumococcal serotypes that cause invasive disease in children aged 5 years and under, listed in decreasing order of prevalence for each geographical region.

Region	IPD-causing serotypes
United States and Canada	4, 14, 9V/N/A, 6B/A, 12F/A
Europe	14, 3, 9V/N/A, 19F/A, 1
Asia	1, 3, 6B/A, 5, 19F/A
Africa	1, 19A, 14, 6A, 3
Latin America	1, 6B/A, 3, 18C/A, 12
Oceania	14, 4, 19F/A, 9V/N, 1

Table 1-4: Pneumococcal serotypes that cause invasive disease in children over 5 years of age and adults, listed in decreasing order of prevalence for each geographical region.

In children, serotype 14 is generally the most prominent serotype worldwide (Table 1-4), being accountable for approximately 20-25% of paediatric IPD on each continent, followed by serogroups 6 and 19; each responsible for 10-20% of disease

(Hausdorff 2007). In the UK, serotype 14 is responsible for up to 36.9% of all IPD in children <5 years of age (Clarke *et al.* 2006).

However, it should be noted that epidemiological data is scare from large areas of the world, particularly Eastern Europe, South East Asia and Africa. This is reflected in the serotype formulation of the heptavalent vaccine. Serogroups represented in PCV-7 are responsible for 90% of disease in young children in the USA and Canada and at least 60% of IPD in all other regions, except Asia where vaccine coverage is just 45% (Hausdorff *et al.* 2000). However, this may be largely attributable to the more substantial contribution of serotype 1 to IPD in these regions than in North America. In all regions, serotypes 1, 6, 14, 19 and 23 are amongst the most commonly isolated from paediatric IPD. In older children and adults, serotype 3 is also among the most prominent. The relative proportion of disease caused by these serotypes, and the contributions of other serotypes to disease burden however, varies between regions, and individual countries.

1.3.6.1 Pneumococcal Serotypes in bacteraemic pneumonia

Isolation of pneumococci from the blood allows identification of serotypes which are able to cause invasive (bacteraemic) pneumonias. Although the relative frequencies of the most prevalent serotypes varies between individual countries, serotypes 14, 1, 6 and 19 consistently account for at least 65% of bacteraemic pneumonias in all regions (Hausdorff and Dagan 2008). It should be noted that these findings cannot be extrapolated to non-bacteraemic pneumonias, due to the mucosal nature of their colonisation and invasion.

1.3.6.2 Pneumococcal Serotypes in complicated pneumonias and empyemas

When pneumococcal pneumonia is complicated by an empyema or a parapneumonic effusion, the aetiology can be determined by analysis of the pleural fluid, obtained by thoracocentesis. The microbiology of disease is assessed by culture and, more recently, by PCR (Saglani *et al.* 2005) and antigen detection (Fletcher *et al.* 2006).

Before the introduction of PCV7, several studies demonstrated that serotype 1 was the predominant serotype in complicated pneumonias and empyemas globally

(Eastham *et al.* 2004; Byington *et al.* 2006; Fletcher *et al.* 2006). A study in the United States has demonstrated that pneumococcal serotype 1 is responsible for a significantly larger proportion of infections in children with complicated pneumonia (24.4%) compared with patients with uncomplicated disease (3.6%) (Tan *et al.* 2002), as illustrated in Figure 4.

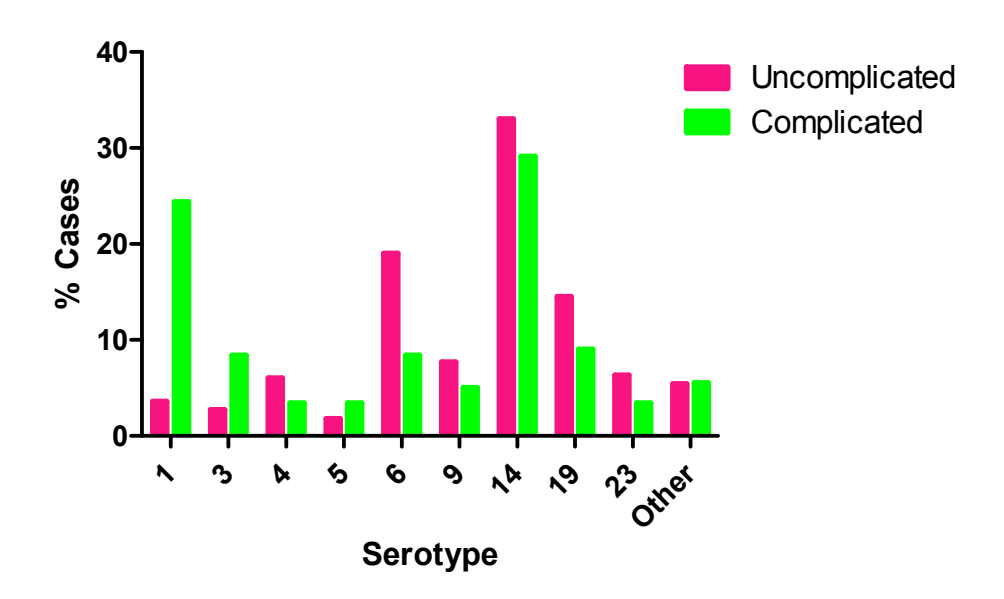


Figure 1-7: Pneumococcal serotypes isolated from children with uncomplicated versus complicated pneumonia.

Figure adapted from data presented by Tan et al. (Tan et al. 2002).

In the UK, serotype 1 has been implicated in at least 60% of empyemas (Eltringham *et al.* 2003) while in the United States, Hausdorff and Dagan reported that serotype 1 accounted for 46% of all empyemas (Hausdorff and Dagan 2008). This proportion decreased to 34% following the incorporation of the vaccine into the US immunisation schedule, although serotype 1 continued to predominate. In addition, the proportion of empyemas caused by the other non-vaccine serotypes 3 and 19A increased by 20% and 14% respectively and, during the course of the study, the total proportion of empyemas caused by non-vaccine serotypes increased from 63 to 83%. Similarly, studies in Spain (Obando *et al.* 2008) and France (Bekri *et al.* 2007), where

the introduction of PCV7 has been much less complete than in the US, have reported that serotype 1 is responsible for 50% and 52% of empyemas respectively.

Strikingly, despite its high propensity to cause invasive disease, serotype 1 is very rarely carried in the nasopharynx of children, nor is it the commonest serotype in overall invasive pneumococcal disease in the US or the UK (Eltringham *et al.* 2003). The results of these studies are summarised in Table 1-6 below:

Country	Empyema causing Serotypes	References
USA	1, 14, 9, 19, 18, 12, 29	Byington et al., 2002
		Tan <i>et al.</i> , 2002
UK	1, 14, 4, 3, 7F, 9V, 23F	Eltringham et al., 2003
		Fletcher et al., 2006
Spain	1, 3, 5, 14, 7F, 19A	Obando et al, 2008.
France	1, 3, 5, 6B, 7F, 9V, 14, 18C, 19A, 23F	Bekri <i>et al.</i> , 2007.

Table 1-5: Empyema-causing pneumococcal serotypes, ranked in decreasing order of prevalence.

Collectively, these data suggest that serotype 1 has a major role in complicated pneumonias, in both the pre- and post- vaccine environments. However, it is important to note that empyema due to serotype 1 appears to be limited to children over the age of 2 years, whereas serotypes 14 and 19A are the most common in younger children (Hausdorff and Dagan 2008).

1.3.6.3 Effect of PCV-7 on pneumococcal antibiotic resistance

Pneumococcal resistance to antibiotics complicates treatment choices and can lead to treatment failure, thus increasing disease morbidity and medical costs. The epidemiology of antibiotic resistance however, varies notably between continents and individual countries. In Europe, high resistance rates in pneumococci have been

reported in Spain, France and Eastern-European countries, whereas other regions such as Germany and the more Northern European countries are only marginally affected (Imohl *et al.* 2010). At the time of PCV-7 introduction in the United States, approximately 24% of pneumococcal isolates from invasive disease were resistant to penicillin, and 5 of the 7 serotypes included in the PCV-7 vaccine (6B, 9V, 14, 19F and 23F) accounted for 89% of all penicillin-resistant isolates of *S. pneumoniae* (Richter *et al.* 2009).

Following vaccine introduction, a 78% decrease in invasive paediatric disease caused by vaccine serotypes was reported by Whitney *et al.* (Whitney *et al.* 2003). By 2004, 73% of US children had received at least 3 of the recommended 4 doses of PCV-7, and the incidence of invasive disease caused by penicillin resistant pneumococci decreased by 81% (Kyaw *et al.* 2006). Thus the reduction in disease caused by antimicrobial resistant pneumococci has also been attributed to the conjugate vaccine. However, the increase in the rate of infection by non-vaccine "replacement strains", particularly by serotype 19A, has become apparent and is of obvious ongoing concern.

1.3.7 Pneumococcal Virulence Factors

For many years, the virulence of *Streptococcus pneumoniae* was attributed to the antiphagocytic properties of its polysaccharide capsule. However, numerous studies have now shown that certain other pneumococcal proteins play important roles in the pathogenesis of disease, either as mediators of inflammation, or by interacting directly with host tissues to facilitate pneumococcal colonisation and invasion.

1.3.7.1 The Polysaccharide Capsule

The polysaccharide capsule is a predominant feature of *Streptococcus pneumoniae* and is required for full pathogenicity of the organism (Nelson *et al.* 2007b). The importance of the capsule to the virulence of the pneumococcus results from its ability to inhibit opsonophagocytosis via electrostatic mechanisms. Capsular polysaccharide exerts a highly negative charge and so stearically inhibits the interactions between the complement receptor CR3 on phagocytes and the complement component C3b, and between the Fcγ receptors to the Fc region of IgG fixed to the pneumococcus (van der Poll and Opal 2009). Although unencapsulated mutant strains

have been shown to adhere better to epithelial cells in the nasopharynx (Morona *et al.* 2006), they very rarely cause invasive disease, probably due to their increased susceptibility to complement-mediated phagocytosis (Preston and Dockrell 2008). Unencapsulated strains are also highly attenuated in *in vitro* models of infection (Brown *et al.* 1983). A critical step in the pathogenesis of invasive disease is the ability of pneumococci to adapt to the diverse environments it encounters, for example the nasopharynx and the bloodstream. This is achieved by the phenomenon of spontaneous phase variation, during which the genes that encode for capsular polysaccharide are switched on and off. Downregulation of capsule expression results in a transparent phenotype, and these variants exhibit an increased ability to adhere to buccal cells (Weiser *et al.* 1994; Cundell *et al.* 1995b). By contrast, opaque capsule-expressing variants are better adapted for invasion since the antiphagocytic activity of the capsule is required to evade host immune defences once the pneumococcus has traversed the epithelium (Weiser *et al.* 1994).

1.3.7.2 Surface proteins

The surface of the pneumococcus bears a range of surface proteins that play specific roles in disease pathogenesis. These proteins can either be covalently anchored to the cell wall via the Gram-positive attachment motif (LPXTG), or be attached noncovalently via interaction with cell wall teichoic acid phosphorylcholine residues (choline-binding proteins, Cbps). Some of these Cbps include:

1.3.7.2.1 Choline-binding protein A (CbpA)

Pneumococcal adherence to host cells is the essential first step in colonisation and infection. CbpA is a 75kDa polypeptide and is a predominant constituent in mixtures of Cbps isolated from pneumococci (Jedrzejas 2001). This protein promotes adhesion to host cells by interacting with the polymeric immunoglobulin receptor on secretory IgA (Graham and Paton 2006) and may also impair the protective function of the antibody. Like other Cbps it has a C-terminal repeat region, consisting of 10, 20-amino acid repeats, which is responsible for attachment of the protein to teichoic acid choline residues. The functional N-terminal module binds to human cell

glycoconjugates, thus the molecule acts as a bridging unit between pneumococci and the host and it has been suggested that CbpA is responsible for up to 50% of the adherence of pneumococci to nasopharyngeal cells (Rosenow *et al.* 1997). However, this interaction is restricted to cytokine-activated cells suggesting that this process is involved in advancing pneumococcal disease from colonisation to invasion.

1.3.7.2.2 Pneumococcal surface protein A (PspA)

PspA is a pneumococcal surface protein with a variable molecular weight, ranging from 67-99kDa (Waltman *et al.* 1990) and is present on every strain of *S. pneumoniae*. This protein serves as a protective antigen for pneumococci, by preventing the activation of the host complement system (Tu *et al.* 1999). Structural studies have shown that PspA is a highly polar electrostatic molecule. The electropositive end of the molecule serves to stabilise the electronegative pneumococcal capsule, while the electronegative part of the molecule prevents complement activation and deposition (Jedrzejas 2001). In turn, this reduces complement-mediated clearance and phagocytosis of pneumococci during infection. Furthermore, a study by Graham and Paton suggested that expression of PspA suppressed the CXC chemokine response of respiratory epithelial cells, and may be a further means by which *Streptococcus pneumoniae* evades the host response (Graham and Paton 2006).

1.3.7.2.3 Autolysin

Autolysin (LytA) is a 36kDa cell wall degrading enzyme which is localised to the cell envelope of the pneumococcus. It is bound to choline moieties of lipoteichoic acid, which is anchored to the cell membrane, and in this conformation autolysin is inactive. However, in circumstances where cell wall biosynthesis ceases, such as nutrient starvation or penicillin treatment, the association of the enzyme with lipoteichoic acid is disrupted and autolysin is activated. The enzyme cleaves the covalent bond between the glycan chain and the peptide side-chain of the cell wall resulting in autolysis of the bacterial cell (Briese and Hakenbeck 1985). Cell wall degradation products, such as teichoic acid and peptidoglycan, are released into the periphery, causing local inflammation. In addition, the autolytic action of the enzyme contributes to

pneumococcal virulence by releasing other active intracellular components such as pneumolysin.

1.3.7.3 Pneumococcal enzymes

1.3.7.3.1 Pneumolysin

The 53-kDa polypeptide pneumolysin is a well-characterised pneumococcal virulence factor, which is expressed by virtually all clinical isolates of S. pneumoniae (Paton 1996). This enzyme is located in the cytoplasm of pneumococci and is dependent on the action of autolysin for its release. It is a member of the thiol-activated cytolysin family of toxins which bind to cholesterol in eukaryotic cell membranes resulting in the insertion of the toxin into the lipid bilayer. Lateral diffusion and oligomerisation of 20-80 of these toxin molecules into a ring structure results in the formation of transmembrane pores which induce cell lysis (Paton 1996). Recent studies have also highlighted other non-cytolytic activities of pneumolysin including its ability to activate complement, which limits the opsonisation of pneumococci by the classical pathway (Preston and Dockrell 2008)

1.3.7.3.2 Neuraminidases

The *S. pneumoniae* genome encodes 3 neuraminidase enzymes, NanA, NanB and NanC. NanA and NanB are present in all pneumococcal strains and have molecular masses of ~108kDa and ~75kDa respectively (Jedrzejas 2001). These enzymes cleave terminal sialic acid residues from a wide variety of glycolipids, glycoproteins, mucins and oligosaccharides on host cell surfaces or in bodily fluids and thus have the potential to cause extreme damage to host tissues. In addition, such changes in host glycosylation patterns may expose further surface receptors for potential interaction with pneumococci, leading to increased adhesion (Krivan *et al.* 1988). More recently, NanA expression by pneumococci has been reported to also contribute to nasopharyngeal colonisation and subsequent spread to the lung of mice (Orihuela *et al.* 2004).

1.3.7.3.3 Hyaluronidase

Hyaluronidase is an enzyme produced by the pneumococcus, which degrades the hyaluronic acid component of host connective tissue. This facilitates translocation of pneumococci between tissues, for example from the lung to the pleura. Hyaluronidase-deficient mutants have been shown to have a decreased capacity to invade the blood stream in an animal model of pneumonia when compared to wild-type pneumococci (Mitchell 2006), demonstrating the important role played by hyaluronidase in invasive disease.

1.3.7.3.4 Superoxide dismutase (SOD)

The pneumococcus contains two types of superoxide dismutase, FeSOD and MnSOD. These are metalloenzymes that catalyse the conversion of superoxide molecules into hydrogen peroxide and oxygen. As well as enabling the anaerobic pneumococcus to cope in the *in vivo* oxygenic environment, these enzymes also protect the bacterium from the oxidative killing mechanisms of neutrophils (Yesilkaya *et al.* 2000).

It is also possible that pneumococci produce other virulence factors similar to those produced by other pathogenic streptococci. *Streptococcus pyogenes* produces specific proteases that degrade CXC chemokines, thus impairing bacterial clearance from infected tissues (Hidalgo-Grass *et al.* 2006) and it has been shown that *S. pyogenes* and *S. pneumoniae* share homology in the streptococcal invasion locus (sil) (Claverys and Havarstein 2002).

The exact contribution of any of the known pneumococcal virulence factors, and of others as yet uncharacterised, to empyema is yet to be fully elucidated.

1.4 Immunity to the pneumococcus

As with all bacteria, the host's first line of defence against pneumococcal infection is the innate immune system, which is comprised of such non-specific defences as mucocilliary clearance, complement, and neutrophils and macrophages. These primary defence mechanisms are essential for the prevention and impedence of pneumococcal disease.

1.4.1 Complement

The contributions of complement system conponents to host immunity against pneumococcal infection pertains to their role in neutrophil chemotaxis, opsonisation of the microbial surface and bactericidal activity via formation of the membrane attack complex (Paterson and Orihuela 2010).

The significance of complement to the human anti-pneumococcal response is evidenced by the recurrent infections suffered by people with genetic complement deficiencies (Paterson and Mitchell 2006). Studies performed in knockout mice deficient for specific complement components has also elucidated that it is the classical pathway of complement activation that is dominant in the innate response to the pneumococcus. The cascade is triggered by recognition of capsular teichoic acid by natural IgM antibodies, as well as activation by acute-phase proteins such as C reactive protein and also the direct binding of the component C1q to the pneumococcal surface (Brown *et al.* 2002).

The fact that pneumococci possess elaborate complement evasion mechanisms indicates the importance of the complement system to the innate response to pneumococci. The major pneumococcal virulence factor, the polysaccharide capsule, largely exerts its pathogenic effects by protecting the bacterium from complement-mediated opsonophagocytosis via mechanisms previously described in Section 1.3.7.1. In addition, the lytic protein pneumolysin has been shown to activate the classical complement pathway in the absence of specific antibodies to the toxin (Mitchell *et al.* 1991). Yutse and co-workers demonstrated that deletion of the gene encoding pneumolysin resulted in an increase in opsonophagocytic clearance of pneumococci via the classical complement pathway (Yutse *et al.* 2005). These investigators proposed that the complement cascade is activated by pneumolysin secreted distally, thus reducing the amount available for bacterial binding. Furthermore, increased complement activation may contribute to host tissue damage, thereby facilitating pneumococcal invasion.

1.4.2 Toll-like Receptors

The best characterised of the germline encoded pathogen recognition receptors (PRRs) are the family of Toll-like receptors (TLRs), which provide early recognition of highly conserved microbial antigens. At least 10 TLRs have been characterised in humans, with each recognising a unique ligand repertoire (Janeway and Medshitov 2002), some of which are implicated in the innate response to pneumococci (Paterson and Orihuela 2010).

TLR2 binds pneumococcal lipoteichioc acid and cell wall peptidoglycan and other lipoproteins (Schwander *et al.* 1999). Studies in TLR2 knoockout mice in models of meningitis, septicaemia and pneumonia have shown increased susceptibility to pneumococcal disease than wildtype mice (Echchannaoui *et al.* 2005; Knapp *et al.* 2004; Koedel *et al.* 2003). TLR4 is a key component of the innate immune response against Gram-negative infections due to its recognition of bacterial lipopolysaccharide (LPS). However Malley *et al.* demonstrated that the proinflammatory effect of pneumolysin on macrophages *in vitro* was TLR4 dependent, (Malley *et al.* 2003) and Srivastava *et al.* subsequently showed that pneumolysin interacts directly with this receptor (Srivastava *et al.* 2005). These researchers found that in addition to TLR-mediated inflammation, the ligation of pneumolysin and TLR4 induced host cell apoptosis both *in vitro* and *in vivo*, which appeared to be a protective host response.

The unmethylated cytosine-phosphate-guanosine (CpG) motifs present in bacterial DNA are recognised by TLR9 (Bauer *et al.* 2001). the autolytic nature of the organism also renders the interaction between the liberated bacterial DNA and TLR9 of likely importance during pneumococcal infection.

The roles of TLRs 1 and 6 in the host defence against pneumococci are less well defined. Both of these receptors have been shown to dimerise with TLR2, with TLR2/6 and TLR1/2 heterodimers recognising diacylated and triacylated lipoproteins respectively (Schenk *et al.* 2009).

The transduction pathway through which TLRs signal has been well described (Akira and Takeda, 2004). Ligand binding to a TLR generates a signal via recruitment of the adaptor molecule MyD88, which leads to intracellular association with IL-1

receptor-associated kinase 4 (IRAK4) and thereby the subsequent association and phosphorylation of IRAK1. In turn, TNF receptor-associated factor 6 (TRAF6) is recruited to the receptor complex by association with phosphorylated IRAK1. Phosphorylated IRAK1 and TRAF6 then dissociate from the receptor to form a complex with TGF-β-activated kinase 1 (TAK1) and TAK1-binding protein 1 (TAB1) and TAB2 at the membrane, thereby inducing the phosphorylation of these proteins. At the membrane, IRAK1 is degraded and the remaining complex then translocates to the cytosol where it associates with ubiquitin ligases. This leads to the ubiquitilation of TRAF6, thus inducing the activation of TAK, which subsequently phosphorylates both mitogen-activated (MAP) kinases and the inhibitor of nuclear factor-κB (IκB)-kinase (IKK) complex. The IKK complex rapidly phosphorylates IkB, leading to its ubiquitylation and subsequent degradation. This finally permits the nuclear translocation of nuclear factor-κB (NF-κB). NF-κB is a potent transcription factor which activates the promoters of the genes for a broad range of cytokines and proinflammtory peptides such as TNF-α, IL-1, IL-6 and IL-8. This stimulation of cytokine production by TLRs is a key event in the recruitment of other important components of the host's innate immune system.

1.4.3 Nucleotide binding and Oligomerisation Proteins

In addition to the TLRs, other PRRs have been more recently identified as innate microbial sensors, notably, the Nucleotide Binding and Oligomerisation (NOD) proteins, including Nod1, Nod2 and ice-protease activating factor (IPAF). These intracellular cytosolic receptors are characterised by a tripartite structure, composed of a C-terminal LRR domain, a central NOD domain, and an N-terminal caspase and recruitment domain (CARD) and recognise highly conserved bacterial peptidoglycan molecules.

Peptidoglycan (PG) is a cell wall component, common to nearly all bacteria except *Mycoplasma*, which provides shape and mechanical rigidity to the organisms. PG is composed of polysaccharide chains of alternating *N*-acetylmuramic acid and *N*-acetylglucosamine crosslinked linked by pentapeptides. The nature of the third residue in the pentapeptide is an important feature in bacterial PG. In most Gram-negative

bacteria this residue is a meso-diaminopimelic acid (DAP), whereas lysine is found in the third position in Gram-positive organisms (Giarardin *et al.* 2003). During the course of the bacterial life cycle, PG is constantly degraded by specific hydrolases and resynthesised with newly incorporated subunits to enable biological processes such as cell division (Carneiro *et al.* 2007). This biosynthetic process releases small muropeptides into the periphery and it is these molecules which constitute the minimum unit for NOD recognition (Chedid, 1983), although Nod1 and Nod2 recognise different moieties of these PG degradation products. Specifically, the ligand for Nod2 is muramyl dipeptide (MDP) which is conserved in the PG of both Grampositive and Gram-negative bacteria, thus both can be detected by Nod2 (Giarardin *et al.* 2003; Inohara *et al.* 2003). In contrast, Nod1 has narrow specificity, binding only DAP type PG from Gram-negative bacteria (Giarardin *et al.* 2003).

Ligation of NOD receptors has been shown to induce NF-κB-dependent transcription of inflammatory mediators (Opitz *et al.* 2004) and also pyroptosis; a caspase-1-dependent form of cell death which is highly inflammatory (Bryan and Fitzgerald 2009; Chen *et al.*, 2009).

1.4.4 Recognition of the Polysaccharide Capsule

The pneumococcal polysaccharide capsule is recognised by other PRRs present on various components of the innate immune system. The C-type lectin SIGN-related 1 (SIGN-R1) is expressed on the surface of macrophages, and has been demonstrated to bind purified capsular polysaccharide as well as to whole bacteria, promoting their uptake (Kang *et al.* 2004). In addition, SIGN-R1 activates the classical complement pathway via the binding of the component C1q, promoting C3 deposition on the pneumococcus.

Scavenger receptors are a diverse family of glycoproteins which are primarily expressed on the surface of macrophages, dendritic cells and endothelium (Murphy *et al.* 2005). The scavenger receptors- Macrophage Receptor with Collagenous Structure (MARCO) and SR-AI/II expressed on alveolar macrophages have been demonstrated

to mediate uptake of pneumococci (Arredouani *et al.* 2006) although the bacterial motifs recognised by these receptors is yet to be elucidated.

The key PRRs involved in the innate innume response against the pneumococcus are illustrated in Figure

Figure 1.8 Key Pathogen Recognition Receptors involved in the innate recognition of *Streptococcus pneumoniae*

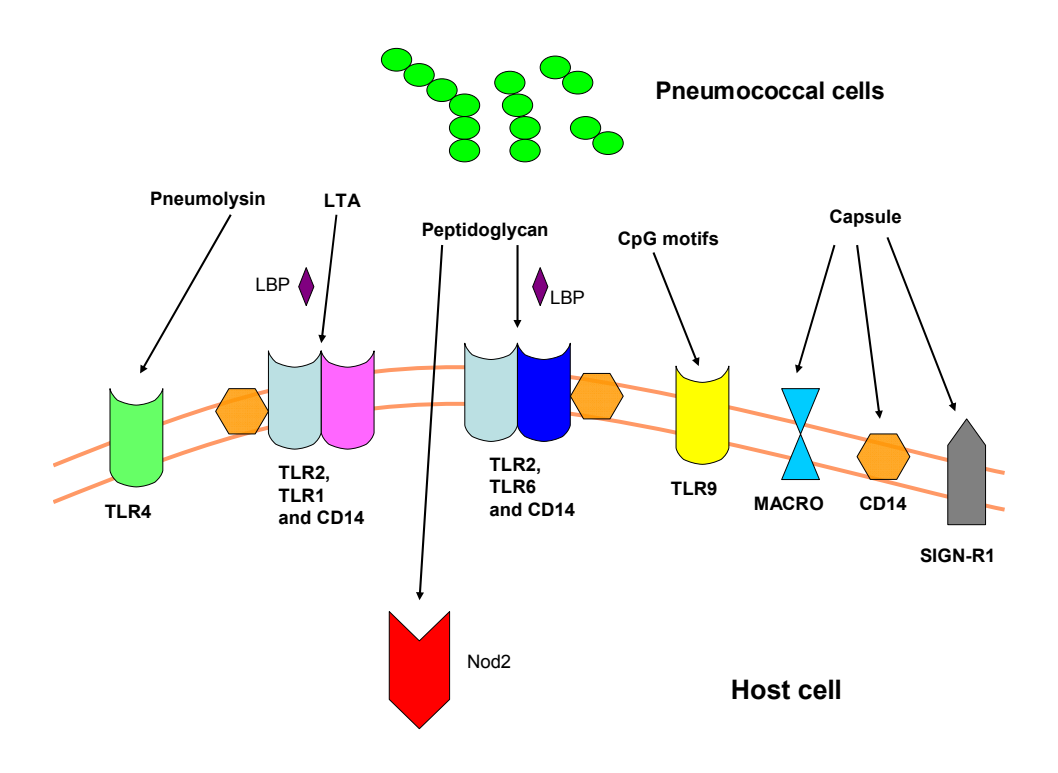


Figure adapted from Paterson and Mitchell (2006).

1.5 Hypotheses and Objectives

As discussed previously, epidemiological data on the incidence of invasive pneumococcal disease demonstrate differences between pneumococcal strains in their propensity to cause disease, although the molecular mechanisms which account for these differences are not well understood. Although the functions of several individual pneumococcal virulence factors have been characterised (as described in Section 1.3.7), the importance of these genes specifically to the manifestation and pathogenesis of empyema is unknown. It is the proposal of the current study that the pathogenesis of empyema is multifactorial to which both bacterial and host factors contribute, and the following hypotheses will be tested: that,

- 1. strains of *Streptococcus pneumoniae* isolated from clinical empyema patients express factors which facilitate the adhesion to and invasion of pleural cells and thus will exhibit qualitative and quantitative differences in their interactions with a human pleural mesothelial cell line, when compared to reference strains.
- 2. pneumococcal strains deficient in key virulence factors will have a decreased capacity to adhere to, invade and cause cytotoxicity to pleural cells.
- 3. human pleural mesothelial cells play a role in initiating the innate immune response to pneumococcal infection, via the production of pro-inflammatory cytokines and chemokines.
- 4. upon interaction with human pleural mesothelial cells *in vitro*, pneumococci will differentially regulate genes necessary for interaction with cells of the pleura and the manifestation of empyema.
- 5. the transcriptional response of human pleural mesothelial cells will differ following infection with empyema-causing pneumococcal isolates when compared to the response to reference strains.

CHAPTER 2 MATERIALS AND METHODS

All experimental procedures involving the handling of pathogens and cell lines were conducted in accordance with ethically approved local standard operating procedures in class II cabinets. Unless otherwise stated, all incubations were in a humidified incubator at 37° C and 5% (v / v) CO₂ (Labheat Incubator, Borolabs, UK).

2.1 General Reagents

Distilled water was produced by reverse osmosis using a euRO40 system (Triple Red Ltd., Thame, UK) and then further purified to $18.0 \text{m}\Omega$ -cm with a NANOpure DIamond ultrapure system (Barnstead-Thermolyne, Iowa, USA) to yield ultra high quality (UHQ) water.

Phosphate buffered saline (PBS) tablets (Oxoid, Basingstoke, UK) were dissolved in UHQ to give a buffer of pH 7.3.

Both water and PBS were sterilised by autoclaving at 2.68kg/cm² at 121°C for 15 minutes before use.

Foetal calf serum (Lonza, Belgium) was decomplemented (dFCS) prior to use by heating to 56°C for 1 hour in a waterbath, and stored at -20°C.

2.2 Characterisation of Human Pleural Mesothelial Cell Line

2.2.1 Culture and passage

The human pleural mesothelial cell line Met-5A was purchased from LGC Standards UK (ATCC–CRL-9444). These were originally established by transfecting normal human pleural mesothelial cells with a plasmid containing Simian virus (SV40) early region DNA, and they express SV40 large T antigen.

Materials:

Complete Growth Medium: Medium 199 containing Earles' balanced salt

solution (BSS), glutamine, 4-(2-hydroxyethyl)-1-

piperazineethanesulphonic acid (HEPES) and

sodium carbonate (Lonza, UK), supplemented

with 10% (v / v) dFCS, 3.3nM epidermal growth

factor (EGF), 870nM insulin and 400nM

hydrocortisone (all from Sigma-Aldrich, UK).

Trypsin EDTA: Hanks' Balanced Salt Solution containing

0.5mg/ml and 0.2mg/ml

ethylenediaminetetraacetic acid (EDTA) (Lonza,

UK).

Storage Medium: Complete growth medium containing 10% (v/v)

dimethyl sulphoxide (DMSO) (BDH, UK).

Initially, Met-5A cells were cultured in complete growth medium in 75cm^2 cell culture flasks (Greiner BioOne, UK) and passaged at $\approx 90\%$ confluence. Cells were washed twice in PBS, then incubated with 1ml of trypsin EDTA (Lonza) for 5 minutes at room temperature to detach cells. Growth medium ($\sim 8\text{ml}$) was then added to the cell culture flask to deactivate the trypsin and the cell suspension transferred to a sterile universal and centrifuged at 500g for 5 mins (Damon/IEC Ltd., UK). The pellet was then suspended in 10ml of fresh medium, and the suspension then diluted according to requirements and transferred into sterile cell culture flasks or cell culture plates.

2.2.2 Cryopreservation

For long term storage, Met-5A cells were isolated from a confluent monolayer grown in a 75cm² flask as described in Section 1.2.1. The pellet was suspended in 5ml of storage medium, then 1ml aliquots were transferred to cryovials (Alpha Laboratories, UK). Vials were stored at -80°C overnight before being transferred to liquid nitrogen for long term storage at -196°C.

2.2.3 Resuscitation of cryopreserved cells

Cryopreserved cells were resuscitated by rapid thawing of the cryovial at 37°C in a water bath. The contents were diluted in growth medium and centrifuged at 300g for 3 minutes to aggregate cells. The supernatant was then discarded to remove DMSO, and the pellet suspended in fresh growth medium and seeded into a 75cm² cell culture flask.

2.2.4 Immunocytochemistry of cellular markers in cultured human pleural mesothelial cells

Human pleural mesothelial cells were immunocytochemically characterised by Simsir *et al.* who demonstrated that the expression of cytokeratin along with E-cadherin and calretinin could aid the distinction of pleural cells from other cell types of mesothelial origin (Simsir *et al.*, 1999). Thus the cell line used in the current study were characterised by immunofluorescent staining for these markers.

Materials:

Block Buffer: PBS containing 10% (v/v) rabbit serum (Invitrogen).

Met-5A cells were grown to confluence in LabTekII 8-well chamber slides (BD Biosciences, UK) in growth medium. The mesothelial cell markers investigated are detailed in Table 2-1.

Antigen	Primary Antibody	Secondary Antibody	Fluorochrome
Cytokeratin	Mouse anti- human (BioLegend, USA)	Rabbit anti-mouse (Invitrogen)	Fluorosceneisothiocyanat e (FITC)
Calretinin	Mouse anti- human (Abgent)	Rabbit anti mouse	FITC
E-cadherin	Mouse anti- human (Biolegend)	Rabbit anti-mouse	FITC

Table 2-1: Antibodies used for the staining of cellular markers

Culture medium was removed and the cell monolayers washed three times in PBS. The monolayers were then fixed for ten minutes with ice-cold 100% methanol. Fixative was removed and the cells washed three times in PBS before the addition of 400µl / well of blocking buffer at room temperature (RT) for 1 hour to reduce nonspecific binding of the primary antibody. Primary antibodies were diluted at a ratio of 1:20 in blocking buffer (400µl), and the cell monolayers were maintained with these antibodies for 16-18 hours at 4°C. The slide was then removed from the refrigerator and allowed to equilibrate to RT for 30 minutes. The monolayers were washed three times in PBS before the addition of 400µl of the appropriate secondary antibody, diluted at a ratio of 1:100 in blocking buffer, for 1 hour in the dark at RT. Following a further three washes in PBS, the cells were incubated with propidium iodide (Sigma-Aldrich) (400µl) at a dilution of 1:100, for 10 mins at RT, in order to visualise the cell nucleus. Monolayers were then washed 4 times in PBS before being mounted with antifade fluorescent mounting medium (Dako, Denmark) onto a clean glass microscope slide. Cell staining was visualised under a LP2 fluorescent microscope (Leica Microsystems, Germany).

2.2.5 Characterisation of Toll-Like Receptor expression in MET-5A cells

Toll-Like Receptors (TLRs) are important in innate immune recognition of pathogens. The expression of TLRs on the surface of Met-5A cells was investigated by Fluorescence-activated cell sorting (FACS).

Materials:

FACS Buffer: Sterile PBS containing 0.5% (w/v) Bovine serum albumin (BSA) and 2mM EDTA.

Met-5A cells were grown to confluence in a 75cm² cell culture flask and detached by trypsinisation as described in Section 2.2.1. Detached cells were then suspended in complete growth medium and the concentration adjusted to yield a 1x10⁵ cells/ml suspension. Aliquots (1ml) of the cell suspension were then transferred to sterile Eppendorf tubes, and centrifuged at approximately 500g for 2 minutes to pellet the cells. The pellet was then suspended in FACS buffer and the cell suspension was centrifuged again for 6 minutes at 400g and 4°C. The supernatant was discarded and

the pellet was suspended in 50µl of FACS buffer containing 10% (v/v) human IgG Fcγ blocker (Sigma–Aldrich) and kept on ice for 10 minutes before being transferred to a FACS tube (Marathon Labs, UK). The appropriate anti-TLR antibody (e-biosciences, USA) was then added to the cell suspension (5µl for TLR4 and 20µl for TLR2) and the volume of each tube was then made up to 100µl with FACS buffer. The mixture was then maintained on ice for 30 minutes in the dark, before 2ml of FACS buffer was added to each tube. The tubes were again centrifuged for 6 minutes at 400g and 4°C to pellet the cells and the supernatant, containing any unbound antibody, was discarded. The pellet was suspended in 500µl of FACS buffer and the cell suspension was filtered through 100µm strainer caps (Marathon Labs) to remove any large cell aggregates. Expression data were then acquired on a FACSAria cell sorting machine (BD Biosciences, USA) according to the manufacturer's instructions.

2.3 Characterisation of Streptococcus pneumoniae

The pneumococcal strains used in this study are listed in Table 2-2.

D39 is a serotype 2 strain clinical isolate first obtained by Oswald Avery in 1916 at the Rockefeller Institute for Medical Research, and first described by Martin Henry Dawson in 1928 (Dawson 1928). It was deposited at the British National Collection of Type Cultures (NCTC) in 1948. R6 is an unencapsulated mutant of D39, originally obtained in 1934 following serial passage in the presence of anti-type 2 capsular antibodies. It has been employed for several decades as a transformable, unencapsulated prototype of S. pneumoniae in various physiological, biochemical and genetic studies and thus is very well characterised. The major, and currently only, conclusively documented genetic difference between strain D39 and the unencapsulated derivatives of it is a 7.5 kb deletion of a contiguous segment of the chromosome that originally encoded nine of the type 2 capsule genes. The D39-derived pneumolysin-deficient mutant (D39-ΔPly) used in this study was constructed using site-directed mutagenesis by Kirkham et al. at the University of Glasgow in 2006 (Kirkham et al. 2006). TIGR4 is clinical strain, isolated from a patient with pneumococcal bacteraemia. This isolate was the first pneumococcal strain whose genome was fully sequenced (Tettelin et al. 2002), and as such, current pneumococcal

genomic and transcriptomic analyses have been developed using the genome of this strain. The serotype 1 non haemolytic (S1-NH) and haemolytic (S1-H) isolates used in this study are clinical isolates, obtained from paediatric empyema patients. These have been characterised as pneumococcal serotype 1 and were a gift from Professor T. J. Mitchell from the University of Glasgow.

2.3.1 In vitro culture of pneumococcal strains

Materials:

Brain Heart Infusion Medium (BHI): UHQ containing 37g/l BHI (Oxoid, UK), sterilised by autoclaving at 2.68kg/cm for 15 minutes at 121°C.

BHI Agar Plates: BHI medium containing 10g/l bacteriological agar (Oxoid).

Plastic MicroBankTM beads (ProLab Diagnostics, Canada) (Section 2.3.2) were plated onto Columbia Blood Agar Plates (E&O Laboratories Ltd., UK) with a sterile 10μl inoculating loop, and an optochin disc (Mast Group, UK) placed in the centre to identify any contamination. The plates were then incubated overnight. A loopful of bacterial growth was then subcultured onto a blood plate with an optochin disc and incubated for 6-8 hours. The bacterial lawn was then suspended in 2ml of liquid Brain Heart Infusion medium (BHI) (Oxoid, UK) and then briefly centrifuged at 500g for 1 minute to pellet any debris. Serial ten-fold dilutions of the bacterial suspensions were made to a final dilution of 1:100,000, which was then incubated for 12 hours to achieve log phase growth. Bacterial suspensions were then used for infection experiments.

Strain	Source	Serotype	Characteristics	Reference
D39	NTCT (NTCT 7466)	2	Haemolytic	(Dawson 1928)
D39-ΔPly	(T. J. Mitchell	2	Pneumolysin Deficient	(Kirkham et al. 2006)
	University of Glasgow)		Non-haemolytic	
R6	ATCC (BAA- 225)	Acapsular (Serotype 2 background)	Capsule Deficient Haemolytic	(Hoskins et al. 2001)
TIGR4	ATCC (BAA – 334)	4	Haemolytic	(Tettelin et al. 2002)
S1 – NH	(T. J Mitchell, University of Glasgow)	1	Non-haemolytic, clinical empyema isolate, highly mucoid.	N/A
S1 – H	(T. J Mitchell, University of Glasgow)	1	Haemolytic, clinical empyema isolate, highly mucoid.	N/A

Table 2-2: Streptococcus pneumoniae strains used in this study.

2.3.2 Cryopreservation of bacteria

Bacteria were stored on porous MicrobankTM beads (Pro-Lab, Canada) to enable reliable preservation of cultures, rather than repetitive subculture, which can result in contamination, lost organisms or changed characteristics.

Pneumococci were grown overnight on blood agar plates as described in section 2.3.1 A MicrobankTM cryovial was inoculated with a loopful of colonial growth and then gently inverted to emulsify the organisms. Excess cryopreservative liquid was then aspirated and the vial stored at -80°C.

2.3.3 Quantification of bacterial suspensions

Pneumococcal strains were cultured as described above and a 1:100,000 dilution prepared. The optical density (OD) of the culture at $\lambda600$ nm was measured every 2 hours using a HITACHI U-1100 spectrophotometer (Maidenhead, UK), using uninfected liquid BHI as a blank, and samples were also taken for viable counting. Serial ten-fold dilutions of the sample were made and 20 μ l volumes were pipetted onto BHI agar plates, in triplicate. The plates were incubated for 48 hrs and bacterial colonies were then counted using an automated Protocol colony counter (Synoptics, UK). Growth curves were generated (colony forming units (cfu) vs. OD) which were then used to calculate experimental infective doses.

2.3.4 Preparation of infection suspensions

Pneumococcal strains were grown to log phase as described in section 2.3.1. At 12 hours, the bacterial suspension was further diluted at a 1:5 ratio and incubated for 2 hours to obtain a log phase culture. Optical density at $\lambda600$ nm was then measured to determine bacterial concentration from the growth curves of each strain. The bacterial suspension was then centrifuged at 2000g for 5 minutes and the pellet suspended in 1ml of PBS. The suspension was then diluted in infection medium to generate infective doses of 10^1 , 10^2 , 10^4 , 10^6 and 10^8 colony forming units (cfu) per ml.

2.3.5 Characterisation of capsule expression

The presence or absence of a polysaccharide capsule was determined for all pneumococcal strains by the use of a negative staining protocol.

Materials:

Congo Red solution: UHQ containing 1% (w/v) Congo Red (Sigma-Aldrich).

Crystal Violet solution: UHQ containing 1% (w/v) Crystal Violet (Difco, Germany)

A single drop of Congo Red solution was added to a clean glass microscope slide with a sterile Pasteur pipette. A single bacterial colony was then mixed with the solution to create an emulsion which was then spread thinly over the slide and allowed to air-dry. The slide was then flooded with crystal violet solution for 2 minutes, and then gently washed under running tap water. After air-drying, samples were visualised using a Nikon 4500 light microscope (Nikon, Japan) under immersion oil with a x40 objective lens.

2.3.6 Characterisation of haemolytic activity

The haemolytic activity (and thus functionality of the pneumolysin protein) of each pneumococcal strain was characterised by standard a haemolytic assay. Bacterial lysates were prepared as described in Section 4.8.2. PBS (50μl) was dispensed into each well of a sterile U-bottomed 96-well plate (Greiner BioOne, UK) and 50μl of crude bacterial lysate pipetted into the first well of each row. Serial dilutions were then made across each row by pipetting 50μl into each subsequent well. Erythrocytes were prepared by washing 1ml of sheep's blood (Oxoid, UK) by centrifugation at 8000g for 1 minute. The supernatant containing lysed cells was discarded and the pellet suspended in 1ml PBS. This wash step was then repeated to remove all lysed cells. A 2% (v/v) suspension of red blood cells was then prepared in PBS, which was then transferred to each well (50μl), before incubating the plate for 30 mins at 37°C and then 30 mins at RT. In negative wells, the red blood cells aggregate at the bottom of the well and a pellet is visible. In positive wells, where there is pneumolysin activity, the blood cells are lysed and no pellet is visible.

2.4 Investigation of bacterial association with human pleural mesothelial cells Materials:

Infection Medium: Medium 199 containing Earles' balanced salt

solution (BSS), glutamine, HEPES and sodium carbonate (Lonza), supplemented with 1% (v/v)

dFCS.

Lysis Buffer: PBS containing 1% (w/v) saponin (Sigma-

Aldrich) and sterilised using a 0.2µm filter

(Nalgene, Denmark).

Gentamicin Solution: Infection medium containing 200µg/ml

gentamicin (Lonza)

Cytochalasin D (CD): Maintenance medium containing 2µg/ml CD

(Lonza).

For all bacterial association experiments, Met-5A cells were grown to confluence in sterile 24 well culture plates (Greiner BioOne) as described in section 2.2.1. Growth medium (1ml/well) was replaced 24 hours prior to infection with infection medium to allow confluent monolayers to adjust to the reduced FCS concentration used during experiments.

2.4.1 Quantification of total bacterial association

Pneumococcal suspensions were prepared as described in section 2.3.1 and adjusted to a concentration of 10⁸ cfu/ml in infection medium. Serial dilutions were made to also yield bacterial suspensions of 10¹, 10², 10⁴, 10⁶ cfu/ml. Viable counts were performed by serially diluting each suspension in PBS and inoculating BHI agar plates with 20µl of each dilution. This enabled the retrospective calculation of the exact infective doses. Met-5A cells were washed twice with PBS (1ml/well) and triplicate monolayers were infected with 1ml/well of the appropriate bacterial dose and then incubated under standard culture conditions. At 3, 6, 9 and 24 hours post-challenge, supernatants were aspirated from each well and the monolayers washed 4x with PBS. Prior to aspiration, a viable count was performed on the supernatants, as described

above, so that bacterial growth in the medium and the percentage of bacterial association could be calculated. To liberate associated bacteria, 250µl of lysis buffer was added to each well and incubated for 15 minutes at 37°C. Lysates from triplicate wells were pooled into bijoux tubes and mixed by vortex to ensure uniform distribution of bacteria. Serial ten-fold dilutions of each lysate were made in PBS depending on the infective dose and time point, and triplicate plates were inoculated as described above. The plates were incubated for 48 hours and colonies then counted using a Protocol Colony Counter (Synoptics).

2.4.2 Quantification of bacterial invasion of pleural mesothelial cells

In order to determine whether pneumococci were able to invade pleural cells, Met-5A cell cultures and a bacterial suspension was prepared to a concentration of 10⁴ cfu/ml as described in Section 2.3.1. Prior to infection, cells were washed twice in PBS and the appropriate wells were treated with 500µl of cytochalasin D for 30 minutes. An equal volume of infection medium alone was added to control wells. Cytochalasin D is a cell permeable mycotoxin and a potent inhibitor of actin polymerisation, which is essential in the process of internalisation for many bacteria (Wells et al. 1998) and so was used as an inhibitor of potential invasion in this assay. Triplicate wells were inoculated with the bacterial suspension and incubated under standard culture conditions for either 3, 6 or 9 hours. Cell monolayers were then washed four times with PBS and the appropriate wells treated with 1ml of gentamicin solution (200µg/ml) for 90 minutes in order to kill any extracellular bacteria. Again, control wells were treated with infection medium alone. In addition, monolayers were treated with both cytochalasin D and gentamicin, so that true invasion could be distinguished from artefact such as bacteria adherent to the plastic. Monolayers were then washed, lysed with saponin, processed and enumerated as previously described in Section 2.3.3. Data were then analysed using a students' t-test to determine the significance of pneumococcal invasion; a P value of ≤ 0.05 was considered significant.

2.4.3 Visualisation of pneumococcal adherence to Met-5A cells by Scanning Electron Microscopy

In order to confirm the data obtained from bacterial association assays, Met-5A cells were infected with pneumococci and their adherence to pleural cells visualised by scanning electron microscopy (SEM).

Materials:

PIPES Buffer: 0.1M piperazine-NN'-bis-2-ethanesulphonic acid,

pH 7.2

Fixative: 0.1M PIPES buffer containing 3% (v/v)

gluteraldehyde and 4% (v/v) formaldehyde.

Post fixative: PIPES buffer containing 1% (w/v) osmium

tetroxide (Oxchem, Oxford).

Graded Alcohols: 30, 50, 70, and 95% (v/v) ethanol in UHQ;

absolute ethanol.

Cells were grown to confluence on 0.4µm pore Transwell membranes (Greiner BioOne) and the complete growth medium was replaced 24 hours prior to infection with infection medium as described in Section 1.6. Monolayers were then infected with either 10⁴ cfu/monolayer and incubated under standard conditions for 3, 6, 9 or 24 hours. At each time point, infection medium was aspirated and the monolayers gently washed four times in PBS to remove any non-adherent bacteria. Fixative (500µl) was then added to the monolayers followed by incubation at 37°C for at least 1 hour. The fixed monolayers were then washed twice for 10 mins with PIPES buffer and then kept in post-fixative for 1 hour at RT. The samples were again washed twice for 10 mins in PIPES buffer before being dehydrated through a series of graded ethanol solutions at 30, 50, 70 and 95% (v/v) (1x10 mins each) and then in absolute ethanol (2x20 mins). Whilst in the 50% (v/v) ethanol solution, the membrane was carefully cut out from the insert to ensure that the samples did not desiccate.

2.5 Antigenic stimulation of pleural mesothelial cells.

In order to ascertain whether Met-5A cells possessed an innate immune response mechanism, a series of experiments were performed in which cells were challenged with various stimuli and the cytokine response was assessed.

2.5.1 Pre-Stimulation of pleural mesothelial cells with TNF-α

Met-5A cells were grown to confluence in 24 cell culture plates as described in section 2.2.1 and maintained in infection medium for 48 hours prior to infection. Bacterial suspensions were prepared as described previously in section 2.4.3 and adjusted to give a multiplicity of infection (MOI) of 1, 10, 50, 100 or 200 bacteria per cell. Monolayers were washed twice in PBS and treated with 1ml of human recombinant TNF-α (PeproTech, UK) at a concentration of 100ng/ml and incubated under standard conditions for 4 hours. Again, control wells were treated with infection medium alone. Triplicate monolayers were then infected with 1ml of the appropriate bacterial suspension and incubated for 24 hours. Supernatants were then collected into 2ml tubes (Eppendorf, UK) and centrifuged for 5 mins to pellet the bacteria, before being transferred to fresh tubes and stored at -20°C until analysis for cytokine production.

2.5.2 Production of bacteria-derived antigens

In order to assess the capacity of pleural cells to mount a cytokine response via antigen recognition by TLRs and other PRRs, they were challenged with various bacterially derived stimuli. The pneumococcal antigens (including whole bacteria) used in this assay were derived from the reference strain D39.

2.5.2.1 Production of pneumococcal lysates

Log phase bacterial suspensions were prepared as previously described in Section 2.3.4 and centrifuged for 5 mins at 2000g and the pellet suspended in ~5ml of PBS. The suspension was then centrifuged for a further 5 minutes to wash the bacteria and remove any bacterial debris or residual BHI medium. The pellet was then suspended in 2ml of PBS and transferred to a Lysis Matrix B tube (MP Biomedicals, UK). The

bacteria were then mechanically lysed using a Ribolyser (Biorad, USA) according to the following protocol. The tube was placed on ice for 30 seconds between each spin.

Ribolyser Speed Setting	Time (s)
6	40
6	20
4.5	40
4.5	20

From this crude lysate, the protein fraction could be isolated by passing the lysate through a 0.4µm filter to remove bacterial debris and large polysaccharides.

2.5.2.2 Heat-attenuation of pneumococci

Pneumococci were pelleted, washed and suspended in PBS as described in section 1.8.2. The suspension was then transferred to a 2ml Eppendorf tube and heated to 96°C for 4 minutes in a Dri-block (Techne, UK). Viable counting confirmed that this method killed 100% of pneumococci.

2.5.2.3 Quantification of bacterial proteins by Bradford Assay

Materials:

BCA Protein Assay Kit (Pierce Biotechnology)

Bovine serum albumin (BSA) protein standard solutions were prepared as detailed below.

Vial	Volume of Diluent (μl)	Volume and Source of BSA	Final BSA Concentration (μg/ml)
A	0	300µl of stock	2000
В	125	375µl of stock	1500
C	325	325µl of stock	1000
D	175	175µl of vial B	750
E	325	325µl of vial C	500
F	325	325μl of vial E	250
G	325	325µl of vial F	125
Н	400	100μl of vial G	25
I	400	0μ1	0

Each of the standards and samples (25μl) were transferred into duplicate wells of a 96 well microtitre plate (Nunc, Denmark). Crude lysate and protein fraction samples were tested neat and also at dilutions of 1 in 10 and 1 in 25 (in UHQ). The working reagent was prepared by mixing Reagent B with Reagent A at a ratio of 1:50, and then adding 200μl of working reagent to each well. The plate was then covered and incubated for 30 minutes at 37°C on an R100 RotaShaker plate shaker (Luckham Ltd., UK) to ensure thorough mixing. The absorbance of the wells was then measured at 570nm on the MPM6 microplate reader (Biorad), and the manufacturer's software was used to generate a standard curve and to calculate the protein content of each sample.

2.5.3 Stimulation of pleural cells with antigens

Met-5As were grown to confluence in 24-well culture plates as previously described in Section 2.2.1 and monolayers were then challenged with infection medium

containing either; whole live pneumococci, crude lysate, the protein fraction of the crude lysate or heat attenuated bacteria, each at a concentration of 100µg/ml (as determined by the Bradford assay described in Section 2.5.2.3). Lipopolysacchariderich meningococcal outer membranes preparations, derived from *Neisseria meningitidis* strain MC58 (a gift from Dr. Jeanette Williams) were used, at the same concentration of total protein, as a positive control. Monolayers were incubated for 24 hours under standard conditions before the supernatants were harvested for cytokine quantification.

2.5.4 Assessment of cytokine degradation by pneumococci

Materials:

Stimulation Medium: Infection medium containing 100ng/ml of recombinant human TNF-α.

In order to test the hypothesis that TNF- α is bound and/or degraded by pneumococci, bacterial suspensions were prepared in stimulation medium to a concentration of approximately 2 x 10⁶ cfu/ml (equivalent to an MOI of 50 in the presence of Met-5A cells). Bacterial suspensions (1ml) were then transferred into triplicate wells of a 24 well plate and incubated for 24 hours under standard conditions. Supernatants were then aspirated, bacteria removed by centrifugation and TNF- α concentrations quantified by cytokine ELISA.

2.6 Quantification of cytokine production by pleural mesothelial cells following bacterial association and antigen stimulation.

The innate response of MET5-A cells to pneumococcal infection was investigated by the quantification of cytokines in the cell culture supernatants of infected cells.

Materials:

Ready - SET - Go!® ELISA Kit (eBiosciences, USA) containing:

Capture Antibody

Detection antibody

Recombinant Cytokine Standard

Horseradish peroxidise

5X Assay Diluent

Tetramethylbenzine (TMB) substrate

Wash Buffer: PBS containing 0.05% (v/v) Tween-20

Stop Solution: 2N H₂SO₄

Capture antibodies were diluted at a ratio of 1:250 in assay buffer according to manufacturers instructions and then dispensed (100µl) into each well of a MaxiSorp® 96 well plate (Thermo Fisher, UK). The plate was kept overnight at 4°C to allow binding of the antibody. The plate was then washed four times with wash buffer to remove any unbound antibody, and blocked for 1 hour with proprietary assay buffer to reduce non-specific protein binding. A 2-fold series of the recombinant cytokine standard was prepared in assay buffer, ranging from 8,000-3.14 pg/ml. Following the blocking stage, plates were washed twice in wash buffer before 100µl of each of the standards and samples was added to the wells. The plate was then kept at 4°C for 16-18 hours to allow proteins to bind. Plates were then washed four times with wash buffer before addition of 100µl/well of biotin-conjugated detection antibody, which was diluted at a ratio of 1:250 according to the manufacturer's instructions. The plate was then incubated at RT for 1h. Following a further wash stage, 100µl/well of avidinhorseradish peroxidise, diluted 1:250 in assay buffer, was added to each well and the plate incubated for 30 minutes at RT. Plates were finally washed five times in wash buffer, before 100µl of TMB substrate solution was added to each well and the plate

then incubated in the dark at RT for 15 minutes. Stop solution (50µl) was then added to the wells and the absorbance of the wells measured immediately on the MPM6 microplate reader (Biorad). The manufacturer's software was then used to manipulate the data and to calculate cytokine concentration.

2.7 Analysis of pneumococcal gene expression profile during infection of human pleural mesothelial cells.

To test the hypothesis that *Streptococcus pneumoniae* differentially expresses virulence-associated genes which are involved in the pathogenesis of empyema, the transcriptome of pleural cell-associated pneumococci was analysed by microarray.

2.7.1 Recovery of pneumococci from pleural mesothelial cell monolayers

In order to investigate gene expression in adherent bacteria, it was necessary to detach them from the cell monolayer, to prevent contamination by eukaryotic RNA. Following a series of trial methods (detailed in Chapter 4, Section 4.1), the procedure finally used for bacterial RNA extraction was based on a protocol devised by Ryan *et al.* (2007), in which dilute trypsin was used to detach bacteria from cell monolayers, while leaving the monolayer intact.

Confluent Met-5A cell monolayers were grown in 30x 75cm² cell culture flasks and were infected with pneumococci at a multiplicity of infection (MOI) of 200:1 bacteria/cell, and incubated for 2 hours at 37°C. At 2 hours post challenge, flasks were washed twice with PBS to remove any non-adherent bacteria and the monolayers were then treated with 0.005% (v/v) trypsin-EDTA (Lonza) (5ml) for 10 minutes at 37°C, in order to detach adherent bacteria, while leaving the pleural mesothelial cell monolayer intact. For control bacteria, maintained in infection medium, the suspension was centrifuged at 2000g to pellet the bacteria, and the pellet was suspended in trypsin solution. The trypsin solution was removed and pooled into sterile universals and then centrifuged at 2000g for 5 minutes to pellet the detached bacteria. The supernatant was discarded and the bacterial pellet was suspended in 700µl of RNA Protect Bacteria Reagent (Qiagen, UK) and incubated at RT for at least 10 minutes in order to stabilise the bacterial RNA. The suspension was centrifuged again at 2000g for 5 minutes to

pellet the bacteria, and then the supernatant was carefully removed with a pipette. The pellet was then suspended in the proprietary lysis buffer RLT (Qiagen) and transferred to Lysis Matrix B tubes (MP Biomedicals) and mechanically lysed as described in Section 2.5.2. Bacterial RNA was then isolated as described in Section 2.7.2.

2.7.2 Extraction of RNA from adherent pneumococci and Met-5A cells

Bacterial and host cell RNA was extracted using an RNeasy Minikit (Qiagen, UK). All reagents and consumables were provided with the kit unless otherwise stated. Bacterial lysates were produced as described in Section 2.7.2 and Met-5A cells were disrupted by the addition of 700µl of the lysis buffer RLT directly to the cell culture flask. From this point RNA extraction procedures for host and bacterial RNA are the same.

The lysate was transferred into a 2ml collection tube and 700µl of ethanol (70% (v/v) for eukaryotic RNA and 100% (v/v) for bacterial RNA) was then added and mixed thoroughly by pipetting. The sample was then transferred into an RNeasy spin column and centrifuged at 8000g for 15 seconds on a Heraeus Biofuge (Hereaus, UK) and the flow through was discarded. The column was then washed by the addition of the wash buffer RW1 (700µl), and then centrifuged at 8000g for 15 seconds. Again the flow through was discarded. The buffer RPE (500µl) was then added to the column and centrifuged for 2 minutes at 8000g. The long centrifugation ensures that the spin column membrane is completely dry and ensuring that no ethanol is carried over during RNA elution as residual ethanol may interfere with downstream reactions. The spin column was then transferred into a new collection tube and 50µl of RNase-free water was added directly to the membrane. The column was then centrifuged at 8000g for 1 minute to elute the RNA. The elution step was then repeated with a further 50µl of RNase-free water to maximise the RNA yield.

2.7.3 Assessment of RNA quantity and integrity

Materials: RNA 600 Nano Kit (Agilent, USA).

RNA concentration was initially quantified on a Nanodrop 1000 spectrophotometer (Thermo Scientific, USA), according to the manufacturer's instructions. The purity of the sample was determined by analysis of the absorbance of

the sample at 280nm relative to the absorbance at 260nm. A 260nm absorbance value that is twice the magnitude of the 280nm value indicates that there is no detectable protein contamination in the sample (Figure 2.1).

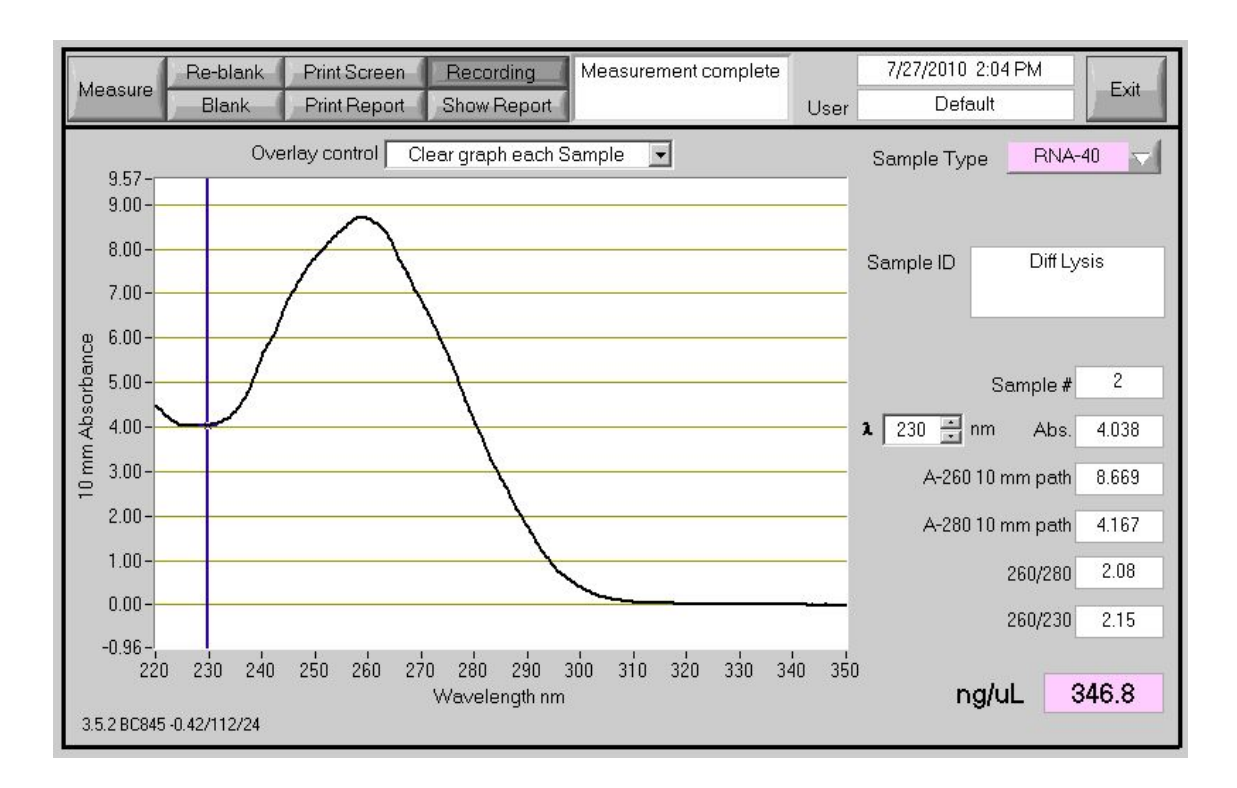


Figure 2-1: Spectrophotometric analysis of bacterial and human RNA.

RNA extracted from Streptococcus pneumoniae and Met-5A cells was analysed at A260 on a Nanodrop 1000 spectrophotometer to ensure a sufficient quantity for microarray analysis. A discrete peak at A260 indicates the high integrity and homogeneity of the sample.

In order to assess the homogeneity of the RNA sample and detect any human RNA contamination, samples were analysed on a Bioanalyser 2100 (Agilent, USA) using an RNA Nano Kit 6000. Unless otherwise stated, all materials used for RNA analysis were proprietary reagents provided with the kit and prior to use, all reagents were allowed to equilibrate to room temperature for 30 minutes. First, 550µl of the matrix gel was pipetted onto the membrane of a spin filter tube and the tube was spun at 1500g for 10 minutes. Filtered gel was then divided into 65µl aliquots and stored at 4°C until use. Dye concentrate (1µl) was added to a gel aliquot and the tube mixed by vortexing before being centrifuged at 13,000g for 10 minutes at RT. Aliquots (1µl) of

the RNA ladder and the test samples were transferred to nuclease-free Eppendorfs and were heated at 70°C for 2 minutes to minimise any secondary structure. An RNA Nano chip was then placed onto the chip priming station and 9µl of the gel-dye mix was pipetted into the indicated well. The priming station was then closed and locked and the plunger was pressed down for exactly 30 seconds in order to pressurise the chip and promote capillary movement of the gel-dye mix throughout the sample wells. The priming station was then opened and a further 9µl of gel-dye mix was pipetted into the indicated wells (Figure 2.2a). Nano marker (5µl) was then pipetted into each of the sample wells (b) and also the well marked with the ladder symbol (c). The denatured samples and the RNA ladder (1µl) were pipetted into corresponding wells, before the chip was vigorously agitated for 1 minute on the IKA vortex mixer (Agilent). RNA Nanochips were then analysed on the Bioanalyser using the Prokaryote Total RNA Nano protocol.

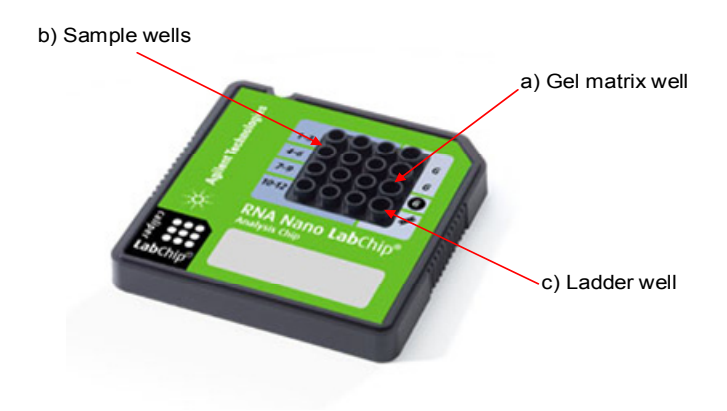


Figure 2-2: Agilent RNA Nano Chips used to assess the integrity and homogeneity of bacterial RNA.

2.7.3.1 Concentration of bacterial RNA by vacuum desiccation

Where Nanodrop measurements found bacterial RNA concentration to be insufficient for microarray, samples were concentrated by vacuum desiccation using a GeneVac CVP100 (GeneVac, UK) whilst centrifuging on a SpeedVac (Savant, USA) on the medium drying rate setting for 20 minutes.

2.7.4 Bacterial RNA Labelling

For each RNA sample (*i.e.* each biological condition), 2 fluorochrome labelled cDNA samples were prepared. One sample was labelled with Cy3 and the other with Cy5 (GE Healthcare, UK). This technique is called dye-swap, and by calculating the mean of both arrays, the variable of dye-bias is negated. RNA (10μl) was added to a microfuge tube (Alpha Laboratories, UK) with 1μl of random primers (Invitrogen, UK) (stock concentration 3μg/μl) and 11μl of nuclease-free water (Sigma-Aldrich). The mixture was heated to 95°C for 5 minutes and then snap cooled on ice and pulse centrifuged for 10 seconds. The RNA was then labelled by the addition of the labelling mixture (Invitrogen) as below:

Component	Volume
5x First Strand Buffer	5µl
100mM Dithiothreitol (DTT)	2.5µl
dNTPs (5mMdA/G/TTP, 2mM dCTP)	2.3μ1
Cy3 or Cy5	1.7µl
SuperScript II (200U/μl)	2.5µl

The labelling mixture was then incubated at 25°C in the dark for 10 minutes followed by 42°C in the dark for 90 minutes. During this incubation, a prehybridisation solution was prepared as follows in a Coplin jar (Fisher Scientific, UK) and left at 65°C to equilibrate:

Component	Volume
20x Saline Sodium Citrate (SSC)	8.75ml
20% (w/v) Sodium Dodecyl Sulphate (SDS)	250μ1
100mg/ml Bovine Serum Albumin (BSA)	5ml
UHQ	To 50ml

The microarray slide was incubated in the pre-heated prehybridisation solution at 65° C for 20 minutes and then rinsed with H₂0 for 1 minute by vigorous agitation of a slide rack in a staining trough, followed by a 1 minute rinse in 100% propan-2-ol. The slide was then centrifuged in a 50ml tube at 500g for 5 minutes to thoroughly dry it, before it was stored in the dark in a dust-free box until hybridisation (<1h).

The fluorochrome labelled cDNA was purified using a MinElute column (Qiagen, UK), as per the manufacturer's instructions. Cy3 and Cy5 labelled cDNA samples were combined in a single tube and 250 μ l of buffer PB was added. The mixture was then applied to the MinElute column and centrifuged at 8000g for 1 minute, and the flow through was discarded. The column was then washed by the addition of 500 μ l of buffer PE to the membrane and the centrifugation step was repeated. This wash step was then repeated with 250 μ l of buffer PE and the flow through discarded. The column was then centrifuged at 8000g for an additional 1 minute to remove residual ethanol. The column was then transferred to a fresh collection tube and 23 μ l of H₂0 was pipetted directly onto the membrane of the column and allowed to stand for one minute before the cDNA was eluted by centrifugation at 8000g for 1 minute.

The prehybridised slide was then placed into a hybridisation cassette (Corning Lifesciences, USA) and $2x15\mu l$ aliquots of H_20 were pipetted into the wells of the cassette to ensure a humidified environment The purified Cy3/Cy5-labelled cDNA

(19.5μl) was added to hybridisation solution which contained filtered 20x SSC (6μl) and filtered 2% (w/v) SDS (4.5μl). The mixture was heated to 96°C for 2 minutes and then was allowed to briefly cool and pulse centrifuged. A LifterSlip (VWR International, UK) was placed over the printed area of the array slide, then the hybridisation solution was pipetted under one corner of the slip allowing the solution to be drawn completely across the array by capillary action. The hybridisation cassette was then sealed and submerged in a water bath at 65°C in the dark for 16-20 hours.

Wash buffer A containing 20x SSC (20ml), 2% (w/v) SDS (1ml) made up to 400ml with H₂0, was prepared in a sealed bottle and incubated at 65°C overnight. The preheated wash buffer A was then added to a preheated staining trough. The microarray slide was then removed from the hybridisation cassette and initially washed carefully in the trough to remove the LifterSlip. Once the slip was displaced, the slide was placed in a slide rack and vigorously agitated in wash buffer A for a further 2 minutes. Slides were then immediately transferred to a trough containing wash buffer B (H₂0 containing 0.06x SSC) and agitated for 2 minutes before being washed in a second trough of wash buffer B for a further 2 minutes to ensure thorough washing of the slide to minimise any non-specific fluorescence. The slide was then placed in a 50ml centrifuge tube and centrifuged at 500g for 5 minutes to thoroughly dry it before it was scanned by an Affymetrix GeneChip analyser (Affymetrix, USA), and gene expression analysed using GeneSpring GX software (Agilent, USA).

2.8 Validation of bacterial gene expression

2.8.1 Primer Design

Pneumococcal genes were selected for RT-qPCR validation using the random stratification method described in Section 4.2. Gene sequences were obtained from the J. Craig Venter Institute's (JCVI) online Comprehensive Microbial Resource by searching for each of the selected genes' locus number. Sequences were then entered into Primer3 primer design software (http://frodo.wi.mit.edu/primer3/) (Rozen and Skaletsky 1999) and primers were designed to be at least 18 (optimally 20) base pairs in length and to have a GC content of greater than 50% to ensure a high melting

temperature, thus minimising the level of non-specific binding. The primer pairs generated by the software were then analysed using NetPrimer Software (PREMIER Biosoft, USA) to avoid the formation of hairpins within the primers and primer heteroand homo- dimers. The selected primer pair sequences are shown in Table 2-3. (http://www.premierbiosoft.com/servlet/com.pbi.crm.clientside.FreeToolLoginServlet#).

Gene Name	Sense Primer Sequence	Antisense Primer Sequence
Gdh A	TGCTCAAGGCGTTATCTGTG	AGCTTTTGCAGGTCCGTAGA
SP_1914	GGGAATGCAACCGTCTATGT	CTTCCCAAAAGCCACATCTC
SP_0136	CGAGAAGAGGAGAAGACCGATT	ACAACACCGTCCTGATGTGA
<i>psaB</i>	AGGAATGCGTCTCGTTAGGA	TAGTCAGCTAGGCCGACGAT
SP_0858	ACCTTTGGACTCAAGCAACG	GCTGCTTCTCCCATAGGTTG
glnQ	GACCCTGAGATGGTTGGAGA	CGAGGGTGTTGTGGGTTATC
SP_0857	GGTTCTGCCATGAAACACCT	GATGAAGCTGTTGGCATCAA
SP_1992	AGTGGCTCCTAATGCTGCTC	TTGTTGCCACCACTAGACCA
pdxK	TATCAAGGGAGGCAATCGTC	CAAAGGTACAACCTGCACCA
Nox	CTGTTGGTGACTGTGCGACT	TGTAGGCACCAACGATACCA
SPR1178	CACCGAAATTTCCTCAGCTC	GAGGCAATGGCCTGTTCTAA
Pdx1	CTGATGACCGTTTCCATGTG	CTGTCCCTGGTTCTCCTTTG
glnA	TCTTGAGTTGCGTTCAGTGG	TTCGATAGGAGCTGGTGCTT
lytB	TCAAAGCAGATGGACAGCAC	TTGGCACCACTAGCATTCAC
SP_0138	GGTTACCCTTTGAGCCAACA	GACGTTCACAAGCTAACCTGTCT
adhE	TGCTCCTGAAAACTGTGTGC	ACCTACCCCAAGAGCTGGTT
adhP	TTCTTGGGCACGAAGGTATC	GTTCAGCCATACCACCGTCT
trpD	GATATTCGTGGTGGGAATGC	CAACCCCTTCCTTGATGCTA
trxA	ACTTCTGGGCAACTTGGTGT	GTTTGACAACTTGGCCGTCT
SP_1775	GCCAGCAAGAACGAAAGAAC	TCCATAAGTCCCATGGTAGTCC
SP_2187	CTCTGGGCTCACATCAGTCA	CGGAACCTTTCTCAGCAAAC
SP_1069	CATGGCCGCTATTACAGACC	TTCACATTCGGTGTCAGAGC
purl	ACTCCCAGAAGAGCGTCAAA	CGTCCAACAGAGCAGTCAAA
purF	TCTACTTTGCTCGCCCTGAT	TAGGGAAGAATTGGGCACAC
GyrA	GCGAGCTCTTCCTGATGTTC	TTACCCATGACATCCCCTGT

Table 2-3: Primer pairs for RT-qPCR validation of differentially expressed pneumococcal genes.

2.8.2 Synthesis of cDNA by reverse transcription

Materials: Superscript® VILOTM cDNA Synthesis Kit (Invitrogen)

A two-step RT-qPCR method was used to quantify pneumococcal gene expression. Reverse transcription reactions were performed using the following recipe to yield first-strand cDNA.

Component	Volume
5X VILO™ Reaction Mix	4µl
10X SuperScript® Enzyme Mix	2µl
RNA	2µl
Nuclease Free Water	12μ1

The contents of the tube were mixed by gentle agitation with a pipette. The reaction was then incubated in a Biometra T3 thermocycler (Goettingen, Germany) at 25°C for 10 minutes, followed by 42°C for 60 minutes. The reaction was then terminated by heating to 85°C for 5 minutes.

2.8.3 Quantitative Polymerase Chain Reaction

Materials: EXPRESS SYBR® GreenER™ qPCR Supermix (Invitrogen)

Bacterial cDNA was synthesised as described in section 1.14.2. A 10-fold dilution of cDNA was made in nuclease free water (Qiagen). Reactions were set up in 96-well PCR plates, on ice, according to the following recipe:

Component	Volume
EXPRESS SYBR® GreenER TM qPCR Supermix Universal	10μ1
10μM forward primer (200nM final)	0.4μ1
10μM reverse primer (200nM final)	0.4μ1
Template DNA	2.5μ1
Nuclease-free water	6.7µl

Real-Time quantitative polymerase chain reaction (RT-qPCR) was then performed using a CFX-96 RT-qPCR detection system (Biorad, USA). Plates were incubated at 50°C for 2 minutes followed by heating to 95°C for 2 minutes. Genes were then amplified for a total of 40 cycles; each cycle consisted of 95°C for 15 seconds, followed by 60°C for 1 minute. Using the manufacturer's software, melt curve analysis was also performed on each sample over a range of 60 - 95°C to ensure the presence of only a single PCR product, and to allow the detection of primer dimers.

2.9 Analysis of gene expression profile of Met-5A cells during infection with Streptococcus pneumoniae

The host innate immune response to pneumococcal infection was investigated by analysis of the transcriptome of Met-5A cells during infection. Pleural mesothelial cell cultures were grown to confluence in 75cm² flasks as described in Section 2.2.1 and infectious suspensions of pneumococci were prepared as described in Section 2.3.4. Met-5A cells were then infected at an MOI of 200:1 bacteria/cell and incubated at 37°C for 2 hours as described in Section 2.4.1. RNA was extracted from infected cells according to the protocol described in Section 2.7.1 and its quantity and quality assessed as described in Section 2.7.3.

All reagents and consumables used in the preparation of human microarray probes were provided in an Amino Allyl MessageAmpTM II aRNA proprietary kit (Ambion, USA), unless otherwise stated.

2.9.1 Manufacture and Quality Control of Human Microarray Slides

The human microarrays used in the current study were printed in-house at the Post-Genomic Technologies Facility at the University of Nottingham (http://genomics.nottingham.ac.uk) using a BioRobotics Microgrid II 600 robot (Isogen Life Science, Netherlands). For each of the 32,000 human genes represented on the array, a cDNA probe corresponding to the mRNA of that gene, was synthesised. Probes were then spotted on to the surface of Nexterion A+ slides (Schott, UK) at a predetermined position by an array of fine pins, with each spot measuring approximately 80µm in diameter.

Following printing, all slides from the batch were scanned using an Agilent BA scanner (Agilent Technologies, USA), to detect autofluorescence and thus the precise location of each spot. Each image was then processed using GenePix® Pro v6.0 software (Molecular Devices LLC, USA), which aligns a reference grid to the array and generates data on individual spot quality, based on their size and uniformity. This software also detects the absence of spots, and a tolerance threshold of <1% maximum missing spots (<320 out of 32488) was applied to all arrays used in this study.

To ensure homogeneity between spots, cDNA distribution within each spot was quantified on two slides from both the beginning and end of each print run. The printed arrays, as well as a proprietary calibrator slide, were hybridised for 5 mins with Genetix SpotcheckTM solution (Molecular Devices) which contains a nucleic-acid dye. Slides were then washed for 5 mins in PBS and scanned at λ555nm. The signal intensities from the spots on the printed slide were then compared to those on the control slide and the relative quantity of cDNA was calculated by the manufacturer's quality control software (Agilent Technologies). Spots with signal intensities below that of the lowest calibrator were then excluded from analysis.

To control for inter-batch variation, an additional two slides from the print batch were assessed using the Lucidea Microarray ScoreCard system (Amersham Biosciences, USA) (Samartzidou 2001). In this, a set of 10 artificial genes, selected from yeast intergenic regions which show no cross-hybridisation with human, mouse, rat or *E. coli* are printed onto each array. These are hybridised to corresponding control probes at a predefined concentration and ratio labelled with a mixture of Cy3 and Cy5. Lucidea Microarray ScoreCard software (Amersham Biosciences) was then used to evaluate the target attachment, probe labelling efficiency, hybridisation uniformity, signal detection limits and dynamic range of each slide and apply quality control criteria (Samartzidou *et al.* 2001). Comparison of these parameters both intra- and inter- experimentally also provides a method of data normalisation. However, to negate any error arising from inter-batch variability, all slides used in the current study originated from the same print run.

2.9.2 Synthesis of First Strand cDNA

Total RNA (1µg) was added to an appropriately labelled RNAse-free microfuge tube. T7 Oligo(dT) primer (1µl) was added to the tube and the total volume made up to 12µl with nuclease-free water, before being incubated for 10 minutes at 70°C in an Omnigene thermal cycler (Hybaid, UK). Microtubes were then briefly centrifuged for 5 seconds in an AccuSpin 17R Microfuge (Fisher Scientific, UK) and then placed immediately on ice. A reverse transcription reaction was then performed on each sample according to the following recipe:

Component	Volume
10X First Strand Buffer	2μ1
dNTP Mix	4μ1
Ribonuclease Inhibitor	1μ1
Array Script	1µl

All components were mixed thoroughly by gentle pipetting and then incubated for 2 hours at 42°C in a hybridisation oven (Hybaid). Samples were again briefly centrifuged for 5 seconds and returned immediately to ice.

2.9.3 Synthesis of Second Strand cDNA

Synthesis of the second strand of cDNA immediately followed first strand synthesis according to the following protocol.

Component	Volume
Nuclease-free water	63µl
10X Second Strand Buffer	10μ1
dNTP Mix	4μ1
DNA polymerase	2μ1
RNAse H	1µl

Components were mixed thoroughly using a pipette and maintained in a waterbath (Grant Instruments, UK) at 16°C for 2 hours.

2.9.4 Purification of cDNA

cDNA binding buffer (250µl) was added to each of the newly synthesised cDNA samples, and was gently mixed by pipetting. The mixture was then transferred directly to the membrane of a cDNA filter cartridge and centrifuged at 10,000g for 1 minute. The flow-through was discarded and 500µl of cDNA wash buffer was applied to the membrane of the cartridge before again being centrifuged at 10,000g for 1 minute. The flow-through was again discarded and the cartridge was centrifuged for a further minute to ensure the removal of trace amounts of ethanol. The filter cartridge was then transferred to an elution tube and then 9µl of nuclease-free water, pre-heated to 50°C, was added to the centre of the membrane. The cartridge was incubated at RT for 2

minutes and then centrifuged at 10,000g for 2 minutes to elute the cDNA. The elution step was then repeated with a further 9µl of nuclease-free water.

2.9.5 *In-vitro* transcription to synthesise amino-allyl RNA (aRNA).

The purified cDNA obtained in Section 2.15.3 was next transcribed in the presence of amino-allyl labelled uracil triphosphate (aaUTP) to yield amino-allyl-labelled RNA (aRNA) according to the following recipe:

Component	Volume
Double stranded purified cDNA	14µl
aaUTP (50mM solution)	3μ1
ATP, GTP, CTP (25mM solution)	12μ1
UTP (50mM solution)	3μ1
T7 10X Reaction Buffer	4μ1
T7 Enzyme Mix	4µl

All components were gently mixed by pipetting and then centrifuged briefly for 5 seconds before being incubated for 16-18 hours at 37°C. The reaction was then terminated by the addition of 60µl of nuclease-free water and was gently vortex-mixed (Lab Dancer, Fisher Scientific).

2.9.6 Purification of aRNA

In order to optimise the ionic charge of the aRNA for binding to the filter cartridge membrane, aRNA binding buffer (350µl) was added to each aRNA sample followed by 250µl of 100% ethanol. The mixture (700µl) was then immediately pipetted directly onto the membrane of an aRNA filter cartridge and centrifuged at 10,000g for 1 minute. The flow-through was discarded and then 650µl of aRNA wash

buffer was added to the cartridge before being centrifuged again at 10,000g for 1 minute. The flow-through was again discarded and the tube was centrifuged for a further minute at 10,000g to remove any residual ethanol. Nuclease-free water (50µl), preheated to 50°C was applied directly to the filter membrane and incubated at RT for 2 minutes before being centrifuged at 10,000g for 2 minutes to elute the aRNA. The elution step was then repeated with a further 50µl of water to maximise aRNA yield. Incorporation of amino allyl-labelled UTP was confirmed by measurement on a Nanodrop® ND1000 spectrophotometer (Nanodrop®, USA).

2.9.7 Dye-coupling and clean up of aRNA

The concentration of aRNA was maximised by precipitating it in ethanol to remove all water. Samples (10µg) were transferred to nuclease-free microfuge tubes then a 0.1X volume of 3M sodium acetate solution (pH 5.0 - 5.2) and a 2.5X volume of 100% ethanol were added. The mixture was mixed by gentle inversion of the tubes and stored at -20°C for 1 hour to precipitate the aRNA. Tubes were then centrifuged for 30 minutes at 15,000g and 4°C. The supernatant was carefully removed with a pipette and the pellet was suspended in 250µl of 70% (v/v) ethanol before being centrifuged at 15,000g and 4°C for 8 minutes. The supernatant was again carefully removed with a pipette and the pellet allowed to air dry for 2 minutes to remove any residual ethanol. The pellet was then re-dissolved in 9µl of proprietary dye coupling buffer. One lyophilised dye aliquot per sample was prepared per sample by the addition of 11µl of dimethyl sulphoxide (DMSO) and then added to the aRNA samples and incubated at RT in the dark for 30 minutes. Test samples were coupled to Cy3 whilst control aRNA was labelled with Cy5. Hydroxylamine (4.5ul) was then added to the tube in order to quench the reaction and remove the active amine residues on any unincorporated dye molecules, and the sample volume was then made up to 30µl by the addition of 5.5µl of nuclease-free water.

2.9.8 Purification of dye-labelled aRNA

Proprietary aRNA binding buffer (105μ l) and 100% ethanol was then added to each aRNA sample, and the mixture (210μ l) was immediately pipetted directly onto the membrane of an aRNA filter cartridge. The cartridge was then centrifuged for 1 minute at 10,000g and the flow through was discarded. The membrane was then washed by the

application of 500µl of aRNA wash buffer and then centrifuged again for 1 minute at 10,000g. The flow through was discarded and the tubes then centrifuged for a further minute to remove all traces of ethanol. To elute the dye-labelled aRNA, 10µl of nuclease-free water, preheated to 50°C, was added to the membrane and incubated at RT for 2 minutes, before being centrifuged at 10,000g for 2 minutes. The elution step was then repeated with a second 10µl aliquot of nuclease-free water. The frequency of dye incorporation was measured on the Nanodrop using the microarray setting and the probes were then kept on ice until use.

2.9.9 Pre-hybridisation processing of microarray slides.

Prior to probe hybridisation, microarray chips were processed through a series of detergent-containing buffers to ensure that they were clean and free from dust and other debris that might compromise the quality of the microarray. Slides were placed into metal slide racks and then immersed in wash stations containing 0.2% (w/v) SDS buffer, preheated to 45°C and gently agitated for 1 minute. This wash step was repeated with a second container of fresh 0.2% (w/v) SDS buffer and subsequently with 2 containers of UHQ. Slide racks were then immersed in PBS containing 0.1M Sodium Borohydride (NaBH₄) at 45°C for 10 minutes. Slides were then washed again for 1 minute in each of 3 containers of 0.2% SDS buffer, 2 containers of UHQ and finally in a container of 100% ethanol, before being dried by centrifugation at 3,000g for 1 minute. Processed slides were then stored in plastic slide holders in a low humidity chamber and protected from light.

2.9.10 Fragmentation of microarray probes

For each slide to be hybridised, 500ng of both test sample and control sample aRNA were transferred to a nuclease-free microfuge tube and the volume made up to 4.5µl with nuclease-free water. Fragmentation buffer (Ambion, USA) was then added to the tube and incubated at 70°C for 2 minutes. The reaction was then quenched by the addition of 0.5µl of stop solution (Ambion). The tubes were then placed on ice and 2µl of lithium heparin and 1µl of Cot-I human DNAse (Ambion) was added to inhibit none-specific probe hybridisation. Finally, Schott 1X hybridisation buffer (110µl), preheated to 50°C was added to the probe just prior to slide hybridisation.

2.9.11 Microarray slide hybridisation

All reagents used in the preparation of the hybridisation buffers were purchased from Fisher Scientific, UK.

Materials:

Buffer 1: UHQ containing 4X SSC and 0.2% (v / v) SDS.

Buffer 2: UHQ containing 2X SSC and 0.1% (v / v) SDS

Buffer 3: UHQ containing 1X SSC and 0.1% (v / v) SDS

Buffer 4: UHQ containing 0.1X SSC and 0.2% (v / v) SDS

Buffer 5: UHQ containing 0.1X SSC

Buffer 6: UHQ

Blocking Solution: UHQ containing 5X SSC, 0.2% (v / v) SDS and 1% BSA.

Microarray hybridisations were performed on a HS48000 hybridisation station (Tecan Ltd., Switzerland). Buffers were loaded into the appropriate reservoirs and slides were placed into the hybridisation chambers. An automated program was then run on the machine as follows:

Step	Buffer	Temperature	Time	Cycles
Wash	6	45°C	1 min	1
Blocking	Blocking Solution	45°C	10 mins	1
Wash	6	42°C	30 secs	5
Wash	1	50°C	15 mins	1
Probe Injection	N/A	50°C	N/A	N/A
Hybridisation	N/A	50°C	16 h	1
Wash	2	40°C	2 mins	4
Wash	3	40°C	2 mins	2
Wash	4	40°C	2 mins	2
Wash	5	23°C	2 mins	2
Slide drying	N/A	23°C	2 mins	N/A

Following hybridisation, microarray slides were scanned on an Agilent BA scanner (Agilent Technologies, USA) and data were analysed as described in Chapter 5, Section 5.1.

CHAPTER 3 RESULTS – PNEUMOCOCCAL INTERACTIONS WITH HUMAN PLEURAL MESOTHELIAL CELLS

3.1 Characterisation of the human pleural mesothelial cell line Met-5A

To verify the mesothelial origins of Met-5A cells, cultures were immunocytochemically characterised using fluorescent antibodies targeted against known mesothelial cell markers. Zeng *et al.* reported that *ex vivo* mesothelioma cells stained heavily for cytokeratin (Zeng *et al.* 1994). More specifically, the concurrent expression of E-cadherin and calretinin has been shown to distinguish pleural cells from other cell types of mesothelial origin (Simsir *et al.* 1999).

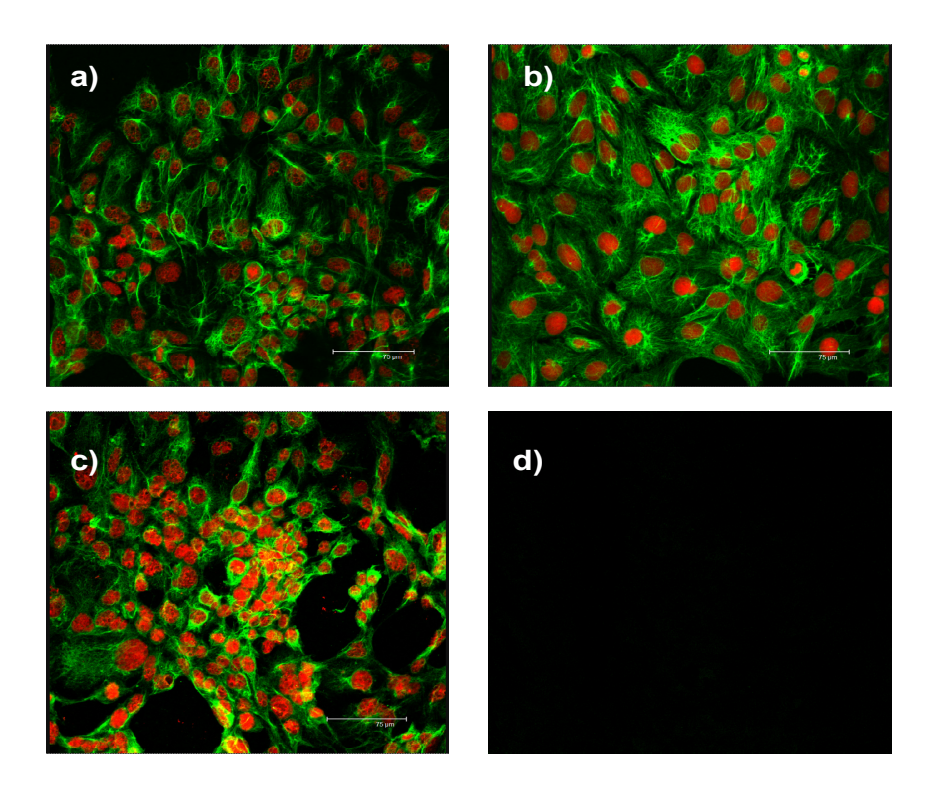


Figure 3-1: Immunocytochemical characterisation of Met-5A cells.

Met-5A cell monolayers were characterised as pleural mesothelial cells by the positive staining for cytokeratin (a) in conjunction with calretinin (b) and E-cadherin (c). Cellular markers were detected with FITC-conjugated antibodies (green) and cell nuclei were counter-stained with propidium iodide (red) so that the cellular localisation

of the markers could be determined. The specificity of antigen staining was confirmed by the low degree of background fluorescence in the negative antibody control (d).

Immunocytochemical analysis of Met-5A cells verified their pleural mesothelial origin. Both cytokeratin and calretinin were visualised as diffusely distributed molecules present in the cytoplasmic fibres of the cells. E-cadherin was similarly localised in the cell cytoplasm, but also appeared to more concentrated around the nucleus, appearing as a concentrated "halo" of fluorescence, suggesting that this junctional protein is also expressed intracellularly in these cells.

3.2 Characterisation of capsule expression in *S. pneumoniae* isolates

A negative capsule stain was used to investigate the expression of polysaccharide capsule in each of the pneumococcal strains. Congo red is an acidic dye which stains the background and the bacteria, but is not able to penetrate the dense capsule, which is visualised as a clear 'halo' around encapsulated bacteria.

Encapsulation was evident in all pneumococcal strains examined (Fig 3.2), except for the capsule-deficient mutant R6 (Fig 3. 2 c). Notably, the clinical isolate S1-NH (Fig 3.2 e), and to a lesser degree S1-H (Fig. 3.2 f), appeared to have thicker capsules than the laboratory reference strains, and had a more mucoid phenotype in liquid culture.

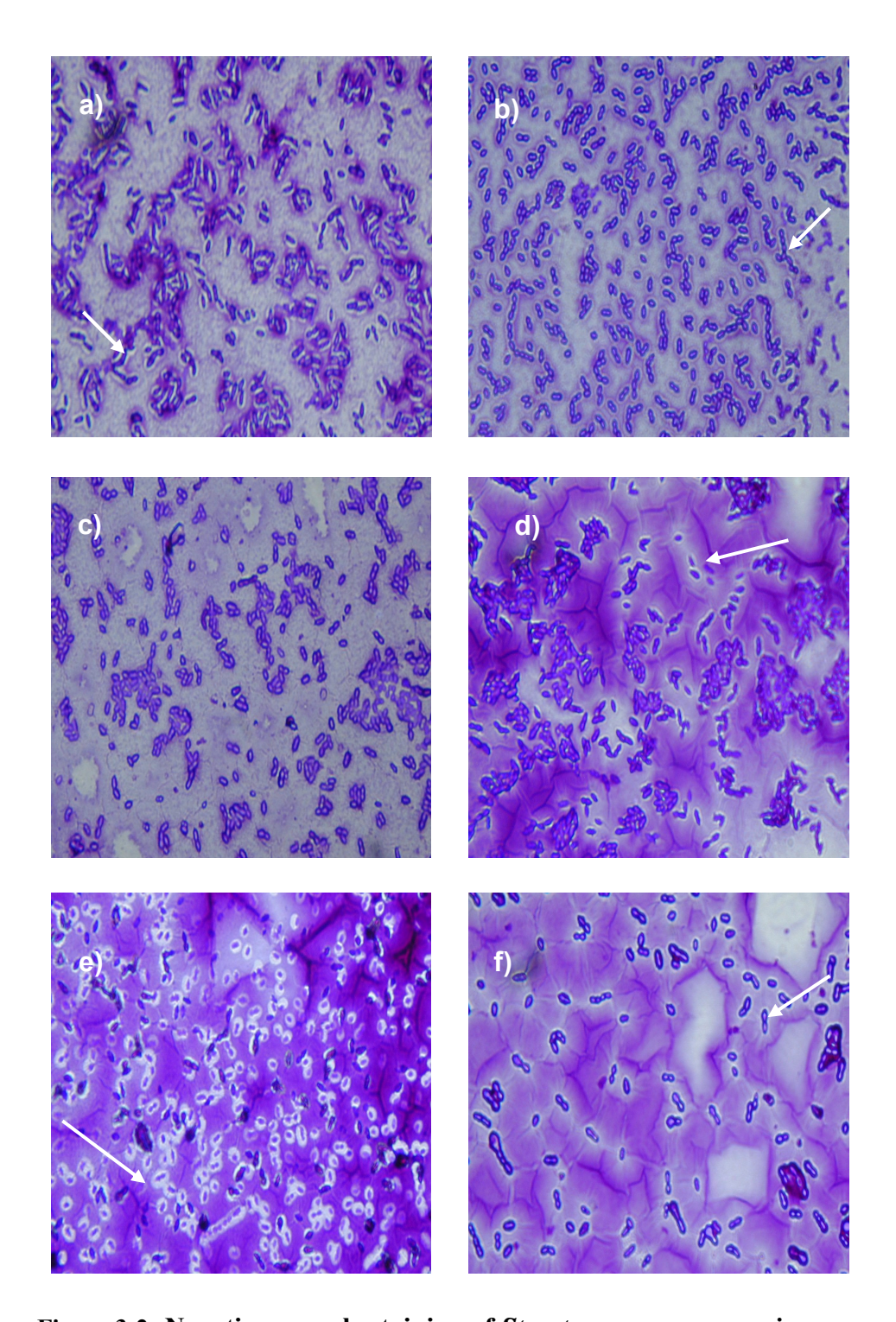


Figure 3-2: Negative capsule staining of Streptococcus pneumoniae.

Pneumococcal laboratory reference strains D39 (a), D39- Δ Ply (b), R6 (c) and TIGR4 (d) and also the paediatric empyema clinical isolates S1-NH (e) and S1-H (f) were stained with Congo Red to investigate expression of polysaccharide capsule. The capsule is visualised as a clear halo around the bacterial cells, as denoted by the arrows. Magnification x100.

3.3 Association of *Streptococcus pneumoniae* with human pleural mesothelial Met-5A cells

In the current study, the hypothesis that the adherence of *Streptococcus pneumoniae* to cells of the pleural mesothelium is a critical prerequisite step in the pathogenesis of empyema was tested. Met-5A cells were infected with the well characterised *Streptococcus pneumoniae* serotype 2 reference strain D39 (Figure 3.3a), a D39-derived pneumolysin deficient mutant (D39-ΔPly) (b), an unencapsulated D39-derived strain R6 (c) and the serotype 4 strain, TIGR4 (d). In addition, cell cultures were infected with serotype 1 clinical strains which had been isolated from paediatric empyema patients. Total bacterial association with pleural mesothelial cells was quantified over a time course and at a range of bacterial concentrations in order to mimic events that may occur in the lung during the pathogenesis of empyema, whereby small numbers of bacteria are believed to enter the pleural cavity and then rapidly proliferate. The association dynamics of each pneumococcal strain are shown in Figure 3.3.

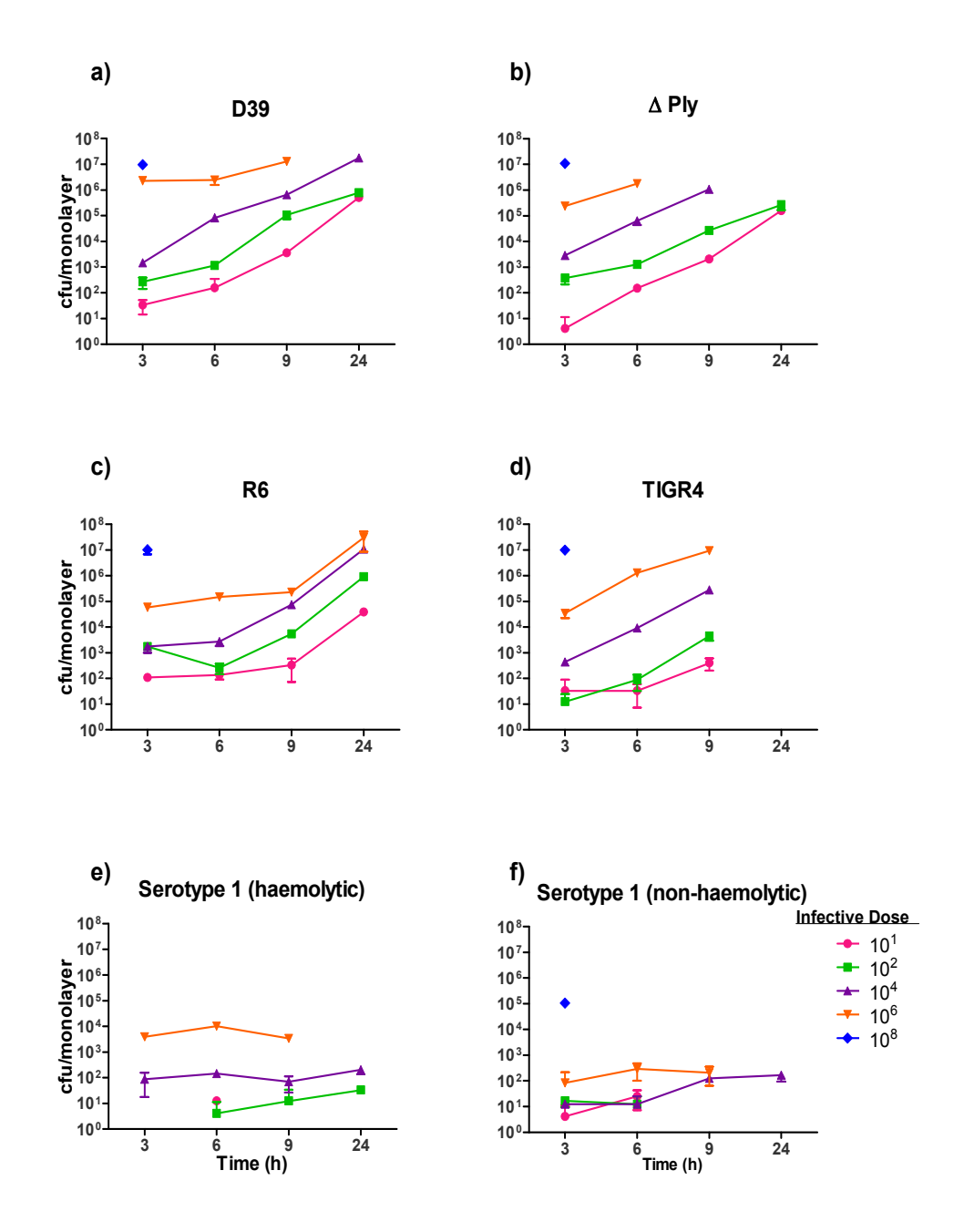


Figure 3-3: Total association of pneumococci with human pleural mesothelial cells.

Met-5A cells were infected with pneumococci over a dose range of $10^1 - 10^8$ cfu/monolayer. Total association of bacteria with the cells was quantified at 3, 6, 9 and 24 hours using viable counting methods, as described in Materials and Methods, Section 2.6.1. Monolayers were visualised by light microscopy at each time point and measurements were not taken where the cell monolayer had been destroyed. Graphs are representative of at least n=3 experiments, where symbols denote the mean and the error bars denote the standard deviation of triplicate samples.

All of the laboratory-passaged pneumococcal strains exhibited similar trends of association with Met-5A cells, adhering to the monolayer in a dose and time dependent manner (Figure 3.3a-d). Challenge with the highest concentrations (10⁶ and 10⁸ cfu/monolayer) of these strains resulted in the rapid saturation of the mesothelial cell monolayers, whilst a significant time lag was observed with the lower inocula (10¹-10⁴ cfu/monolayer). At an infective dose of 10^8 cfu/monolayer, all of the reference pneumococcal strains had saturated the monolayer by 3hrs, with approximately 10% (10⁷ cfu) of the original inoculum being adherent by this time point. By 6hrs postchallenge there was sufficient destruction of the monolayer that further analyses of bacterial adherence could not be performed for any strain (Figure 3.3 a-d). At a bacterial concentration of 10⁶ cfu/ml, D39, D39-ΔPly and TIGR4 strains had completely destroyed the monolayer by 24hrs post-challenge. However, monolayers infected with R6 remained largely intact allowing quantification of association at this time point (Fig. 3.3 c). Remarkably, monolayers challenged with the non-haemolytic mutant D39-ΔPly at concentrations of 10⁴ and 10⁶ cfu/monolayer were destroyed by 9 hours, whereas those infected with wildtype D39 remained intact (Figure 3.3a-b), suggesting that the cytotoxic capacity of the mutant was not attenuated by knock-out of pneumolysin.

Despite large numbers of adherent bacteria (approximately 3 x 10⁷), R6 did not cause cytotoxicity to Met-5A cells suggesting the reduced virulence of this unencapsulated variant compared to its encapsulated parent strain D39 and also to the other reference strains tested. By contrast, monolayers infected with TIGR4 were completely absent at 24hrs, regardless of the initial infective dose (Figure 3.3 d), illustrating that this strain is more cytotoxic to mesothelial cells than the other reference strains tested.

The clinical pneumococcal isolates displayed notably different association dynamics to the reference strains. The capacity of these isolates to adhere to the pleural cell monolayers was significantly reduced (p<0.05) at all infective doses when compared to reference laboratory strains of pneumococci (Figure 3.3e-f). In addition, bacterial association did not appear to noticeably increase over time with no significant difference between the number of adherent bacteria at 3 hours and at 24 hours at the

intermediate concentration of 10^4 cfu/monolayer, and between 3 hours and 9 hours at a dose of 10^6 cfu/monolayer (p<0.05).

Despite poor association, these strains still elicited cytotoxicity in Met-5A cells. At the highest bacterial concentration of 10⁸ cfu/monolayer, the haemolytic clinical isolate had destroyed the monolayer by 3 hours; thus, association could not be quantified for this inoculum. With the non-haemolytic strain, the monolayer was completely absent 6 hours post-challenge with the highest infective dose. Contrastingly, at the lowest infective doses of 10¹ and 10² cfu/monolayer, poor adherence of these strains to Met-5A cells resulted in failure to recover any bacteria at certain time points and missing data here was due to this rather than destruction of the monolayer preventing quantitation.

Bacterial growth in the infection medium was observed for all of the laboratory-passaged pneumococcal strains. At the lowest infective dose of 10^1 cfu/monolayer, numbers of adherent bacteria were between $4x10^4$ and $5x10^5$ cfu by 24 hours. However, the clinical isolates did not exhibit the same trend with less than 10^1 bacteria adherent at 24 hours, suggesting that these strains are more fastidious and less adaptable to growth in culture conditions.

The growth of each bacterial strain in the culture medium and also the proportion of total bacteria that were adherent to the monolayer was monitored over the course of infection experiments. Experimental supernatants from cells challenged with the intermediate infective dose of 10⁴ cfu/monolayer were sampled at each time point and bacteria were enumerated using viable counting methods as described in Section 2.6.1. At the earliest time points, all of the reference pneumococcal strains exhibited similar rates of adherence (≤5%). However, by 9 hours the unencapsulated strain R6 was more adherent than the other laboratory strains tested with 21% of total bacteria being adherent to the monolayer, although by 24 hours the adherence rate of R6 was comparable to its encapsulated parent strain D39. The clinical isolates that exhibited heavy encapsulation (Section 3.2), associated poorly with the monolayer with less than 1% of total bacteria being adherent up to 24 hours post challenge. Together, these data are concordant with the suggestion that capsule expression is detrimental to pneumococcal adherence to mesothelial cells.

-		•		
Ka	cte	rI	Пr	n
Da	···		uı	

% adhered pneumococci

	3hrs	6hrs	9hrs	24hrs
D39	3	5	6	50
D39-ΔPly	3	4	2	n/m
R6	2	2	21	40
TIGR4	1	1	2	n/m
S1-H	<1	<1	<1	<1
S1-NH	<1	<1	<1	<1

Table 3-1: The proportion of total bacteria adherent to Met-5A cell monolayers.

Media samples were taken at 3, 6, 9 and 24 hours from wells infected with a dose of 10^4 cfu and bacteria were quantified by viable counting. Using the association data, the number of adherent bacteria was then calculated as a percentage of total bacteria (associated and non-associated) in the well. Data represent mean bacterial association of n=3 experiments for each strain. Samples were not taken where total association was not measured (n/m) due to cell death.

3.4 Visualisation of bacterial association by Scanning Electron Microscopy

In order to confirm pneumococcal adherence to and destruction of pleural mesothelial cells, infected cell monolayers were visualised over a time course by scanning electron microscopy (SEM) (Figure 3.4).

The laboratory reference strain D39 was employed for these analyses since the association data obtained in the current study showed that this strain exhibited good rates of adherence (Table 3-1) yet did not induce rapid cell death at intermediate infective doses. To allow analysis over a time course of 24 hours and to optimise the visualisation of host-pathogen interactions, an infective dose of 10⁴ cfu/ml was used.

Micrographs illustrated the progressive destruction of pleural cell monolayers over the infection time course, which was concurrent with evident bacterial proliferation. In support of the data obtained in association experiments, at 3 hours post infection, cell monolayers appeared intact and very few pneumococci were associated

(Figure 3.4a). Similarly, at 6 hours few bacteria were adhered to the cells, although the integrity of cellular junctions appeared reduced when compared to at 3 hours. However, by 9 hours post-infection, bacterial association with cells was evident with numerous pneumococci adhered to each cell. Pleural cells appeared rounded and necrotic and cell-cell attachment was severely compromised. At 24 hours post-infection the integrity of pleural cell monolayers was obviously compromised, but although a high degree of cell death was evident, monolayers were not completely destroyed by this infective dose, as seen in our adherence experiments. At high rates of bacterial attachment, pleural cells appear to produce a "stringy" matrix (c) and (d). This perhaps could be a mechanism by which pleural cells attempt to maintain membrane integrity, yet contribute to the fibrosis seen in the pleura in empyema.

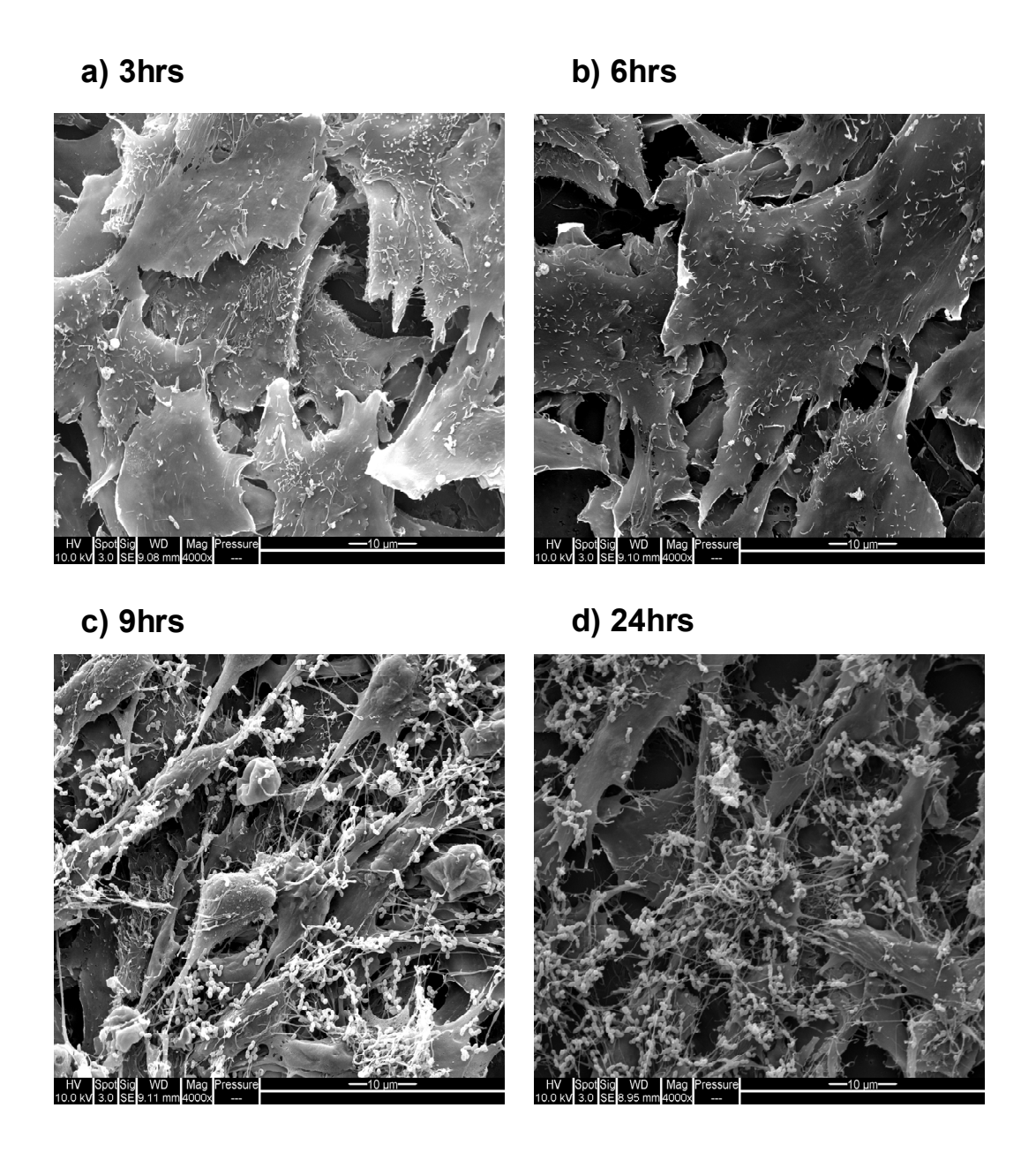


Figure 3-4: Scanning Electron Micrographs of pneumococcal interactions with pleural mesothelial cells.

Met-5A cells were grown to confluence on transwell membranes and were then infected with pneumococcal strain D39 at an infective dose of 10⁴ cfu/ml. At 3, 6, 9 and 24 hours post-infection, membranes were fixed and processed for visualisation by scanning electron microscopy. Images were taken at a 4000X magnification.

3.5 Invasion of human pleural mesothelial cells by Streptococcus pneumoniae.

Invasion of host cells is an essential step in the pathogenesis of IPD, enabling the bacteria to translocate and disseminate to other parts of the host (Agarwal and Hammerschmidt 2009). Additionally, the ability of bacteria to enter non-phagocytic cells may be advantageous for their survival, since internalised bacteria are protected from host innate immune defences and antibiotic therapies (Mandell 1973).

The capacity of pneumococcal strains to invade pleural cells was investigated by isolation of viable bacteria from monolayers challenged with each strain, following treatment with gentamicin. In preliminary experiments, a dose of 200µg/ml of gentamicin was shown to kill >99.9°% of pneumococci within 90 minutes. Invasion experiments were optimised and a final infective dose of 10⁴ cfu/monolayer was used for reference pneumococci and 10⁶ cfu/monolayer for the clinical isolates. This ensured sufficient bacterial association to allow quantification of invasion up to 9hrs post infection without destruction of pleural cell monolayers.

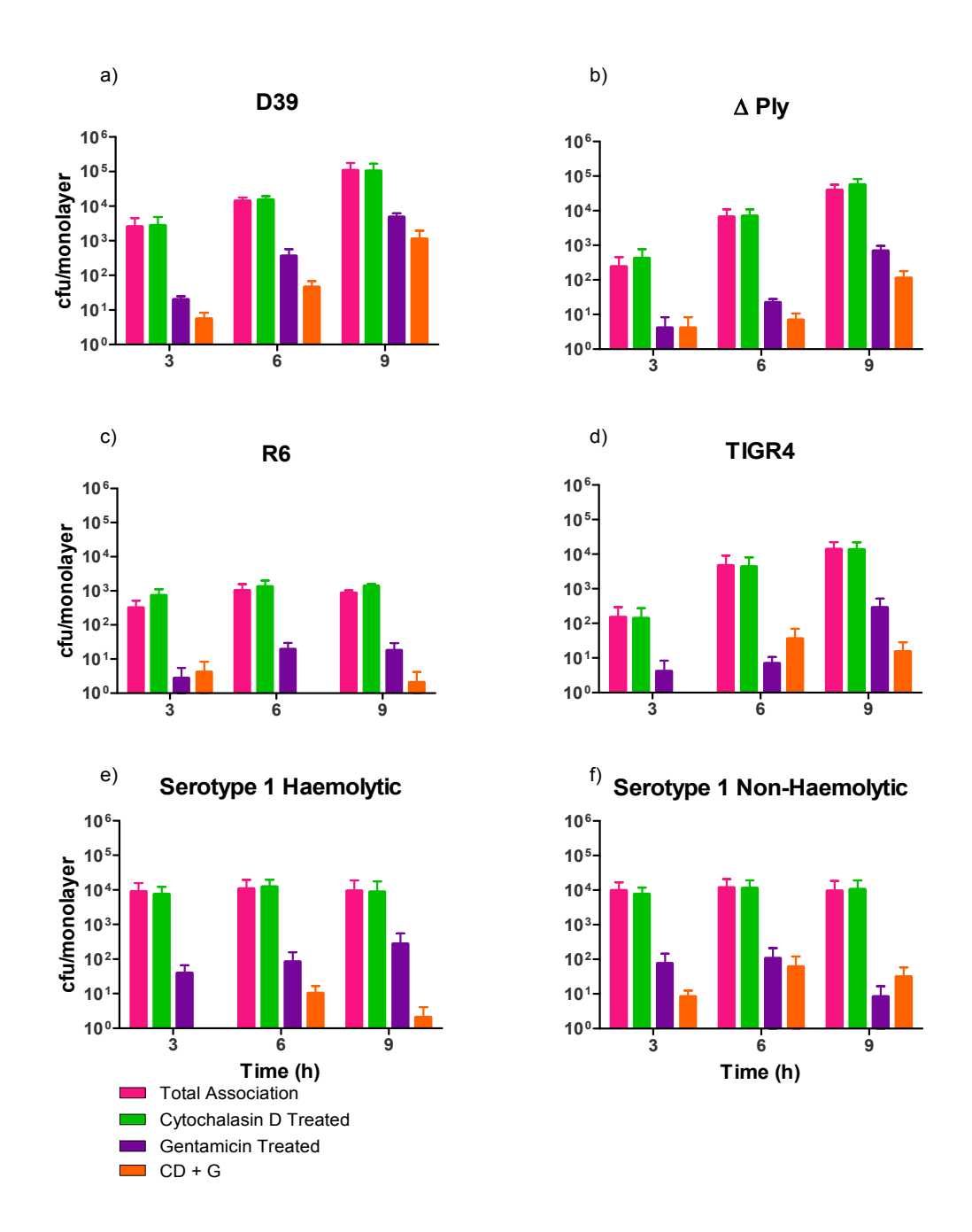


Figure 3-5: Invasion of Met-5A cells by S. pneumoniae.

MET5-A cell monolayers were infected with pneumococcal reference strains D39 (a), D39- Δ Ply (b), R6 (c) and TIGR4 (d) at an infective dose of 10^4 cfu / ml and also the clinical isolates S1 H (e) and S1 – NH (f) at an infective dose of 10^6 cfu / ml and total bacterial association (TA) was measured. Invasive capability of pneumococci was assessed by pre-treating cells with cytochalasin D (CD) to inhibit internalisation of bacteria. Gentamicin (G) treatment of infected monolayers removed extracellular pneumococci and cells were then saponin lysed to liberate invasive bacteria. Comparison of cells treated with gentamicin alone with cells treated with both gentamicin and cytochalasin D (CD+G) suggests the proportion of true invasion. Columns represent the mean bacterial cfu counts and the error bars represent the SEM of n=3 independent experiments.

As seen previously, (Section 3.3) all pneumococcal strains adhered to MET5-A cells in a time dependent manner (Figure 3.3 a-f) and at 9 hours the monolayers were intact. When compared with total bacterial association, pre-treatment of mesothelial cells with cytochalasin D did not affect the capacity of any of the pneumococcal strains to adhere (p>0.05) with no reduction in the number of recovered bacteria. Cytochalasin D is a cell permeable, potent inhibitor of actin polymerisation and as such, it inhibits endocytosis, which is essential to the process of bacterial internalisation. Since internalised bacteria are protected from antimicrobial agents, the invasive potential of pneumococci was investigated by treating Met-5A cells with gentamicin to remove any extracellular bacteria. Viable counts were also performed in samples treated with both cytochalasin D and gentamicin, in order to identify any artefact *e.g.* bacteria adherent to the culture well or that were resistant to gentamicin. True invasion was quantified by comparison of samples treated with gentamicin alone and those treated with both cytochalasin D and gentamicin, and this was calculated as a proportion of the total associated bacteria.

Invasive potential was exhibited by all of the tested pneumococcal strains, albeit to varying degrees, and by 9hrs all strains had significantly invaded the mesothelial monolayer (Table 3-2). At 9hrs, D39-ΔPly was more invasive than its parent strain D39 (1.7% invasion compared to 0.4% respectively). The D39-derived unencapsulated strain R6 was the most invasive strain, with ~2% of adherent bacteria invading by 6 hours, whereas the other stains were non-invasive at this time point. This suggests that decreased capsule expression is advantageous to pneumococcal invasion, perhaps due to increased exposure of surface adhesins and invasins. At 9 hours TIGR4 exhibited a similar rate of invasion to D39-ΔPly and R6, with 2.1% of adherent bacteria being invasive.

Strain	Time Point (Hrs)	% Invasion (of Total Associated)	Significant Invasion
D39	3	0.79	N
	6	2.57	Y
	9	4.50	Y
D39-ΔPly	3	1.71	N
	6	0.33	N
	9	1.74	Y
R6	3	0.87	N
	6	1.89	Y
	9	2.08	Y
TIGR4	3	2.79	N
	6	0.14	N
	9	2.07	Y
S1 – H	3	0.44	Y
	6	0.77	Y
	9	2.95	Y
S1 – NH	3	0.77	Y
	6	0.90	N
	9	0.08	N

Table 3-2: Invasion of pneumococci as a proportion of total associated bacteria.

3.6 Quantitation of Cytotoxicity of S. pneumoniae to Met-5A cells

In vitro, lactate dehydrogenase (LDH) levels are used as a general indicator of tissue damage. To quantify the cytotoxicity elicited in Met-5A cells by infection with pneumococci, monolayers were infected over a bacterial dose range and (LDH) release was measured at 9 hours. In preliminary experiments, no LDH release was detected at the earlier time points of 3 and 6 hours.

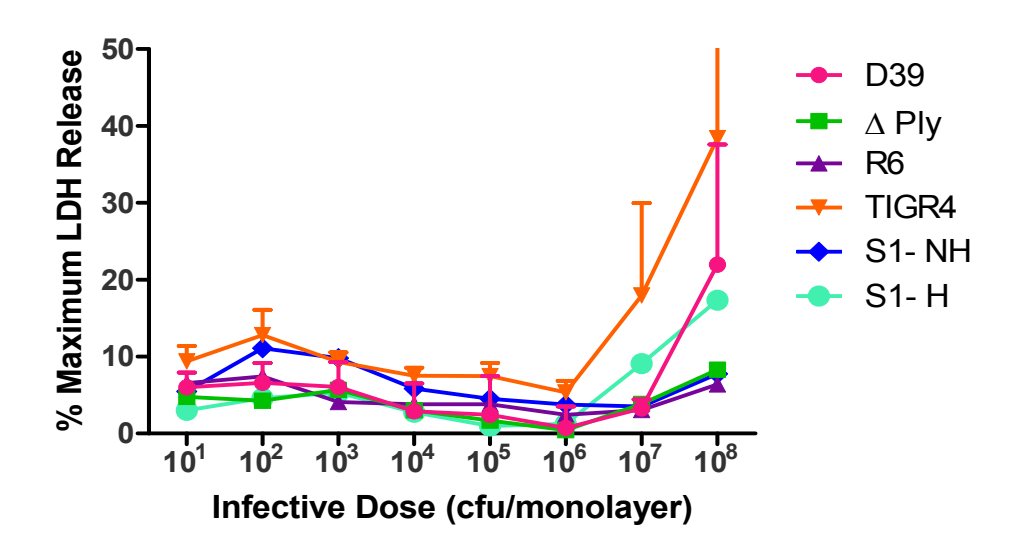


Figure 3-6: Lactate Dehydrogenase release from Met-5A cells following infection with S. pneumoniae.

Pleural mesothelial cell monolayers were infected with the pneumococcal strains D39, D39-ΔPly, R6, TIGR4, S1-NH and S1-H, over a dose range of 101-108 cfu/monolayer. LDH release from cells was quantified at 9 hours, and calculated as a proportion of maximal release, which was determined by chemical lysis of a positive control well. Data represent mean measurements from at least n=3 experiments and the error bars denote the SEM.

In concordance with the total association data, TIGR4 was the most cytotoxic strain at every infective dose, although only at the highest infectious doses of 10^7 and 10^8 cfu / ml was LDH release (18% and 38% of the maximum respectively) significant in comparison to the other bacterial strains. This was also true of S1-H (17%), whilst D39 infection resulted in significant LDH release only at a dose of 10^8 cfu / monolayer (22%). At infective doses of between 10^1 and 10^6 , no LDH-release dependence on dose

was evident for any of the pneumococcal strains. The virulence factor deficient mutants Δ Ply and R6 and the non-haemolytic serotype 1 strain did not exhibit a dose-dependent response for LDH production at 9 hours regardless of bacterial inoculum, with LDH release ranging from 0.5 - 10% of the maximum.

3.7 Cytokine Responses of Met-5A cells to bacterial infection

Cytokines are a heterogeneous group of polypeptide structures which have multiple biological functions. These molecules are key effectors in the initiation, perpetuation and resolution of inflammatory responses (Janeway 2005). Most cells of the immune system, as well as many other host cell types, release cytokines and also respond to them via specific cytokine receptors, although the innate and adaptive immune responses signal through different cytokine molecules (Janeway 2005).

The innate immune system is the primary defence against pneumococcal infection, characterised by the secretion of pro-inflammatory cytokines such as IL-1 β IL-6, IL-8 and TNF- α (Paterson and Mitchell 2006). In order to investigate the nature of the immune response of the human pleura following infection with *Streptococcus pneumoniae*, the production of the pro-inflammatory cytokines IL-6, (Figure 3.6a), IL-8 (b), IL-1 β (c) and TNF- α (d) by Met-5A cells was measured by ELISA.

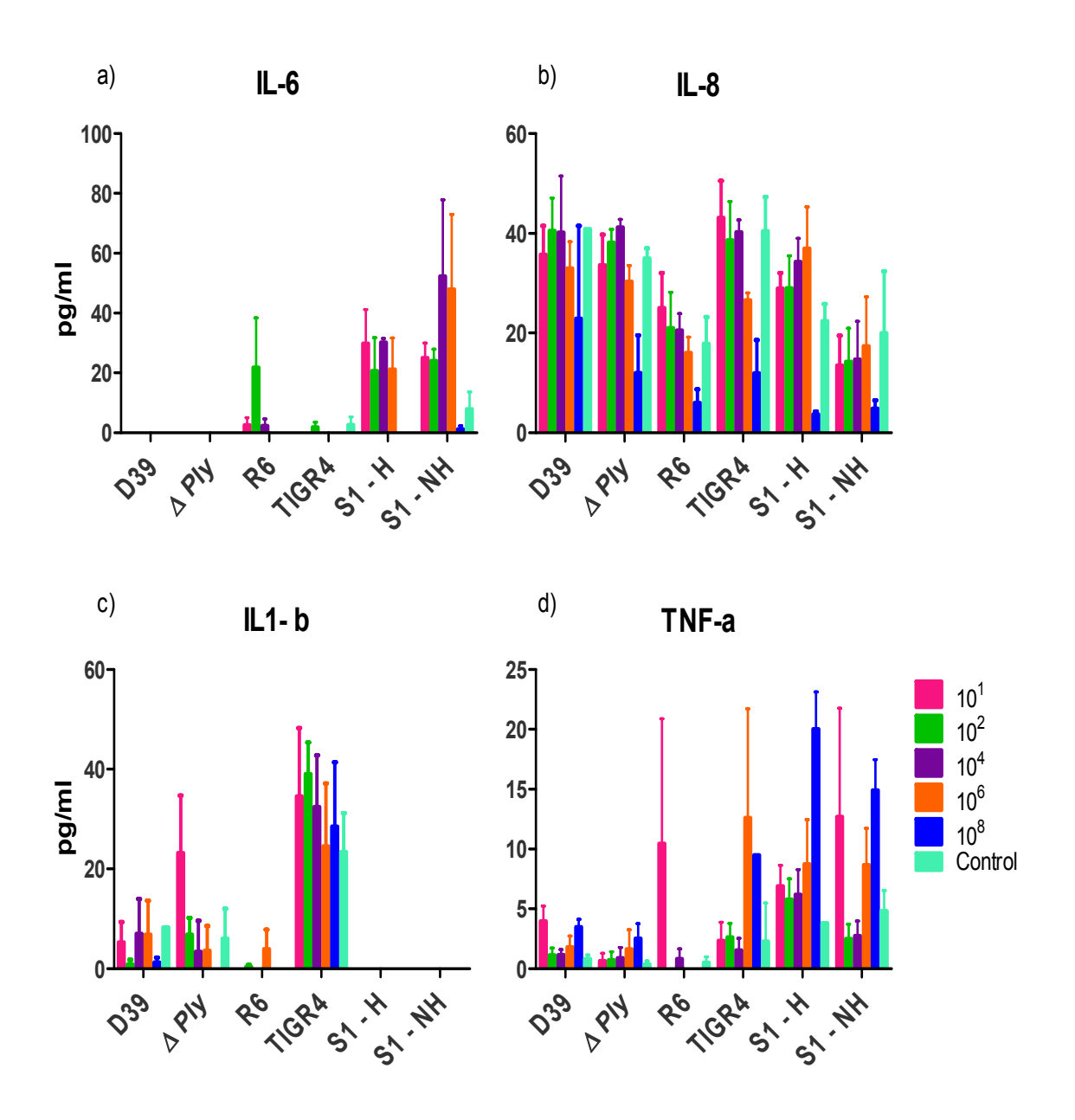


Figure 3-7: The pro-inflammatory response of Met-5A cells to pneumococcal infection.

Met-5A cells were infected with pneumococcal strains D39, D39- Δ Ply, R6 and TIGR4, S1-H and S1-NH at a range of infective doses. Culture supernatants were harvested after 24h, and the immune response of these cells to infection, characterised by secretion of the cytokines IL-6 and IL-8, IL-1 β and TNF- α was quantified by ELISA. Results were subjected to linear regression analysis and data represent the mean measurements of n=3 independent experiments, while error bars represent the SEM.

Unexpectedly, the pro-inflammatory response of Met-5A cells to pneumococcal infection was characterised by very low cytokine production (Figure 3.6 a-d) with all measurements remaining in the pg/ml range, and for all of the cytokines tested, no dose response was apparent.

None of the pneumococcal strains tested induced significant IL-6 production in MET-5A cells when compared with their individual control measurements (Figure 3.6a), although the IL-6 response to both of the clinical isolates was slightly increased relative to reference pneumococci. Conversely, IL-1 β was completely absent in supernatants from cells infected with clinical isolates, but was slightly increased in samples from cells infected with reference strains, albeit negligible levels when compared to their controls, demonstrating the degree of inter-experimental variability. Similarly, when compared to their individual controls, none of the bacterial strains elicited a significant IL-8 or TNF- α response in Met-5A cells. In addition, no consistent dose-response could be observed for any of the cytokines tested. Summarily, none of the tested pneumococcal isolates elicited a pro-inflammatory response in Met-5A cells that was significantly increased from background levels (p>0.05).

The pro-inflammatory response of endothelial cells to bacterial products has been shown to be modulated by anti-inflammatory cytokines such as IL-10, TGF- β and IL-4 (Chen 1995); Bogdan *et al.*, 1991; Kasama *et al.*, 1995). These investigators demonstrated that in the presence of these anti-inflammatory cytokines, the IL-6 and IL-8 responses to LPS in HUVEC cells were abrogated in an additive manner. To test the hypothesis that the absence of a pro-inflammatory response in the current study was due to immune modulation by anti-inflammatory cytokine production by pleural cells, IL-10 and TGF- β were also quantified in experimental supernatants (Figure 3.7).

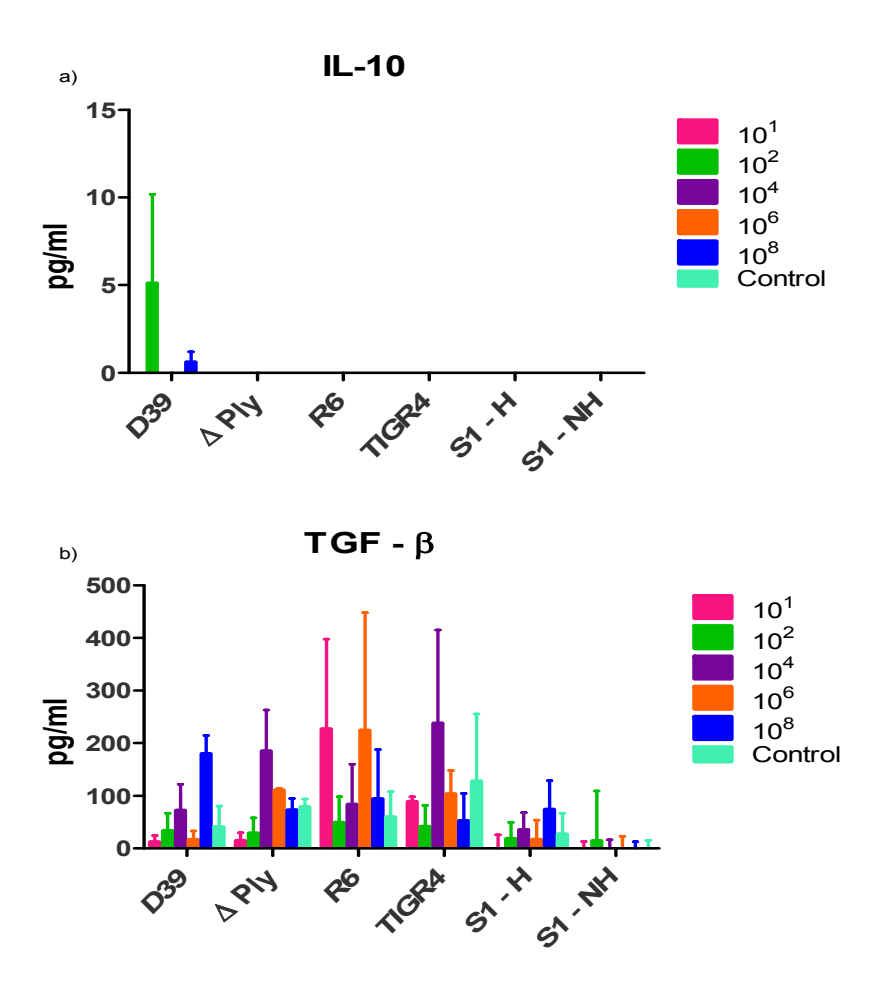


Figure 3-8: The anti-inflammatory response of Met-5A cells to pneumococcal infection.

Met-5A cells were infected with pneumococcal strains D39, D39- Δ Ply, R6 and TIGR4, S1-H and S1-NH at a range of infective doses. Culture supernatants were harvested after 24h, and the production of the anti-inflammatory mediators IL-10 (a) and TGF- β (b) was quantified by ELISA. Results were subjected to linear regression analysis and data represent the mean measurements of n=3 independent experiments, while error bars represent the SEM.

IL-10 was not detected in the experimental supernatants from infections with any of the tested pneumococcal strains (Figure 3.8a). The negligible amount detected in the sample from cells infected with D39 (5pg/ml) was below the detection limit of the ELISA kit used. TGF- β was present in the supernatants at generally higher concentrations than any of the other cytokines measured. Cells infected with TIGR4 or D39- Δ Ply at a dose of 10⁴ cfu/monolayer produced TGF- β at concentrations of 224 and 184 pg/ml respectively, while D39 infection at 10⁸ and R6 at 10⁶ cfu/monolayer

produced 179 and 224 pg/ml respectively. However, a relatively high concentration of the cytokine was also detected in the samples from R6 infection at the lowest bacterial inoculum, illustrating that this effect was not dose dependent. Indeed, although the concentrations of TGF-β in infection culture supernatants were higher than for any other cytokine measured in this system, they were not significantly increased relative to negative controls (p>0.05) (Figure 3.8b). This suggests that rather than being produced directly in response to pneumococcal infection in order to modulate the innate immune response, TGF-β is produced at basal levels by pleural cells.

3.8 Pre-stimulation of Met-5A cells with TNF-a

The mechanisms responsible for the observed absence of cytokine production by pleural cells during pneumococcal infection were further investigated by stimulation of Met-5A cells with TNF- α and the subsequent measurement of the induced inflammatory response. The objective of these experiments was to determine whether low cytokine production by Met-5A cells was due to a refractory property of the cells or a pneumococcal-specific observation. Therefore, the effect that pneumococcal infection had on TNF- α induced cytokine production was assessed.

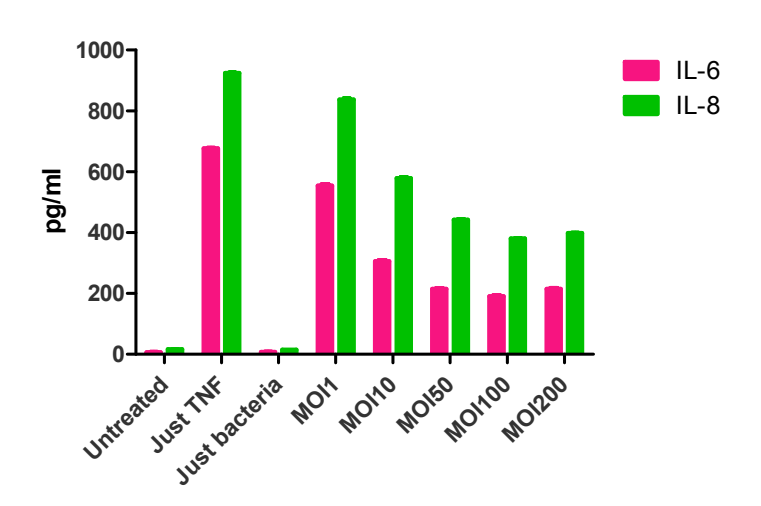


Figure 3-9: TNF-α – induced pro-inflammatory cytokine production in Met-5A cells

Met-5A cells were pre-treated with 100ng/ml of TNF-α for 4 hours prior to infection. Cell monolayers were challenged with *S. pneumoniae* strain D39 at an MOI of 1, 10, 50, 100 or 200 bacteria/cell. Culture supernatants were harvested after 24 hours and IL-6 and IL-8 production was quantified by ELISA.

Stimulation with TNF- α increased the production of both IL-6 and IL-8 by Met-5A cells by >98% when compared to stimulation with pneumococci alone (p<0.05). Introduction of pneumococci to TNF- α pre-stimulated monolayers abrogated the production of both cytokines in a dose dependent manner (Figure 3.9) up to an MOI of 100. Thereafter, this effect was maintained and at an MOI of 200, the percentage of inhibition was in the range of ~60% and 70% for IL8 and IL-6 respectively. At any given MOI, IL-6 production was proportionally more inhibited than IL-8 (*Table 3-3*). In addition, significant inhibition of IL-6 (55% p = 0.0068) was achieved by an MOI of 10 whereas IL-8 production was only significantly inhibited by a bacterial MOI of 50 (52.2% p = 0.0018) or greater. These data demonstrate that Met-5A cells possess the necessary intracellular apparatus to produce cytokines and lend support to the hypothesis that the inflammatory immune response in the pleura is actively suppressed by *S. pneumoniae*.

Cytokine	IL-6		IL-6 IL-8		3
MOI	Inhibition (%)	P-value	Inhibition (%)	P- value	
1	18.1	0.2840	9.5	0.6518	
10	54.9	0.0068	37.4	0.0809	
50	68.3	0.0003	52.2	0.0018	
100	71.8	0.0002	58.8	0.0003	
200	68.3	0.0007	56.9	0.0006	

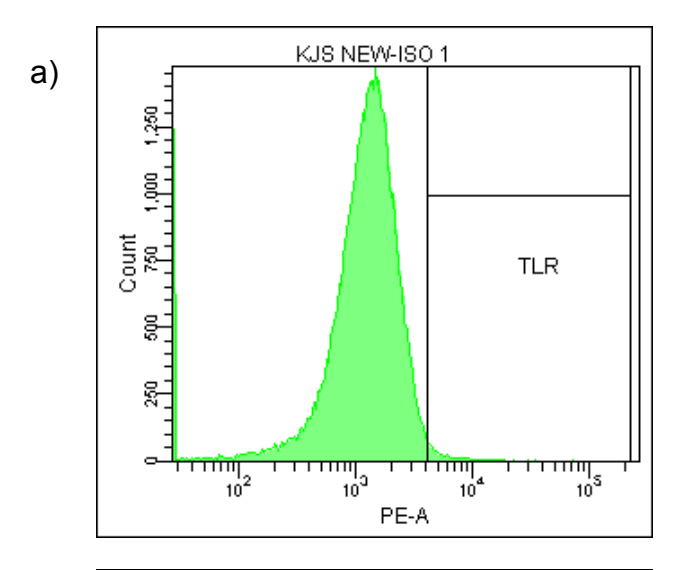
Table 3-3: Inhibition of TNF- α -induced production of pro-inflammatory cytokines by Met-5A cells following pneumococcal infection.

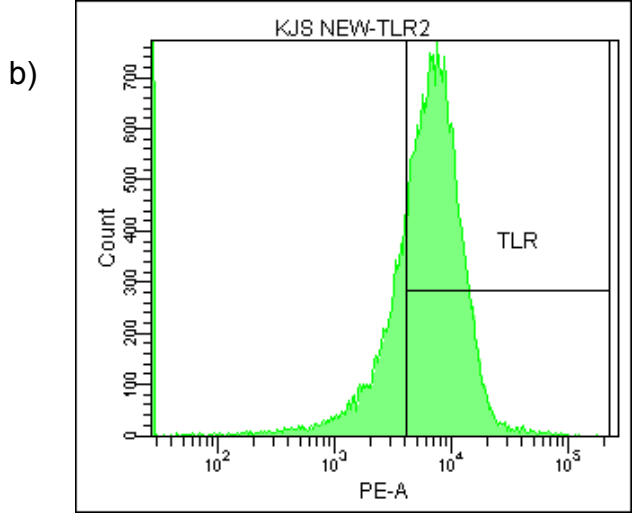
The inhibition of cytokine production is expressed as the proportional decrease in IL-6 or IL-8 production relative to samples treated with TNF- α alone. Data were analysed using a students' t-test, and p-values ≥ 0.05 were considered significant.

3.9 Investigation of Toll-like Receptor Expression in Pleural Mesothelial Cells

The innate immune response to bacterial infections is largely dependent on recognition of bacterial components by pathogen recognition receptors including TLRs. TLR2 is generally thought to be the most important receptor in Gram-positive infections (van der Poll and Opal 2009), since it recognises the cell wall components peptidoglycan, lipoteichoic acid and other surface expressed lipopeptides (Knapp *et al.* 2004; Mogensen *et al.* 2006; Seo *et al.* 2008), whilst the major pneumococcal virulence factor pneumolysin is recognised by TLR4 (Srivastava *et al.* 2005) Low or absent expression of these receptors would compromise the ability of host cells to recognise and bind bacteria and subsequently mount a cytokine response. Thus, in the current study TLR expression in Met-5A cells was characterised by FACS analysis.

The histograms for both Toll-like receptors exhibited a shift to the right relative to the isotype control (Figure 3.10a), albeit to a lesser degree in the case of TLR4 (c) than TLR2 (b). This shift demonstrated that these receptors are expressed in Met-5A cells. Analysis by FACS showed that the proportion of live cells expressing TLR2 was 72% and that 41% of cells expressed TLR4, thereby demonstrating that Met-5A cells possess the PRRs necessary for recognition of key pneumococcal components. The absence of an innate inflammatory response in our infection model therefore, was not due to poor bacterial recognition.





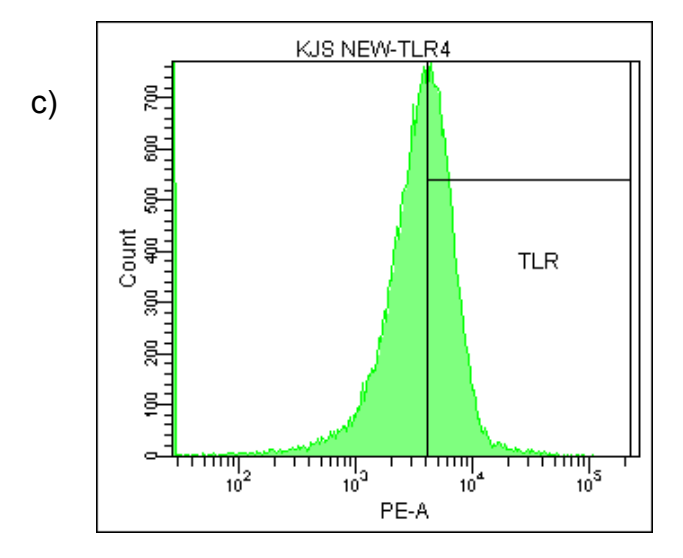


Figure 3-10: Toll-Like Receptor Expression in Met-5A cells.

Met-5A cells were stained with specific PE-conjugated antibodies specific for TLR2 (b) or TLR4 (c) and receptor expression was then analysed by FACS. The TLR expression gate was set at 1% of the isotype control (a). Analysed showed that 72% of Met-5A cells expressed TLR2 and 41% expressed TLR4.

3.10 Antigenic stimulation of Met-5A cells

Since TLR expression data demonstrated that Met-5A cells possessed the capacity to recognise bacterial antigens and TNF-α stimulation experiments showed that these cells were capable of cytokine synthesis, the response of pleural cells to bacterially derived stimuli was investigated. To test the hypothesis that host innate immune responses are actively suppressed by a pneumococcus-specific mechanism, Met-5A cells were treated with differentially derived bacterial antigens and the proinflammatory response to these was quantified (Figure 3.11).

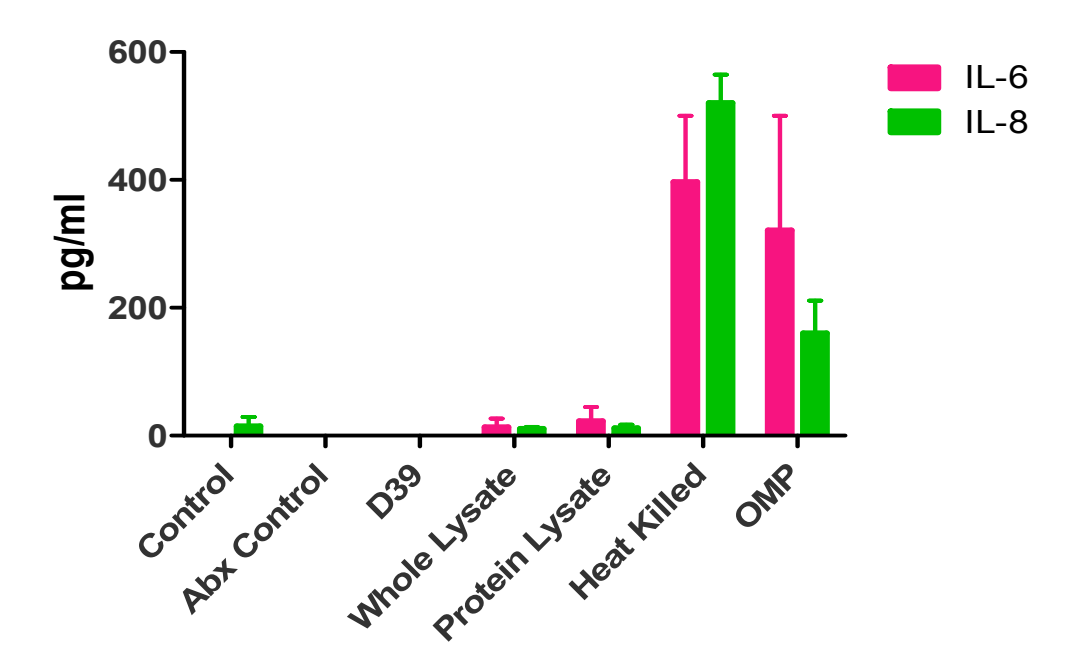


Figure 3-11 Stimulation of Met-5A cells with bacterially derived antigens.

Pleural cell monolayers were challenged with either whole D39 strain pneumococci, whole crude lysate from mechanically lysed bacteria, the protein fraction of the crude lysate or heat-attenuated pneumococci. In addition, monolayers were challenged with whole outer membrane preparation (OMP) derived from the Gram-negative *Neisseria meningitidis* strain MC58. Prior to challenge, total protein concentration in each of the lysates and OMP was quantified by Bradford assay as described in Materials and Methods Section 2.8.4. and cells were subsequently stimulated with 100ng / ml of total protein. Suspensions of whole-live and heat-attenuated bacteria were then adjusted by the same volume factor as the whole lysate to yield an equivalent total protein concentration. Lysates were also treated with gentamicin antibiotic (Abx) to remove any remaining viable bacteria.

As seen previously, infection of pleural mesothelial cell monolayers with whole bacteria did not elicit a cytokine response. When challenged with crude bacterial lysate and the protein fraction of the bacterial lysate the production of both IL-6 and IL-8 was slightly increased in comparison to whole bacteria, but was negligible relative to the negative control (p>0.005). When bacteria were heat attenuated however, production of IL-6 and IL-8 was increased by approximately 400 and 500-fold respectively when compared to the control. Similarly, stimulation of the cells with meningococcal OMP elicited cytokine production that was 320 and 160-fold greater than the control for IL-6 and IL-8 respectively. Notably, IL-8 was induced at higher concentrations than IL-6 when cells were stimulated with heat-killed pneumococci, as was also seen with TNF-α stimulated monolayers (Figure 3.9). However, the converse was true in samples from OMP stimulated pleural cells, where IL-8 concentrations were approximately 50% less than IL-6 concentrations. Together, these data substantiate the hypothesis that *Streptococcus pneumoniae* actively suppresses innate immune mechanisms in host cells, employing factors that are heat labile.

3.11 Cytokine Degradation by S. pneumoniae

Hidalgo-Grass described a bacterial enzyme employed by *Streptococcus pyogenes* to evade host clearance mechanisms by cleavage and degradation of CXC cytokines (Hidalgo-Grass *et al.* 2006). Previous to this, other investigators had shown that *S. pneumoniae* shares homology with *S. pyogenes* at this so called 'streptococcal invasion locus' (sil) (Claverys and Havarstein 2002).

The potential of pneumococci to degrade inflammatory cytokines was therefore investigated in the current model. Bacteria were incubated with TNF- α at a known concentration, which was then quantified after 24 hours.

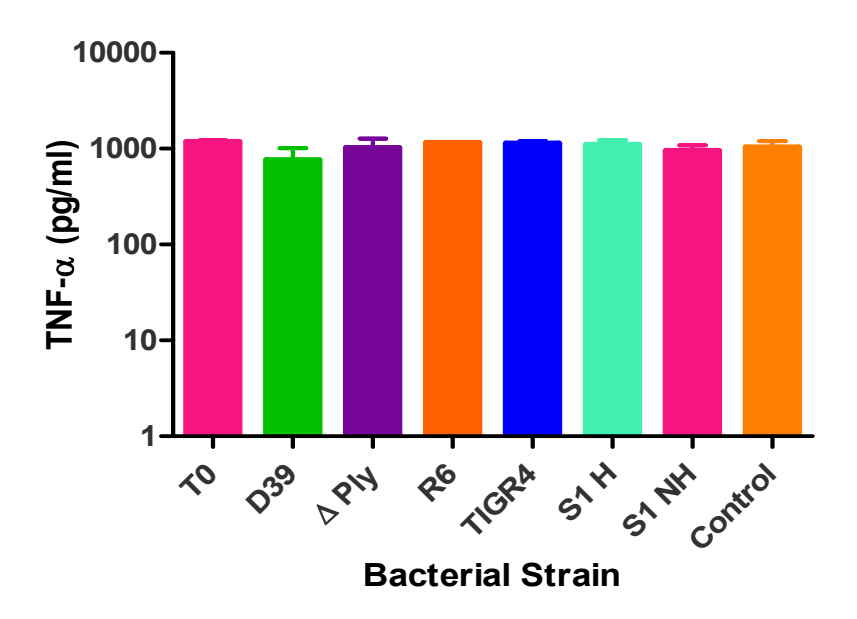


Figure 3-12: Investigation of the potential of pneumococci to degrade TNF-α in vitro.

Pneumococcal strains D39, D39- Δ Ply, R6, TIGR4, S1-H and S1-NH were incubated in infection medium containing 1000pg/ml of TNF- α for 24 hours. TNF- α was then quantified in the medium by ELISA.

Relative to both the TNF- α measurements made at T=0 hours and in the control containing no bacteria, none of the pneumococcal strains tested had reduced the concentration of TNF- α in the culture medium by 24 hours (P>0.005) suggesting that cytokines were not being degraded by pneumococci in our model.

3.12 Summary

The aim of the investigations described hitherto was to characterise the *in vitro* model used in this study and to investigate the interactions of pneumococci with cells of the human pleura. In particular, the hypothesis that pneumococcal strains isolated from clinical empyema patients would exhibit quantifiable differences in their capacity to interact with pleural mesothelial cells was tested.

The association dynamics of clinical isolates differed significantly to those of all reference pneumococci, in that their capacity to adhere to human pleural mesothelial cells was significantly reduced. This reduction in adhesive capacity is correlated with enhanced expression of the major pneumococcal virulence factor, the polysaccharide capsule, as demonstrated by negative staining. Notwithstanding the reduced adhesion of clinical isolates to Met-5A cells, these strains induced cytotoxicity in pleural cells, characterised by destruction of the monolayers, at a comparable, if not enhanced, rate to the reference strains. Conversely, the capsule deficient mutant R6 was able to adhere in greater numbers than its parent and related strains and was the least cytotoxic strain tested in this study, reflecting the virulence exerted by the pneumococcal capsule.

In contrast, pneumolysin expression did not affect the capacity of the bacteria to adhere to and kill Met-5A cells, indicating that this virulence factor is not involved in the initial host-pathogen binding interaction in this model of pathogenesis.

Neither infection with clinical isolates nor reference pneumococci elicited an inflammatory cytokine response from Met-5A cells. FACS analysis of TLR2 and 4 expression on the surface of Met-5A cells confirmed that the absence of an innate immune response was not due to the inability of these cells to recognize pneumococcal antigens. To determine whether the lack of cytokine response was specific to pneumococci, pleural cells were challenged with antigens derived from *Neisseria meningitidis*. The immune response to such antigens and also to heat attenuated pneumococci was significantly increased compared to live pneumococcal infection. Moreover, stimulation of the pleural cell monolayers with TNF-α induced a vigorous IL-6 and IL-8 response, which was abrogated by the introduction of pneumococci in a dose dependent manner. These data demonstrate that Met-5A cells are not refractory to cytokine production, and invite the postulation that the pneumococcus employs a

mechanism of actively suppressing host innate immune defences, such as cytokine production. However, in the current study, it was demonstrated that TNF- α is not degraded by pneumococci, suggesting that these bacteria do not repress the immune response via degradation of cytokine proteins produced by host cells.

CHAPTER 4 RESULTS – GENE EXPRESSION IN STREPTOCOCCUS PNEUMONIAE FOLLOWING HUMAN CELL INTERACTION

4.1 Analysis of differential gene expression in *Streptococcus pneumoniae* during infection of Met-5A cells.

In the current study, the hypothesis that specific virulence genes necessary for the pathogenesis of pleural empyema are differentially expressed in *Streptococcus pneumoniae* upon interaction with pleural cells was tested using a microarray approach. Initially, various methods of bacterial RNA extraction were investigated in order to optimise the model and obtain a sufficient yield of high-quality RNA, whilst simultaneously minimising mammalian RNA contamination.

4.1.1 Optimisation of bacterial RNA extraction method

i) Differential chemical lysis of human pleural mesothelial cells and Streptococcus pneumoniae

It is well documented that methods in which bacterial RNA is co-extracted with host RNA seldom yield microarray-grade RNA (Di Cello et al., 2005). Therefore, we initially sought to employ a method of differential lysis of bacteria and pleural cells to liberate adherent pneumococci for RNA analysis. Due to the inherent instability and short half-life of RNA, the stabilisation reagent RNA Bacteria Protect (Qiagen) was used during the extraction process in order to preserve the integrity of bacterial RNA and allow accurate analysis of the pneumococcal transcriptome during infection of pleural cells. This reagent stabilises RNA in situ without disrupting the bacterial cell wall. Its potential as a differential lysis buffer for bacteria and pleural cells was assessed by comparison of the total RNA yield from Met-5A cell monolayers treated with Bacteria Protect and those lysed by a guanidine thiocyanate (GTC) based buffer RLT (Qiagen, USA). These reagents were applied directly to cell culture flasks and RNA was extracted as described in Materials and Methods Section 2.7.2. Lysis of a confluent monolayer of Met-5A cells with GTC yielded 150ng/µl of RNA, while those treated with RNA protect yielded only 8ng/µl. Visualisation by light microscopy revealed that the Bacteria Protect reagent detached Met-5A cells from the culture vessel but did not sufficiently lyse them to warrant use as a differential lysis buffer.

Many Gram-positive bacteria and mycobacteria are resistant to chemical and detergent modes of lysis due to the production of complex cell walls (Mangan *et al.* 2002). Accordingly, we observed that pneumococci were resistant to chemical lysis with RLT buffer, with a >90% recovery rate of viable bacteria after 10 minutes incubation in the buffer, whereas Met-5A cells were lysed immediately upon contact. Therefore, we investigated the potential use of buffer RLT as a differential lysis buffer in our model, in which infected cell monolayers were lysed, and the lysate centrifuged to pellet bacteria. However, the lysate of Met-5A cells following disruption with RLT was extremely viscous thus rendering adequate removal of the supernatant (containing human cell components) difficult.

ii) Mechanical differential lysis of human pleural mesothelial cells and Streptococcus pneumoniae

Orihuela and colleagues (Orihuela *et al.* 2004) employed a mechanical method of differential lysis, using glass beads to mechanically disrupt mammalian cells, while leaving bacteria intact. In the current study, this method was adapted by scraping cell monolayers from the surface of the culture flask, using a plastic cell-scraper (Greiner BioOne) and transferring them into a bijoux tube with 3mm glass beads, which was then vigorously vortex mixed for 1 minute.

The RNA extracted from bacteria following cell lysis via these methods was analysed by on-chip electrophoresis as described in Materials and Methods Section 2.7.3. The samples appeared to be heavily contaminated with human RNA and proteins and more importantly, no distinct bacterial ribosomal bands were evident (Figure 4.1). This was most likely due to the inefficiency of bacterial isolation from the lysates. However, the presence of endogenous nuclease enzymes, coupled with the inherent instability of RNA reinforced the necessity for timely treatment with protective reagent, and also minimal manipulation of the bacteria prior to RNA extraction. These data indicated that isolation of sufficient quantities of high quality and pure pneumococcal RNA via differential lysis of bacteria and mammalian cells was not viable.

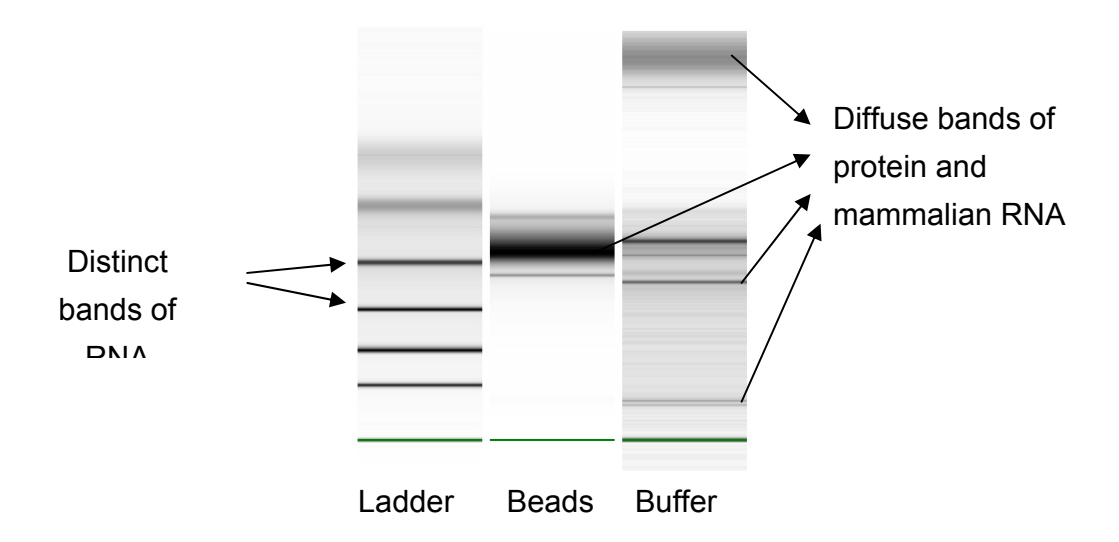


Figure 4-1: Analysis of bacterial RNA quality following disruption of Met-5A cells and pneumococci using various methods of differential lysis.

RNA obtained via each extraction method was analysed by on-chip electrophoresis. Differential lysis of pneumococci and pleural cells resulted in heavy contamination of samples with mammalian RNA, DNA and protein.

iii) Trypsin detachment of pneumococci from pleural cells.

Ryan *at al.* described a method in which *Streptococcus pyogenes* was detached from pharyngeal cell monolayers by trypsin, used at a concentration of 0.005% (v/v) in PBS (Ryan *et al.* 2007). The efficiency of this method (detailed in Section 4.1) of separating adherent bacteria from host cells was also assessed in our infection model. In order to determine the infective dose required to obtain a sufficient yield of bacterial RNA for microarray analysis, pleural cells were infected at various MOIs ranging from 1-200 ($\sim 3 \times 10^6 - 6 \times 10^7$ bacteria/monolayer). At a MOI of 200 bacteria per cell, a recovery rate of >95% was achieved. However, when infected with a lesser MOI of 50 bacteria per cell this proportion decreased to just 13% and no bacteria were recovered at MOIs below this. Due to the observed resistance to chemical lysis, recovered pneumococci were lysed mechanically using lysis matrix tubes as described in Section 2.7.2 and viable counts demonstrated that this method effectively disrupted more than

70% of pneumococci recovered from the monolayer. In addition, mechanical disruption of bacteria negated any potential effects that chemical or enzymatic lysis may have had on bacterial gene transcription.

For microarray analysis at least 2µg of total bacterial RNA is required, hence, a large MOI was necessary to achieve a sufficient yield. In the current study, the highest dose used in association experiments was 10⁸ cfu/monolayer, which corresponded to a MOI of ~250 bacteria/cell. Thus, this MOI was also used for transcriptome analysis. However, the data obtained in the previous infection experiments demonstrated that this high infective dose induced rapid cell death (Section 3.3), which prescribed that only gene expression in adherent pneumococci at the early time point of 2 hours could be investigated. Quantification of the bacterial RNA obtained from experiments in which Met-5A cells were infected for 2 hours with pneumococci at an MOI of 250 bacteria/cell indicated that thirty 75cm² cell cultures flasks would be required in order to obtain a sufficient RNA yield for microarray analysis (Figure 4.2)

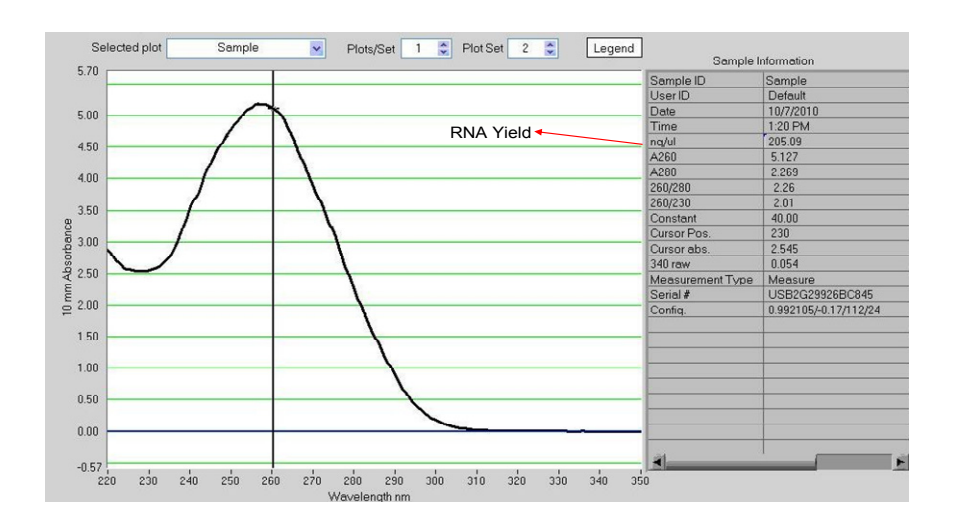


Figure 4-2: Quantification of bacterial RNA following infection of 30x 75cm² cell culture flask with pneumococci at an MOI of 250 bacteria/cell.

Spectrophotometric analysis of RNA extracted from pneumococci detached from Met-5A cells with dilute trypsin demonstrated that 30 cell culture flasks were required to achieve a bacterial RNA yield of $\geq 2\mu g/\mu l$. The smooth peak at A260 indicates the presence of homogeneous RNA

and the A260/A280 ratio of ~2 also demonstrated that the RNA obtained was of high quality and free from significant DNA and protein contamination.

Upon spectrophotometric analysis, RNA samples exhibited absorbance peaks which corresponded with those of control samples, albeit at lower concentrations, thus confirming the presence of RNA in the sample (Figure 4.3a). On-chip electrophoresis of the samples revealed that the integrity and purity of bacterial RNA obtained using the trypsinisation method was much improved in comparison to the samples obtained by differential lysis, although the efficiency of bacterial desorption by trypsin and also of the lysis procedure was variable (Figure 4.3b). Sample 1 demonstrates distinct bands of RNA which correspond to the bands appearing in the respective bacterial control. Similarly, bands of bacterial RNA are evident in sample 3 when compared to its control, although moderate contamination with human RNA was also detected in this sample. However, the quality of sample 2 was poor, with heavy contamination and no distinguishable bands of RNA, and thus this sample was not used for microarray hybridisation.

The effect of trypsin detachment on pneumococcal gene transcription was assessed in a pilot experiment in which RNA from pneumococci treated with trypsin was compared to that from untreated controls by bacterial microarray. The SPv2.0.0 microarrays utilised in this work were manufactured by the Bacterial Microarray Group at St. George's Hospital, University of London as oligonucleotide (60mer) microarrays, designed to sequences from EnsemblBacteria version 5 (http://bacteria.ensembl.org). The arrays were originally designed based on the entirely sequenced TIGR4 genome (Tettelin et al. 2002) and PCR products were amplified to 2236 target genes. However, they have since been extended to include an additional 117 genes from several other pneumococcal strains including R6 (Hoskins et al. 2001). Comparison of gene expression in trypsin treated bacteria with control bacteria was performed by 'dye swap' analysis of microarray slides as described in Section 2.12. In concordance with reports by Ryan and colleagues (Ryan et al. 2007) microarray data from this pilot experiment concluded that there were no differences in gene expression between bacteria treated with trypsin and controls (personal communication, Dr Jason Hinds), thus validating the trypsin detachment method for bacterial transcriptome analysis

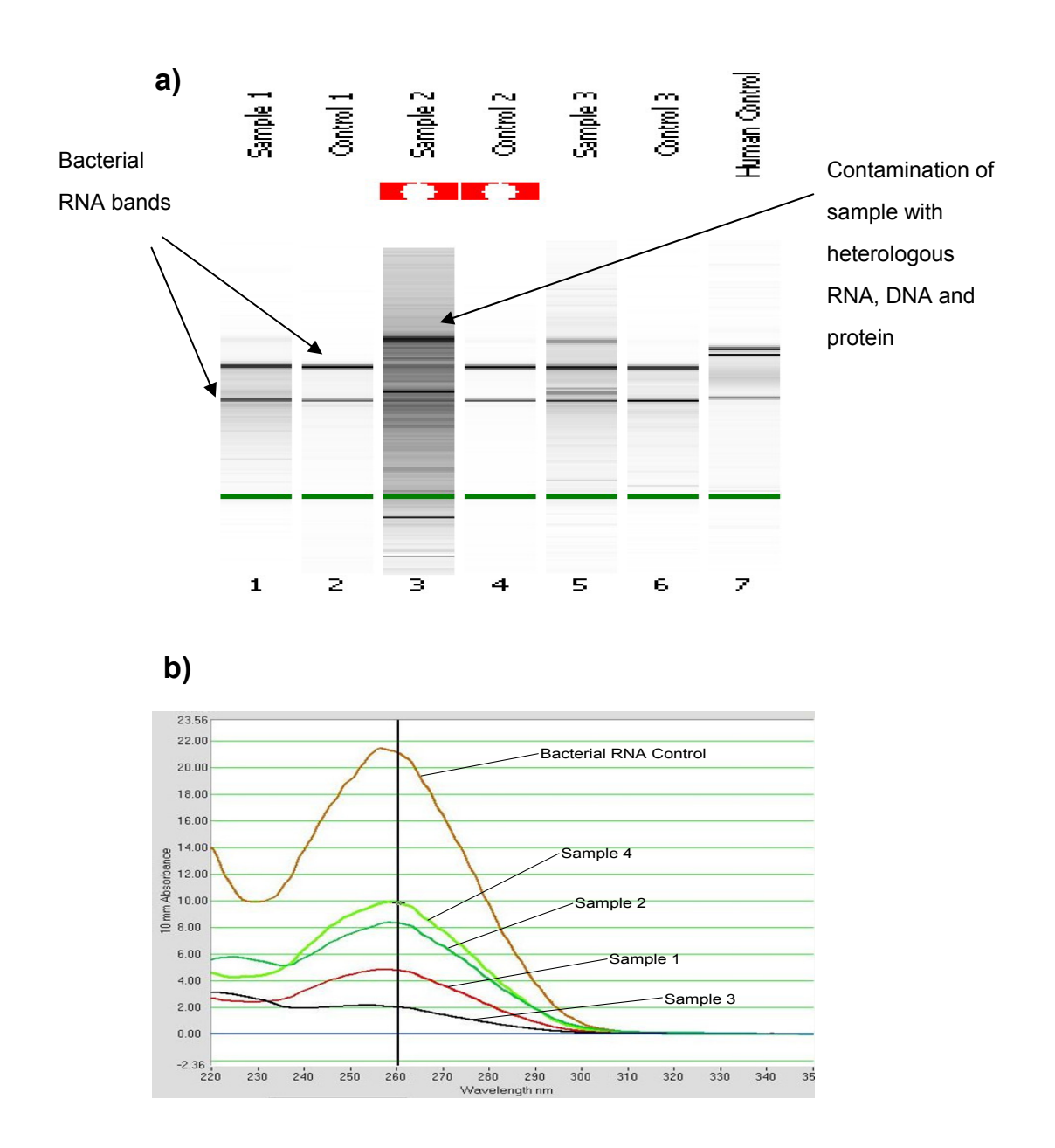


Figure 4-3: Analysis and quantification of bacterial RNA following trypsin detachment.

Confluent monolayers of Met-5A cells in thirty 75cm2 cell culture flasks were infected with D39 strain pneumococci at a MOI of 250 bacteria per cell for 2 hours. Bacteria were recovered from the monolayers using PBS containing 0.005% trypsin and the RNA extracted. On-chip electrophoresis (a) and spectrophotometric analysis (b) showed variability in sample quantity and integrity. Bands of bacterial RNA corresponding to control samples were evident in most test samples, although some host RNA contamination was also detected.

4.2 Microarray analysis of differential gene expression in *Streptococcus* pneumoniae following association with Met-5A cells.

Gene expression in *Streptococcus pneumoniae* during infection of pleural mesothelial cells was investigated by microarray. Probes were prepared and hybridised to a SPv2.0.0 microarray slide as described in Materials and Methods Section 2.13 and data were acquired using an Affymetrix GeneChip analyser (Affymetrix, USA).

A photomultiplier tube is an optical energy detector which amplifies the fluorescent signal emitted by individual spots on the microarray. The photomultiplier tube gain value is defined as the total number of electrons collected at the anode as a result of a single electron emission at the cathode, thus an increase in gain results in increased signal amplification. The gain was optimised for each microarray individually, so that signal intensity could be maximised without any spot becoming saturated. This ensured more accurate quantitation of changes in gene expression.

A gridmap was then assigned to each array, using BlueFuse for Microarrays 3.5© software (BlueGnome Ltd., UK), which defined the exact location and the parameters of each spot. The fluorescent intensity and homogeneity of each spot was then analysed to calculate a confidence value. A data acquisition protocol was then run, which filtered out controls and spots with a confidence value of < 0.1.

Heterogeneity between slide batches, differences in spot morphology and the degree of background signal introduce variability into microarray experiments. Thus a process of data normalisation is required to enable direct comparison between microarrays. Differences between Cy3 and Cy5 dye incorporation were normalised by dye swap normalisation as described in Materials and Methods Section 2.13. A local weighted scatterplot smoothing (LOWESS) normalisation algorithm was then applied to each array, which assumed that no change would be observed in most genes and so normalised to a mean red:green ratio of 1 as illustrated in Figure 4.4. Filtering algorithms were then applied to the fused data in GeneSpring GX v7.3.1 software to identify differentially expressed pneumococcal genes as illustrated in Fig 4.5.

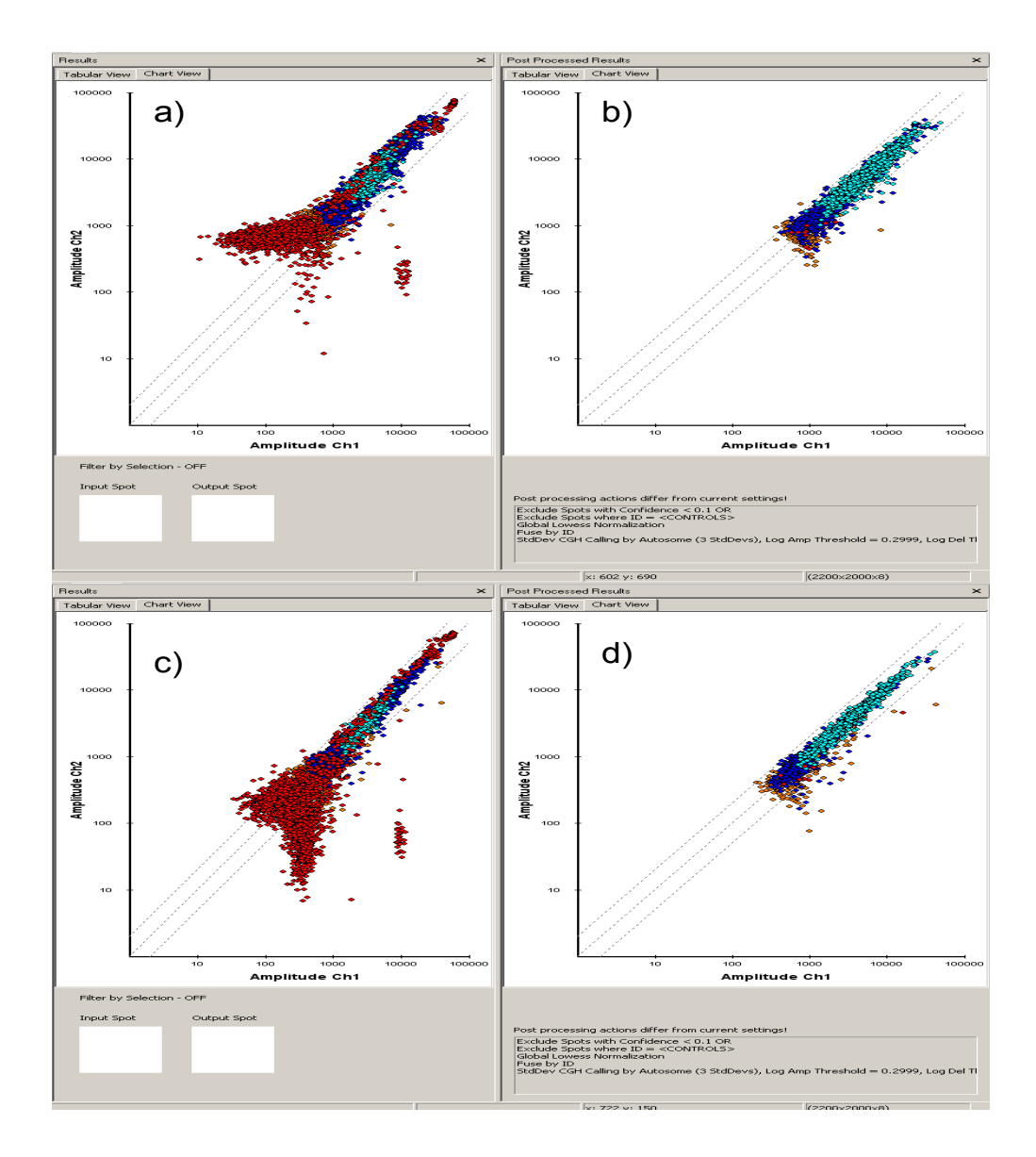


Figure 4-4: LOWESS normalisation was applied to bacterial microarrays to compensate for heterogeneity between slides and inherent experimental variability.

Scatterplots in Figure 4.4a and c correspond to two separate dye swap experiments for a single sample replicate. In (a) the control was labelled with Cy3 and the test sample was labelled with Cy5, while in (c) the control was labelled with Cy5 and the test with Cy3. This allowed for the normalisation of bias introduced by differences in dye incorporation efficiency, and also the identification of any staining artefact. For both there are significant "tail artefacts" resulting from low signal hybridisations. Scatterplots (b) and (d) were generated when Global LOWESS normalisation was applied to the data. Such normalisation also compensates for differences in PMT gain values between arrays. Data for duplicate spots on individual arrays was then fused, although the confidence value of each duplicate was weighted accordingly and mean expression fold-change was calculated for individual genes.

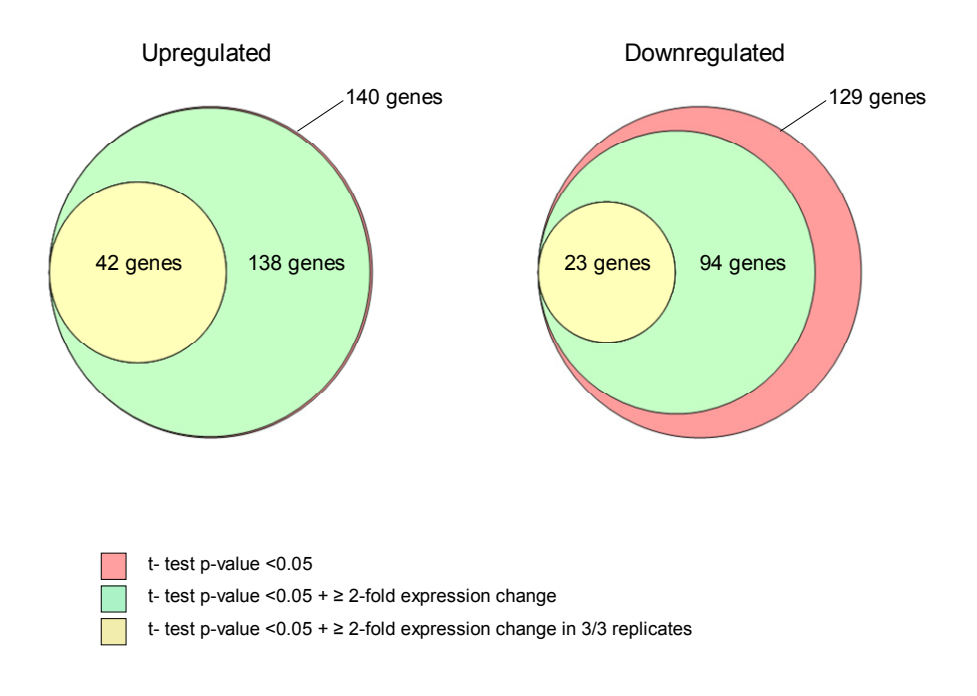


Figure 4-5: Differentially expressed bacterial genes were identified by the application of a series of filtering algorithms to the data.

Gene lists generated by GeneSpring GX software were initially filtered using the students' t-test analysis of variance (shown in pink) to yield only those genes that showed a p-value of > 0.05. Of these genes, only those displaying a mean ≥ 2 -fold expression change were considered further (shown in green). A final filtering algorithm was then applied to these genes, in which only those genes that passed the previous filtering criteria in all biological replicates for a particular experimental condition (shown in yellow) were considered further.

Of the 138 genes that demonstrated a mean 2-fold up-regulation, 96 genes (69.6%) failed to meet the filtering condition that expression change be at least 2-fold in all biological replicates. Of these, 80 genes (83.3%) were filtered out based on the failure of only one replicate in the set to exhibit at least 2-fold upregulation, Of note, included in these was the canonical virulence gene pneumolysin, which had a mean 4-fold increase in expression, but was only upregulated 1.4-fold in one of the replicate set. Similarly, the adhesion lipoprotein, laminin-binding protein, had a mean 2.1-fold expression increase, but just 1 of the replicate set failed to meet the established criteria for transcription analysis. The remaining 16 genes (16.7%) were removed from the gene list based on the failure of 2 biological replicates failing to exhibit at least 2-fold

upregulation. A comprehensive list of gene expression in individual replicates can be found on the accompanying appendix CD.

Ninety four genes exhibited a mean 2-fold downregulation, but of these only 23 were downregulated in all replicates. Of the other 71 genes, 50 were failed by just 1 of the replicate set and 21 genes by 2 failures. Interestingly, included in those genes which failed to meet cut-off criteria in just 1 replicate were 4 of the serotype 2 capsular loci, namely cpsH, cpsI, cpsJ and cpsL which had fold-expression decreases of 2.6, 2.7, 2.2 and 2.2 respectively (Appendix CD). In total 65 pneumococcal genes were identified as satisfying all of the criteria of the filtering algorithms described in section 4.2. Of these, 42 genes (64.6%) were upregulated and 23 genes (35.4%) were down-regulated (Figure 4-6).

Differentially expressed genes in adherent pneumococci were involved in metabolic and homeostatic pathways. Fold increases in expression levels ranged from 2.4- to 10.0-fold. The most highly upregulated gene was SP-1242 or *glnQ*, with a 10-fold increase in expression, although SpTIGR4-1306 or *gdhA*, which had a fold expression increase of 8.7 had the smallest p-value of all the upregulated genes (Table 4-1). Fold expression changes in downregulated genes ranged from a 2.1-fold decrease in SpTIGR4-2022 or *ptcC* to a 28.4-fold downregulation of the gene SpTIGR4-2026 or *adhE* (Table 4-2).

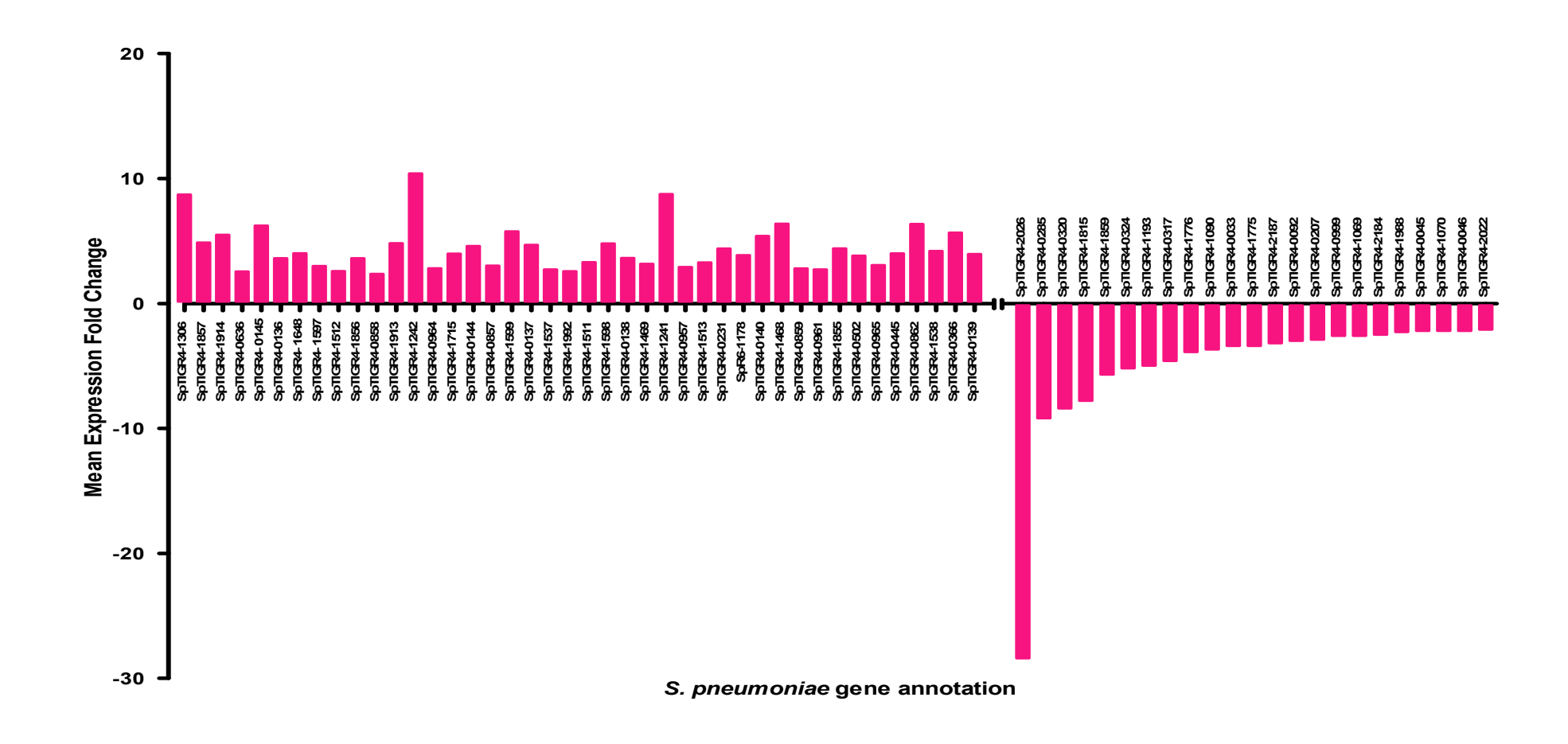


Figure 4-6: Mean expression fold changes in pneumococcal genes which exhibited \geq 2-fold differential expression.

Pneumococcal gene expression data were analysed with a series of filtering algorithms. The expression fold changes of genes which satisfied all of the filtering criteria are shown above.

Gene	Gene Symbol	t-test p- value	Mean Fold- Expression Change	TIGR4 Gene Product
SpTIGR4-1306	gdhA	0.0000353	8.7	Glutamate dehydrogenase
SpTIGR4-1857	czcD	0.0000353	4.9	Cation efflux system protein
SpTIGR4-1914	SP_1914	0.0000353	5.5	Hypothetical protein
SpTIGR4-0636	ABC-NBD	0.000134	2.6	ABC transporter, ATP-binding protein
SpTIGR4-0145	SP_0145	0.000135	6.2	Hypothetical protein
SpTIGR4-0136	SP_0136	0.000156	3.6	glycosyl transferase, family 2
SpTIGR4-1648	psaB	0.000216	4	Manganese ABC transporter, ATP-binding protein
SpTIGR4-1597	SP_1597	0.000216	3	Hypothetical protein
SpTIGR4-1512	atpF	0.000216	2.6	F0F1 ATP synthase subunit B
SpTIGR4-1856	SP_1856	0.000227	3.6	Transcriptional regulator, MerR family
SpTIGR4-0858	SP_0858	0.000227	2.4	Hypothetical protein
SpTIGR4-1913	SP_1913	0.000245	4.8	
SpTIGR4-1242	glnQ	0.000302	10	Amino acid ABC transporter, ATP-binding protein
SpTIGR4-0964	pyrD	0.000401	2.8	Dihydroorotate dehydrogenase 1B
SpTIGR4-1715	ABC-NBD	0.000407	4	ABC transporter, ATP-binding protein
SpTIGR4-0144	SP_0144	0.000407	4.6	hypothetical protein
SpTIGR4-0857	SP_0857	0.000433	3	
SpTIGR4-1599	truA	0.000447	5.8	tRNA pseudouridine synthase A
SpTIGR4-0137	ABC-NP	0.000447	4.7	ABC transporter, ATP-binding protein
SpTIGR4-1537	SP_1537	0.000447	2.7	hypothetical protein
SpTIGR4-1992	SP_1992	0.000447	2.6	cell wall surface anchor family protein
SpTIGR4-1511	atpH	0.000547	3.3	F0F1 ATP synthase subunit delta
SpTIGR4-1598	pdxK	0.000547	4.8	Phosphomethylpyrimidine kinase

SpTIGR4-0138	SP_0138	0.00055	3.6	hypothetical protein
SpTIGR4-1469	Nox	0.000609	3.2	NADH oxidase
SpTIGR4-1241	glnP	0.000721	8.8	Amino acid ABC transporter, amino acid-binding protein/permease protein
SpTIGR4-0957	SP_0957	0.000838	2.9	ABC transporter, ATP-binding protein
SpTIGR4-1513	atpB	0.000988	3.3	F0F1 ATP synthase subunit A
SpTIGR4-0231	Adk	0.00113	4.4	Adenylate kinase
SpR6-1178	SPR1178	0.00116	3.9	
SpTIGR4-0140	Ugd	0.00117	5.4	
SpTIGR4-1468	Pdx1	0.00138	6.4	pyridoxine biosynthesis protein
SpTIGR4-0859	SP_0859	0.00143	2.8	Membrane protein
SpTIGR4-0961	rplT	0.00207	2.7	50S ribosomal protein L20
SpTIGR4-1855	adhB	0.00268	4.4	alcohol dehydrogenase, zinc- containing
SpTIGR4-0502	glnA	0.00268	3.8	Glutamine synthetase, type I
SpTIGR4-0965	lytB	0.00339	3.1	endo-beta-N- acetylglucosaminidase
SpTIGR4-0445	ilvB	0.00382	4	acetolactate synthase catalytic subunit
SpTIGR4-0862	rpsA	0.00393	6.4	30S ribosomal protein S1
SpTIGR4-1538	SP_1538	0.00409	4.2	Cof family protein/peptidyl-prolyl cis-trans isomerase, cyclophilin type
SpTIGR4-0366	aliA	0.00586	5.7	oligopeptide ABC transporter, oligopeptide-binding protein AliA
SpTIGR4-0139	SP_0139	0.00604	4	hypothetical protein

Table 4-1: Up-regulated pneumococcal genes following adherence to human pleural mesothelial cells.

Differential gene expression was analysed by microarray in pneumococci adherent to Met-5A cells at 2 hours post challenge. Genes demonstrating \geq 2-fold up-regulation in all (n=3) replicates are listed in rank order of significance (t-test p-value).

Gene	Symbol	t-test p-value	Mean Fold- Expression Change	TIGR4 Gene Product
SpTIGR4- 2026	adhE	0.00407	28.4	alcohol dehydrogenase,
SpTIGR4- 0285	adhP	0.00895	9.2	alcohol dehydrogenase
SpTIGR4- 0320	Gno	0.0068	8.4	Gluconate 5-dehydrogenase
SpTIGR4- 1815	trpD	0.0466	7.8	Anthranilate phosphoribosyltransferase
SpTIGR4- 1859	SP_1859	0.00267	5.7	transporter, putative
SpTIGR4- 0324	PTS-EII	0.00501	5.2	PTS system, IIC component
SpTIGR4- 1193	lacA	0.0119	5.0	Galactose-6-phosphate isomerise subunit LacA
SpTIGR4- 0317	kdgA	0.00531	4.6	keto-hydroxyglutarate- aldolase/keto-deoxy- phosphogluconate aldolase
SpTIGR4- 1776	trxA	0.0108	3.9	Thioredoxin
SpTIGR4- 1090	SP_1090	0.00642	3.7	redox-sensing transcriptional repressor Rex
SpTIGR4- 0033	SP_0033	0.00993	3.4	hypothetical protein
SpTIGR4- 1775	SP_1775	0.0309	3.4	hypothetical protein
SpTIGR4- 2187	SP_2187	0.0225	3.2	hypothetical protein
SpTIGR4- 0092	ABC- SBP	0.0309	3.0	ABC transporter, substrate-binding protein
SpTIGR4- 0207	SP_0207	0.0233	2.9	hypothetical protein
SpTIGR4- 0999	ccdA	0.00501	2.6	cytochrome c-type biogenesis protein CcdA
SpTIGR4- 1069	ABC- SBP	0.00727	2.6	hypothetical protein
pTIGR4-2184	glpF	0.0135	2.5	glycerol uptake facilitator protein

SpTIGR4- 1988	SP_1988	0.00304	2.3	immunity protein, putative
SpTIGR4- 0045	purL	0.00451	2.2	phosphoribosylformylglycinamidin e synthase, putative
SpTIGR4- 1070	ABC- MSP	0.0158	2.2	hypothetical protein
SpTIGR4- 0046	purF	0.0154	2.2	Amidophosphoribosyltransferase
SpTIGI	R _' ptcC	0.00022	2.1	PTS system, IIC component

Table 4-2: Downregulated pneumococcal genes following adhesion to human pleural mesothelial cells.

Pneumococcal gene expression following adherence to pleural mesothelial cells was analysed by microarray at 2 hours post challenge. Genes demonstrating \geq 2-fold upregulation in all (n=3) replicates are listed in rank order of mean fold expression change.

To lend support to specific biological models, microarray experiments have typically been validated on a gene by gene basis, often with only the most differentially expressed genes being selected for validation (Song et al. 2008b); (de Saizieu et al. 2000; Hendriksen et al. 2007). However Miron et al. purported that the validation of just a few arbitrarily selected genes was not reflective of the authority of the entire microarray experiment, since such validation procedures failed to meet optimal sampling and statistical requirements. For example, sampling of only those genes with the largest fold-changes in expression level exacerbates the statistical artefact of "regression towards the mean", which can result in underestimation of the global level of agreement between microarrays and validated samples. Instead, these investigators proposed a model of global validation, advocating the selection of genes through a random process, which allows evaluation of the general quality of the experiment, and also the extrapolation of the validation results of a subset of genes to the remainder of the microarray. The most robust of the sampling methods trialled in their study was one in which differentially expressed genes were stratified and then genes randomly selected from each stratum for validation (Miron et al. 2006). The degree of agreement between the fold change measurements in the microarray experiments and the RTqPCR validated genes can then be represented by the concordance correlation coefficient (CCC), which subsequently can be applied to all genes on the array as a means of global validation.

Thus, in the current study, this methodology was employed for validation of the bacterial gene expression microarray. Both the up- and down- regulated gene lists above were divided into strata each containing 3 genes. Random number generating software (Apple Inc., USA) was used to select a number between 1-3 for each stratum, and the corresponding gene was then selected for validation. The genes highlighted in yellow in Tables 4-1 and 4-2 above are those that were selected using this random stratification method. Those highlighted in green are the most differentially expressed genes in each list and these were validated separately. Gene expression in these samples was quantified by RT-qPCR. However, the selected house-keeping gene DNA gyrase (*GyrA*) was also highly expressed by pneumococci in this study, therefore the bacterial microarray data obtained could not be validated within the scope of the current study.

4.3 Summary

Transcriptomic analyses of pneumococci adherent to Met-5A cells were undertaken to address the hypothesis that empyema-causing pneumococci differentially express genes which enable the manifestation of pleural disease.

Various experimental techniques were trialed in order to optimise the process of bacterial RNA extraction, since low RNA yield and excessive contamination with host materials in such investigations is often encountered (DiCello *et al.* 2005). A method of trypsin detachment was used to isolate bacteria adherent to Met-5A cells and preliminary investigations confirmed that treatment of bacteria with dilute trypsin did not affect gene transcription. Optimisation experiments also determined that a high pneumococcal MOI of 250:1 bacteria/cell, and infection of a total of thirty 75cm² cell culture flasks was necessary to obtain sufficient bacterial RNA to perform microarray analysis.

Stringent filtering criteria were applied to the microarray data, allowing only those genes that were consistently differentially regulated in all replicates to be considered. This method rendered a total of 65 differentially expressed genes for further analysis, lending support to the hypothesis that pneumococci differentially modulate their gene expression during interaction with cells of the human pleura. Most of these 65 gene perturbations were upregulations, although the most significant fold-change overall was the 28-fold downregulation of the pneumococcal gene *adhE*, which codes for an alcohol dehydrogenase enzyme.

The imposition of rigorous filters excluded many genes based on the failure of only a single replicate within a set to satisfy the criteria. Interestingly, among these were the canonical virulence factors pneumolysin and the polysaccharide capsule which were up- and down-regulated respectively. These observations lend further support to the data obtained in Chapter 3, whereby capsule expression was demonstrated to be detrimental to pneumococcal interaction with pleural mesothelial cells. Despite omitting such "interesting" genes from the experimental read-out, the method of analysis used in the current study affords confidence that the results reported are robust and reproducible. The arbitrary design of filtering algorithms used in microarray studies, however, is a well described limitation of this technology, since no

universal system of analysis exists and exclusion criteria differ widely between studies, thus impeding ready comparison.

RT-qPCR validation of differential expression of those genes identified by microarray would further substantiate the data, but incidental high expression of the chosen housekeeping gene, DNA gyrase, did not allow for PCR verification within the scope of this study.

CHAPTER 5 RESULTS - GENE EXPRESSION IN HUMAN PLEURAL MESOTHELIAL CELLS FOLLOWING CHALLENGE WITH PNEUMOCOCCI

5.1 Analysis of gene expression in human pleural mesothelial cells following challenge with *Streptococcus pneumoniae*.

To investigate the innate immune response of the human pleura to pneumococcal infection, Met-5A cell monolayers were challenged with either the laboratory reference strain D39, the clinical empyema isolate S1-H, the corresponding crude lysate of each of these strains or heat attenuated pneumococci. RNA was extracted from cells at 2 hours post-challenge and the transcriptome of Met-5A cells following infection with pneumococci was analysed by microarray as described in Section 2.15.

The human microarray slides used in this work were manufactured in the Post-Genomic Technologies Facility at the University of Nottingham, (http://genomics.nottingham.ac.uk/) and contain approximately 34, 000 gene targets. Hybridised slides were scanned on an Agilent BA scanner (Agilent Technologies, USA), first at 570nm to excite Cy3 and then at 650nm to excite Cy5 and the gain value was optimised individually for each array, as described previously. For each array, 2 digital images were obtained, which were overlaid using the manufacturer's software (Figure 5-1). Images were then exported to and analysed using GenePix® Pro v6.0 software (Molecular Devices LLC, USA), in which fluorescent intensity values were assigned to each spot. Pixels surrounding each spot were also analysed to calculate local background and spots that were less than 2 standard deviations above background were removed from further analysis. The median of duplicate spots was calculated for each image and raw data was then expressed as a log ratio of Cy5/Cy3 (sample/control probe). Intra- and inter-array global LOWESS normalisation was then performed in J-Express Pro software (MolMine, Norway) and ratios were then used to rank genes and calculate fold changes. False discovery rate (FDR) is the expected proportion of false positives in a data set. An FDR limit of $\leq 5\%$ was applied to the genelists and genes with an FDR above this cut-off were excluded from analysis. The 10 most differentially up and down regulated genes for each condition are shown in Tables 5-1-5-10.

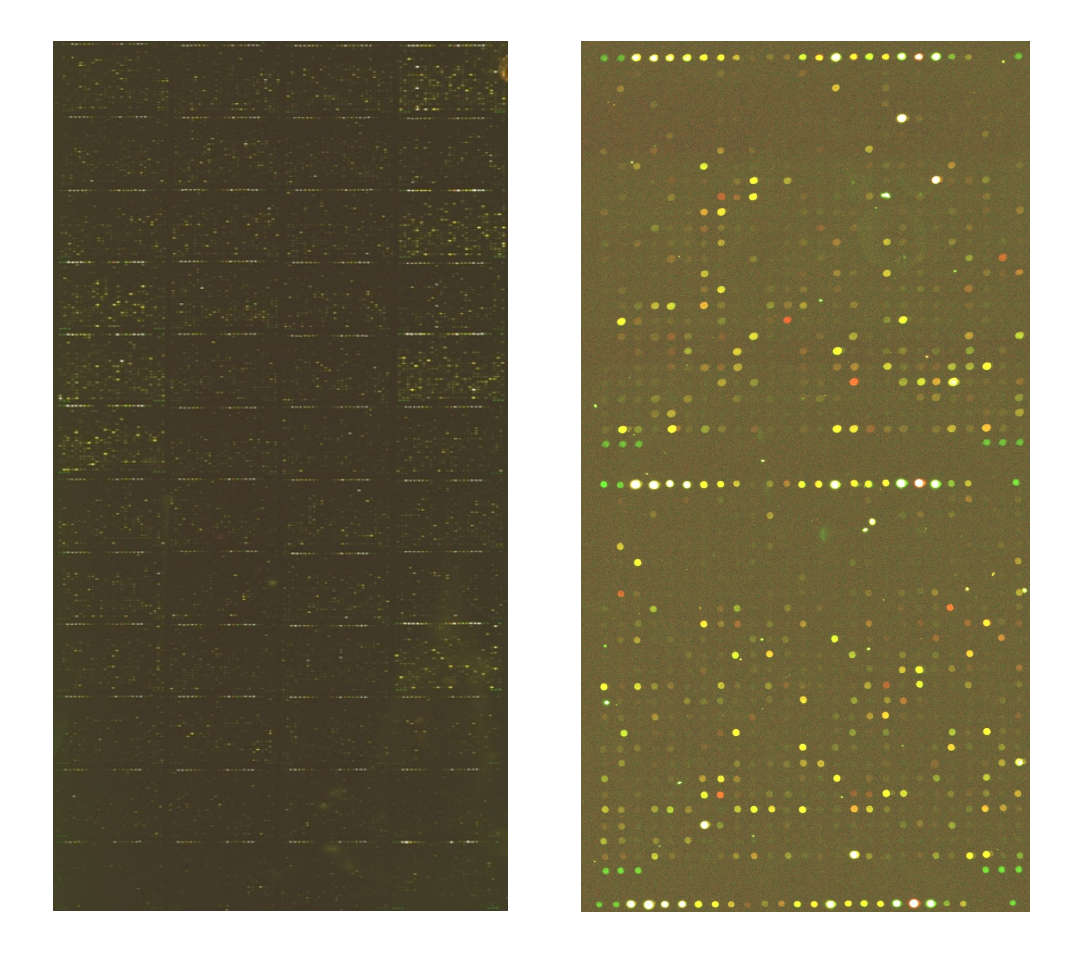


Figure 5-1: Overlaid microarray scan images illustrating differential gene expression in human pleural mesothelial cells following infection with *Streptococcus pneumoniae*.

Two digital images were generated by scanning each microarray slide at 570nm and 650nm to excite the Cy3 and Cy5 fluorophores respectively. Images were then overlaid to generate relative intensity data for each spot on the array, from which relative expression of each gene was calculated. Test samples were labelled with Cy3 and controls were labelled with Cy5, therefore, genes that were up-regulated relative to the control fluoresce red whilst down-regulated genes appear green. Where the expression level of a gene in the test sample is equivalent to expression of that gene in the control, the corresponding spot appears yellow on the array.

Gene Symbol	Entrez Gene Name	Expression fold-change	Subcellular localisation	Function / Role in cellular processes
DBI	Diazepam binding inhibitor (GABA receptor modulator, Acyl- CoA binding protein)	5.2	Cytoplasm	Acyl – CoA binding, benzodiazepine receptor binding. Role in proliferation and mitogenesis
OPTN	Optineurin	3.8	Cytoplasm	Function in replication and cell death
RPL6	Ribosomal protein L6	3.8	Ribosome	DNA binding, RNA binding, structural component of ribosome. Role in translation
EIF4G2	Eukaryotic transcription-initiation factor 4 gamma 2.	3.7	Cytoplasm	Nucleic acid binding translation factor, protein binding, translation initiation factor, translation regulator. Function in translation, cell cycle progression, cell death, growth, transformation, apoptosis, shunting, morphology, differentiation.
SRSF4	Serine/argenine-rich splicing factor 4	3.7	Nucleus	Nucleotide binding, RNA binding. RNA splicing.
DNAJB6	DnaJ (Hsp40) homologue, subfamily B, member 6	3.6	Cytoplasm / Nucleus	ATPase stimulator, chaperone binding, DNA binding, heat shock protein binding, transcription regulator. Active in cell death, organization, growth, formation.
NCL	Nucleolin	3.6	Nucleus	Nuclear localisation sequence, RNA binding, telomeric DNA binding. Role in proliferation, apoptosis, synthesis, maturation, migration, macropinocytosis, transduction.
CNOT6	CCR4-NOT transcription complex, subunit 6	3.5	Nucleus	Transcription
ATF4	Activating transcription factor 4	3.5	Nucleus	DNA binding transcription factor and transcription regulator. Expressed in apoptosis, cell death, cell cycle progression and is recruited in the endoplasmic reticulum stress response.
CTGF	Connective tissue growth factor	3.4	Extracellular space	Fibronectin, heparin and integrin binding protein. Expressed in cell-cell adhesion processes, cell proliferation and growth.

Table 5-1: Differential gene up-regulation in Met-5A cells following infection with D39 strain Streptococcus pneumoniae.

Met-5A cells were infected with pneumococci at an MOI of 200 bacteria / cell for 2 hours. RNA was then extracted from pleural cells and analysed by microarray. Mean fold expression changes were calculated for each gene from n=5 experiments and a \geq 2-fold increase was considered significant. The 10 most differentially up-regulated genes for this condition are detailed in the table above and the remainder can be seen on the accompanying compact disk appendix.

Gene Symbol	Entrez Gene Name	Expression fold-change	Subcellular localisation	Function / Role in cellular processes
SET	SET nuclear oncogene	8.5	Nucleus	Histone binding, nuclear localisation sequence, phosphatise. Role in apoptosis, cell disassembly, cell death.
BST2	Bone marrow stromal cell antigen 2	7.9	Plasma Membrane	Signal transducing transmembrane protein, protein ubiquitination.
EEF1A1	Eukaryotic translation elongation factor 1 alpha 1	6.1	Cytoplasm	GTP binding, protein-synthesising GTPase, translation regulator. Active in proliferation and cell death.
HNRNPC	Heterogeneous nuclear ribonucleoprotein C	5.3	Nucleus	mRNA binding, nuclear localisation sequence. Functional during transcription, cell differentiation and apoptosis
OAZ1	Ornithine decarboxylase antizyme 1	5.2	Cytoplasm / cytosol	Ornithine decarboxylase inhibitor. Role in cell death and cytostasis.
GPX4	Glutathione peroxidase 4	5.1	Cytoplasm	Regulator of apoptosis, cellular organization, cell integrity, motility, damage, cell viability.
TK1	Thymidine kinase 1,	4.6	Cytoplasm, / cytosol	Zinc ion binding. Phosphorylated during apoptosis and necrosis.
ACTB	Actin, beta	4.3	Cytoplasm	Structural constituent of cytoskeleton. Important for cell morphology, motility, formation, endocytosis, apoptosis, chemotaxis, growth, constriction, cell spreading, pathogen entry.
SNRPB	Small nuclear ribonucleoprotein polypeptides B and B1	4.2	Cytoplasm	RNA splicing
ARF4	ADP-ribosylation factor 4	4.1	Cytoplasm	GTPase, transport.

Table 5-2: Differential gene down-regulation in Met-5A cells following infection with D39 strain Streptococcus pneumoniae.

Met-5A cells were infected with pneumococci at an MOI of 200 bacteria / cell for 2 hours. RNA was then extracted from pleural cells and analysed by microarray. Mean fold expression changes were calculated for each gene from n=5 experiments and a \geq 2-fold decrease was considered significant. The 10 most differentially down-regulated genes for this condition are detailed in the table above and the remainder can be seen on the accompanying compact disk appendix.

Gene Symbol	Entrez Gene Name	Expression fold-change	Subcellular localisation	Function / Role in cellular processes
SET	SET nuclear oncogene	4.9	Nucleus	Histone binding, nuclear localisation sequence, phosphatise. Role in apoptosis, cell disassembly, cell death.
GAPDH	Glyceraldehyde-3-phosphate dehydrogenase	4.5	Cytoplasm	Erythrose-4-phosphate dehydrogenase, glyceraldehyde 3-phosphate dehydrogenase, glyceraldehyde-3-phosphate dehydrogenase (phosphorylating). Gluconeogenesis, glycolysis, caspase-independent cell death.
EEF1A1	Eukaryotic translation elongation factor 1 alpha 1	4.4	Cytoplasm	GTP binding, protein-synthesising GTPase, translation regulator. Active in proliferation and cell death.
GPX4	Glutathione peroxidase 4	4.2	Cytoplasm	Regulator of apoptosis, cellular organization, cell integrity, motility, damage, cell viability.
OAZ1	Ornithine decarboxylase antizyme 1	4.2	Cytoplasm / cytosol	Ornithine decarboxylase inhibitor. Role in cell death and cytostasis.
ACTB	Actin, beta	3.8	Cytoplasm	Structural constituent of cytoskeleton. Important for cell morphology, motility, formation, endocytosis, apoptosis, chemotaxis, growth, constriction, cell spreading, pathogen entry.
MYL9	Myosin, light chain 9, regulatory	3.8	Cytoplasm	Structural constituent of muscle. Role in cytokinesis, metaphase / anaphase transition, gene rearrangement.
TUBA1A	Tubulin, alpha 1a	3.4	Cytoplasm	Function in cellular morphology, assembly, apoptosis, regulation, metaphase, differentiation.
SNRPB	Small nuclear ribonucleoprotein polypeptides B and B1	3.4	Cytoplasm	RNA splicing
TK1	Thymidine kinase 1	3.4	Cytoplasm / cytosol	Zinc ion binding. Phosphorylated during apoptosis and necrosis.

Table 5-3: Differential gene up-regulation in Met-5A cells following challenge with the lysate of D39 strain Streptococcus pneumoniae.

Met-5A cells were challenged with whole crude lysates of D39 strain pneumococci, at the equivalent MOI of 200 bacteria / cell, for 2 hours. RNA was extracted and the transcriptome of pleural cells was analysed by microarray. Mean fold expression changes were calculated for each gene from n=5 independent experiments and a \geq 2-fold increase was considered significant. The 10 most differentially up-regulated genes for this condition are detailed in the table above and the remainder can be seen on the accompanying compact disk appendix.

Gene Symbol	Entrez Gene Name	Expression fold-change	Subcellular localisation	Function / Role in cellular processes
SF3B14	Splicing factor 3B, 14 kDa subunit	5.6	Nucleus	Replication in necroptosis, apoptosis.
SH3KBP1	SH3-domain kinase binding protein 1	4.7	Cellular membrane / cytoplasm	Role in apoptosis, cell clustering, migration, cell death.
LOC100290142 /USMG5	Up-regulated during skeletal muscle growth 5 homologue (mouse)	4.6	Cytoplasm	Unknown.
H3F3A/H3F3B	H3 histone, family 3B (H3.3B)	4.3	Nucleus	Cell cycle progression, morphology, transcription, differentiation, growth, apoptosis, gene silencing.
BUB1	Budding uninhibited by benzimidazoles 1 homologue (yeast)	4.2	Nucleus	Active in checkpoint control, apoptosis, mitosis, senescence, segregation, polyploidisation, cell cycle progression, missegregation, aneuploidy.
PAIP1	Poly(A) binding protein interacting protein 1	4.2	Cytoplasm	Initiation of translation. Protein biosynthesis.
SNRPG	Small nuclear ribonucleoprotein polypeptide G	3.9	Nucleus	Maturation.
ITM2B	Integral membrane protein 2B	3.9	Plasma Membrane	Bcl-2 homology 3 domain protein. Active in apoptosis.
ATP5A1	ATP synthase, H+ transporting, mitochondrial F1 complex, alpha subunit 1	3.7	Cytoplasm	ADP binding ATPase, hydrogen-transporting ATP synthase activity. Role in proliferation, growth and metabolism.
SNRPF	Small nuclear ribonucleoprotein polypeptide F	3.5	Nucleus	RNA binding. Role in DNA replication.

Table 5-4: Differential gene down-regulation in Met-5A cells following challenge with the lysate of D39 strain Streptococcus pneumoniae.

Met-5A cells were challenged with whole crude lysates of D39 strain pneumococci, at the equivalent MOI of 200 bacteria / cell, for 2 hours. RNA was extracted and the transcriptome of pleural cells was analysed by microarray. Mean fold expression changes were calculated for each gene from n=5 independent experiments and a \geq 2-fold decrease was considered significant. The 10 most differentially down-regulated genes for this condition are detailed in the table above and the remainder can be seen on the accompanying compact disk appendix.

Gene Symbol	Entrez Gene Name	Expression	Subcellular	Function / Role in cellular processes
•		fold-change	localisation	-
KRT7	Keratin 7	3.5	Cytoplasm	Active during interphase and cellular disassembly.
PITPNM	Phosphatidylinositol transfer protein, membrane-associated 1	3.3	Cytoplasm	Phosphatidylinositol transporter. Role in cytokinesis, cellular morphology, retraction and extension.
MLF2	Myeloid leukaemia factor 2	3.2	Nucleus	Unknown.
CELA2A	Chymotrypsin-like elastase family, member 2A	3	Extracellular Space	Role chemotaxis, cell cycle progression, transcription and apoptosis.
LEPR	Leptin receptor	2.9	Plasma Membrane	Polypeptide hormone binding, protein-hormone receptor, STAT3 binding. Active in proliferation and apoptosis.
MKNK2	MAP kinase interacting serine/threonine kinase 2	2.7	Cytoplasm	Protein serine/threonine kinase.
CDC42SE1	CDC42 small effector 1	2.6	Plasma Membrane	GTPase inhibitor. Role in cellular blebbing.
STK10	Serine/threonine kinase 10	2.5	Cytoplasm	Unknown
MRPL4	Mitochondrial ribosomal protein L4	2.5	Mitochondria	Structural constituent of mitochondrial ribosome
PHLDA3	Pleckstrin homology-like domain,	2.3	Plasma	Phosphatidylinositol-3,4,5-triphosphate binding, phosphatidylinositol-4,5-bisphosphate
	family A, member 3		Membrane	binding. Functions in DNA damage response and apoptosis.

Table 5-5: Differential gene up-regulation in Met-5A cells following infection with S1-H strain Streptococcus pneumoniae.

Met-5A cells were infected with pneumococci at an MOI of 200 bacteria / cell for 2 hours. RNA was then extracted from pleural cells and analysed by microarray. Mean fold expression changes were calculated for each gene from n=4 experiments and $a \ge 2$ -fold increase was considered significant. The 10 most differentially up-regulated genes for this condition are detailed in the table above and the remainder can be seen on the accompanying compact disk appendix.

Gene Symbol	Entrez Gene Name	Expression fold-change	Subcellular localisation	Function / Role in cellular processes
GAPDH	Glyceraldehyde-3-phosphate dehydrogenase	5.1	Cytoplasm	Erythrose-4-phosphate dehydrogenase, glyceraldehyde 3-phosphate dehydrogenase, glyceraldehyde-3-phosphate dehydrogenase (phosphorylating). Gluconeogenesis, glycolysis, caspase-independent cell death.
EEF1A1	Eukaryotic translation elongation factor 1 alpha 1	4.4	Cytoplasm	GTP binding, protein-synthesising GTPase, translation regulator. Active in proliferation and cell death.
SET	SET nuclear oncogene	4.2	Nucleus	Histone binding, nuclear localisation sequence, phosphatise. Role in apoptosis, cell disassembly, cell death.
TUBA1A	Tubulin, alpha 1a	3.9	Cytoplasm	Function in cellular morphology, assembly, apoptosis, regulation, metaphase, differentiation.
MGATB	mannosyl (alpha-1,3-)- glycoprotein beta 1,4-N- acetylglucosaminyltransferase, isozyme B	3.4	Cytoplasm	Functions in cellular growth.
GPX4	Glutathione peroxidase 4	3.4	Cytoplasm	Regulator of apoptosis, cellular organization, cell integrity, motility, damage, cell viability.
OAZ1	Ornithine decarboxylase antizyme 1	3.2	Cytoplasm / cytosol	Ornithine decarboxylase inhibitor. Role in cell death and cytostasis.
TK1	Thymidine kinase 1	3.1	Cytoplasm / cytosol	Zinc ion binding. Phosphorylated during apoptosis and necrosis.
SLC38A2	Solute carrier family 38, member 2	2.9	Plasma Membrane	Amino acid transporter.
ACTB	Actin, beta	2.8	Cytoplasm	Structural constituent of cytoskeleton. Important for cell morphology, motility, formation, endocytosis, apoptosis, chemotaxis, growth, constriction, cell spreading, pathogen entry.

Table 5-6: Differential gene down-regulation in Met-5A cells following infection with S1-H strain *Streptococcus pneumoniae*.

Met-5A cells were infected with pneumococci at an MOI of 200 bacteria / cell for 2 hours. RNA was then extracted from pleural cells and analysed by microarray. Mean fold expression changes were calculated for each gene from n=4 experiments and $a \ge 2$ -fold increase was considered significant. The 10 most differentially down-regulated genes for this condition are detailed in the table above and the remainder can be seen on the accompanying compact disk appendix.

Gene Symbol	Entrez Gene Name	Expression fold-change	Subcellular localisation	Function / Role in cellular processes
EEF1A1	Eukaryotic translation elongation factor 1 alpha 1	5.9	Cytoplasm	GTP binding, protein-synthesising GTPase, translation regulator. Active in proliferation and cell death.
SET	SET nuclear oncogene	5.8	Nucleus	Histone binding, nuclear localisation sequence, phosphatise. Role in apoptosis, cell disassembly, cell death.
NOL7	Nucleolar protein 7	3.9	Mitochondria / Nucleus	Unknown.
BST2	Bone marrow stromal cell antigen 2	3.6	Plasma Membrane	Signal transducing transmembrane protein, protein ubiquitination.
RPL7	Ribosomal protein L7	3.3	Cytoplasm	DNA binding, RNA binding, Transcription regulator.
LAPTM4B	Lysosomal protein transmembrane 4 beta	3.1	Unknown	Role in cell survival.
SLC38A2	Solute carrier family 38, member 2	3.1	Plasma Membrane	Amino acid transporter.
PAIP1	Poly(A) binding protein interacting protein 1	3.0	Cytoplasm	Initiation of translation. Protein biosynthesis.
EIF3M	Eukaryotic translation initiation factor 3, subunit M	2.9	Unknown	Initiation of translation.
MRPS18C	Mitochondrial ribosomal protein S18C	2.8	Mitochondria / mitochondrial matrix	Unknown

Table 5-7: Differential gene up-regulation in Met-5A cells following challenge with the lysate of S1-H strain Streptococcus pneumoniae.

Met-5A cells were challenged with whole crude lysates of S1-H strain pneumococci, at the equivalent MOI of 200 bacteria / cell, for 2 hours. RNA was extracted and the transcriptome of pleural cells was analysed by microarray. Mean fold expression changes were calculated for each gene from n=4 independent experiments and a \geq 2-fold decrease was considered significant. The 10 most differentially up-regulated genes for this condition are detailed in the table above and the remainder can be seen on the accompanying compact disk appendix.

Gene Symbol	Entrez Gene Name	Expression	Subcellular	Function / Role in cellular processes
		fold-change	localisation	
NARF	Nuclear prelamin A recognition	3.9	Nucleus	Lamin binding.
	factor			
TMPRSS13	Transmembrane protease, serine	2.5	Cellular	Proteolysis
	13		Membrane	
PPP1R15A	Protein phosphatise 1, regulatory	2.5	Cytoplasm /	Functions in apoptosis, DNA damage response, cell cycle progression, growth inhibition,
	(inhibitor) subunit 15A		Endoplasmic	and endoplasmic reticulum stress response.
			reticulum	
SRSF4	Serine/argenine-rich splicing factor	2.5	Nucleus	Nucleotide binding, RNA binding, RNA splicing
	4			
OPTN	Optineurin	2.5	Cytoplasm	Function in replication and cell death
LEPR	Leptin receptor	2.3	Plasma	Polypeptide hormone binding, protein-hormone receptor, STAT3 binding. Active in
			Membrane	proliferation and apoptosis.
NAV1	Neuron navigator 1	2.3	Cytoplasm	Enzyme involved in cellular migration.
RNF10	Ring finger protein 10	2.2	Cytoplasm	Active during proliferation and reverse transcription.
ZC3H7B	Zinc finger CCCH-type containing	2.2	Nucleus	Unknown
	7B			
KNTC1	Kinetochore associated 1	2.2	Nucleus	Function in checkpoint control and mitosis.

Table 5-8: Differential gene down-regulation in Met-5A cells following challenge with the lysate of S1-H strain *Streptococcus* pneumoniae.

Met-5A cells were challenged with whole crude lysates of S1-H strain pneumococci, at the equivalent MOI of 200 bacteria / cell, for 2 hours. RNA was extracted and the transcriptome of pleural cells was analysed by microarray. Mean fold expression changes were calculated for each gene from n=4 independent experiments and $a \ge 2$ -fold decrease was considered significant. The 10 most differentially down-regulated genes for this condition are detailed in the table above and the remainder can be seen on the accompanying compact disk appendix.

Gene Symbol	Entrez Gene Name	Expression fold-change	Subcellular localisation	Function / Role in cellular processes
EEF1B2	Eukaryotic translation elongation factor 1 beta 2	20.5	Cytoplasm	Translation regulator. Role in cell proliferation
PAIP1	Poly(A) binding protein interacting protein 1	19.0	Cytoplasm	Initiation of translation. Protein biosynthesis.
NPM1	Nucleophosmin	19.0	Nucleus	Histone binding, NF-kappaB binding, nuclear export signal molecule, nuclear localization sequence, oligomerisation domain, ribosome binding, RNA binding, rRNA binding, transcription co-activator, transcription regulator. Active in apoptosis, proliferation, growth, cell cycle progression, biosynthesis, aging.
ITM2B	Integral membrane protein 2B	17.9	Plasma Membrane	Bel-2 homology 3 domain protein. Active in apoptosis.
LOC100290142 /USMG5	Up-regulated during skeletal muscle growth 5 homologue (mouse)	17.4	Cytoplasm	Unknown.
SF3B14	Splicing factor 3B, 14 kDa subunit	16.9	Nucleus	Replication in necroptosis, apoptosis.
RPL7	Ribosomal protein L7	16.5	Cytoplasm	DNA binding, RNA binding, Transcription regulator.
SH3KBP1	SH3-domain kinase binding protein 1	15.1	Cellular membrane / cytoplasm	Role in apoptosis, cell clustering, migration, cell death.
ATP5A1	ATP synthase, H+ transporting, mitochondrial F1 complex, alpha subunit 1	11.4	Cytoplasm	ADP binding ATPase, hydrogen-transporting ATP synthase activity. Role in proliferation, growth and metabolism.
CALM1	Calmodulin 1	11.2	Nucleus	Calcium ion binding. Role in cytokinesis and neurogenesis,

Table 5-9: Differential gene up-regulation by Met-5A cells following challenge with heat-attenuated D39 strain S. pneumoniae.

Met-5A cells were challenged with pneumococci, which had been previously heat-attenuated by heating to 96°C for 4 minutes, at an MOI of 200 bacteria / cell. At 2 hours post-challenge, RNA was extracted from pleural cells and analysed by microarray. Mean expression fold-changes were calculated for each gene from n=3 independent experiments and a \geq 2-fold increase was considered significant. The 10 most differentially upregulated genes for this condition are detailed in the table above and the remainder can be seen on the accompanying compact disk appendix.

Gene Symbol	Entrez Gene Name	Expression fold-change	Subcellular localisation	Function / Role in cellular processes	
MYL9	Myosin, light chain 9, regulatory	15.0	Cytoplasm	Structural constituent of muscle. Role in cytokinesis, metaphase / anaphase transition, gene rearrangement.	
GAPDH	Glyceraldehyde-3-phosphate dehydrogenase	5.8	Cytoplasm	Erythrose-4-phosphate dehydrogenase, glyceraldehyde 3-phosphate dehydrogenase, glyceraldehyde-3-phosphate dehydrogenase (phosphorylating). Gluconeogenesis, glycolysis, caspase-independent cell death.	
THOC3	THO complex 3	4.0	Nucleus	RNA binding, mRNA processing, mRNA export from nucleus, RNA splicing.	
TUBA1A	Tubulin, alpha 1a	4.0	Cytoplasm	Function in cellular morphology, assembly, apoptosis, regulation, metaphase, differentiation.	
ADIPOR2	Adiponectin receptor 2	3.9	Plasma Membrane	Hormone binding, cellular growth, M2 polarization.	
NBPF3	Neuroblastoma breakpoint family, member 3	3.6	Cytoplasm	Unknown	
SNRPB	Small nuclear ribonucleoprotein polypeptides B and B1	3.5	Cytoplasm	RNA splicing	
SET	SET nuclear oncogene	3.4	Nucleus	Histone binding, nuclear localisation sequence, phosphatise. Role in apoptosis, cell disassembly, cell death.	
ZFP91	Zinc finger protein 91 homologue (mouse)	3.4	Nucleus	Transcription regulator, ubiquitin-protein ligase.	
C2orf28*	Chromosome 2 open reading frame 28	3.2	Unknown	Unknown	

Table 5-10: Differential gene down-regulation by Met-5A cells following challenge with heat-attenuated D39 strain S. pneumoniae.

Met-5A cells were challenged with pneumococci, which had been previously heat-attenuated by heating to 96°C for 4 minutes, at an MOI of 200 bacteria / cell. At 2 hours post-challenge, RNA was extracted from pleural cells and analysed by microarray. Mean expression fold-changes were calculated for each gene from n=3 independent experiments and a \geq 2-fold decrease was considered significant. The 10 most differentially down-regulated genes for this condition are detailed in the table above and the remainder can be seen on the accompanying compact disk appendix.

	D39	D39 Lysate	S1	S1 Lysate	Heat Killed
Up-regulated	DBI	SET	KRT7	EEF1A1	EEF1B2
	OPTN	GAPDH	PITPNM1	SET	PAIP1
	RPL6	EEF1A1	MLF2	NOL7	NPM1
	EIF4G2	GPX4	CELA2A	BST2	ITM2B
	SRSF4	OAZI	LEPR	RPL7	LOC100290142/USMG5
	<i>DNAJB6</i>	ACTB	MKNK2	<i>LAPTM4B</i>	SF3B14
	NCL	MYL9	CDC42SE1	SLC38A2	RPL7
	CNOT6	TUBA 1 A	STK10	PAIP1	SH3KBP1
	ATF4	SNRPB	<i>MRPL4</i>	EIF3M	ATP5A1
	CTGF	TK1	PHLDA3	MRPS18C	CALM1
Down-regulated	SET	SF3B14	GAPDH	NARF	MYL9
Down-regulated	BST2	SH3KBP1	EEF1A1	TMPRSS13	GAPDH
	EEF1A1	LOC100290142/USMG5	SET	PPP1R15A	ТНОС3
	HNRNPC	<i>H3F3A/H3F3B</i>	TUBA1A	SRSF4	TUBA1A
	OAZ1	BUB1	MGAT4B	OPTN	ADIPOR2
	GPX4	PAIP1	GPX4	LEPR	NBPF3
	TK1	SNRPG	OAZ1	NAV1	<i>SNRPB</i>
	ACTB	ITM2B	TK1	RNF10	SET
	SNRPB	ATP5A1	SLC38A2	ZC3H7B	ZFP91
	ARF4	SNRPF	ACTB	KNTC1	C2orf28

Figure 5-2: Illustration of commonly expressed genes in Met-5A cells following challenge with live or heat-attenuated pneumococci, or pneumococcal lysates. The matrix above illustrates differentially expressed genes that are common between data sets. Shortlisted up- and down-regulated genes for each challenge condition are shown in rank order of expression fold-change, and genes common to 2 or more gene lists are shown in the same colour to facilitate the identification of genes that are similarly or oppositely expressed in different challenge conditions.

5.1.1 Differential gene expression in Met-5A cells infected with pneumococciderived antigens.

The total number of differentially expressed genes in infected pleural cells did not significantly differ between any of the conditions, with between 882 (S1-H) and 894 (heat-attenuated) genes satisfying filtering criteria. When the 10 most differentially up and down-regulated genes in every challenge condition were considered, just 65 different genes appeared across all of the data sets, and of these 22 genes were common to 2 or more gene lists. When only the 10 most highly up-regulated genes in each data set were considered, 46 different genes were listed and of these, 4 genes were up-regulated in 2 or more data-sets; namely *SET*, *EEF1A1*, *PAIP1* and *RPL7*. Forty different genes appeared in the 10 highest ranked down-regulated genes when each of the data sets were considered together, however 9 of these were commonly down-regulated in 2 or more of the challenge conditions, specifically; *SET*, *EEF1A1*, *OAZ1*, *GPX4*, *TK1*, *ACTB*, *SNRPB*, *GAPDH* and *TUBA1A* (Figure 5-2).

For both D39 and S1-H, comparison between gene lists generated following infection with whole bacteria and their corresponding lysates, revealed opposite expression in several genes. For example, whole D39 and S1-H induced an 8.5 and 4.2 fold decrease in expression of the nuclear oncogene SET respectively, whilst challenge with the lysates of these strains increased expression of SET by 4.9 and 5.8 fold. This gene, which is involved in apoptosis and cell disassembly, was also down-regulated 3.4-fold by pleural cells following stimulation with heat-attenuated pneumococci. A similar pattern was also observed for the translation regulator *EEF1A1*, whereby it was down-regulated following infection of Met-5A cells with whole D39 (6.1-fold) and S1-H (4.4-fold) bacteria, but up-regulated following stimulation with their respective lysates (4.4 and 5.9 fold). The closely related gene, EEF1B2 was up-regulated 20.5fold by Met-5A cells following stimulation with heat-killed bacteria. Genes encoding ornithine decarboxylase inhibitor 1 (OAZI), which functions during cell death and cytostasis, beta-actin (ACTB), which is an essential component of the mammalian cytoskeleton and thymidine kinase 1 (TKI), which is phosphorylated during cellular apoptosis and necrosis, were also down-regulated following D39 infection and upregulated in response to challenge with the lysates of both D39 and S1-H. These data demonstrate that regardless of antigen challenge condition, the genes that were subject to significant differential expression, whether it be up- or down-regulation, were highly similar in this study.

5.1.2 Pathway analysis of differential human gene expression

Tables 5-1 – 5-10 list individual differentially expressed genes in rank order. However, when investigating the pathology of disease it is useful to examine how changes in gene expression impact upon cellular functions and processes and what pathways are most perturbed by these induced changes. Thus, the data obtained from microarray experiments were also analysed using Ingenuity Pathways Analysis (IPA) software v7.6 (Ingenuity® Systems, USA) in order to identify the signalling and metabolic pathways that were most affected in each data set. This was determined by calculation of the number of differentially expressed genes in each pathway as a proportion of the total number of genes involved in that pathway. A minimum threshold of 5% gene perturbations was then imposed on pathways and those which met these inclusion criteria were then ranked according to the proportion of gene perturbations. The 20 most highly ranked pathways for each challenge condition are presented in Figures 5-3 a-e.

For every challenge condition analysed, oxidative phosphorylation pathways incurred the highest number of gene expression perturbations, with approximately 22% of all genes in that pathway being differentially expressed (Figure 5-3 a-e). In cells infected with live D39, 10% of genes involved in oxidative phosphorylation processes were up-regulated and 12% were down-regulated (Figure 5.3a). Down-regulation of oxidative phosphorylation genes was exaggerated in pleural cells challenged with D39 lysates (18%) and only 4% of genes were up-regulated (b). Infection with whole live S1-H brought about up-regulation of 13% of genes involved in this pathway, while 9% were down-regulated (c). However, challenge with S1-H lysates (d) and heat-killed pneumococci (e) increased the number of up-regulated genes to 18% and reduced down-regulation to 4% of genes.

Commonly amongst these differentially expressed genes were ATP synthase enzymes. Pleural cells challenged with both D39 and D39 lysates down-regulated the enzyme *ATP5A1* by 2.0- and 3.7- fold respectively. Conversely, ATP5A1 was upregulated in cells challenged with S1-H lysate (2.4-fold) and heat-attenuated bacteria

(11.4-fold) while the closely related enzyme *ATP6V1E1* was up-regulated 2-fold in cells infected with whole live S1-H pneumococci. Other genes that were differentially expressed in multiple conditions included various cytochrome c regulatory genes. The cytochrome c oxidase enzyme *COX6A1* was upregulated 2-fold following infection with whole D39 bacteria, while the reductase *COX8A* was up-regulated 3.2-fold in cells challenged with D39 lysates, but down-regulated with heat-attenuated bacteria. Similarly, challenge with S1-H lysate induced a 2-fold down-regulation in the cytochrome oxidase gene *COX7C* in Met-5A cells.

Of the toxicological pathways assessed by IPA, mitochondrial dysfunction mechanisms were the most affected by challenge with all of the pneumococcal antigens with 17% of the total number of genes involved in these pathways being differentially expressed. Whole live D39 elicited more up-regulation (9%) of genes involved in mitochondrial dysfunction when compared to uninfected control cells, whereas D39 lysates induced down-regulation (13%) of these genes. This is reflective of gene expression patterns when live D39 were compared to D39 lysates, whereby challenge with lysates generally elicited gene down-regulation in pathways that were upregulated by infection with whole pneumococci, for example the DNA damage checkpoint regulation pathway and ubiquinone biosynthesis pathway. Furthermore, genes involved in such cellular processes as the spliceosomal cycle and antigen presentation, were oppositely expressed in cells challenged with D39 and D39 lysates. In these pathways, all genes that were differentially expressed in response to whole bacteria were up-regulations, whereas lysates induced only down-regulations in these pathways. In the antigen presentation pathway, 10% of all genes (4 genes) in the pathway were differentially expressed, namely the proteasome subunits PSMB5 and *PSMB6* the transporter protein *TAP2*, and the protein disulphide isomerase *PDIA3*.

Contrastingly to D39, S1-H generally induced more down-regulation of genes than its corresponding lysate in most of the 20 highest ranked pathways (Figure 5-3). An anomaly to this pattern was the cleavage and polyadenylation of pre-mRNA pathway, in which 17% of genes were down- and up-regulated by whole S1-H and S1-H lysates respectively. In the mitochondrial dysfunction pathway, whole S1-H caused down-regulation of 11% of genes, compared to just 4% by S1-H lysates.

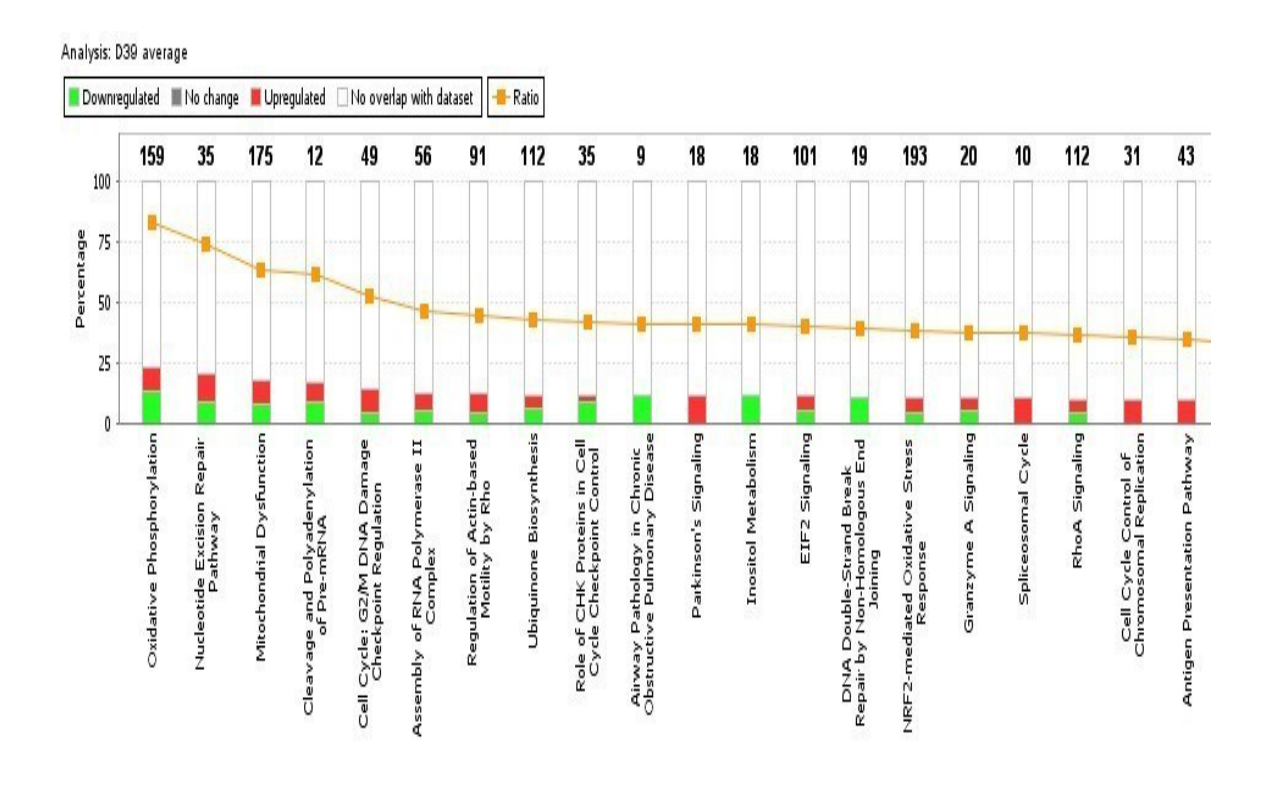


Figure 5-3a: Met-5A cells infected with D39 strain pneumococci

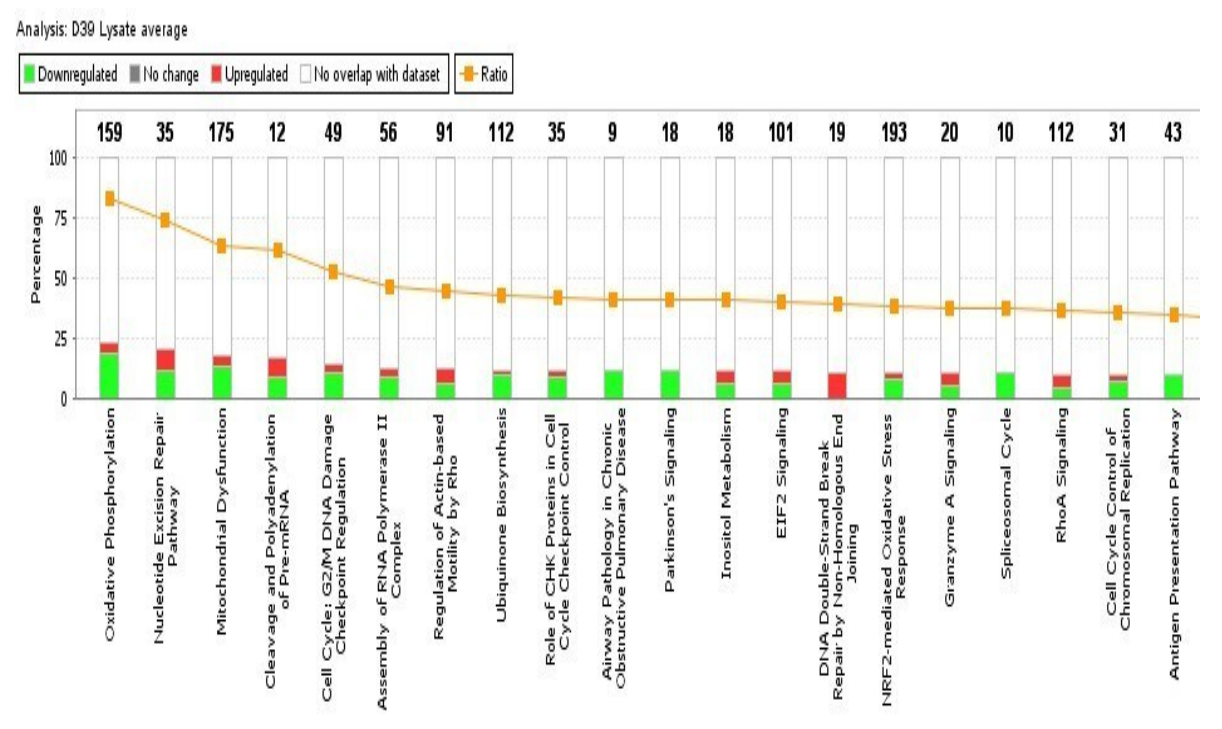


Figure 5-3b: Met-5A cells challenged with the lysate of D39 strain pneumococci.

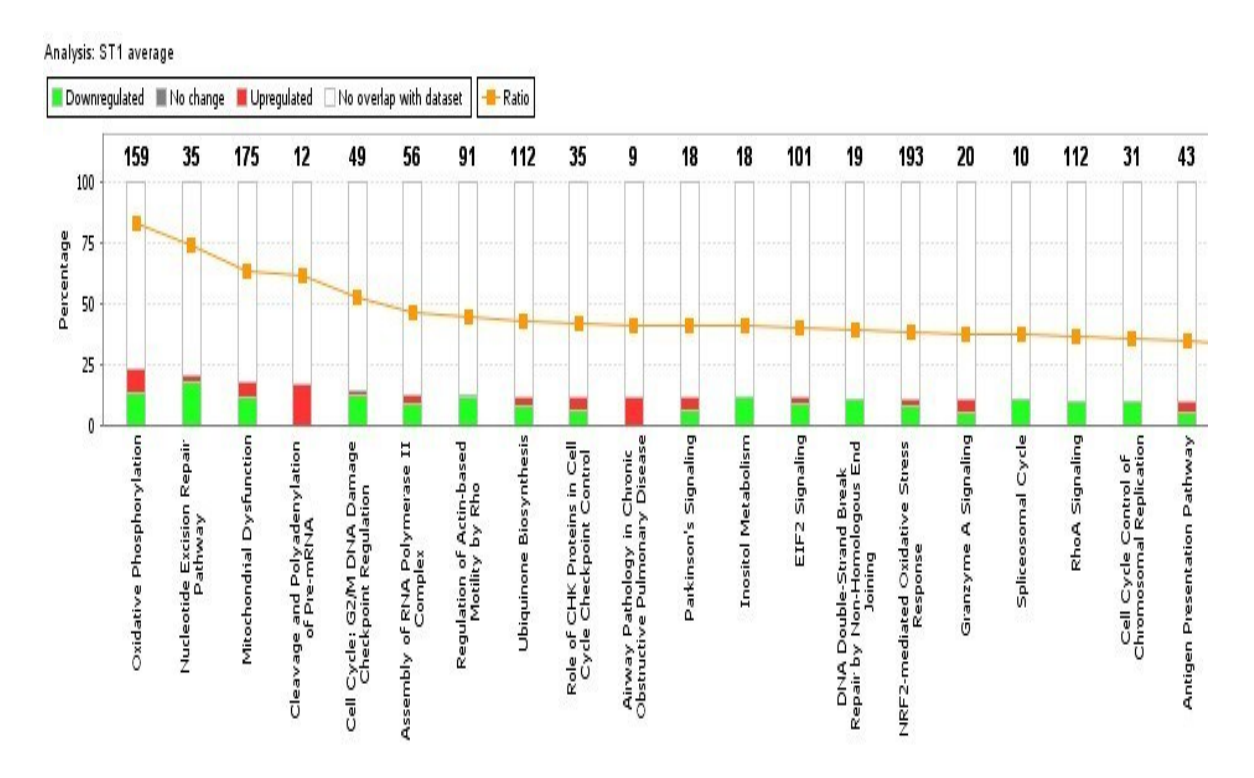


Figure 5-3c: Met-5A cells infected with S1-H strain pneumococci.

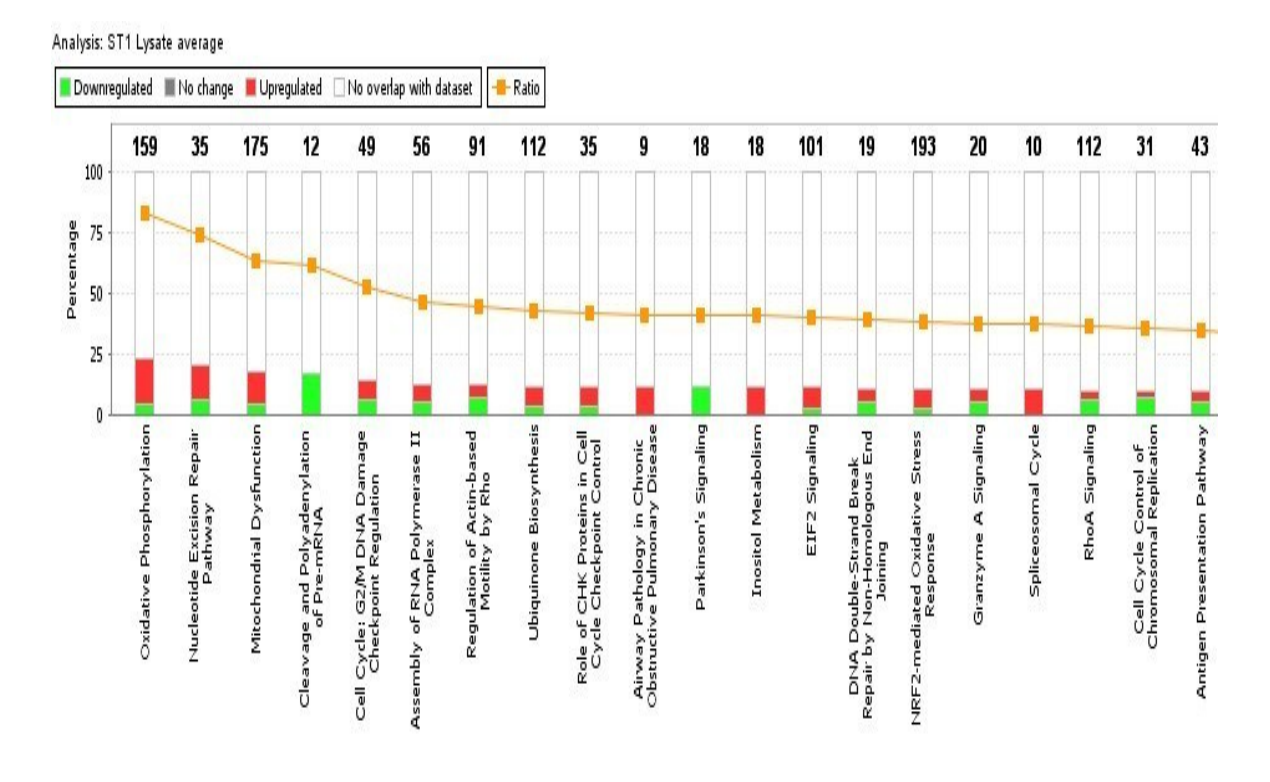


Figure 5-3d: Met-5A cells challenged with the lysate of S1-H strain pneumococci

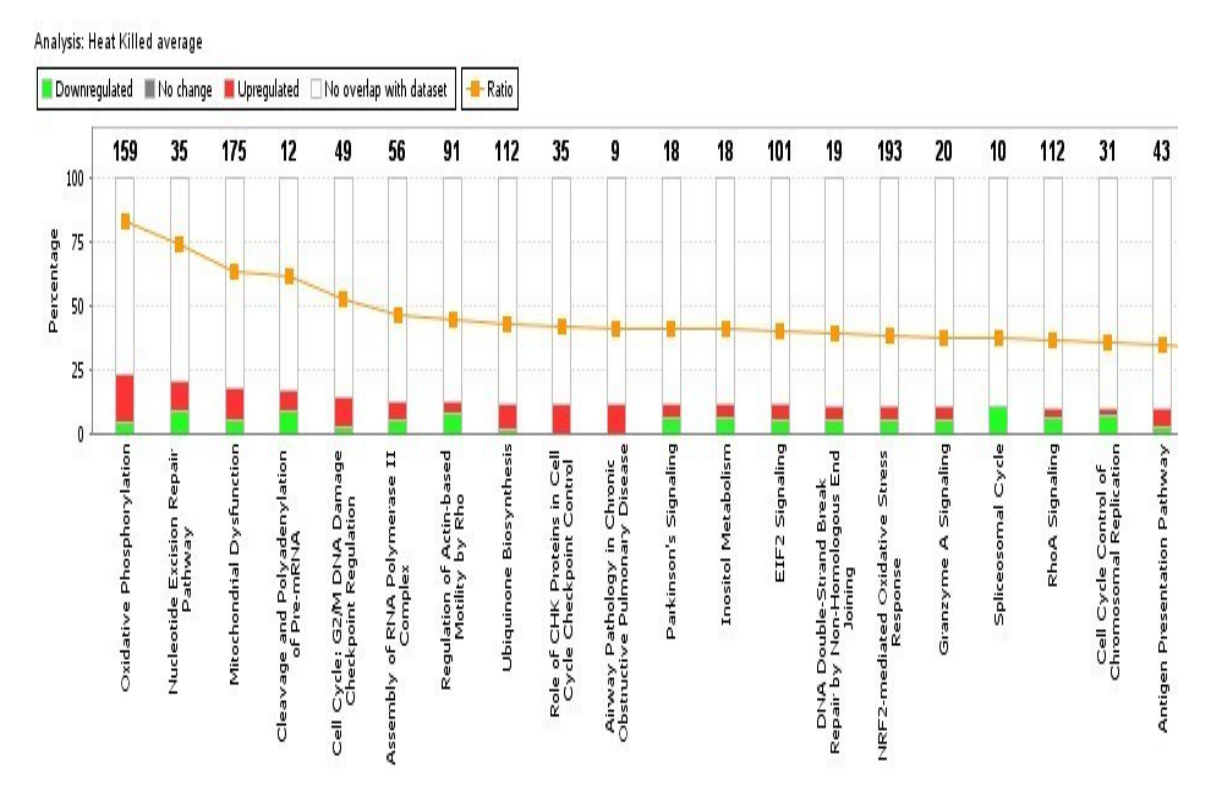


Figure 5-3e: Met-5A cells challenged with heat-attenuated pneumococci.

Figure 5-3: Pathway analysis of differential gene expression in Met-5A cells following challenge with *S. pneumoniae* derived antigens.

All genes that satisfied all of the filtering criteria for differential expression were analysed using IPA software to determine the signalling and metabolic pathways most affected by pneumococcal infection. Pathways were ranked according to the number of differentially expressed genes as a percentage of the total number of genes involved in that pathway. Gene up-regulation is denoted by red and down-regulation by green. The number above each column gives the total number of genes associated with each pathway.

Perhaps the most interesting observation of gene pathway perturbations in pleural cells is that following infection of Met-5A cells with both the clinical empyema isolate S1-H and its lysate, genes involved in airway pathology during the inflammatory condition Chronic Obstructive Pulmonary Disease (COPD) were up regulated. However, this was not observed when cells were infected with the laboratory strain D39 or with its lysate. In each case, the chymotrypsin-like elastase enzyme, *CELA2A*, was the most

differentially expressed gene, which was up-regulated 3-fold following infection with the clinical isolate and down-regulated 2-fold with D39.

As described previously, gene expression fold-changes induced by challenge with heat killed pneumococci were much greater than in any of the other conditions. Pathway analysis demonstrated that most differential gene expression in cells challenged with heat-attenuated bacteria were up-regulations, with 115 genes (65%) being up-regulated compared with 61 (35%) down-regulated genes in the top 20 canonical pathways. Similarly to the clinical empyema isolates, heat-killed pneumococci brought about up-regulation of genes involved in the airway pathology pathway, again with *CELA2A* being the most highly expressed with a fold change of 3. In addition there was exclusive up-regulation of genes involved in the *CHK* protein regulation of cell cycle checkpoints, foremost, the cyclin-dependent kinase *CDK1* which exhibited a 4-fold expression increase.

5.2 Summary.

The aim of investigations into the transcription profile of pleural cells following pneumococcal challenge was to discern whether differences in the disease-causing propensities of pneumococcal strains was partially due to the variation in the host's immune response to them. The hypothesis that the induced response of Met-5A cells to infection with a clinical empyema isolate would be distinct to the response to a reference strain was tested.

However, the data obtained in this chapter suggest that rather than differing between strains, the transcriptional response of pleural mesothelial cells differed between pneumococcal strains and their corresponding lysates, where opposite patterns of expression were evident. For example, the nuclear oncogene *SET*, which is involved in apoptotic processes, was downregulated following infection with whole pneumococci of both strains, but upregulated following lysate challenge. An interesting exception to this pattern however, was the observed difference between the reponses induced by the clinical empyema isolates and reference strains in genes involved in airway pathology, particularly the expression of *CELA2*.

The observed differences between the response to whole pneumococci and lysates corroborates the protein expression data presented in Chapter 3, in which the IL-6 and IL-8 response of Met-5A cells to pneumococcal lysates was significantly increased relative to whole bacteria. In addition, challenge with heat-killed pneumococci typically induced greater fold-changes in differentially expressed genes, which also lends support to the new hypothesis that host cellular responses are actively suppressed by the pneumococcus.

When the most significant changes in gene expression were considered across all of the challenge conditions, the data showed that a large proportion of genes subject to differential regulation were common to several challenge conditions. Cellular processes involving oxidative phosphorylation were found to be the most affected, regardless of the antigen challenge condition. Analysis of toxicological pathways revealed that genes involved in mitochondrial dysfunction were subject to differential regulation within each of the challenge groups.

As described for pneumococcal microarray analysis, these data are limited by the arbitrary nature of the filtering criteria imposed, due to the lack of consensus regarding microarray interpretation approaches. However, performance of pathway analysis, which collates global gene expression data to illustrate the functional processes most perturbed within a cell, provides a reliable overview of pleural mesothelial cell responses to pneumococcal antigens.

CHAPTER 6 DISCUSSION AND CONCLUSIONS

6.1 Interactions of *Streptococcus pneumoniae* with pleural mesothelial cells

Although the mechanisms of infection have been described in various models of pneumococcal disease, including pneumococcal pneumonia, the direct interactions of this bacterium with cells of the pleural mesothelium has never been investigated. Therefore, in current study the interactions of pneumococci with human mesothelial cells in an *in vitro* model of pleural empyema were examined. Adherence of pneumococci to host cells is an essential prerequisite step in the pathogenesis of disease (Bogaert *et al.* 2004). Initially, the adherent properties of reference pneumococci, including various virulence gene mutants, were investigated and compared to pneumococci isolated from clinical paediatric empyema samples.

Laboratory passaged bacteria adhered to pleural cells in a dose and time dependent manner, with the higher inocula rapidly saturating and destroying cell monolayers. No significant differences were observed in the capacity of wild type pneumococci and pneumolysin-deficient mutants to associate with pleural cells (p>0.05). The role of pneumolysin in pneumococcal pathogenesis is subject to much contradictory evidence. In concordance with the findings of the current study, Rubins and Janoff demonstrated that expression of pneumolysin in a serotype 14 background pneumococcus was not a major determinant of successful nasopharyngeal colonisation in a murine model (Rubins and Janoff 1998). These investigators showed that pneumolysin-deficient bacteria adhered to the mouse nasopharynx in comparable numbers to the wild type, and also observed only modest differences in adherence rates between pneumolysin-sufficient and deficient serotype 2 strains with epithelial cells in vitro, indicating that the contribution of the toxin varies between strains (Rubins and Janoff 1998). Furthermore, Rayner et al. showed that pneumococcal adhesion to ex vivo tissue of the human respiratory mucosa was not inhibited by pneumolysin deficiency (Rayner et al. 1995). Kadioglu and colleagues however, reported that colonisation of cells of the upper respiratory tract and the lung by pneumolysin-deficient bacteria in a murine model was significantly impaired in comparison to the wild-type (Kadioglu et al. 2002). Similarly, the role of pneumolysin in the early pathogenesis of invasive pneumonia has been demonstrated in in vivo experimental models. In mice,

pneumolysin deficient strains cause less lethal infection, decreased damage to the alveolar interstitium, a reduced capacity to proliferate in the lung and a decreased ability to penetrate the alveolar/capillary barrier and invade the bloodstream when compared to wild type strains (Rubins and Janoff 1998); (Canvin *et al.* 1995); (Berry *et al.* 1992); (Berry *et al.* 1995). Moreover, distinct from its activity as a pore-forming toxin, pneumolysin has been shown to potentiate colonisation of the respiratory tract and subsequent invasive disease via numerous other mechanisms. Several investigators have shown that the protein facilitates the propagation of disease via the disruption of tight junctions between bronchial epithelial cells (Rubins and Janoff 1998; Cockeran *et al.* 2002), and also by eliciting ciliary beat dyskinesia in epithelial and ependymal cells, thus impeding muco-ciliary clearance and facilitating spread of infection to the lower respiratory tract (Steinfort *et al.* 1989; Steinfort *et al.* 1989; Hirst *et al.* 2004). However, Hirst and colleagues also demonstrated that pneumococci that were rendered pneumolysin-deficient retained the capacity to cause culinary stasis, albeit less pronounced, via release of hydrogen peroxide (Hirst *et al.* 2000).

Doubt has been cast upon the absolute requirement for pneumolysin in disease pathogenesis by data obtained by Lock *et al.* who reported great variation in the levels of haemolytic activity amongst clinical strains (Lock *et al.* 1996). More recently, naturally occurring pneumolysin-deficient strains have been identified in highly-invasive disease isolates (Kirkham *et al.* 2006; Jefferies *et al.* 2007). Furthermore, the requirement for pneumolysin for virulence appears to differ between pneumococcal disease manifestations (Mitchell and Mitchell 2010). In animal models of pneumococcal meningitis, pneumolysin-deficient strains exhibit reduced virulence, appearing in lower numbers in the cerebrospinal fluid (CSF) and brain homogenates and causing less damage to the ultrastructure of the cerebral cisternae (Braun *et al.* 2002; Wellmer *et al.* 2002; Hirst *et al.* 2008).In contrast, data obtained by Sato and coworkers indicated that pneumolysin was not essential for disease pathogenesis in a chinchilla model of otitis media (Sato *et al.* 1996). Since D39-ΔPly was not attenuated in our model, one can surmise that the toxin is not important for the damage caused to pleural cells during pneumococcal empyema.

Despite describing an impediment in the capacity of pneumolysin deficient bacteria to colonise the murine nasopharynx, Kadioglu *et al.* also reported that capsular

phenotype was a more important determinant of the efficiency of colonisation and emphasised that the relative contribution of pneumolysin to adherence should be considered in context with other pneumococcal adherence factors (Kadioglu et al. 2002). Indeed, when considering the evidence on the relevance of pneumolysin in an infection model, it is important to draw distinction between its importance as a "virulence factor" in the overall establishment of invasive disease and its role as an "adhesion factor" in the initial binding interaction with host cells. Pneumolysin is a cytoplasmic protein which is released following autolysis of bacterial cells and as such, it is unlikely to be directly involved in the initial interaction between the pneumococcal surface and the host epithelium. Thus, as observed in the current study, pneumolysin deficiency is unlikely to impact upon early adhesion analyses in vitro. Infection of pleural mesothelial cells with D39-ΔPly at infective doses of 10⁶ and 10⁴ cfu / monolayer actually induced cell death earlier than did wild-type D39, suggesting the importance of other pneumococcal factors in the current model of infection. Canvin et al. reported the production of a second haemolysin by pneumococci that was distinct from pneumolysin and characterised by the alpha haemolysis of horse blood and inhibition by cholesterol (Canvin et al. 1997). However, this protein remains unidentified and its role, if any, in virulence has never been elucidated. Nevertheless, it is conceivable that this and other such poorly characterised factors play a role in the host-pathogen dynamics in the current study and others and explain, at least in part, the seeming non-requirement for pneumolysin for pneumococci to be able to adhere to and kill epithelial cells in vitro.

Pneumolysin function has also been closely linked to the expression of the major pneumococcal autolysin, LytA (Mitchell 2000). Unlike other thiol-activated toxins, pneumolysin lacks an N-terminal signal sequence which allows transport out of the cell (Walker *et al.* 1987). This observation led to the supposition that pneumolysin release is dependent upon LytA mediated autolysis of pneumococci, which occurs during the stationary phase of growth or upon treatment with antimicrobial agents (Paton 1996). This hypothesis was substantiated by the findings of Berry *et al.*, who demonstrated that insertion duplication mutagenesis of LytA in D39 pneumococci completely abrogated pneumolysin release (Berry *et al.* 1992) and several studies showed that these mutants were highly attenuated in mouse models of pneumonia and septicaemia

(Canvin *et al.* 1995; Orihuela *et al.* 2004). The expression of autolysin was not quantified in the current study. Differences in the constitutive expression levels of this enzyme, and thus the level of pneumolysin release, between the pneumococcal strains tested in this study may also partially account for observed differences in elicited cytotoxicity.

However, this proposed mechanism of autolytic pneumolysin release was later contested by Balachandran and co-workers, who demonstrated that pneumolysin can also be secreted via an autolysin-independent mechanism in some pneumococcal strains (Balachandran *et al.* 2001). Using D39, these investigators also observed that although pneumolysin release could be quantified in a mouse model of bacteraemia, extracellular secretion of pneumolysin was not observed *in vitro* cell cultures, suggesting that some exogenous *in vivo* stimulus is required for pneumolysin release in some pneumococcal strains. Failure of D39 to secrete pneumolysin *in vitro* lends support to the data obtained in the current study in which wild-type D39 was no more cytotoxic to pleural cells than was the pneumolysin mutant D39-ΔPly and may also account for the controversial observations made on the requirement for pneumolysin in different disease models.

Aside from its toxicity, pneumolysin also promotes the propagation of bacterial disease by modulation of the immune system. The toxin is able to inhibit phagocyte and immune cell function through direct cytolytic effects on these cells (Rubins and Janoff 1998) and in addition, at sublytic concentrations, pneumolysin has been shown to inhibit neutrophil and monocyte respiratory burst, chemotaxis and bactericidal activity (Paton and Ferrante 1983); (Nandoskar M 1986); (Johnson *et al.* 1981) as well as the production of lymphokines and immunoglobulins (Ferrante 1984). Consideration of these reports emphasises the multifaceted contribution made by pneumolysin to the pathogenesis of disease. Differences in the cellular composition of human tissue at diverse disease sites, such as the lung and the meninges, may account for the contrasting role of pneumolysin in different disease manifestations and the variation in observations between cell culture models. Furthermore, observed differences in the potency of pneumolysin between animal and cell culture infection models may be due to the fact that in the *in vivo* models, pneumolysin propagates disease primarily via its immunomodulatory effects rather than its direct toxicity.

In agreement with Kadioglu *et al.*, in our infection model, the capsular phenotype appeared to be a more important virulence determinant than pneumolysin (Kadioglu *et al.* 2002). The clinical empyema isolates were shown by negative staining to express thicker polysaccharide capsules than the encapsulated laboratory passaged strains, whilst the unencapsulated state of R6 was confirmed. The clinical isolates adhered to pleural cells significantly less than any of the laboratory strains, whilst R6 was proportionally the most adherent strain by 9 hours post infection. These data suggest that over-expression of polysaccharide capsule is inhibitory to pneumococcal adhesion in our model.

There is a considerable body of evidence purporting the absolute requirement for encapsulation in systemic disease (Magee and Yother 2001; Paterson and Mitchell 2006; Nelson et al. 2007b), the primary function of which is the evasion of opsonophagocytosis. Conversely, in vitro adhesion studies have consistently shown that capsule expression is inhibitory to bacterial attachment to host cells (Hammerschmidt et al. 2005; Nelson et al. 2007a). Intrastrain phase variation, characterised by differences in opacity between colonies, has been shown to correlate with the amount of capsular polysaccharide produced, with opaque variants synthesising up to 6 times more capsule than transparent variants of the same type (Kim and Weiser 1998). Several studies have demonstrated that transparent phase variants of pneumococci adhere more efficiently to host cells in vitro (Cundell et al. 1995b; Morona et al. 2006) and also in animal models of nasopharyngeal carriage (Weiser et al. 1994) and that pneumococcal virulence levels are directly correlated with the quantity of capsule produced (MacLeod and Krauss 1950; Kim and Weiser 1998). It is thought that the enhanced adhesive capacity of unencapsulated strains is due to increased exposure of cell surface adhesins, such as CbpA and PspA (Hammerschmidt et al. 2005; Hammerschmidt 2006; Bootsma et al. 2007). In fact, several cholinebinding proteins, and in particular CbpA, have been found in greater amounts on transparent variants of pneumococci, correlating with the increased teichoic acid content associated with this phenotype (Rosenow et al. 1997). Additionally, unencapsulated strains of pneumococci, have been shown to have higher neuraminidase activity than capsule-producing strains in models of upper and lower respiratory tract infection (Manco et al. 2006), invasion of the brain endothelium (Uchiyama et al.

2009), and particularly ocular diseases such as conjunctivitis (Norcross *et al.* 2010); (Williamson *et al.* 2008). *S. pneumoniae* encodes 3 neuraminidase enzymes which function as sialidases, cleaving sialic acid residues from cell surface glycans and mucins thus facilitating colonisation of mucosal surfaces. King *et al.*, demonstrated that desialylation of the host proteins lactoferrin and secretory component (SC) by the pneumococcal neuraminidase NanA was associated with enhanced bacterial binding (King *et al.* 2006).

Notwithstanding its enhanced capacity for adherence to Met-5A cells, R6 was less cytotoxic than all the capsule producing strains tested, including its parent strain D39 and the closely related strain D39-ΔPly. This is consistent with epidemiological data that show that unencapsulated strains very rarely cause invasive disease (Hausdorff et al., 2000) and are highly attenuated in models of systemic infection. However, unencapsulated strains are frequently isolated from non-invasive mucosal diseases such as conjunctivitis (Ertugrul et al. 1997; Hanage et al. 2006; Norcross et al. 2010) . These data suggest that capsular polysaccharide is required for the full pathogenicity of the organism in invasive disease. In summation, experimental evidence suggests that the pneumococcus is able to utilise a complex array of molecules for colonisation of the host. Since host ligands vary depending on the environment, the individual contributions of virulence factors depend on the site of infection (Kadioglu et al. 2008; Kline et al. 2009). Indeed, in a large scale study designed to delineate the exact contributions of different virulence genes to various disease manifestations, Orihuela et al., confirmed that the relative contribution and thus importance of individual virulence factors to disease pathogenesis was tissue specific (Orihuela et al. 2004). The identity of the host signals that trigger expression of such tissue specific factors however, remains to be fully elucidated (Hava et al. 2003). Such investigations into the dynamics of pathogen-host interactions serve to highlight the complex multifactorial nature of pneumococcal virulence and the numerous "contingency mechanisms" that are utilised by the organism. In support of the findings of the current study, in which virulence gene knock-out mutants were still able to adhere to and kill pleural cells, studies into pneumococcal virulence suggest that incapacitation of a single virulence gene is unlikely to attenuate these bacteria.

The serotype 4 strain, TIGR4, was more cytotoxic to the pleural cell monolayer than the serotype 2 strains, causing complete destruction of the monolayer by 24h, regardless of the initial infective dose. This observation is reflective of epidemiological data, which identifies serotype 4 as one of the most common pneumococcal serotypes isolated from invasive disease in large areas of the world (Hausdorff et al., 2000) and one of the most common paediatric-empyema causing serotypes in the UK (Eltringham et al., 2003; Fletcher et al., 2006). The earlier cell death elicited by TIGR4 in our study is supported by the observations of Balachandran and colleagues who showed that serotype 4 strains secreted pneumolysin at an earlier stage of the bacterial growth cycle than D39 in vitro (Balachandran et al., 2001). Similarly, in substantiation of the epidemiological literature, the clinical isolates obtained were identified as serotype 1, which is the most common causative serotype of pneumococcal empyema in the UK (Eltringham et al., 2003; Fletcher et al., 2006) and indeed worldwide (Byington et al., 2002; Tan et al., 2002). Analysis of the haemolytic activity of these clinical strains identified a haemolysin deficiency in one isolate, which was then denoted serotype 1 non-haemolytic (S1-NH) in this study. Kirkham et al., reported that expression of non-functional pneumolysin in clinical disease isolates was the result of a mutation in the pneumolysin gene and was associated with serotype 1 pneumococci with a sequence type (ST) 306 background (Kirkham et al. 2006). Therefore, it is highly likely that the non-haemolytic variant used in the current study is of ST306 origin. Different STs within the same serotype have been shown to have different propensities to cause invasive disease, and is therefore another variable which may impact upon association dynamics in studies of disease pathogenesis. A limitation of this study is that the clinical isolates were obtained from the blood of paediatric empyema patients, which correlates with the increased capsule expression observed in these strains. Ideally, bacteria isolated from infected pleural fluid would be used to establish our model, which would allow assessment of pneumococcal phenotype, particularly the degree of capsule expression, as in situ. However, no unnecessary invasive therapies are employed in the treatment of paediatric empyema and therefore such samples were unobtainable.

In recent years it has become increasingly clear that, in addition to providing a passive barrier function, the airway epithelium actively contributes to host defence

(Diamond et al. 2000; Holgate et al. 2000; Bals and Hiemstra 2004). The innate immune functions of airway epithelial cells are of significance to bacterial pathogenesis, since these cells form the first line of defence against microbial colonisation and the manifestation of disease (Bals and Hiemstra, 2004). The anatomy of the pleura dictates that pleural mesothelial cells are the first to come into contact with invading microorganisms in empyema (Hage et al. 2004) and therefore investigations into their capacity to initiate innate immune responses to bacterial infection have been conducted. Cytokine production by mesothelial cells mediates the transmesothelial migration of acute inflammatory cells to the site of infection (Visser et al. 1998; Mutsaers 2004), which is facilitated by the expression of adhesion molecules and integrins such as lymphocyte function-associated antigen-1 (LFA-1), CD11a/CD18 and CD11b/CD18 on leucocytes and intercellular adhesion molecule-1 (ICAM-1) on mesothelial cells (Liberek et al. 1996). In patients with bacterial parapneumonic effusion, the pleura is involved in a vigorous inflammatory response (Hage et al., 2004; (Mohammed et al. 2000) characterised by the release of both C-X-C and C-C cytokines into the pleural fluid (Antony 2003; Odeh and Oliven 2005; Chiu et al. 2008). In fact, several investigators have recently described methods of using pleural fluid cytokine measurements to differentially diagnose complicated parapneumonic effusions and empyemas (Utine et al. 2005; Chiu et al. 2008; Martha et al. 2010).

Differential TLR activation patterns (Mogensen *et al.* 2006) and cytokine expression profiles have been exhibited by mesothelial cells in response to different bacterial species, and indeed, to different strains within a species (Grundmeier *et al.* 2010). Visser *et al.* described a potent IL-8 response of cultured mesothelial cells to infection with both *Staphylococcus aureus* and *Staphylococcus epidermidis* (Visser *et al.* 1998) and similarly, Mohammed *et al.*, reported a C-C cytokine response to infection with *Mycobacterium tuberculosis* (Mohammed *et al.* 1998). However, in agreement with the data obtained in the current study, Zeillemaker *et al.* observed a negligible IL-8 response to pneumococci when compared with various bacteroides species in an *in vitro* model of the pleural mesothelium (Zeillemaker *et al.* 1996; Zeillemaker *et al.* 1999). Differential cytokine expression in response to pneumococci is not, however, limited to models of respiratory infection. Fowler *et al.* found that, in contrast to the other meningitis causing organisms *Neisseria meningitidis*, *Haemophilus*

influenzae and Escherichia coli, pneumococcal infection did not induce significant secretion of IL-6, IL-8, MCP-1, RANTES or GM-CSF by cells of the leptomeninges (Fowler et al. 2004). These differential patterns of host cell activation by different bacterial species, and even intra-species strains may account for observed differences in morbidity and mortality between strains and the propensity of each to cause disease.

The innate immune response to pneumococci has been shown to be largely dependent on recognition of components from the cell wall rather than the capsule (Tuomanen et al. 1985) and in particular recognition of lipoteichoic acid by TLR2 (Yoshimura et al. 1999; Han et al. 2003; Schröder et al. 2003; Kadioglu and Andrew 2004; Kawai and Akira 2006). Also, TLR4 which is traditionally regarded as the key receptor in LPS recognition during Gram negative infections, has been shown to also bind pneumolysin (Malley et al. 2003; Srivastava et al. 2005) resulting in the activation of the transcription factor NF-κB (Koedel et al. 2003; Schmeck et al. 2006). As detailed previously, increased teichoic acid expression is associated with unencapsulated transparent-phase pneumococci, therefore one might expect an enhanced inflammatory response to unencapsulated bacteria compared to their capsuleproducing counterparts due to increased TLR2 ligation. Additionally, as aforementioned, pneumococci isolated from systemic disease are almost invariably heavily encapsulated. One may surmise that in addition to the well documented antiphagocytic benefits, expression of capsule masks cell wall teichoic acid, minimising TLR mediated inflammation. However, in the present study, neither R6 nor the capsule-sufficient strains induced production of IL-8, IL-6, IL-1β or TNF-α in pleural mesothelial cells. FACS analysis of Met-5A cells confirmed the expression of TLR2 and TLR4, proving that pleural cells possess the apparatus necessary for pneumococcal recognition. Moreover, the observation that Met-5A cells exhibited the capacity to mount a pro-inflammatory response to LPS-containing meningococcal outer membrane preparations, primarily via TLR4, proved that the TLR signal transduction mechanism was functional in our model.

The lack of inflammation observed in our study is in agreement with the findings of Xu *et al.*, who reported that infection of alveolar epithelial cells with *S. pneumoniae* resulted in negligible TNF-α production (Xu *et al.* 2008). The failure of pneumococci to induce an inflammatory response in mesothelial cells may in itself be regarded as a

putative virulence mechanism via which the bacteria inhibit leucocyte recruitment. Barbuti et al. reported that pneumococci were able to induce mast cell degranulation in vitro without the concomitant production of pro-inflammatory cytokines and subsequent neutrophil recruitment (Barbuti et al. 2006), whilst Martner et al. reported that pneumococcal infection of peripheral blood mononuclear cells resulted in up to 30fold less TNF-α production than infection with other closely related streptococcal species (Martner et al. 2009). In addition, Kerr et al., demonstrated that increased susceptibility of CBA/Ca mice to pneumococcal pneumonia was correlated with reduced TNF-α expression in the lungs in the early stages of infection (Kerr et al. 2002). In contrast, direct stimulation of phagocytic cells with individual pneumococcal components including capsular polysaccharide, lipoteichoic acid and pneumolysin has been demonstrated to induce pro-inflammatory cytokine production in vitro (Riesenfeld-Orn et al. 1989; Houldsworth et al. 1994; Simpson et al. 1994; Kerr et al. 2002; Weber et al. 2003). Taken together with the current study, these investigations suggest that the pneumococcus may employ a mechanism to actively suppress cytokine production and is a strategy by which the bacterium evades phagocytic recruitment and clearance providing it with an advantage for disease propagation.

In support of this concept of active inflammatory suppression, the data obtained in the present study demonstrates that TNF- α induced production of IL-8 and IL-6 is abrogated by pneumococci in a dose dependent manner. Furthermore, in support of the data obtained by Beren *et al.*, we showed that heat-attenuation of pneumococci induced secretion of IL-8, IL-6, IL-1 β and TNF- α by Met-5A cells, indicating that the suppressive factor is heat labile, although the exact molecular mechanism by which these bacteria exert this effect is as yet poorly characterised (Beran *et al.* 2011). However, Graham and Paton described modulation of the immune responses of the respiratory epithelial cell lines A549 and Detroit-562 by the pneumococcal adhesion proteins CbpA and PspA, as evidenced by an increase in the secretion of IL-8 and MIP- 2α by cells infected with knockout mutants for these proteins compared to wild type pneumococci (Graham and Paton, 2006). In the present model, these proteins were not found by microarray to be differentially expressed in pneumococci during interaction with Met-5A cells. However, analysis of constitutive expression levels of these factors in the bacteria used in our model may reveal correlation between expression levels and

cytokine production. Recently, Witzenrath *et al.* demonstrated that IL-1 β production in cultured monocytes was inhibited in pneumolysin deficient pneumococci, including D39- Δ Ply and a serotype 1 ST306 non haemolytic variant as used in the current study, due to reduced activation of the Nod-like receptor (NLR) inflammasome (Witzenrath *et al.* 2011). These authors hypothesise that single nucleotide polymorphisms in the pneumolysin gene or down-regulation of pneumolysin may confer a selective advantage to pneumococci under some conditions by decreasing NLR inflammasome mediated inflammation. In the current study however, no IL-1 β secretion was detected in culture supernatants from Met-5A cells infected with either pneumolysin sufficient or deficient strains.

Another mechanism by which other streptococcal species has been shown to evade host defences is via degradation of elicited cytokines. *Streptococcus pyogenes* produces specific proteases that degrade C-X-C chemokines, thus impairing bacterial clearance from infected tissues (Hidalgo-Grass *et al.*, 2006). These proteases are encoded within the so-called streptococcal invasion locus (sil), in which *S. pneumoniae* has been shown to share homology (Claverys and Havarstein, 2002). However, experiments conducted in the present study demonstrated that TNF- α was not degraded by any of the pneumococcal strains used.

The inhibition of TLR mediated antibacterial responses, however, is not exclusive to pneumococci. Other colonisers of the respiratory epithelium, *Moraxella catarrhalis*, *Neisseria meningitidis*, and *Haemophilus influenzae*, have been shown to exploit host cell carcinoembryonic antigen-related cell adhesion molecules (CEACAMs) to inhibit TLR2 initiated NF-κB-dependent inflammatory responses in pulmonary epithelial cells (Slevogt *et al.* 2008). Ligation of CEACAMs by bacterial proteins promotes the recruitment of a Src homology 2 domain-containing cytoplasmic protein tyrosine phosphatase 1 (SHP-1) to the membrane. This limits the phosphorylation of a phosphoinositide 3-OH kinase (PI(3)K) which has been shown to be important for TLR2 induced activation of NF-κB (Arbibe *et al.* 2000). Although a homologous CEACAM binding molecule has not been described in pneumococci, it is possible that these pathogens use this or an equally elegant mechanism of immune suppression. However, considerable further investigation is required in order to fully

elucidate the molecular mechanisms by which pneumococci are able to modulate cytokine production in host cells.

From the perspective of the host, an alternative mechanism by which the airway epithelium may afford protection from bacterial infection is by secretion of anti-inflammatory cytokines (Kerr *et al.*, 2002). The production of anti-inflammatory molecules such as IL-10 and TGF- β modulates the production of pro-inflammatory mediators (Bogdan *et al.* 1991; Kasama *et al.* 1995), thereby limiting damage to the host and therefore bacterial invasion and has also been shown to down-regulate the expression of adhesion molecules (Willems *et al.* 1994). In the current study, IL-10 was not detected in the infected culture supernatants, although this was not unexpected since this cytokine is primarily expressed by monocytes *in vivo*. However, the presence of TGF- β at relatively high basal levels may have inhibited the production of pro-inflammatory cytokines by Met-5A cells and is a possible mechanism by which the pleura modulates *in situ* inflammation and prevents excessive immune responses.

Since our investigations, in concordance with others, have shown that pneumococci do not induce a pro-inflammatory response by pleural mesothelial cells *in vitro*, it appears that the rigorous cytokine response consistently seen in clinical empyema cases (Utine *et al.*, 2005) is not augmented by these cells. Mohammed *et al.*, observed that more the induction of acute pleural inflammation in a murine model of staphylococcal empyema was dependent upon the activity of CD4+ T-cells (Mohammed *et al.*, 2000). It is likely then, that the elevated local and systemic levels of inflammatory cytokines seen in clinical empyema are primarily produced by more specialised cells, such as resident neutrophils and serous macrophages.

6.2 Microarray analysis of differential gene expression in *Streptococcus* pneumoniae following adherence to human pleural mesothelial cells.

Pneumococcal gene regulation during interactions with host tissues is not well defined and research has been limited by the technical difficulties of isolating sufficient quantities of intact and pure bacterial RNA from infected human cells (Hinton *et al.* 2004). In the current study, we have optimised a method of bacterial RNA extraction which has enabled examination of the gene expression profile of *Streptococcus pneumoniae* during interaction with human pleural mesothelial cells in order to identify

bacterial factors which may be important to the pathogenesis of pleural empyema. The use of microarray technology allowed the interrogation of the entire pneumococcal genome without prior bias as to which genes or pathways might be involved in pathogenesis, as opposed to conventional PCR and reporter fusion techniques which limit analysis to a limited number of arbitrarily selected transcripts (Handfield and Levesque 1999; Di Cello *et al.* 2005).

Ideally, gene expression would be analysed in pneumococci isolated directly from invasive disease, since expression of virulence genes *in vivo* would verify their importance to the pathogenesis of empyema. However, in addition to the aforementioned technical difficulties of obtaining a sufficient RNA yield, invasive techniques would be required to isolate pneumococci from the pleural fluid and these are not readily employed in the treatment of empyema, particularly in paediatric patients. Therefore, the use of pleural fluid isolates was not viable in this study. Conversely, a limitation of using bacteria isolated directly from clinical disease is that no appropriate control is available and thus differential gene expression cannot be accurately examined. In addition, the yield of bacterial RNA from organisms recovered directly from the pleura is unlikely to be sufficient for analyses. In our *in vitro* model however, gene expression was compared between pneumococci adherent to pleural cells and bacteria maintained in the same cell culture medium. Perturbations in gene expression then, are in response to either direct cell contact or to components secreted by the cell both during normal physiology and in response to bacterial infection.

In order to identify genes that were most likely to be important in pneumococcal pathogenesis, stringent filtering criteria were applied to the data (Section 4.2), and only those genes that were consistently altered across all biological replicates were further analysed. Using these filtering algorithms, no differential expression was shown in any of the canonical, well characterised pneumococcal virulence genes. Indeed, of a set of 20 known virulence determinants described by Orihuela and colleagues (*Table 6-1*), none were represented in our shortlist (Chapter 4, Tables 4.1 and 4.2) (Orihuela *et al.* 2004). However, when data were screened with the condition that only 2 out of 3 biological replicates need exhibit \geq 2-fold expression changes, 5 of these virulence genes satisfied the criteria. Of these perturbations, 3 genes were upregulated, namely pneumolysin (*Ply*), laminin binding protein (*lmb*) and pneumococcal

histidine triad precursor D (*phtD*). The serotype 2 equivalents of *cps4A* and *cps4C*, along with 3 other subunits of the serotype 2 capsular biosynthesis locus, were all significantly down-regulated in 2 of 3 replicates.

Gene Symbol	TIGR4 Annotation	Function
blpU	SpTIGR4-0041	Bacteriocin
cps4A	SpTIGR4-0346	Capsular polysaccharide biosynthesis
cps4C	SpTIGR4-0348	Capsular polysaccharide biosynthesis
pspA	SpTIGR4-0117	Pneumococcal surface protein A
cbpJ	SpTIGR4-0378	Choline-binding protein J
cbpG	SpTIGR4-0390	Choline-binding protein G
cbpF	SpTIGR4-0391	Choline-binding protein F
blpK	SpTIGR4-0533	Bacteriocin associated protein
blpY	SpTIGR4-0545	Immunity protein
prtA	SpTIGR4-0641	Protective antigen A
spxB	SpTIGR4-0730	Pyruvate oxidase
Lmb	SpTIGR4-1002	Adhesion lipoprotein
phtD	SpTIGR4-1003	Pneumococcal histidine triad precursor D
xseA	SpTIGR4-1207	Exodeoxyribonuclease VII, large subunit
Ply	SpTIGR4-1923	Pneumolysin
lytA	SpTIGR4-1937	Autolysin
cbpA	SpTIGR4-2190	Choline-binding protein A
cbpD	SpTIGR4-2201	Choline-binding protein D
htrA	SpTIGR4-2239	Serine protease
spoJ	SpTIGR4-2240	Homologue of sporulation protein

Table 6-1: List of known virulence determinants of *Streptococcus* pneumoniae.

The putative adhesin choline-binding protein A (CbpA) contributes to pneumococcal virulence primarily by facilitating bacterial adhesion to host cells (Rosenow et al. 1997; Robson et al. 2006) via exploitation of the secretory component of the human polymeric immunoglobulin receptor (pIgR) (Hammerschmidt et al. 2000; Zhang et al. 2000). In the current study, the expression of CbpA, or indeed any member of the choline-binding protein family, was not altered in pneumococci adherent to pleural cells compared to control bacteria. In agreement with our data, Song et al. reported that pneumococci adherent to lung epithelial cells for 1 hour in vitro did not differentially express CbpA (Song et al. 2008a). Conversely however, Orihuela et al., observed a 2.3 fold increase in CbpA expression in pneumococci following epithelial cell contact (Orihuela et al., 2004). Likewise LeMessurier et al. reported an increase in mRNA transcripts for CbpA in pneumococci adhered to the murine nasopharynx in vivo (LeMessurier et al. 2006). CbpA-deficient mutants have been demonstrated to have up to a 90% reduction in their capacity to invade host nasopharyngeal cells compared to the parent wild type (Zhang et al., 2000), indicating that expression of this protein is necessary for invasive disease (Zhang et al., 2000). Consideration of all these data, in combination with the results of the present study, promotes the hypothesis that very early adhesion events are not dependent on choline-binding proteins, but that these molecules are up-regulated soon after host cell ligation to facilitate epithelial transmigration and tissue invasion. In the current study, gene expression analyses were performed at 2 hours post infection, as necessitated by the high multiplicity of infection used. Since, gene transcription is a highly dynamic process, a larger scale experiment would allow analysis of later gene transcription events and the identification of factors involved in pneumococcal pathogenesis following initial host cell adherence.

In pathogenic bacteria, divalent cations serve as essential micronutrients for the growth and survival of the organism. Thus, an innate immune mechanism by which the host is able to limit bacterial colonisation of tissues is by ion sequestration via high-affinity metal binding proteins (Corbin *et al.* 2008). Many bacteria, however, have evolved metal-chelating scavenging mechanisms, involving ion-specific transport systems, which enable them to counteract these host defences. The best characterised of these is the Mn²⁺ binding and virulence-associated protein pneumococcal surface antigen A (PsaA) (Dintilhac *et al.* 1997; Marra *et al.* 2002). Although no differential

expression was observed for PsaA in the current study, the closely related protein PsaB, which is also involved in manganese transport, exhibited a 4-fold increase in expression in pneumococci adherent to pleural cells. These data are substantiated by the findings of Orihuela et al. who observed 3.7-fold increase in PsaB following bacterial association with Detroit pharyngeal epithelial cells (Orihuela et al., 2004). Song et al. also reported the induction of PsaC following colonisation of lung epithelial cells (Song et al., 2008a). The absolute requirement for the proteins of the psa operon in infection is evidenced by complete attenuation of PsaA, PsaB and PsaC mutants individually (Marra et al., 2002). Moreover, the zinc efflux protein czcD exhibited a mean 4.9-fold up-regulation in our model. Recently, Ogunniyi et al., showed that czcD, which is activated by elevated levels of Zn²⁺, (Kloosterman et al. 2007), was also upregulated under conditions of Mn²⁺ stress. This suggests that increases in cellular Zn²⁺ are correlated with decreases in Mn²⁺ and that czcD plays a role in manganese acquisition (Ogunniyi et al. 2010). The importance of manganese to pneumococcal virulence is becoming increasingly apparent, particularly its role in the regulation of the oxidative-stress-response genes pyruvate oxidase (spxB) and superoxide dismutase (SOD) (Kehres and Maguire 2003; Johnston et al. 2006). Of note, in the current model, the gene encoding spxB was up-regulated in all 3 biological replicates with a mean fold increase of 1.8. However, this gene was removed from analysis by the filtering algorithm as none of the individual replicates exhibited a \geq 2-fold change. This enzyme is involved in the generation of hydrogen peroxide (H₂O₂) and has been implicated as an important factor in the pathogenesis of pneumococcal disease (Spellerberg et al. 1996). The production of H₂O₂ has been demonstrated to promote pneumococcal colonisation, both by exerting bactericidal effects on competing nasopharyngeal flora (Pericone et al. 2000) and by inhibiting ciliary beating, thereby facilitating the progression of bacterial infection to the lungs (Hirst et al., 2000; Feldman et al., 2002). The data obtained in our study is in concordance with data obtained by other investigators which shows that the expression of spxB is negatively correlated with expression of capsule (LeMessurier et al., 2006) and is selected for in the transparent phenotype of pneumococci during phase variation (Overweg et al. 2000). Albeit not significant, the up-regulation of spxB coincided with the down-regulation of 5 individual polysaccharide capsule subunits in our model. This observed downregulation of genes of the capsular operon during early host cell interaction concurs

with data discussed previously, in which capsule expression was demonstrated to hinder adhesion (Hammerschmidt *et al.* 2005).

The pneumococcal Zn²⁺-binding histidine triad precursor D (phtD) protein is a highly immunogenic antigen which affords protection against heterologous pneumococci in immunised mice (Adamou et al. 2001) and is also recognised by convalescent phase sera from patients with pneumococcal bacteraemia (Adamou et al., 2001) and otitis media (Simell et al. 2009). This surface expressed protein has recently been shown to contribute to virulence by regulating bacterial intracellular zinc concentrations in the various host niches encountered during invasion of host tissue (Loisel et al. 2011). Of additional interest, this gene lies directly downstream of the gene lmb, which is homologous to a laminin-binding protein described as an important adhesin for Streptococcus anginosus (Allen and Höök 2002) and which was upregulated in all 3 biological replicates in our study. Panina et al. suggested that disruption of the pneumococcal zinc transport system may reduce expression of laminin adhesion proteins that are likely contributors to pneumococcal colonisation and invasion (Panina et al. 2003). These data suggest that the role of phtD in pneumococcal pathogenesis may be underappreciated and that considerable further investigation is warranted.

The ability to adapt to changes in nutrient availability is essential to bacterial survival within the host. Several studies have shown that glutamine metabolism in particular plays a role in bacterial virulence by providing the cell with a source of nitrogen (Tamura et al. 2002; Hendriksen et al. 2008). In the pneumococcus, glutamine metabolism is under the control of the transcriptional regulator GlnR (Kloosterman et al. 2006), which consists of the gene encoding the glutamate dehydrogenase (gdhA) enzyme, the genes glnP and glnQ which encode the major pneumococcal glutamine/glutamate transporter and the gene encoding glutamine synthase (glnA). Strikingly, in the current study, all of the genes in this regulon were on the shortlist of most differentially up-regulated genes (Table 4-1). A study by Hendriksen and colleagues demonstrated that pneumococci deficient in glnA were attenuated in their ability to colonise the nasopharynx in a murine model, while glnP was shown by microarray analysis to be involved in adherence to Detroit cells in vitro (Hendriksen et al. 2008). Interestingly, in group B streptococci, glnQ has been shown to mediate

bacterial adherence to host cells by binding to fibronectin (Tamura *et al.*, 2002). Since every gene in the GlnR regulon was significantly and reproducibly up-regulated in the current study, the data strongly suggest that proteins involved in glutamine metabolism are essential to the pathogenesis of empyema, perhaps by directly mediating adhesion by binding molecules such as fibronectin on the surface of pleural mesothelial cells. The oligopeptide binding protein aliA was also one of the most significantly up-regulated genes in the current study, exhibiting a 5.7-fold increase in expression. This gene was first implicated in adhesion by Cundell *et al.* who showed that mutations in this gene decreased pneumococcal binding to pulmonary epithelial cells via the GalNAc-β-1-4Gal glycoconjugate receptor (Cundell *et al.* 1995a). More recently though, Kerr *et al.* demonstrated that aliA contributes to adhesion but is not required in invasive disease (Kerr *et al.* 2004). In light of these data, one might hypothesise that since the pneumococcus has to adapt to the varying supply of micronutrients available at discrete host niches, it is likely that virulence gene expression is modulated by metabolic regulators.

Another interesting observation is that the expression of 2 genes associated with purine ribonucleotide synthesis, purF and purL, was down-regulated in our model. Differential regulation of purine ribonucleotide biosynthesis genes was highlighted in a study by Song *et al.* who observed significant down-regulation of 11 pneumococcal genes involved in this process in the avirulent strain R6 following interaction with human lung cells (Song *et al.*, 2008a). Other studies have shown significant upregulation of these genes in pneumococci isolated from blood (Orihuela *et al.*, 2004), suggesting that ribonucleotide biosynthesis may contribute to host-pathogen interactions and warrants further investigation.

In the present study, although pneumolysin was up-regulated in all 3 biological replicates, differential expression was not consistently significant and therefore pneumolysin did not satisfy the filtering criteria set out in our study. In fact, analysis of pneumolysin expression in individual replicates, which ranged from 16 - 1.4-fold increases, illustrated the degree of inter-experimental variation in bacterial gene expression. This observation advocates the stringent filtering method used in the identification of differentially expressed genes and strengthens the reliability and reproducibility of the results reported herein.

Accordingly, our conclusion that expression of pneumolysin is not consistently altered in our model is substantiated by the data obtained in other *in vitro* studies of pneumococcal adherence to cells of the respiratory tract (Orihuela *et al.* 2004; Song *et al.* 2008a). In addition, LeMessurier demonstrated that pneumolysin was not differentially regulated in pneumococci isolated from the nasopharynx, the blood or the lung when compared to bacteria grown *in vitro* (LeMessurier *et al.*, 2006). This apparent redundancy of pneumolysin during early adhesion interactions is supportive of the adherence data obtained in our model, in which no differences in adhesive capacity were exhibited between D39 and D39-ΔPly. Notwithstanding the consistent absence of differential pneumolysin expression in adherence models, pneumolysin has been shown to play a critical role in invasive infections (Hirst *et al.*, 2004). Thus it has been proposed that pneumolysin production is regulated at a post-transcriptional level or that regulation of pneumolysin is independent of environmental stimuli (Kwon *et al.* 2003).

The multiplicity of pneumococcal virulence is becoming evermore apparent and the contribution of individual virulence genes to pathogenesis has been shown to vary between different manifestations of pneumococcal disease (Mitchell and Mitchell, 2010). Accordingly, patterns of differential gene expression have likewise been shown to differ between bacteria isolated from distinct host niches. Orihuela and co-workers observed a greater number of gene perturbations in pneumococci following exposure to epithelial cells than blood and CSF, and found a large number of genes that were differentially expressed at only one site (Orihuela *et al.*, 2004). Similarly, LeMessurier *et al.* reported differential transcription of known pneumococcal virulence genes at discrete host niches, indicating variation in the contributions made by individual virulence factors in different diseases (LeMessurier *et al.*, 2006). The premise of the current study was to identify pneumococcal genes involved specifically in the pathogenesis of pleural empyema. These observations of disparate gene expression between different disease sites emphasise the requirement for understanding pneumococcal pathogenesis on a disease-specific basis.

It has also been reported that differential expression of some virulence genes, including pneumolysin, CbpA and CbpG within a defined host niche, varies between pneumococcal serotypes (Desa *et al.* 2008). Such observations are likely to account for the epidemiological differences in the propensity of pneumococcal serotypes to cause

disease. Since such disparate gene expression has been shown between serotypes, a limitation of the current model of empyema is that pneumococcal gene expression analyses were performed in the serotype 2 strain D39 which is not a common causative serotype of invasive pneumococcal disease. However, since the serotype 1 clinical empyema isolates adhered poorly to pleural cells in our study, a sufficient yield of bacterial RNA could not be obtained for microarray analysis. Moreover, D39 is a well-characterised strain which is commonly used in both *in vitro* and *in vivo* adherence and gene expression analyses and therefore use of this stain in the current model allows ready comparison of our data to that obtained by other researchers. However, it should be acknowledged that since no standardised protocol for microarray analysis has been formulated, much disparity exists between methods used to analyse and assign significance to gene expression. Therefore, when comparing gene expression data between studies, it is important to consider the "cut off" criteria used by individual researchers to assign significance and to interpret the results presented in the appropriate context.

Although microarrays are powerful tools that provide guidance on dynamic processes occurring within cells, it should be acknowledged that this technology reports differential expression between a test and a control condition, and not absolute gene expression levels. This is relevant to the current study since lack of differential expression does not eliminate the possibility that putative virulence genes are involved in pleural cell interaction and in the pathogenesis of empyema. Similarly, post-transcriptional regulation mechanisms mean that gene transcription does not necessarily result in the expression of the corresponding protein. Moreover, expression of a protein may not necessarily have a pathological effect (Gygi *et al.* 1999). Therefore, absolute quantitation of putative virulence genes by RT-qPCR and other protein-based techniques may reveal that proteins that are imperative for pneumococcal adhesion and virulence are constitutively expressed by these bacteria.

6.3 Gene expression in human pleural mesothelial cells following infection with *Streptococcus pneumoniae*.

Concurrent to the analysis of the pneumococcal transcriptome in our model of empyema, early gene expression in pleural mesothelial cells in response to pneumococcal infection was assessed.

In order that the infection conditions were consistent in our model, the pneumococcal reference strain D39 was used to challenge Met-5A cells in our analyses of host cell gene transcription, since it was in this strain that the bacterial transcriptome was assessed. In addition, microarray analysis of pleural cell transcription was performed following infection with the clinical empyema isolate S1-H, in order to discern whether empyema-causing isolates exert differential effects on the host compared to non-empyema-causing pneumococci. Differences in the capability of the host to recognise and respond to different pneumococcal strains may account for the disparate propensities of pneumococcal strains to cause invasive disease.

The data obtained in the current investigation however, suggest that host gene expression differs more between live bacteria and their homologous lysates than between different strains. Indeed, a number of genes were oppositely expressed in cells infected with whole bacteria and lysates. Strikingly, the expression of the nuclear oncogene SET, which is involved in apoptosis and cell disassembly, was downregulated following infection with live D39 and S1-H pneumococci, but up-regulated following stimulation with their respective lysates. The same was true of other genes that are phosphorylated during proapoptotic and necrotic processes, including OAZI, GPX4 and TK1. Apoptosis is sometimes a defensive mechanism employed by host cells during infection, particularly with intracellular organisms (Tilney and Portnoy 1989). Thus an ambitious hypothesis may be that, in our model, live pneumococci are able to actively inhibit apoptosis during early interactions with host cells in order to promote colonisation and the propagation of disease, whilst recognition of bacterial components in lysates results in the transcription of proapoptotic genes in the host. Terminal deoxynucleotidyl transferase mediated dUTP nick end labelling (TUNEL) techniques could be used to further develop this hypothesis. In contrast to our data, Mohammad et al., described the potent induction of the proapoptotic genes Bad and Bak in pleural mesothelial cells infected with Staphylococcus aureus in a murine model of empyema

(Mohammed *et al.* 2007). Similarly, Bootsma *et al.* reported the downregulation of the antiapoptotic gene *AP15* in an *in vitro* model of pneumococcal colonisation of the nasopharynx (Bootsma *et al.* 2007).

In the current study, we demonstrated the expression of TLRs 2 and 4 on Met-5A cells, which recognise the key pneumococcal components peptidoglycan and pneumolysin respectively. In addition, we demonstrated the ability of these cells to mount a TLR-mediated cytokine response following challenge with LPS-rich meningococcal-derived outer membrane preparations. This led to the postulation that pneumococci are able to actively suppress host immune responses. Graham and Paton demonstrated that the pro-inflammatory response of both airway epithelial cells and pneumocytes to CbpA-deficient pneumococci was significantly increased compared to the wildtype in vitro, suggesting that this putative adherence molecule is involved in immune modulation (Graham and Paton, 2006). Thus, to investigate the possibility of active immune modulation in our model, we also challenged pleural cells with mechanically disrupted and heat-attenuated bacteria. As previously described, bacterial lysates did not elicit an innate response in Met-5A cells with cytokine protein levels comparable to those observed in cells treated with live bacteria. One may surmise then, that any suppressive component is perhaps either secreted or preserved in its native conformation in bacterial lysates and therefore retains its function. The observation that gene expression fold-changes were greatly elevated in cells challenged with heatattenuated pneumococci also lends support to the hypothesis that pneumococci produce a factor which inhibits gene transcription, since heating would denature such a protein, rendering it inactive.

In support of our cytokine quantitation data, transcriptomic analysis of pleural cells challenged with both live bacteria and lysates did not reveal the differential expression of any genes encoding cytokines or chemokines, or indeed, any genes involved in the signal transduction pathways that result in cytokine production. However, it should be acknowledged that this was also true in pleural cells challenged with heat-attenuated pneumococci, which in our antigen-stimulation experiments did elicit a robust inflammatory response. However, host gene expression was assessed at the early time point of 2 hours post infection and it is likely that during sustained infection, genes that contribute significantly to host immunity are transcribed at a later

In contention of our hypothesis, Mohammed and colleagues reported the expression of the potent chemokines MIP-1α and MCP-1 by *ex vivo* human pleural mesothelial cells from patients with *Mycobacterium tuberculosis* (Mohammed *et al.* 1998). As with any cell culture model, our investigation is limited in that as a transformed cell line, Met-5A cells may respond to infection in a disparate manner to primary cells due to alterations to controls on growth and differentiation. In addition, cellular responses to infection *in vivo* are modulated by the presence of a variety of other cell types and soluble factors which cannot be mimicked in an *in vitro* monoculture. Co-culture of pleural mesothelial cells with immune effector cell types *e.g.* neutrophils may help to further elucidate the host-pathogen interactions that occur during the pathogenesis of empyema.

Distinct patterns of host gene transcription have been described in response to different pathogens (Schubert-Unkmeir *et al.* 2009). In fact, such is the degree of this heterogeneity, that Evans *et al.* purport that the aetiology of infectious disease can be predicted from gene expression profiles, with diagnostic accuracy of around 95% (Evans *et al.* 2010). Furthermore, distinct transcriptional responses have been described between different strains of pneumococci (Bootsma *et al.*, 2007; Rogers *et al.*, 2003). These reports serve to emphasise the complex multiplicity of pathogen host interactions during the pathogenesis of disease. Indeed, the plethora of data obtained in the current investigation, and indeed all microarray studies, serve to augment models of infection

and refine hypotheses on mechanisms of both microbial pathogenesis and host defence rather than provide definitive answers about these interactions.

Pathway analysis is a useful tool to identify cellular processes and functions that are most perturbed during infection. In the current study, mitochondrial dysfunction was the most consistently affected toxicological pathway following challenge with pneumococcal antigens. This is consistent with the data obtained by Mohammed et al. who describe the release of mitochondrial cytochrome-c during pleural infection with Staphylococcus aureus (Mohammed et al., 2007). In addition to the direct toxic effects of pneumococcal virulence genes, it is possible that these bacteria exert cytotoxicity to host cells by inhibiting host metabolic and homeostatic processes thereby effectively "shutting down" the cell. In substantiation our data, a study by Brealey et al. implicated bioenergetic failure as a result of mitochondrial dysfunction as an important mechanism in the pathophysiology of haematological sepsis (Brealey et al. 2002). In addition to this bioenergetic failure, another pathway that incurred a high number of perturbations was the transcription regulation pathway in which pre-RNA is cleaved and polyadenylated. Although no distinct pattern of regulation was evident between challenge conditions for this pathway, the higher levels of overall gene expression in cells challenged with heat-attenuated pneumococci compared to all other challenge conditions suggests that levels of overall gene transcription may be non-specifically reduced by pneumococci, for example by down-regulation of genes encoding ribosomal subunits and transcription factors. One can surmise that infection-induced alterations in host transcription processes maybe another strategy by which bacteria attempt to evade host defences such as cytokine production.

6.4 Future work.

The current study has characterised the interactions of *Streptococcus pneumoniae* with human pleural mesothelial cells in an *in vitro* model of empyema on a cellular and transcriptomic level. The data obtained has allowed the refining of the initial hypotheses and identification of further investigations that would more precisely define these interactions.

- Analysis of more clinical empyema strains including, if possible, different seroptypes, in the cell culture model would reveal whether the observations seen in the current study, such as poor adhesion of these strains to pleural cells, is a universal feature of all empyema isolates.
- Ideally, future clinical isolates would be obtained directly from pleural fluid during therapeutic chest drain, to identify the features of empyema-causing strains as *in situ*. The advantages of using disease isolates for transcriptome studies is obvious, however, the limitations involved *e.g.* identification of an appropriate control, have been discussed.
- Use of co-culturing techniques with other cell types found in the pleura, or more ideally, primary pleural tissue, would address the limitation of the homogeneity of the current cell culture model.
- Engineered promoter sequences could be used to overexpress genes identified in pneumococci as differentially upregulated, such as laminin binding protein, to discern whether this confers hypervirulence. Depending on the cellular localisation of these genes, the generation of antibodies or use of gene silencing techniques could be investigated to attenuate disease causing bacteria.
- To expand upon the current investigation, the essentiality of individual genes to pneumococcal virulence in empyema could be dertermined by the use of further knock out mutants, both for putative virulence genes already described and for genes identified by microarray in this study, such as pyruvate oxidase and superoxide dismutase. In addition, the capsular loci could be knocked out in the clinical isolates used in the current study to test our supposition that increased

capsule expression was the inbitory factor in adhesion of these strains to pleural cells.

- Since the pneumococcal proteins PspA and CbpA have been shown to modulate immune reponses in other *in vitro* models, the constitutive expression of these factors in the pneumococcal isolates used herein, and also any future empyema samples obtained, could be quantified by PCR and ELISA or western blot.
- The new hypothesis that pneumococci actively suppress the innate immune response of the host could be investigated by stimulation of pleural cells with capsular polysaccharide alongside recombinant proteins generated for individual pneumococcal virulence genes to identify factors involved in this mechanism.
- Microarrays were performed at a relatively early timepoint, and mRNA transcription and translation is a highly dynamic process. Therefore, RT-qPCR could be used to quantify specific transcripts temporally.
- Since the data obtained in the current study demonstrate that pneumolysin deficiency does not attenuate pneumococci in this model, knockout mutants could be engineered for the second haemolysin described by Canvin *et al.* (Canvin *et al.* 1997), to determine whether this toxin is alternatively used in some disease manifestations, or in cases where pneumolysin has been attenuated.
- Constitutive expression of *LytA* in each pneumococaal strain could be measured by PCR, since the expression of this gene has been correlated with pneumolysin release (Mitchell 2000). Thus differences in expression levels of this enzyme could account for relative virulence and disease-causing propensity.
- Both bacterial and microarray data would be further substantiated simply by increasing the number of replicates. Imposition of strict filtering algorithms as described in the present study may further isolate genes and pathways critical for the manifestation of empyema.

- As detailed previously, more accurate quantification of selected genes by RTqPCR would validate the data obtained in microarray experiments.
- Cytotoxicty of pneumococcal infection to pleural cells could be more accurately
 quantified by TUNEL and PCR for apoptotic and necrotic factors such as
 caspases. Similarly, mitochondrial dysfunction in pleural cells could be
 confirmed by measurement of cytochrome c proteins in infected culture
 supernatants.

These investigations would further elucidate the molecular mechanisms employed by pneumococci during the manifestation of disease and may ultimately lead to the advent of novel anti-microbial prophylactics and therapies.

CHAPTER 7 REFERENCES

- (APPG), A.-P. P. G. (2008). Improving Global Health by Preventing Pneumococcal Disease. London, UK.
- Adamou, J. E., *et al.* (2001). "Identification and Characterization of a Novel Family of Pneumococcal Proteins That Are Protective against Sepsis." <u>Infect. Immun.</u> **69**(2): 949-958.
- Agarwal, V. and S. Hammerschmidt (2009). "Cdc42 and the phosphatidylinositol 3-kinase-Akt pathway are essential for PspC-mediated internalization of pneumococci by respiratory epithelial cells." <u>Journal of Biological Chemistry</u> **284**(29): 19427-19436.
- Allen, B. L. and M. Höök (2002). "Isolation of a putative laminin binding protein from Streptococcus anginosus." <u>Microbial Pathogenesis</u> **33**(1): 23-31.
- Ampofo, K., *et al.* (2008). "Seasonal Invasive Pneumococcal Disease in Children: Role of Preceding Respiratory Viral Infection." Pediatrics **122**(2): 229-237.
- Andrews, P. M. and K. R. Porter (1973). "The ultrastructural morphology and possible functional significance of mesothelial microvilli." <u>The Anatomical Record</u> **177**(3): 409-426.
- Antony, V. B. (2003). "Immunological mechanisms in pleural disease." <u>European Respiratory</u> Journal **21**(3): 539-544.
- Arbibe, L., *et al.* (2000). "Toll-like receptor 2-mediated NF-kappa B activation requires a Rac1-dependent pathway." Nature immunology **1**(6): 533-540.
- Arredouani, M., et al. (2004). "The scavenger receptor MARCO is required for lung defense against pneumococcal pneumonia and inhaled particles". J Exp Med 200, 267–272.
- Austrian, G. (1964). "Pneumococcal Bacteremia with Especial Reference to Bacteremic Pneumococcal Pneumonia." <u>Annals of Internal Medicine</u> **60**(5): 759-766.
- Balachandran, P., *et al.* (2001). "The Autolytic Enzyme LytA of Streptococcus pneumoniae Is Not Responsible for Releasing Pneumolysin." J. Bacteriol. **183**(10): 3108-3116.
- Balfour-Lynn, I. M., *et al.* (2005). "BTS guidelines for the management of pleural infection in children." Thorax **60**(suppl 1): i1-i21.
- Bals, R. and P. S. Hiemstra (2004). "Innate immunity in the lung: how epithelial cells fight against respiratory pathogens." <u>European Respiratory Journal</u> **23**(2): 327-333.
- Barbuti, G., *et al.* (2006). "Streptococcus pneumoniae induces mast cell degranulation." <u>International Journal of Medical Microbiology</u> **296**(4-5): 325-329.
- Bauer, S., Kirschning et al. (2001). "Human TLR9 confers responsiveness to bacterial DNA via species-specific CpG motif recognition.". Proc Natl Acad Sci U S A 98, 9237—
- Bekri, H., *et al.* (2007). "[Streptococcus pneumoniae serotypes involved in children with pleural empyemas in France]. [French]." <u>Archives de Pediatrie</u> **14**(3): 239-243.
- Bentley, S. D., *et al.* (2006). "Genetic Analysis of the Capsular Biosynthetic Locus from All 90 Pneumococcal Serotypes." <u>PLoS Genet</u> **2**(3): e31.
- Beran, O., *et al.* (2011). "Differences in Toll-like receptor expression and cytokine production after stimulation with heat-killed gram-positive and gram-negative bacteria." <u>Folia Microbiologica</u> **56**(2): 138-142.

- Berry, A., *et al.* (1995). "Effect of defined point mutations in the pneumolysin gene on the virulence of Streptococcus pneumoniae." <u>Infect. Immun.</u> **63**(5): 1969-1974.
- Berry, A. M., *et al.* (1992). "Effect of insertional inactivation of the genes encoding pneumolysin and autolysin on the virulence of Streptococcus pneumoniae type 3." <u>Microbial Pathogenesis</u> **12**(2): 87-93.
- Black, S. (2008). "Changing Epidemiology of Invasive Pneumococcal Disease: A Complicated Story." Clinical Infectious Diseases **47**(4): 485-486.
- Bogaert, D., *et al.* (2004). "Streptococcus pneumoniae colonisation: the key to pneumococcal disease." <u>The Lancet Infectious Diseases</u> **4**(3): 144-154.
- Bogdan, C., et al. (1991). "Macrophage deactivation by interleukin 10." The Journal of Experimental Medicine 174(6): 1549-1555.
- Bootsma, H. J., *et al.* (2007). "Analysis of the in vitro transcriptional response of human pharyngeal epithelial cells to adherent Streptococcus pneumoniae: evidence for a distinct response to encapsulated strains." <u>Infection & Immunity</u> **75**(11): 5489-5499.
- Braun, J. S., *et al.* (2002). "Pneumococcal pneumolysin and H2O2 mediate brain cell apoptosis during meningitis." <u>The Journal of Clinical Investigation</u> **109**(1): 19-27.
- Brealey, D., et al. (2002). "Association between mitochondrial dysfunction and severity and outcome of septic shock." The Lancet **360**(9328): 219-223.
- Briese, T. and R. Hakenbeck (1985). "Interaction of the pneumococcal amidase with lipoteichoic acid and choline." <u>European Journal of Biochemistry</u> **146**(2): 417-427.
- Brims, F. J. H., *et al.* (2010). "Empyema thoracis: new insights into an old disease." <u>European Respiratory Review</u> **19**(117): 220-228.
- Brito, D. A., *et al.* (2003). "Serotyping Streptococcus pneumoniae by Multiplex PCR." <u>J. Clin. Microbiol.</u> **41**(6): 2378-2384.
- Brown, E. J., *et al.* (1983). "The Role of Antibody and Complement in the Reticuloendothelial Clearance of Pneumococci from the Bloodstream." <u>Review of Infectious Diseases</u> 5(Supplement 4): S797-S805.
- Brown, J. S *et al.* (2002). "The classical pathway is the dominant complement pathway required for innate immunity toStreptococcus pneumoniae infection in mice. <u>Proc Natl Acad Sci U S A 99</u>, 16969–74.
- Brueggemann, A. B. and B. G. Spratt (2003). "Geographic Distribution and Clonal Diversity of Streptococcus pneumoniae Serotype 1 Isolates." J. Clin. Microbiol. **41**(11): 4966-4970.
- Bryant C, Fitzgerald KA. (2009) "Molecular mechanisms involved in inflammasome activation". Trends Cell. Biol. 2 (19): 455–64.
- Butler, J. C., *et al.* (1999). "Pneumococcal vaccines: history, current status, and future directions." <u>The American Journal of Medicine</u> **107**(1, Supplement 1): 69-76.
- Byington, C. L., *et al.* (2006). "Impact of the pneumococcal conjugate vaccine on pneumococcal parapneumonic empyema." <u>Pediatric Infectious Disease Journal</u> **25**(3): 250-254.
- Byington, C. L., *et al.* (2002). "An epidemiological investigation of a sustained high rate of pediatric parapneumonic empyema: risk factors and microbiological associations." Clinical Infectious Diseases **34**(4): 434-440.
- Calder, A. and C. Owens (2009). "Imaging of parapneumonic pleural effusions and empyema in children." <u>Pediatric Radiology</u> **39**(6): 527-537.

- Calix, J. J. and M. H. Nahm (2010). "A New Pneumococcal Serotype, 11E, Has a Variably Inactivated wcjE Gene." <u>Journal of Infectious Diseases</u> **202**(1): 29-38.
- Canvin, J. R., *et al.* (1995). "The Role of Pneumolysin and Autolysin in the Pathology of Pneumonia and Septicemia in Mice Infected with a Type 2 Pneumococcus." <u>Journal of Infectious Diseases</u> **172**(1): 119-123.
- Canvin, J. R., *et al.* (1997). "Streptococcus pneumoniaeproduces a second haemolysin that is distinct from pneumolysin." <u>Microbial Pathogenesis</u> **22**(3): 129-132.
- Carniero, L. A. M., (2007) "Nod-like proteins in inflammation and disease". <u>J. Pathol.</u>, 214 (2), 136-148.
- Chedid, L., (1983) "Muramyl peptides as possible endogenous immunopharmacological mediators". Microbiol. Immunol. 27 (9), 723-732.
- Chen, C. C. M., A. M. (1995). "Transcriptional regulation of endothelial cell adhesion molecules: A dominant role for NF-kappaB." <u>Agents and Actions Supplements</u>(47): 135-145.
- Chen G,. et al. (2009). "NOD-like receptors: role in innate immunity and inflammatory disease". Annu. Rev. Pathol. 4: 365–98.
- Chiu, C.-Y., et al. (2008). "Proinflammatory Cytokines, Fibrinolytic System Enzymes, and Biochemical Indices in Children With Infectious Para-pneumonic Effusions." The Pediatric Infectious Disease Journal 27(8): 699-703 610.1097/INF.1090b1013e318170b318678.
- Chretien J, B., J Hirsch A, Ed. (1985). <u>The pleura in health and disease</u>. New York, Marcel Dekker.
- Christensen, P. (1975). "AGGLUTINABILITY OF SOME SELECTED STREPTOCOCCI BY IMMUNE COMPLEXES." <u>Acta Pathologica Microbiologica Scandinavica Section C Immunology</u> **83C**(1): 28-34.
- Clarke, S. C., *et al.* (2006). "Pneumococci causing invasive disease in children prior to the introduction of pneumococcal conjugate vaccine in Scotland." <u>Journal of Medical Microbiology</u> **55**(8): 1079-1084.
- Clarke, S. C., *et al.* (2004). "Serotypes and Sequence Types of Pneumococci Causing Invasive Disease in Scotland Prior to the Introduction of Pneumococcal Conjugate Polysaccharide Vaccines." <u>J. Clin. Microbiol.</u> **42**(10): 4449-4452.
- Claverys, J. P. and L. S. Havarstein (2002). "Extracellular-peptide control of competence for genetic transformation in Streptococcus pneumoniae." <u>Frontiers in bioscience : a journal and virtual library 7: d1798-1814.</u>
- Cockeran, R., *et al.* (2002). "The role of pneumolysin in the pathogenesis of Streptococcus pneumoniae infection." <u>Current Opinion in Infectious Diseases</u> **15**(3): 235-239.
- Corbin, B. D., *et al.* (2008). "Metal Chelation and Inhibition of Bacterial Growth in Tissue Abscesses." Science **319**(5865): 962-965.
- Cundell, D., *et al.* (1995a). "Streptococcus pneumoniae anchor to activated human cells by the receptor for platelet-activating factor." <u>Nature</u> **377**: 435 438.
- Cundell, D., et al. (1995b). "Relationship between colonial morphology and adherence of Streptococcus pneumoniae." Infect. Immun. 63(3): 757-761.
- Davies, C. W. H., *et al.* (2003). "BTS guidelines for the management of pleural infection." Thorax **58**(suppl 2): ii18-ii28.

- Dawson (1928). "THE INTERCONVERTIBILITY OF "R" AND "S" FORMS OF PNEUMOCOCCUS The Interconvertibility of R and S forms of pneumococcus." The Journal of Experimental Medicine Volume 47 (4).
- de Saizieu, A., *et al.* (2000). "Microarray-Based Identification of a Novel Streptococcus pneumoniae Regulon Controlled by an Autoinduced Peptide." <u>J. Bacteriol.</u> **182**(17): 4696-4703.
- Deibel, R. H. S., Jr. H. W. (1974). Streptococceae. <u>Bergey's Manual of Determinative Bacteriology</u>. R. E. a. G. Buchanan, N. E. Baltimore, Williams & Wilkins.
- Desa, M. N. M., *et al.* (2008). "Expression analysis of adherence-associated genes in pneumococcal clinical isolates during adherence to human respiratory epithelial cells (in vitro) by real-time PCR." <u>FEMS Microbiology Letters</u> **288**(1): 125-130.
- Di Cello, F., *et al.* (2005). "Approaches to Bacterial RNA Isolation and Purification for Microarray Analysis of Escherichia coli K1 Interaction with Human Brain Microvascular Endothelial Cells." J. Clin. Microbiol. **43**(8): 4197-4199.
- Diamond, G., *et al.* (2000). "Transcriptional Regulation of beta -Defensin Gene Expression in Tracheal Epithelial Cells." <u>Infect. Immun.</u> **68**(1): 113-119.
- Dintilhac, A., *et al.* (1997). "Competence and virulence of Streptococcus pneumoniae: Adc and PsaA mutants exhibit a requirement for Zn and Mn resulting from inactivation of putative ABC metal permeases." <u>Molecular Microbiology</u> **25**(4): 727-739.
- Dowell, S. F., *et al.* (2003). "Seasonal patterns of invasive pneumococcal disease." <u>Emerging Infectious Diseases</u> **9**(5): 573-579.
- Durbin, W. J. (2004). "Pneumococcal Infections." Pediatrics in Review 25(12): 418-424.
- Eastham, K. M., *et al.* (2004). "Clinical features, aetiology and outcome of empyema in children in the north east of England." Thorax **59**(6): 522-525.
- Echchannaoui, H. *et al.* (2005). "CD14 deficiency leads to increased MIP-2 production, CXCR2 expression, neutrophil transmigration, and early death in pneumococcal infection." <u>J Leukoc Biol.</u> 78, 705–715.
- Eltringham, G., *et al.* (2003). "Culture-negative childhood empyema is usually due to penicillin-sensitive Streptococcus pneumoniae capsular serotype 1." <u>Journal of Clinical Microbiology</u> **41**(1): 521-522.
- Ertugrul, N., *et al.* (1997). "BOX-Polymerase Chain Reaction-Based DNA Analysis of Nonserotypeable Streptococcus pneumoniae Implicated in Outbreaks of Conjunctivitis." Journal of Infectious Diseases **176**(5): 1401-1405.
- Evans, S., *et al.* (2010). "Host lung gene expression patterns predict infectious etiology in a mouse model of pneumonia." <u>Respiratory Research</u> **11**(1): 101.
- Feldman, C. and R. Anderson (2009). "New insights into pneumococcal disease." <u>Respirology</u> **14**(2): 167-179.
- Ferrante, A. (1984). "Inhibition of In Vitro Human Lymphocyte Response by the Pneumococcal Toxin Pneumolysin." <u>Infection and Immunity</u> **46**(2): 585-589.
- Finley, C., et al. (2008). "Empyema: an increasing concern in Canada." <u>Canadian respiratory</u> journal: journal of the Canadian Thoracic Society **15**(2): 85-89.
- Fletcher, M., *et al.* (2006). "Childhood empyema: limited potential impact of 7-valent pneumococcal conjugate vaccine." <u>Pediatric Infectious Disease Journal</u> **25**(6): 559-560.
- Fowler, M. I., *et al.* (2004). "Different meningitis-causing bacteria induce distinct inflammatory responses on interaction with cells of the human meninges." <u>Cellular Microbiology</u> **6**(6): 555-567.

- Fraenkel, A. (1886). "Weitere Beitrage zur Lehre von den Mikrococcen der genuinen fibrinosen Pneumonie." Zeitschrift filr Klinische Medicin 11: 437-458.
- Girardin, S. E. *et al.* (2003). "Nod1 detects a unique muropeptide from Gram-negative bacterial peptidoglycan." <u>Science</u> 300, 1584–1587.
- Graham, R. M. A. and J. C. Paton (2006). "Differential Role of CbpA and PspA in Modulation of In Vitro CXC Chemokine Responses of Respiratory Epithelial Cells to Infection with Streptococcus pneumoniae." <u>Infect. Immun.</u> **74**(12): 6739-6749.
- Grundmeier, M., *et al.* (2010). "Staphylococcal Strains Vary Greatly in Their Ability to Induce an Inflammatory Response in Endothelial Cells." <u>The Journal of Infectious Diseases</u> **201**(6): 871-880.
- Gupta, R. and S. Crowley (2006). "Increasing paediatric empyema admissions." <u>Thorax</u> **61**(2): 179-180.
- Gygi, S. P., *et al.* (1999). "Correlation between Protein and mRNA Abundance in Yeast." Mol. Cell. Biol. **19**(3): 1720-1730.
- Hage, C. A., et al. (2004). "Pathogenesis of pleural infection." Respirology 9(1): 12-15.
- Hamm, H. and R. Light (1997). "Parapneumonic effusion and empyema." <u>European</u> Respiratory Journal **10**(5): 1150-1156.
- Hammerschmidt, S. (2006). "Adherence molecules of pathogenic pneumococci." <u>Curr Opin Microbiol</u> **9**(1): 12 20.
- Hammerschmidt, S., *et al.* (2000). "Species-specific binding of human secretory component to SpsA protein of Streptococcus pneumoniae via a hexapeptide motif." <u>Molecular Microbiology</u> **36**(3): 726-736.
- Hammerschmidt, S., *et al.* (2005). "Illustration of pneumococcal polysaccharide capsule during adherence and invasion of epithelial cells." <u>Infect Immun</u> **73**(8): 4653 4667.
- Han, D. C., *et al.* (2003). "Expression of MHC Class II, CD70, CD80, CD86 and proinflammatory cytokines is differentially regulated in oral epithelial cells following bacterial challenge." Oral Microbiology & Immunology **18**(6): 350-358.
- Hanage, W. P., *et al.* (2006). "A Successful, Diverse Disease-Associated Lineage of Nontypeable Pneumococci That Has Lost the Capsular Biosynthesis Locus." <u>J. Clin. Microbiol.</u> **44**(3): 743-749.
- Handfield, M. and R. C. Levesque (1999). "Strategies for isolation of in vivo expressed genes from bacteria." <u>FEMS Microbiology Reviews</u> **23**(1): 69-91.
- Hardie, W., et al. (1996). "Pneumococcal pleural empyemas in children." <u>Clinical Infectious</u> Diseases **22**(6): 1057-1063.
- Hausdorff, W. P. (2007). "The roles of pneumococcal serotypes 1 and 5 in paediatric invasive disease." <u>Vaccine</u> **25**(13): 2406-2412.
- Hausdorff, W. P., *et al.* (2000). "Which Pneumococcal Serogroups Cause the Most Invasive Disease: Implications for Conjugate Vaccine Formulation and Use, Part I." <u>Clinical Infectious Diseases</u> **30**(1): 100-121.
- Hausdorff, W. P. and R. Dagan (2008). "Serotypes and pathogens in paediatric pneumonia." <u>Vaccine</u> **26**, **Supplement 2**(0): B19-B23.
- Hausdorff, W. P., *et al.* (2005). "Epidemiological differences among pneumococcal serotypes." The Lancet Infectious Diseases **5**(2): 83-93.
- Hava, D. L., *et al.* (2003). "From nose to lung: the regulation behind Streptococcus pneumoniae virulence factors." Molecular Microbiology **50**(4): 1103-1110.

- Hendriksen, W., et al. (2007). "Regulation of gene expression in Streptococcus pneumoniae by response regulator 09 is strain dependent." <u>Journal of Bacteriology</u> **189**(4): 1382 1389.
- Hendriksen, W. T., *et al.* (2008). "Site-Specific Contributions of Glutamine-Dependent Regulator GlnR and GlnR-Regulated Genes to Virulence of Streptococcus pneumoniae." Infect. Immun. **76**(3): 1230-1238.
- Hidalgo-Grass, C., *et al.* (2006). "A streptococcal protease that degrades CXC chemokines and impairs bacterial clearance from infected tissues." <u>EMBO J</u> **25**(19): 4628-4637.
- Hinton, J. C. D., *et al.* (2004). "Benefits and pitfalls of using microarrays to monitor bacterial gene expression during infection." <u>Current Opinion in Microbiology</u> **7**(3): 277-282.
- Hirst, R. A., *et al.* (2008). "Streptococcus pneumoniae Deficient in Pneumolysin or Autolysin Has Reduced Virulence in Meningitis." <u>Journal of Infectious Diseases</u> **197**(5): 744-751.
- Hirst, R. A., *et al.* (2004). "The role of pneumolysin in pneumococcal pneumonia and meningitis." Clinical & Experimental Immunology **138**(2): 195-201.
- Hirst, R. A., *et al.* (2000). "Relative Roles of Pneumolysin and Hydrogen Peroxide from Streptococcus pneumoniae in Inhibition of Ependymal Ciliary Beat Frequency." <u>Infect. Immun.</u> **68**(3): 1557-1562.
- Hoffman, O. and J. R. Weber (2009). "Review: Pathophysiology and treatment of bacterial meningitis." Therapeutic Advances in Neurological Disorders 2(6): 401-412.
- Holgate, S. T., *et al.* (2000). "Epithelial-mesenchymal interactions in the pathogenesis of asthma." Journal of Allergy and Clinical Immunology **105**(2, Part 1): 193-204.
- Hoskins, J., *et al.* (2001). "Genome of the Bacterium Streptococcus pneumoniae Strain R6." <u>J. Bacteriol.</u> **183**(19): 5709-5717.
- Houldsworth, S., *et al.* (1994). "Pneumolysin stimulates production of tumor necrosis factor alpha and interleukin-1 beta by human mononuclear phagocytes." <u>Infect. Immun.</u> **62**(4): 1501-1503.
- Imohl, M., *et al.* (2010). "Association of Serotypes of Streptococcus pneumoniae with Age in Invasive Pneumococcal Disease." J. Clin. Microbiol. **48**(4): 1291-1296.
- Inohara N, Ogura Y, Fontalba A, Gutierrez O, Pons F, Crespo J, *et al.* Host recognition of bacterial muramyl dipeptide mediated through NOD2. Implications for Crohn's disease. <u>J Biol Chem</u> 2003; 278: 5509–5512.
- Jaffé, A. and I. M. Balfour-Lynn (2005). "Management of empyema in children." <u>Pediatric</u> Pulmonology **40**(2): 148-156.
- Janeway (2005). Immunobiology: The Immune System in Health & Disease.
- Janeway, C. A., Jr & Medzhitov, R. (2002). "Innate immune recognition". Annu Rev Immunol 20, 197–216.
- Jantz, M. A. and V. B. Antony (2008). "Pathophysiology of the Pleura." <u>Respiration</u> **75**(2): 121-133.
- Jedrzejas, M. J. (2001). "Pneumococcal Virulence Factors: Structure and Function." <u>Microbiol.</u> <u>Mol. Biol. Rev.</u> **65**(2): 187-207.
- Jefferies, Johanna M. C., *et al.* (2007). "Presence of Nonhemolytic Pneumolysin in Serotypes of Streptococcus pneumoniae Associated with Disease Outbreaks." <u>The Journal of Infectious Diseases</u> **196**(6): 936-944.

- Jin, P., *et al.* (2009). "First Report of Putative Streptococcus pneumoniae Serotype 6D among Nasopharyngeal Isolates from Fijian Children." <u>Journal of Infectious Diseases</u> **200**(9): 1375-1380.
- Johnson, M. K., *et al.* (1981). "Effects of pneumolysin on human polymorphonuclear leukocytes and platelets." <u>Infect. Immun.</u> **34**(1): 171-176.
- Johnston, J. W., et al. (2006). "Mn2+-Dependent Regulation of Multiple Genes in Streptococcus pneumoniae through PsaR and the Resultant Impact on Virulence." Infect.Immun. 74(2): 1171-1180.
- Kadioglu, A. and P. W. Andrew (2004). "The innate immune response to pneumococcal lung infection: the untold story." <u>Trends in Immunology</u> **25**(3): 143-149.
- Kadioglu, A., et al. (2002). "Upper and Lower Respiratory Tract Infection by Streptococcus pneumoniae Is Affected by Pneumolysin Deficiency and Differences in Capsule Type." Infect. Immun. 70(6): 2886-2890.
- Kadioglu, A., *et al.* (2008). "The role of Streptococcus pneumoniae virulence factors in host respiratory colonization and disease." <u>Nat Rev Micro</u> **6**(4): 288-301.
- Kang, Y. S. *et al.* (2004). "The C-type lectin SIGN-R1 mediates uptake of the capsular polysaccharide of Streptococcus pneumoniae in the marginal zone of mouse spleen". Proc Natl Acad Sci U S A 101, 215–220.
- Kaplan, S. L., *et al.* (2004). "Decrease of Invasive Pneumococcal Infections in Children Among 8 Children's Hospitals in the United States After the Introduction of the 7-Valent Pneumococcal Conjugate Vaccine." <u>Pediatrics</u> **113**(3): 443-449.
- Kasama, T., *et al.* (1995). "Interleukin-10 expression and chemokine regulation during the evolution of murine type II collagen-induced arthritis." <u>The Journal of Clinical</u> Investigation **95**(6): 2868-2876.
- Kawai, T. and S. Akira (2006). "TLR signaling." Cell Death Differ 13(5): 816-825.
- Kaye, P. M., R. Martin, S. Slack, M. Trotter, C. Jit, M. George, R. Miller, E. (2008). Invasive Pneumococcal Disease (IPD) in England & Wales after 7-valent conjugate vaccine (PCV7); potential impact of 10 and 13-valent vaccines. H. P. Agency. London.
- Kehres, D. G. and M. E. Maguire (2003). "Emerging themes in manganese transport, biochemistry and pathogenesis in bacteria." <u>FEMS Microbiology Reviews</u> **27**(2-3): 263-290.
- Kerr, A. R., *et al.* (2004). "The Ami-AliA/AliB Permease of Streptococcus pneumoniae Is Involved in Nasopharyngeal Colonization but Not in Invasive Disease." <u>Infect. Immun.</u> **72**(7): 3902-3906.
- Kerr, A. R., *et al.* (2002). "Role of Inflammatory Mediators in Resistance and Susceptibility to Pneumococcal Infection." <u>Infect. Immun.</u> **70**(3): 1547-1557.
- Kim, J. O. and J. N. Weiser (1998). "Association of Intrastrain Phase Variation in Quantity of Capsular Polysaccharide and Teichoic Acid with the Virulence of Streptococcus pneumoniae." <u>Journal of Infectious Diseases</u> 177(2): 368-377.
- King, S., *et al.* (2006). "Deglycosylation of human glycoconjugates by the sequential activities of exoglycosidases expressed by Streptococcus pneumoniae." <u>Molecular Microbiology</u> **59**(3): 961 974.
- Kirkham, L.-A. S., *et al.* (2006). "Identification of Invasive Serotype 1 Pneumococcal Isolates That Express Nonhemolytic Pneumolysin." <u>J. Clin. Microbiol.</u> **44**(1): 151-159.
- Kirkman, J. B., *et al.* (1970). "A Microtiter Plate Technique for the Agglutination Typing of Diplococcus pneumoniae." Journal of Infectious Diseases **121**(2): 217-221.

- Kline, K. A., *et al.* (2009). "Bacterial Adhesins in Host-Microbe Interactions." <u>Cell Host & Amp: Microbe</u> **5**(6): 580-592.
- Kloosterman, T. G., *et al.* (2006). "To have neighbour's fare: extending the molecular toolbox for Streptococcus pneumoniae." <u>Microbiology</u> **152**(2): 351-359.
- Kloosterman, T. G., *et al.* (2007). "The novel transcriptional regulator SczA mediates protection against Zn2+ stress by activation of the Zn2+-resistance gene czcD in Streptococcus pneumoniae." <u>Molecular Microbiology</u> **65**(4): 1049-1063.
- Knapp, S., et al. (2004). "Toll-Like Receptor 2 Plays a Role in the Early Inflammatory Response to Murine Pneumococcal Pneumonia but Does Not Contribute to Antibacterial Defense." <u>The Journal of Immunology</u> **172**(5): 3132-3138.
- Koedel, U., *et al.* (2003). "Toll-Like Receptor 2 Participates in Mediation of Immune Response in Experimental Pneumococcal Meningitis." <u>The Journal of Immunology</u> **170**(1): 438-444.
- Krivan, H. C., *et al.* (1988). "Many pulmonary pathogenic bacteria bind specifically to the carbohydrate sequence GalNAc beta 1-4Gal found in some glycolipids." <u>Proceedings of the National Academy of Sciences</u> **85**(16): 6157-6161.
- Kronvall, G. (1973). "A Rapid Slide-Agglutination Method for Typing Pneumococci by Means of Specific Antibody Adsorbed to Protein A-Containing Staphylococci." <u>Journal of Medical Microbiology</u> **6**(2): 187-190.
- Kwon, H.-Y., *et al.* (2003). "Effect of Heat Shock and Mutations in ClpL and ClpP on Virulence Gene Expression in Streptococcus pneumoniae." <u>Infect. Immun.</u> **71**(7): 3757-3765.
- Kyaw, M. H., *et al.* (2006). "Effect of Introduction of the Pneumococcal Conjugate Vaccine on Drug-Resistant Streptococcus pneumoniae." New England Journal of Medicine **354**(14): 1455-1463.
- Langley, J. M., *et al.* (2008). "Empyema associated with community-acquired pneumonia: a Pediatric Investigator's Collaborative Network on Infections in Canada (PICNIC) study." <u>BMC Infectious Diseases</u> **8**(129).
- LeMessurier, K. S., *et al.* (2006). "Differential expression of key pneumococcal virulence genes in vivo." <u>Microbiology</u> **152**(2): 305-311.
- Liberek, T., *et al.* (1996). "Adherence of neutrophils to human peritoneal mesothelial cells: role of intercellular adhesion molecule-1." <u>Journal of the American Society of Nephrology</u> **7**(2): 208-217.
- Lipsitch, M. (2000). "Interpreting Results from Trials of Pneumococcal Conjugate Vaccines: A Statistical Test for Detecting Vaccine-induced Increases in Carriage of Nonvaccine Serotypes." <u>American Journal of Epidemiology</u> **154**(1): 85-92.
- Lock, R. A., *et al.* (1996). "Sequence variation in theStreptococcus pneumoniaepneumolysin gene affecting haemolytic activity and electrophoretic mobility of the toxin." <u>Microbial Pathogenesis</u> **21**(2): 71-83.
- Loisel, E., *et al.* (2011). "Biochemical Characterization of the Histidine Triad Protein PhtD as a Cell Surface Zinc-Binding Protein of Pneumococcus." <u>Biochemistry</u> **50**(17): 3551-3558.
- MacLeod CM, H. R., Heidelberger M, Bernhard WG (1945). "Prevention of pneumococcal pneumonia by immunization with specific capsular polysaccharides. Journal of Experimental Medicine " 1(82:): 445-465.
- MacLeod, C. M. and M. R. Krauss (1950). "RELATION OF VIRULENCE OF PNEUMOCOCCAL STRAINS FOR MICE TO THE QUANTITY OF CAPSULAR

- POLYSACCHARIDE FORMED IN VITRO." <u>The Journal of Experimental Medicine</u> **92**(1): 1-9.
- Magee, A. D. and J. Yother (2001). "Requirement for Capsule in Colonization by Streptococcus pneumoniae." <u>Infect. Immun.</u> **69**(6): 3755-3761.
- Malley, R., et al. (2003). "Recognition of pneumolysin by Toll-like receptor 4 confers resistance to pneumococcal infection." <u>Proceedings of the National Academy of Sciences</u> **100**(4): 1966-1971.
- Manco, S., *et al.* (2006). "Pneumococcal Neuraminidases A and B Both Have Essential Roles during Infection of the Respiratory Tract and Sepsis." <u>Infect. Immun.</u> **74**(7): 4014-4020.
- Mandell, G. L. (1973). "Interaction of Intraleukocytic Bacteria and Antibiotics." <u>The Journal of Clinical Investigation</u> **52**(7): 1673-1679.
- Mangan, J. A., *et al.* (2002). Gene expression during host—pathogen interactions: Approaches to bacterial mRNA extraction and labelling for microarray analysis. <u>Methods in Microbiology</u>. N. D. Brendan Wren, Academic Press. **Volume 33:** 137-151.
- Marra, A., *et al.* (2002). "In vivo characterization of the psa genes from Streptococcus pneumoniae in multiple models of infection." <u>Microbiology</u> **148**(5): 1483-1491.
- Martha, V. F., *et al.* (2010). "Tumor necrosis factor alpha in experimental empyema thoracis." <u>Pediatric Pulmonology</u> **45**(12): 1201-1204.
- Martner, A., et al. (2009). "Streptococcus pneumoniae Autolysis Prevents Phagocytosis and Production of Phagocyte-Activating Cytokines." <u>Infection and Immunity</u> 77(9): 3826-3837.
- McDonald, E. D., B. Cameron, C. (2011). Respiratory bacteria quarterly report quarter two: 1 April to 30 June 2011 (Meningococcal disease, Invasive pneumococcal disease (IPD), Haemophilus influenzae) Edinburgh, UK, Health Protection Scotland. **45**.
- Michailova, K., *et al.* (1999). "Scanning and transmission electron microscopic study of visceral and parietal peritoneal regions in the rat." <u>Annals of Anatomy Anatomischer Anzeiger</u> **181**(3): 253-260.
- Miron, M., *et al.* (2006). "A methodology for global validation of microarray experiments." BMC Bioinformatics 7(1): 333.
- Miserocchi, G. (1997). "Physiology and pathophysiology of pleural fluid turnover." <u>European Respiratory Journal</u> **10**(1): 219-225.
- Mitchell, A. M. and T. J. Mitchell (2010). "Streptococcus pneumoniae: virulence factors and variation." Clinical Microbiology and Infection 16(5): 411-418.
- Mitchell, T. (2006). "Streptococcus pneumoniae: infection, inflammation and disease." <u>Adv Exp Med Biol</u> **582**: 111 124.
- Mitchell, T. J. (2000). "Virulence factors and the pathogenesis of disease causedby Streptococcus pneumoniae." <u>Research in Microbiology</u> **151**(6): 413-419.
- Mitchell, T..J. *et al.* (1991).."Complement activation and antibody binding by pneumolysin via a region of the toxin homologous to a human acute-phase protein". <u>Mol Microbiol.</u> 5, 1883–1888.
- Mogensen, T. H., *et al.* (2006). "Live Streptococcus pneumoniae, Haemophilus influenzae, and Neisseria meningitidis activate the inflammatory response through Toll-like receptors 2, 4, and 9 in species-specific patterns." <u>Journal of Leukocyte Biology</u> **80**(2): 267-277.
- Mohammed, K., *et al.* (2007). "Bacterial Induction of Early Response Genes and Activation of Proapoptotic Factors in Pleural Mesothelial Cells." <u>Lung</u> **185**(6): 355-365.

- Mohammed, K. A., *et al.* (2000). "Induction of Acute Pleural Inflammation by Staphylococcus aureus. I. CD4+ T Cells Play a Critical Role in Experimental Empyema." <u>Journal of Infectious Diseases</u> **181**(5): 1693-1699.
- Mohammed, K. A., *et al.* (1998). "Mycobacterium-Mediated Chemokine Expression in Pleural Mesothelial Cells: Role of C-C Chemokines in Tuberculous Pleurisy." <u>Journal of Infectious Diseases</u> **178**(5): 1450-1456.
- Morona, J. K., *et al.* (2006). "Attachment of capsular polysaccharide to the cell wall of Streptococcus pneumoniae type 2 is required for invasive disease." <u>Proceedings of the National Academy of Sciences</u> **103**(22): 8505-8510.
- Murphy JE, *et al.* "Biochemistry and cell biology of mammalian scavenger receptors". <u>Atherosclerosis</u> 182: 1–15.
- Mutsaers, S. E. (2004). "The mesothelial cell." <u>The International Journal of Biochemistry & Cell Biology</u> **36**(1): 9-16.
- Nandoskar M, F. A. (1986). "Inhibition of human monocyte respiratory burst, degranulation, phospholipid methylation and bactericidal activity by pneumolysin." Immunology **59**: 515-520.
- Nelson, A., *et al.* (2007a). "RrgA is a pilus-associated adhesin in Streptococcus pneumoniae." Molecular Microbiology **66**(2): 329 340.
- Nelson, A. L., *et al.* (2007b). "Capsule Enhances Pneumococcal Colonization by Limiting Mucus-Mediated Clearance." <u>Infect. Immun.</u> **75**(1): 83-90.
- Neufeld, F. (1902). "Ueber die Agglutination der Pneumokokken and iiber die Theorieen der Agglutination." <u>Hyg. Infekt Krankh</u> **40**: 54.
- Noppen, M., *et al.* (2000). "Volume and Cellular Content of Normal Pleural Fluid in Humans Examined by Pleural Lavage." <u>Am. J. Respir. Crit. Care Med.</u> **162**(3): 1023-1026.
- Norcross, E. W., et al. (2010). "Assessment of Streptococcus pneumoniae Capsule in Conjunctivitis and Keratitis in vivo Neuraminidase Activity Increases in Nonencapsulated Pneumococci following Conjunctival Infection." <u>Current Eye</u> Research **35**(9): 787-798.
- O'Brien, K. L., *et al.* (2009). "Burden of disease caused by Streptococcus pneumoniae in children younger than 5 years: global estimates." <u>The Lancet</u> **374**(9693): 893-902.
- Obando, I., *et al.* (2008). "Pediatric parapneumonic empyema, Spain." <u>Emerging Infectious Diseases</u> **14**(9): 1390-1397.
- Odeh, M. and A. Oliven (2005). "Tumor Necrosis Factor-α in Parapneumonic Effusion." <u>Chest</u> **127**(5): 1868-1869.
- Ogunniyi, A. D., *et al.* (2010). "Central Role of Manganese in Regulation of Stress Responses, Physiology, and Metabolism in Streptococcus pneumoniae." <u>J. Bacteriol.</u> **192**(17): 4489-4497.
- Opitz, B., *et al.* (2004). "Nucleotide-binding oligomerization domain proteins are innate immune receptors for internalized Streptococcus pneumoniae". <u>J Biol</u> Chem 279, 36426–36432.
- Orihuela, C., *et al.* (2004). "Tissue-specific contributions of pneumococcal virulence factors to pathogenesis." J Infect Dis **190**(9): 1661 1669.
- Orihuela, C., *et al.* (2004). "Microarray analysis of pneumococcal gene expression during invasive disease." Infect Immun **72**(10): 5582 5596.
- Overweg, K., et al. (2000). "Differential Protein Expression in Phenotypic Variants of Streptococcus pneumoniae." <u>Infect. Immun.</u> **68**(8): 4604-4610.

- Pai, R., *et al.* (2006). "Sequential Multiplex PCR Approach for Determining Capsular Serotypes of Streptococcus pneumoniae Isolates." J. Clin. Microbiol. **44**(1): 124-131.
- Panina, E. M., *et al.* (2003). "Comparative Genomics of Bacterial Zinc Regulons: Enhanced Ion Transport, Pathogenesis, and Rearrangement of Ribosomal Proteins." <u>Proceedings of the National Academy of Sciences of the United States of America</u> **100**(17): 9912-9917.
- Park, I. H., *et al.* (2007). "Discovery of a New Capsular Serotype (6C) within Serogroup 6 of Streptococcus pneumoniae." <u>J. Clin. Microbiol.</u> **45**(4): 1225-1233.
- Park, M. K., *et al.* (2000). "A Latex Bead-Based Flow Cytometric Immunoassay Capable of Simultaneous Typing of Multiple Pneumococcal Serotypes (Multibead Assay)." <u>Clin. Diagn. Lab. Immunol.</u> 7(3): 486-489.
- Pasteur, L. (1881). "Note sur la maladie nouvelle provoquee par la salive d'un enfant mort de la rage." <u>Bulletin de l'Academie de Medicin</u> **10**: 94-103.
- Paterson, G.K., Orihuela, C. J., (2010). "Pneumococci: immunology of the innate host reposnse." <u>Respirol.</u> 15 (7), 1057-1063.
- Paterson, G. K. and T. J. Mitchell (2006). "Innate immunity and the pneumococcus." <u>Microbiology</u> **152**(2): 285-293.
- Paton, J. (1996). "The contribution of pneumolysin to the pathogenicity of Streptococcus pneumoniae." <u>Trends in Microbiology</u> **4**(3): 103-106.
- Paton, J. C. and A. Ferrante (1983). "Inhibition of human polymorphonuclear leukocyte respiratory burst, bactericidal activity, and migration by pneumolysin." <u>Infect. Immun.</u> **41**(3): 1212-1216.
- Pericone, C. D., *et al.* (2000). "Inhibitory and Bactericidal Effects of Hydrogen Peroxide Production by Streptococcus pneumoniae on Other Inhabitants of the Upper Respiratory Tract." <u>Infect. Immun.</u> **68**(7): 3990-3997.
- Playfor, S. D., et al. (1997). "Increase in incidence of childhood empyema." Thorax 52(10).
- Preston, J. A. and D. H. Dockrell (2008). "Virulence factors in pneumococcal respiratory pathogenesis." Future Microbiology **3**(2): 205-221.
- Quadri, A. and A. H. Thomson (2002). "Pleural fluids associated with chest infection." <u>Paediatric Respiratory Reviews</u> **3**(4): 349-355.
- Rayner, C., et al. (1995). "Interaction of pneumolysin-sufficient and -deficient isogenic variants of Streptococcus pneumoniae with human respiratory mucosa." <u>Infect. Immun.</u> **63**(2): 442-447.
- Rees, J. H., *et al.* (1997). "Increase in incidence of childhood empyema in West Midlands, UK." Lancet **349**(9049): 8.
- Richter, S. S., *et al.* (2009). "Changing Epidemiology of Antimicrobial-Resistant Streptococcus pneumoniae in the United States, 2004–2005." <u>Clinical Infectious Diseases</u> **48**(3): e23-e33.
- Riesenfeld-Orn, I., *et al.* (1989). "Production of interleukin-1 but not tumor necrosis factor by human monocytes stimulated with pneumococcal cell surface components." <u>Infect. Immun.</u> **57**(7): 1890-1893.
- Robson, R., *et al.* (2006). "Differential activation of inflammatory pathways in A549 type II pneumocytes by Streptococcus pneumoniae strains with different adherence properties." <u>BMC Infectious Diseases</u> **6**(1): 71.

- Rogers, P. D., *et al.* (2003). "Pneumolysin-dependent and -independent gene expression identified by cDNA microarray analysis of THP-1 human mononuclear cells stimulated by Streptococcus pneumoniae." <u>Infection and immunity</u> **71**(4): 2087-2094.
- Rosenow, C., *et al.* (1997). "Contribution of novel choline-binding proteins to adherence, colonization and immunogenicity of Streptococcus pneumoniae." <u>Molecular Microbiology</u> **25**: 819 829.
- Rosenow, C., *et al.* (1997). "Contribution of novel choline-binding proteins to adherence, colonization and immunogenicity of Streptococcus pneumoniae." <u>Molecular Microbiology</u> **25**(5): 819-829.
- Rozen, S. and H. Skaletsky (1999). Primer3 on the WWW for General Users and for Biologist Programmers
- Bioinformatics Methods and Protocols. S. Misener and S. A. Krawetz, Humana Press. 132: 365-386.
- Rubins, J. B. and E. N. Janoff (1998). "Pneumolysin: A multifunctional pneumococcal virulence factor." <u>Journal of Laboratory and Clinical Medicine</u> **131**(1): 21-27.
- Ryan, P. A., et al. (2007). "Novel Algorithms Reveal Streptococcal Transcriptomes and Clues about Undefined Genes." <u>PLoS Comput Biol</u> **3**(7): e132.
- Saglani, S., et al. (2005). "Empyema: the use of broad range 16S rDNA PCR for pathogen detection." <u>Archives of Disease in Childhood</u> **90**(1): 70-73.
- Samartzidou, H. T., L. Houts, T. (2001). Lucidea Microarray Scorecard: An integrated tool for validation of microarray gene expression experiments. <u>Life Science News Sunnyvale</u>, Amersham Pharmacia Biotech. **8**.
- Sato, K., et al. (1996). "Roles of autolysin and pneumolysin in middle ear inflammation caused by a type 3 Streptococcus pneumoniae strain in the chinchilla otitis media model." Infect.Immun.64(4): 1140-1145.
- Schenk M,. et al. (2009) "TLR2 looks at lipoproteins". Immunity 31: 847-9.
- Schmeck, B., *et al.* (2006). "Pneumococci induced TLR- and Rac1-dependent NF-κB-recruitment to the IL-8 promoter in lung epithelial cells." <u>American Journal of Physiology</u> Lung Cellular and Molecular Physiology **290**(4): L730-L737.
- Schröder, N. W. J., *et al.* (2003). "Lipoteichoic Acid (LTA) of Streptococcus pneumoniaeand Staphylococcus aureus Activates Immune Cells via Toll-like Receptor (TLR)-2, Lipopolysaccharide-binding Protein (LBP), and CD14, whereas TLR-4 and MD-2 Are Not Involved." Journal of Biological Chemistry **278**(18): 15587-15594.
- Schubert-Unkmeir, A., et al. (2009). "Mammalian cell transcriptome in response to meningitis-causing pathogens." Expert Review of Molecular Diagnostics 9(8): 833-842.
- Schwander R., *et al.*, (1999) "Peptidoglycan- and lipoteichoic acid-induced cell activation is mediated by Toll-like receptor 2". <u>J. Biol. Chem.</u> 274, 17 406–17 409.
- Seo, H. S., *et al.* (2008). "Lipoteichoic Acid Is Important in Innate Immune Responses to Gram-Positive Bacteria." Infect. Immun. **76**(1): 206-213.
- Simell, B., *et al.* (2009). "Pneumococcal carriage and acute otitis media induce serum antibodies to pneumococcal surface proteins CbpA and PhtD in children." <u>Vaccine</u> **27**(34): 4615-4621.
- Simpson, S. Q., et al. (1994). "Heat-killed pneumococci and pneumococcal capsular polysaccharides stimulate tumor necrosis factor-alpha production by murine macrophages." <u>American Journal of Respiratory Cell and Molecular Biology</u> **10**(3): 284-289.

- Simsir, A., *et al.* (1999). "E-cadherin, N-cadherin, and calretinin in pleural effusions: The good, the bad, the worthless." <u>Diagnostic Cytopathology</u> **20**(3): 125-130.
- Sleeman, K., *et al.* (2001). "Invasive Pneumococcal Disease in England and Wales: Vaccination Implications." <u>Journal of Infectious Diseases</u> **183**(2): 239-246.
- Slevogt, H., *et al.* (2008). "CEACAM1 inhibits Toll-like receptor 2-triggered antibacterial responses of human pulmonary epithelial cells." <u>Nat Immunol</u> **9**(11): 1270-1278.
- Smart, L. E. (1986). "Serotyping of Streptococcus pneumoniae strains by coagglutination." <u>Journal of Clinical Pathology</u> **39**(3): 328-331.
- Song, X.-M., *et al.* (2008a). "Streptococcus pneumoniae early response genes to human lung epithelial cells." <u>BMC Research Notes</u> **1**(1): 64.
- Song, X. M., *et al.* (2008b). "Microarray analysis of Streptococcus pneumoniae gene expression changes to human lung epithelial cells." <u>Canadian Journal of Microbiology</u> **54**(3): 189-200.
- Sonnappa, S. and A. Jaffe (2007). "Treatment approaches for empyema in children." <u>Paediatric</u> Respiratory Reviews **8**(2): 164-170.
- Sorensen, U. B. (1993). "Typing of pneumococci by using 12 pooled antisera." <u>J. Clin.</u> Microbiol. **31**(8): 2097-2100.
- Spellerberg, B., *et al.* (1996). "Pyruvate oxidase, as a determinant of virulence in Streptococcus pneumoniae." <u>Molecular Microbiology</u> **19**(4): 803-813.
- Spencer, D. A. and D. Cliff (2008). "The changing epidemiology of parapneumonic empyema in children." <u>Paediatrics and Child Health</u> **18**(11): 513-518.
- Srivastava, A., *et al.* (2005). "The Apoptotic Response to Pneumolysin Is Toll-Like Receptor 4 Dependent and Protects against Pneumococcal Disease." <u>Infect. Immun.</u> **73**(10): 6479-6487.
- Steinfort, C., *et al.* (1989). "Effect of Streptococcus pneumoniae on human respiratory epithelium in vitro." <u>Infection and immunity</u> **57**(7): 2006-2013.
- Steinfort, C., *et al.* (1989). "Effect of Streptococcus pneumoniae on human respiratory epithelium in vitro." <u>Infect. Immun.</u> **57**(7): 2006-2013.
- Sternberg, G. M. (1881). "A fatal form of septicaemia in the rabbit, produced by the subcutaneous injection of human saliva." <u>Annual Reports of the National Board of Health</u> 3: 87-108.
- Takeda, K., Akira, S. (2003). "Toll-like receptors". Annu Rev Immunol 21, 335–376.
- Talbot, T. R., *et al.* (2005). "Seasonality of invasive pneumococcal disease: Temporal relation to documented influenza and respiratory syncytial viral circulation." <u>The American Journal of Medicine</u> **118**(3): 285-291.
- Tamura, G. S., *et al.* (2002). "A Glutamine Transport Gene, glnQ, Is Required for Fibronectin Adherence and Virulence of Group B Streptococci." <u>Infect. Immun.</u> **70**(6): 2877-2885.
- Tan, T. Q., et al. (2002). "Clinical characteristics of children with complicated pneumonia caused by Streptococcus pneumoniae." Pediatrics 110(1 Pt 1): 1-6.
- Tettelin, H., *et al.* (2002). "Complete genome sequence and comparative genomic analysis of an emerging human pathogen, serotype V Streptococcus agalactiae." <u>Proceedings of the National Academy of Sciences</u> **99**(19): 12391-12396.
- Tilney, L. G. and D. A. Portnoy (1989). "Actin filaments and the growth, movement, and spread of the intracellular bacterial parasite, Listeria monocytogenes." <u>The Journal of Cell Biology</u> **109**(4): 1597-1608.

- Tu, A.-H. T., *et al.* (1999). "Pneumococcal Surface Protein A Inhibits Complement Activation by Streptococcus pneumoniae." <u>Infect. Immun.</u> **67**(9): 4720-4724.
- Tuomanen, E., *et al.* (1985). "The Induction of Meningeal Inflammation by Components of the Pneumococcal Cell Wall." <u>Journal of Infectious Diseases</u> **151**(5): 859-868.
- Uchiyama, S., *et al.* (2009). "The surface-anchored NanA protein promotes pneumococcal brain endothelial cell invasion." <u>The Journal of Experimental Medicine</u> **206**(9): 1845-1852.
- Utine, G. E., et al. (2005). "Childhood Parapneumonic Effusions*." Chest 128(3): 1436-1441.
- van der Poll, T. and S. M. Opal (2009). "Pathogenesis, treatment, and prevention of pneumococcal pneumonia." <u>The Lancet</u> **374**(9700): 1543-1556.
- Visser, *et al.* (1998). "Chemokines produced by mesothelial cells: huGRO-α, IP-10, MCP-1 and RANTES." <u>Clinical & Experimental Immunology</u> **112**(2): 270-275.
- Walker, J. A., *et al.* (1987). "Molecular cloning, characterization, and complete nucleotide sequence of the gene for pneumolysin, the sulfhydryl-activated toxin of Streptococcus pneumoniae." <u>Infect. Immun.</u> **55**(5): 1184-1189.
- Waltman, W. D., *et al.* (1990). "Variation in the molecular weight of PspA (pneumococcal surface protein A) among Streptococcus pneumoniae." <u>Microbial Pathogenesis</u> **8**(1): 61-69.
- Wang, N. S. (1974). "The regional difference of pleural mesothelial cells in rabbits." <u>The American review of respiratory disease</u> **110**(5): 623-633.
- Weber, J. R., *et al.* (2003). "Recognition of Pneumococcal Peptidoglycan: An Expanded, Pivotal Role for LPS Binding Protein." <u>Immunity</u> **19**(2): 269-279.
- Weinberger, D. M., *et al.* (2011). "Serotype replacement in disease after pneumococcal vaccination." <u>The Lancet.</u>
- Weiser, J. N., *et al.* (1994). "Phase variation in pneumococcal opacity: relationship between colonial morphology and nasopharyngeal colonization." <u>Infect. Immun.</u> **62**(6): 2582-2589.
- Wellmer, A., *et al.* (2002). "Decreased Virulence of a Pneumolysin-Deficient Strain of Streptococcus pneumoniae in Murine Meningitis." <u>Infect. Immun.</u> **70**(11): 6504-6508.
- Wells, C. L., *et al.* (1998). "Cytochalasin-Induced Actin Disruption of Polarized Enterocytes Can Augment Internalization of Bacteria." <u>Infect. Immun.</u> **66**(6): 2410-2419.
- Whitney, C. G., *et al.* (2003). "Decline in Invasive Pneumococcal Disease after the Introduction of Protein–Polysaccharide Conjugate Vaccine." New England Journal of Medicine **348**(18): 1737-1746.
- WHO (2007). "Pneumococcal conjugate vaccine for childhood immunization WHO position paper." Weekly Epidemiological Record **12**(82): 93-104.
- WHO (2009). "Comparative impact assessment of child pneumonia interventions." <u>Bulletin of the World Health Organisation</u>(87): 472-480.
- Willems, F., *et al.* (1994). "Interleukin-10 inhibits B7 and intercellular adhesion molecule-1 expression on human monocytes." <u>European Journal of Immunology</u> **24**(4): 1007-1009.
- Williamson, Y. M., et al. (2008). "Differentiation of Streptococcus pneumoniae Conjunctivitis Outbreak Isolates by Matrix-Assisted Laser Desorption Ionization-Time of Flight Mass Spectrometry." <u>Appl. Environ. Microbiol.</u> **74**(19): 5891-5897.
- Winslow, C. E. A. B., J. Buchanan, R. E. Krumwiede, C. Jr. Rogers, L. A. Smith, G. H. (1920). "The families and genera of the bacteria: final report of the committee of the Society

- of American Bacteriologists on characterization and classification of bacterial types." Journal of Bacteriology 5: 191-229.
- Witzenrath, M., *et al.* (2011). "The NLRP3 Inflammasome Is Differentially Activated by Pneumolysin Variants and Contributes to Host Defense in Pneumococcal Pneumonia." <u>The Journal of Immunology</u> **187**(1): 434-440.
- Wright AE, M. P., Colebrook L, Dodgson RW (1914). "Observations on prophylactic inoculation against pneumococcus infections, and on the results which have been achieved by it." Lancet 1-10: 87-95.
- Xu, F., *et al.* (2008). "Modulation of the Inflammatory Response to Streptococcus pneumoniae in a Model of Acute Lung Tissue Infection." <u>Am. J. Respir. Cell Mol. Biol.</u> **39**(5): 522-529.
- Yesilkaya, H., *et al.* (2000). "Role of Manganese-Containing Superoxide Dismutase in Oxidative Stress and Virulence of Streptococcus pneumoniae." <u>Infect. Immun.</u> **68**(5): 2819-2826.
- Yoshimura, A., *et al.* (1999). "Cutting Edge: Recognition of Gram-Positive Bacterial Cell Wall Components by the Innate Immune System Occurs Via Toll-Like Receptor 2." <u>The Journal of Immunology</u> **163**(1): 1-5.
- Yu, J., *et al.* (2008). "A rapid pneumococcal serotyping system based on monoclonal antibodies and PCR." <u>Journal of Medical Microbiology</u> **57**(2): 171-178.
- Yuste, J., *et al.* (2005). "Additive inhibition of complement deposition by pneumolysin and PspA facilitates Streptococcus pneumoniae septicaemia". <u>J Immunol</u> 175, 1813–1819.
- Zeillemaker, A. M., *et al.* (1999). "Mesothelial Cell Activation by Micro-Organisms." <u>Sepsis</u> **3**(4): 285-291.
- Zeillemaker, A. M., *et al.* (1996). "Peritoneal Interleukin-8 in Acute Appendicitis." <u>Journal of Surgical Research</u> **62**(2): 273-277.
- Zeng, L., *et al.* (1994). "Immunocytochemical characterization of cell lines from human malignant mesothelioma: Characterization of human mesothelioma cell lines by immunocytochemistry with a panel of monoclonal antibodies." <u>Human Pathology</u> **25**(3): 227-234.
- Zhang, J., et al. (2000). "The polymeric immunoglobulin receptor translocates pneumococci across human nasopharyngeal epithelial cells." Cell 102: 827 837.